REPORT DOCUMENTATION PAGE

Form Approved
OMB No. 0704-0188

2. REPORT DATE	3. REPORT TYPE AND DATES COVERED
30 Mar 92	THESIS

4. TITLE AND SUBTITLE

Temporal Monitoring of VHF and LF Atmospherics and Their Relation to Lightning

5. FUNDING NUMBERS

(1)

6. AUTHOR(S)

Arthur E. Zemke, Captain

7. PERFORMING ORGANIZATION NAME(S) AND ADDRESS(ES)

AFIT Student Attending: Tufts University

8. PERFORMING ORGANIZATION REPORT NUMBER

AFIT/CI/CIA- 92-026

9. SPONSORING/MONITORING AGENCY NAME(S) AND ADDRESS(ES)

AFIT/CI
Wright-Patterson AFB OH 45433-6583

10. SPONSORING/MONITORING AGENCY REPORT NUMBER

11. SUPPLEMENTARY NOTES

12a. DISTRIBUTION/AVAILABILITY STATEMENT

Approved for Public Release IAW 190-1
Distributed Unlimited
ERNEST A. HAYGOOD, Captain, USAF
Executive Officer

12b. DISTRIBUTION CODE

13. ABSTRACT (Maximum 200 words)

92

14. SUBJECT TERMS

15. NUMBER OF PAGES
49

16. PRICE CODE

17. SECURITY CLASSIFICATION OF REPORT	18. SECURITY CLASSIFICATION OF THIS PAGE	19. SECURITY CLASSIFICATION OF ABSTRACT	20. LIMITATION OF ABSTRACT

TEMPORAL MONITORING OF VHF AND LF ATMOSPHERICS AND THEIR RELATION TO LIGHTNING

A Thesis Submitted by

Captain Arthur E. Zemke, USAF
B.S.E.E., United States Air Force Academy
(1987)

In Partial Fulfillment of the Requirements
for the Degree of

Master of Science

in

Electrical Engineering

at

TUFTS UNIVERSITY

May 1992

Signature of Author 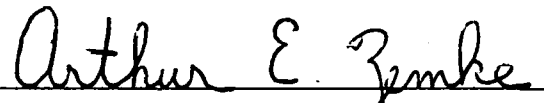
Department of Electrical Engineering, March 30, 1992

Approved by 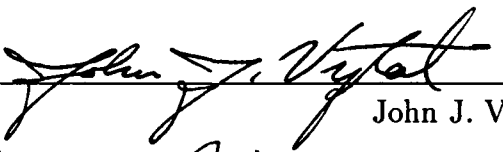
John J. Vytal, CSDL Supervisor

Approved by 
Arthur Uhlir, Professor of Electrical Engineering

Approved by 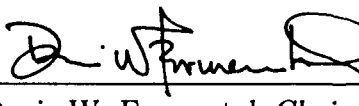
Denis W. Fermental, Chairman, Department of Electrical Engineering

March 31, 1992

This report was prepared at The Charles Stark Draper Laboratory, Inc., under IR&D Project 18754.

Publication of this report does not constitute approval by the Draper Laboratory or the sponsoring agency of the findings or conclusions contained herein. It is published for the exchange and stimulation of ideas.

I hereby assign my copyright of this thesis to The Charles Stark Draper Laboratory, Inc., Cambridge, Massachusetts.

Arthur E Zemke

Arthur E. Zemke

Permission is hereby granted by The Charles Stark Draper Laboratory, Inc. to Tufts University to reproduce any or all of this thesis.

Temporal Monitoring of VHF and LF Atmospherics and their Relation to Lightning

by

Arthur E. Zemke

Submitted to the Department of Electrical Engineering at Tufts University on March 31, 1992, in partial fulfillment of the requirements for the degree of Master of Science in Electrical Engineering.

Abstract

Atmospheric discharges of various types emit electromagnetic radiation over a wide range of frequencies. VHF transients are associated with the discharges that occur during the preliminary charge separation and breakdown processes of lightning. Correlated VHF-LF activity emitted at relatively high magnitudes are normally attributed to lightning's powerful return stroke and recoil streamer discharges. This research hypothesized that VHF atmospherics (precursors) exist at least 1 minute or more before correlated VHF-LF transient activity (return strokes or recoil streamers) is detected during known lightning and thunderstorm periods.

For 56 days, high-sampling-rate digitizers continuously monitored atmospheric conditions in VHF and LF bandwidths and measured the peak magnitude of transients as they occurred. The data was recorded in a computer file and used to characterize transient activity during various weather periods. The experimental results collected throughout confirmed lightning and thunderstorm intervals showed a significant increase in transient activity and that VHF atmospherics were detected on the average at least 3 minutes before any correlated VHF-LF transient activity was measured. In a few cases, the lead time was even greater when the initial VHF existed an average of at least 11 minutes before the onset of correlated VHF-LF. These results suggest that monitoring VHF atmospheric activity could form the basis of lightning hazard warning systems. Also, they could provide status information for activities like artificially triggering lightning. However, in some instances the VHF activity was not always followed by LF indications of lightning and might be considered "false alarms" which could be reduced by more refinements such as radio locating the VHF signal's source.

Thesis Supervisors

Arthur Uhlir, Professor
Department of Electrical Engineering
Tufts University, Medford, MA

John J. Vytal, Leader
HF Communications Group
C.S. Draper Laboratory, Cambridge, MA

ACKNOWLEDGEMENTS

Many people have assisted me at one time or another with completing my graduate program and in particular this research endeavor. Some have made numerous contributions on my behalf and really deserve special recognition.

At Tufts, Professor Arthur Uhlir enhanced my graduate experience in many ways as my advisor. He provided meaningful advice throughout the entire process and shared many of his professional experiences with me. Some of Profersor Uhlir's numerous contributions include helping me select a research subject area, acquiring the Hewlett Packard instrumentation, teaching me how to measure the data collection system parameters, and checking the gain analysis. Other support he provided consisted of proofreading the various drafts and coordinating committee functions.

I would like to thank everyone involved at C.S. Draper Laboratory for offering me a "Fellowship" opportunity, but especially the Education Office who took care of the various details and "brought Tufts on board" with established practices. A special thanks is in order for my Draper Labs supervisor John J. Vytal, who has made my graduate education very meaningful by exposing me to a variety of topics. I am thankful to John for offering me a position in his research group, allowing me to work in a subject area that I found interesting, nudging me to investigate a few topics more thoroughly, and providing technical assistance. In addition, John proofread my proposal and thesis drafts with fine tune precision, coordinated fellowship requirements, and invited me to his group's social functions.

Lt Colonel Mark J.A. Nolen deserves recognition for motivating me to apply for the Draper Lab Fellowship and to approach my schooling with an intense desire to learn. His insight into technical applications associated with the topics I studied presented real world examples of the theories in action. Similarly, he researched, acquired, and furnished hard to find government reports and supplementary textbooks that allowed me to complete course projects.

I would like to also acknowledge those folks who have helped me with specific problems. Warren Gagosian of Tufts kept my test equipment up and running for the early months of the study. John Walsh of the National Climatic Data Center in Asheville provided five months of consolidated weather reports and radar summaries from local observation stations. Ensign Brad Bogan helped me decipher many aspects of Stochastics, DSP, Matlab, and LaTeX and accompanied me in an exploration of Bean Town and Maine.

This section would not be complete if I did not acknowledge the countless sacrifices that my wife Cynthia has made during the last two years. Even as a full time teacher of the deaf, she still found time to take care of many of life's daily details that my studies kept me from attending to. Also, she reviewed the proposal and thesis drafts and offered meaningful suggestions. Most of all, she represented a constant motivation to get done soon so that I could get back to enjoying life with her again.

Contents

List of Figures

List of Tables

TEMPORAL MONITORING OF VHF AND LF ATMOSPHERICS AND THEIR RELATION TO LIGHTNING

Chapter 1

Introduction

Lightning has always been a source of fascination due to its destructiveness and bright luminosity. Its impact has intensified because of the higher sensitivity of electronic equipment, decreased vertical distance between taller structures and charged clouds, and overall growth in aeronautical operations which at times fly through storm systems. For example, some ballistic missiles and rockets have been destroyed or disabled by lightning strokes triggered by conditions created by the launch or by the rapid introduction of the flight vehicle into the high electrostatic fields. As mankind continues to move and work in lightning's territory, the need to find better ways to anticipate this hazard increases.

Today many efforts and systems exist which attempt to protect equipment and personnel from lightning strikes. One way to protect these systems is to detect the earliest stages of lightning's development and take precautionary actions. Fortunately, a lightning discharge possesses several observables that help identify not only that it is occurring, but which phase is transpiring. Atmospherics are one such observable and promise the advantage of all-weather remote detection.

This research focused on detecting electromagnetic radiation emitted specifically at VHF and LF in order to better distinguish the phases of lightning. The main thrust was to determine if VHF atmospherics (precursors), which are radiated by small discharges during lightning's preliminary charge separation and breakdown processes, exist at least 1 minute or more before correlated VHF-LF transients (activity indicative of return strokes or recoil streamers) are detected.

The study consisted of using high-sampling-rate digitizers to continuously monitor atmospheric conditions in two frequency bands. The first goal was to characterize transient activity at both frequencies under different types of weather conditions. With this accomplished, the data collected during confirmed lightning and thunderstorm periods was analyzed to determine when VHF atmospherics were detected in relation to correlated VHF-LF transients. The experimental results yielded two interesting types of VHF transient behavior and strongly suggest the inclusion of local atmospheric activity levels in future lightning hazard warning systems.

Chapter 2

The Problem

2.1 Rationale and Need for the Study

This study is important and timely for several reasons. Lightning's impact on and destructiveness to mankind has intensified in recent years particularly due to the growth of the aviation, space, and missile sectors and increased sensitivity of electronic systems to voltage transients and high-amplitude electromagnetic pulses. The destruction from lightning includes forest fires, livestock fatalities, equipment damage, power outages, and communication interference just to name a few examples. More importantly, human lives are lost due to lightning strikes. A look at statistics concerning fatalities from severe weather shows lightning accounts for an average of around 200 deaths annually[56].

Today's lightning protection efforts concentrate on passive techniques that attempt to minimize the destructive effects of lightning by continually offering a constant level of defense. For example, facilities are designed with lightning rods or appropriate grounding systems and computer networks employ transient voltage suppressors. Active systems, like self-shunting circuits, provide extra and temporary protection against lightning activity during periods of time when lightning is likely, but are not designed to operate continuously. Such systems suffer from limitations imposed by lightning's transitory nature in terms of determining just when to put them into operation or turn them off.

For example, whenever the weather service suggests that thunderstorm activity is probable, one could maintain the passive protection systems already in place and take active measures like moving people and livestock inside, disconnecting a facility from power transmission lines, and activating self-shunting circuits in sensitive electronic equipment. However, this approach could result in long downtime if the facility does not have an alternative power supply. A more appropriate solution to minimize this downtime would be to monitor the local atmospheric conditions, determine when the weather has changed to a state indicating that lightning will probably occur, and then activating additional precautionary measures. The utility of this technique increases as capabilities which give more time proximate warnings of lightning evolve.

Today, some weather surveillance systems attempt to provide more advanced

warnings prior to lightning discharges, but suffer from limitations that make them inadequate for this purpose. Many operate over wide geographic areas to maximize coverage, but are not designed to pinpoint and report conditions to local users. Some can provide warnings to other regions only after thunderstorm activity is confirmed in an initial area. One warning system proposed uses optical sensors, which can detect the luminosity of individual lightning strokes. Unconfirmed reports indicate that optical sensors have been able to detect flashes minutes before the first return stroke, however their full utility is hindered by haze and cloud cover. Weather radar is another system used today and provides warnings due to its ability to determine internal thunderstorm conditions such as precipitation and vertical wind shear intensity from radar echoes[12]. Drawbacks of weather radar are its high acquisition costs and the fact that radar echoes only reveal the precipitation intensity or the height of cloud tops. Even though these are observables that correlate well with thunderstorm development, they do not necessarily confirm lightning.

Field mills can also be employed as part of a lightning warning system due to their ability to locally monitor the earth's electrostatic field or E-field. High static values and changes in polarity of the E-field are conditions that indicate lightning development and thunderstorm movement. Unfortunately, these various E-field conditions usually only exist in the vicinity of the storm and therefore require that field mills or E-field sensors be placed over a wide geographic area to ensure coverage. Also, some form of telemetry is needed to communicate local E-field conditions to a central controller in order to update information. Another minor drawback of field mills providing an early warning concerns the fact that at times, significant E-field variations do not occur until after a recoil streamer is initiated or a half second before a return stroke starts to propagate.

The outlook for the development of new warning systems appears dim, because the focus of a large percentage of current research is on measuring or detecting large scale weather disturbances and phenomena due to their destructiveness. There are studies that correlate maximum lightning flash rates with the peak of vertical wind shear activity[75] or measure the UHF radiation of a return stroke[21]. Other related lightning measurements include tracking frontal movements and thunderstorms by satellite, detecting microbursts with doppler radar, plotting E-field changes of return strokes with field mills[61], and locating stepped leaders with interferometry. Unfortunately these types of measurements do not lend themselves well to affording much of a warning capability, because observation of these phenomena usually occurs when the storm is near or at full strength.

Therefore, to achieve dynamic protection against lightning and reduce its destructive effects, new systems based on lightning's other observables must be developed to overcome the limitations of optical sensors, weather radar, and E-field networks. In addition, the focus should be on observing the initial stages of lightning in order to provide the earliest warning possible.

2.2 Statement of the Problem

Knowing the potential initiating time and location of a recoil streamer or return stroke discharge would greatly enhance capabilities to protect people, structures, and systems from lightning discharges. However, due to lightning's transitory nature, it is difficult or even impossible to predict when and where a flash will hit. Even though weather radar, forecasts, or atmospheric conditions such as overcast skies and frontal movements may suggest that thunderstorm or lightning activity is likely in a particular region, they do not provide a useful advanced warning to allow additional protective measures to be taken without excessive downtime.

In an attempt to furnish the earliest warning possible, this research effort centered on a theme of measuring the initial indications that lightning activity would occur in a specific area. Because atmospherics are radiated during all stages of a lightning flash, the main goal was to test a basis founded on these observables in order to detect the preliminary discharge and breakdown processes. In particular, detection of atmospherics radiated from these earliest charge transfers might allow ample time to warn people and protect all types of systems prior to the launching of a recoil streamer or return stroke. The use of atmospherics offered several advantages over other observables such as their ability to penetrate haze and cloud cover. Similarly, they can travel great distances in short time intervals and be detected by inexpensive receivers even at low signal levels.

2.3 Hypothesis to be Investigated

To obtain the earliest possible warning of a lightning flash, its initial stages of development must be detected. During lightning's preliminary phases, discharges occur while the charge separation process advances. These discharges are relatively small in magnitude, not bright enough to be observed by optical sensors, and do not cause sufficient E-field changes to be confirmed by field mills. Fortunately, the various phases of lightning including preliminary charge transfers also radiate a significant amount of atmospherics. In fact, the phases of lightning can be identified by the spectrum of RF activity. Specifically, significant VHF activity tends to indicate the occurrence of lightning's preliminary phases. Similarly, recoil streamers and return strokes are confirmed by intervals of high magnitude correlated VHF-LF radiation. Historically, the unknown here has been how much earlier do the preliminary stages or VHF start in relation to the first return stroke or recoil streamer. Time estimates range from as little as .5 seconds to as much as 12 minutes. This research effort attempted to refine these estimates and hypothesized that lightning's preliminary charge transfers emit VHF radiation (precursors) at least 1 minute or more before the occurrence of the first recoil streamer or return stroke. To test the hypothesis, high-sampling-rate digitizers were utilized to record the time of occurrence and peak value of atmospherics, particularly the ones emitted during the early stages of thunderstorms.

Chapter 3

Review of Literature

3.1 Historical Overview

According to the well known lightning researcher M.A. Uman, "Lightning and thunder have always produced fear and respect in mankind, as evident from the significant role that they have played in the religions and mythologies of all but the most modern civilizations". Early statues show Buddha carrying and the Egyptian god Typhon hurling thunderbolts. Ancient Verdic books of India tell how the god Indra carried thunderbolts on his chariot while a Sumerian seal (2500 B.C.) depicts the lightning goddess Zarpenik riding on the wind with a bundle of thunderbolts. The ancient Greeks thought Zeus sent lightning as punishment while the Romans also believed Jupiter used lightning as a warning against undesirable behavior. The most famous god associated with lightning was the fierce Norseman Thor, who produced lightning by striking an anvil with his hammer while riding a chariot in the clouds. In America, certain Indian tribes believed that lighting was due to the mystical *Thunderbird.* Some medieval European church bells carried Latin inscriptions which meant, 'I break up the lightning flashes'[70].

The first scientific study of lightning was carried out by Benjamin Franklin around 1774 and proved clouds were electrically charged. Significant progress in understanding lightning began again in the late nineteenth century with the use of time-resolved photography and spectroscopy to identify individual lightning strokes. Lightning current measurements were made by Pockels in Germany around 1899. Modern lightning research began in England with Wilson in 1920, who estimated the charge structure of a thunderstorm and lightning discharge. The period from 1970 to present has been a very active one for lightning research due to motivation produced by lightning damage and development of new techniques of digital data taking[70].

3.2 Research Literature Specific to Thesis Topic

The earth's atmosphere contains a variety of electrical activity that is generated in many ways. The most common source of charge buildup and transfer are natural phenomena and include tornadoes, hurricanes, volcanoes, sand storms, solar activity,

cosmic rays, auroras, and thunderstorms. Natural, as opposed to triggered, lightning from thunderstorms accounts for the largest magnitude charge transfers.

The overall lightning discharge is termed a *flash* and is made up of individual *strokes*. Lightning flashes from thunderstorms are divided into two types, depending on the end points of the discharge. Cloud-to-ground discharges are the most familiar type due to their bright luminosity, interference with communication systems, and overall destructiveness to man's environment. Cloud-to-cloud, cloud-to-air, and intracloud discharges are all grouped together in the second category as Cloud discharges[70]. Intracloud discharges are the most prevalent and account for well over half of all types of lightning discharges[65, 73].

By examining a few subtopics of atmospheric electricity such as the global circuit, the electrification of thunderstorms, charge separation, and the stages of cloud-to-ground and intracloud lightning, clues to observing lightning in its formative stages can be found. In addition, the various stages of lightning are accompanied by many observables. Even though E-field variations and atmospherics are just two of the many observables available, both are important and suggest the use of particular detection schemes to confirm lightning discharges.

3.2.1 Global Circuit

Lightning is just one part of the earth's global circuit and serves as a sort of battery to maintain the earth's ambient or "fair weather" electricity levels. The earth has a negative charge that is maintained primarily by thunderstorm activity. In particular cloud-to-ground lightning, corona point discharges or conduction currents, and rain contribute to the main charge transfer[31, 56]. According to Ogawa[50], in normal weather conditions the atmosphere is electrified at a positive potential and sustains an E-field $E_o \approx 100\ V/m$ at the earth's surface. Basically, the global circuit is a current system in which currents flow upward from thunderstorms through the ionosphere and down to earth's surface in the fair weather regions[43]. This is illustrated in Figure 3.1.

3.2.2 Electrification Theories

Identification of the processes or mechanisms which actually charge up thunderclouds and eventually form lightning remain the most controversial area of lightning research. The discrepancy arises because intense electric fields, $E \approx 3x10^6\ V/m$ and $5x10^5\ V/m$ for dry and humid air respectively, must develop before breakdown can occur within thunderclouds and lightning is initiated[46]. During developed thunderstorms however, measured electric field magnitudes rarely even exceed $E \approx 4x10^5\ V/m$[46]. Therefore, researchers are attempting to develop theories that explain and identify the responsible mechanisms which intensify the local fields enough to initiate and propagate lightning[30]. The subject of electrostatic field changes is revisited in more depth in a later section.

There are two common themes for the theories that explain charge separation. *Gravitational or Precipitation Theories* contend that a microscopic mechanism

separates charge and places negative charge on the larger precipitation and positive charge on the smaller particles, which separate under gravity to form the cloud's dipole structure[30, 39, 56, 75]. *Convective Theories* differ and argue that air motions (windshear, up-drafts, and down-drafts) are the dominant influence in the charge separation process[45, 56].

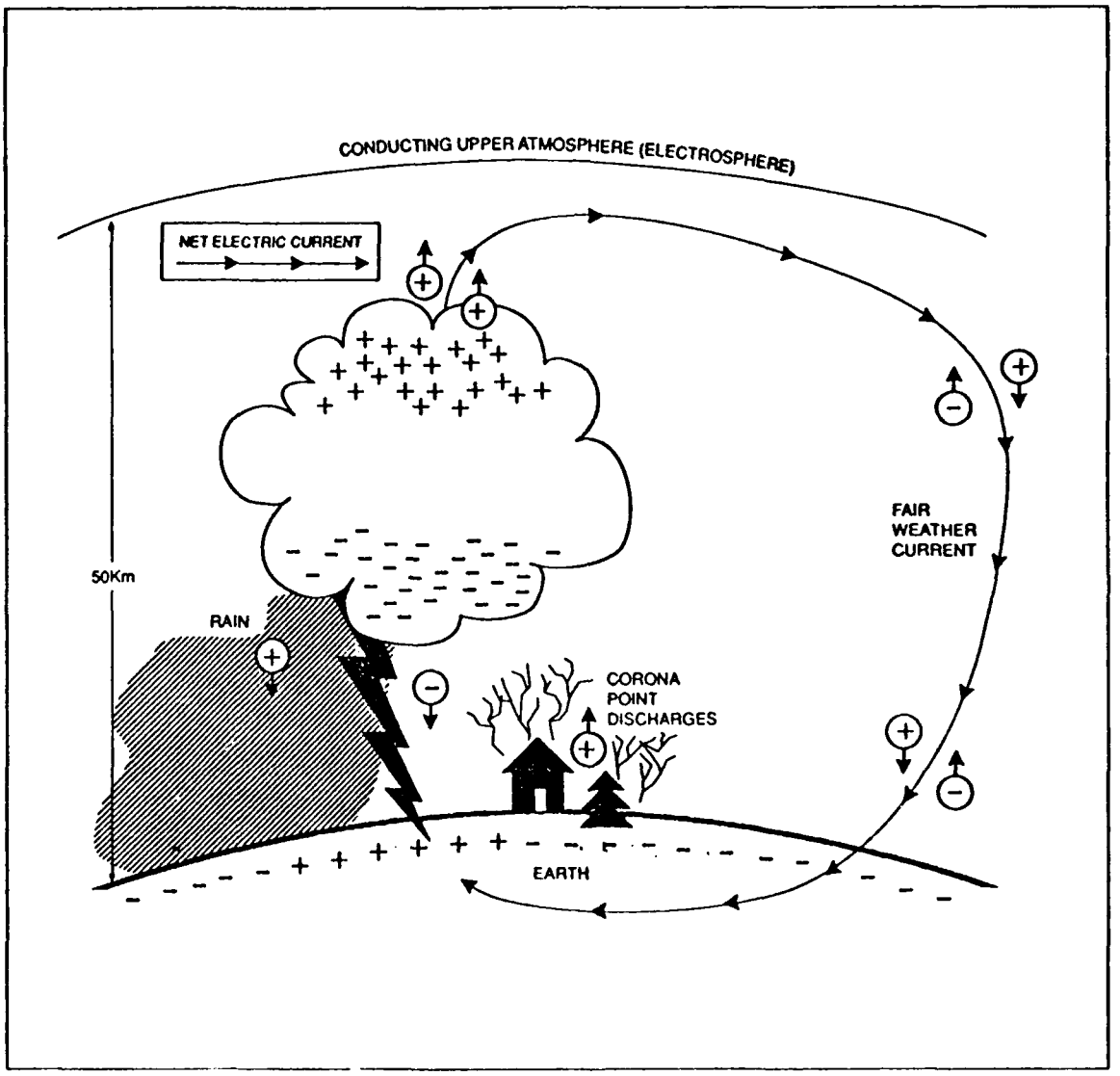

Figure 3.1: Global Circuit Showing Thunderstorm Acting as a Battery to Keep Earth Charged Negatively and Atmosphere Charged Positively. Adapted from M.A. Uman's *The Lightning Discharge.*

There is general agreement among lightning experts that the overall charging process relies on parts of both theories. Gravitational processes such as the formation of hail and ice account for most of the charge separation. Wind shear, however, cannot be ignored as a major contributor as well, due to the magnitude of the vertical components involved. For our purposes, it is not critical to identify the actual charge separation process responsible, but to realize and take advantage of the fact that varying amounts of charge are eventually separated and hence discharges can occur. In fact, the occurrence of preliminary small magnitude discharges (during the initial charge separation processes) is one specific process that this study is attempting to detect.

3.2.3 Charge Structure of Thunderstorms

The structure of a thunderstorm (after charge separation) suggests using vertically-polarized antennas to sense the charge transfer. In a thundercloud, the higher regions of the cloud carry positive charges, the lower regions are negatively charged, and a concentrated small positive charge exists near the lower frontal region of the cloud[5]. The thunderstorm charge structure model (developed in the early 1930's) is basically a vertical electric dipole as seen in Figure 3.2. It is important to note the effective height of the localized charge regions $\mathbf{Q_P}$ (3-4 km), $\mathbf{Q_N}$ (4-5 km), and $\mathbf{Q_P}$ (9-10 km) for a later discussion concerning lightning initiation[70].

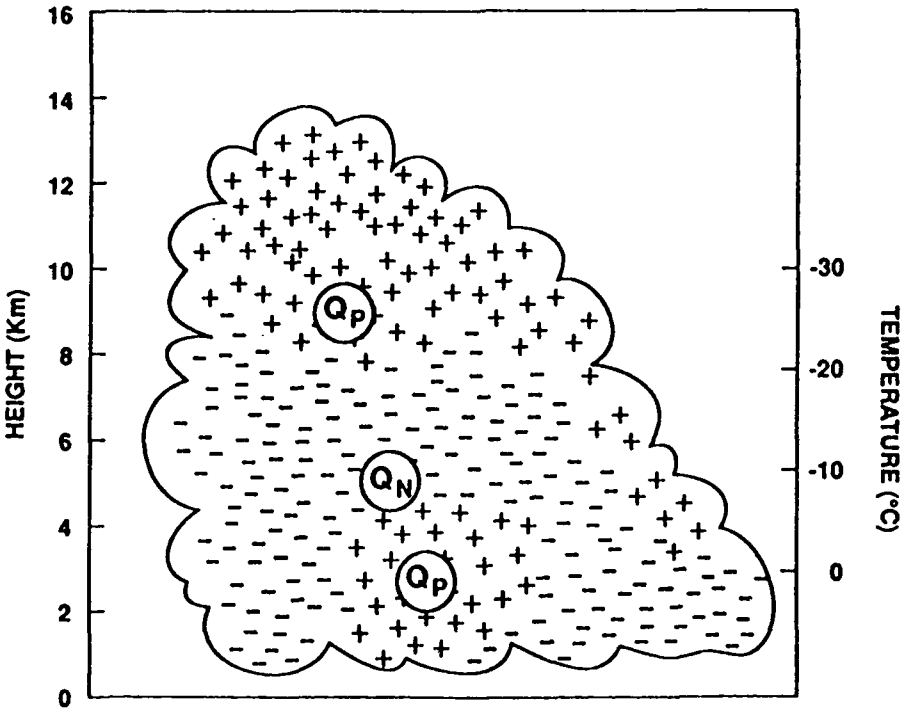

Figure 3.2: Charge Distribution in a Typical Thundercloud. Adapted from M.A. Uman's *The Lightning Discharge.*

3.2.4 Cloud-To-Ground Lightning

Categories

The classification, cloud-to-ground lightning, is further broken down into four categories as illustrated in Figure 3.3. The categories are divided up depending on the charge polarity and direction of the leader that starts the discharge. *Category 1* lightning accounts for over 90% of all cloud-to-ground discharges and is initiated by a downward-moving negatively charged leader. An upward-moving positively charged leader originating from a mountain or tall structure begins *Category 2* lightning. *Category 3* lightning remains more common in winter, usually results in much higher peak currents and charge transfers than Category 1, and is launched by a downward-moving positively charged leader. *Category 4* is even more rare than Category 2 and is initiated by an upward-moving negatively charged Leader[70].

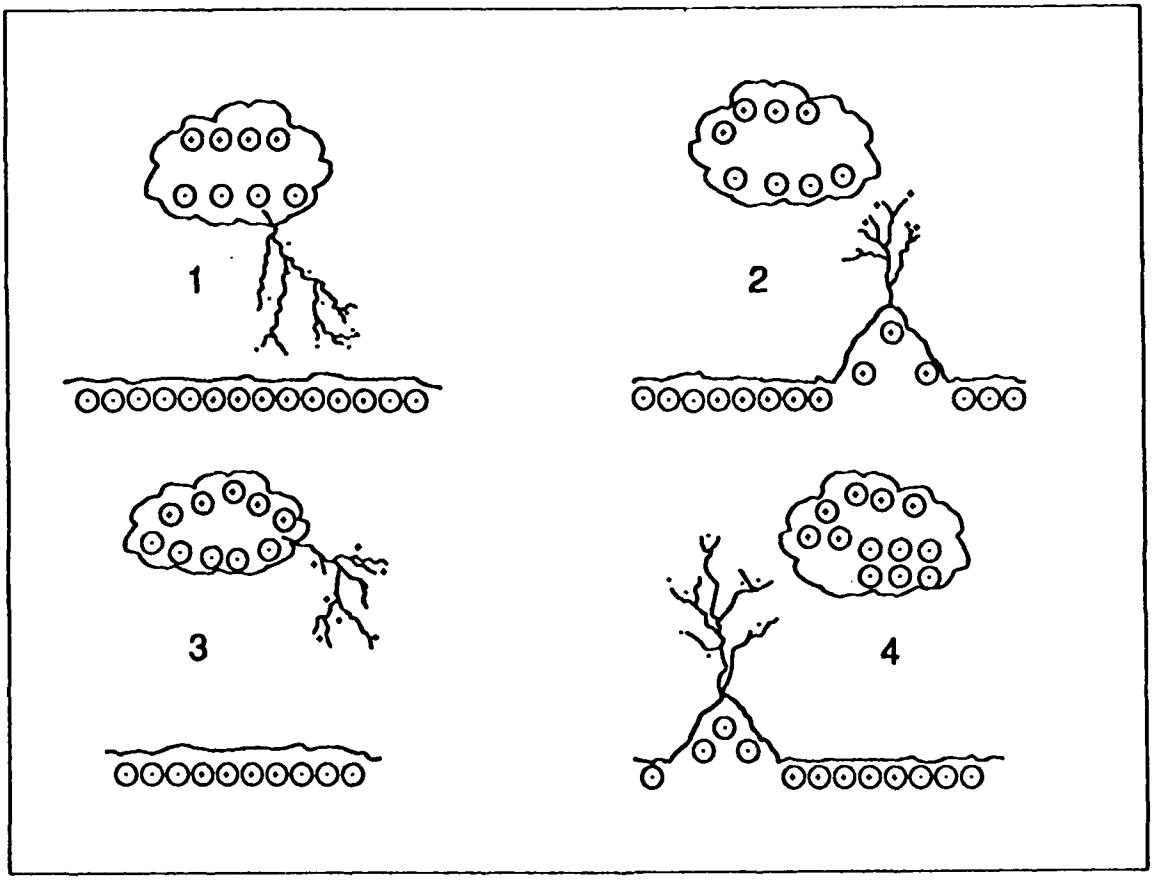

Figure 3.3: Categories 1 - 4 of cloud-to-ground Lightning. Adapted from M.A. Uman's *The Lightning Discharge.*

Category 1 Flash

As mentioned earlier, the most common cloud-to-ground flash is Category 1 lightning. The peak activity and main charge transfer for this flash begins with a negative leader originating from the Q_N region. Initially, it propagates downward toward the Q_p region, but then continues descending until it attaches to the earth. The main charge transfer or return stroke occurs between the Q_N region and the earth and carries negative charge to the earth. At the same time, some of the positive charges in the Q_P region are recombined while the majority are dissipated into the ionosphere. These regions are identified in Figure 3.2.

In more detail, the initial stages of Category 1 lightning start many minutes before a return stroke. The first stage of development, *Preliminary Discharges*, is not fully recognized among the lightning experts. However, it is characterized by minor discharges assumed to be caused by minor streamer processes in the cloud due to charge density fluctuations which start to occur 10 to 15 minutes before the 1st return stroke[76].

The next steps of a Category 1 flash continue the charge buildup and usually generate a return stroke within one second. These stages are illustrated in Figure 3.4 and described in the following excerpt adapted from M.A. Uman's, *The Lightning Discharge.*

> During *Preliminary Breakdown*, a propagating discharge begins and a *Stepped Leader* is initiated within the cloud in the lower part of the cloud between the central negative Q_N and lower positive Q_p regions as seen in Figure 3.2. As small ionized channels and leaders form, E-field changes referred to as *Preliminary Variations* can be recorded when the charge transfer between close and oppositely charge pockets becomes significant[46].
>
> The stepped leader then propagates from cloud to ground in a series of discrete steps typically 1 μs in duration, ten's of meters in length, and with a pause time between steps of 50 μs. A fully developed stepped leader lowers 10 or more coulombs of negative charge in ten's of milliseconds with an average speed $2x10^5\ m/s$. The average stepped leader current is .1-1 kA with step pulse currents of at least 1 kA.
>
> As the stepped leader nears the ground, the E-field at sharp objects or at irregularities on the ground increases until it exceeds the breakdown value of air. Then one or more upward moving discharges is initiated from those points, thus beginning the *Attachment Process.* When one of the upward moving discharges (from the ground) contacts the downward moving stepped leader (approximately 10 m above ground), the stepped leader tip is connected to ground potential. The leader channel is then discharged when a ground potential wave termed the *1st Return Stroke* propagates continuously up the previously ionized and charged leader path.
>
> The upward speed of a return stroke (measured near the ground) is typically 1/3 or more times the speed of light $3x10^8\ m/s$, and the speed decreases with increasing height. The total transmit time from ground to

the top of the channel is typically 100 μs. The 1st return stroke produces a peak current near ground of typically 30 kA with a time from zero to peak of a few milliseconds. Currents measured (at the ground) fall to 1/2 the peak value in about 50 μs.

The next stage is known as *Continuing Current.* It is characterized by a current flow of 100 A or more from cloud to ground, may last a few to hundred's of milliseconds, and registers high E-field changes. During continuing current, impulse brightenings or high luminosity of the channel called *M-Components* can be seen.

The very rapid release of return stroke energy heats the channel to a temperature of 30,000 K and generates a high-pressure channel that expands and creates a shock wave that eventually becomes thunder. The return stroke effectively lowers negative charge originally found in the Q_N region, deposited on the stepped leader channel, or available at the top of its channel to ground.

The *Junction Process* or J-Processes occur in the cloud after a return stroke occurs and are similar to processes that occur in intracloud lightning. The J-Processes are identified with cloud discharges that make charge available (to the top of the previous return stroke channel) to initiate a *Dart Leader. J-Changes* accompany J-Processes, are relatively steady E-field changes (over ten's of milliseconds in duration), can be either positive or negative, and are generally smaller than the field changes found during continuing current.

Recoil Streamers or K-Processes are generally viewed as a small return stokes that occur when a propagating discharge (J-Process) within the cloud encounters a pocket of charge opposite to its own[51]. *K-Changes* accompany recoil streamers and are small, relatively rapid E-field variations occurring at intervals of 2-20 milliseconds which are superimposed on the overall J-changes.

If after one return stroke, the current and charge motion in the cloud cease, then the flash is called a *Single Stroke Flash.* If on the other hand, additional charge is made available to the top of the channel by J-Processes, then a continuous dart leader may propagate down the residual return stroke channel at a speed near $3x10^6\ m/s$. Usually, the dart leader lowers a charge on the order of 1 coulomb by virtue of its current of 1 kA. As the dart leader nears the ground, attachment occurs and a *Subsequent Return Stroke* is initiated. In other cases, some leaders begin as a dart leader, but toward the end of their trip to the ground they start stepping and are known as *Dart-Stepped Leaders.* After the current of the subsequent return stroke and charge motion in the cloud have ceased, the overall process is called a *Multiple Stroke Flash*[70].

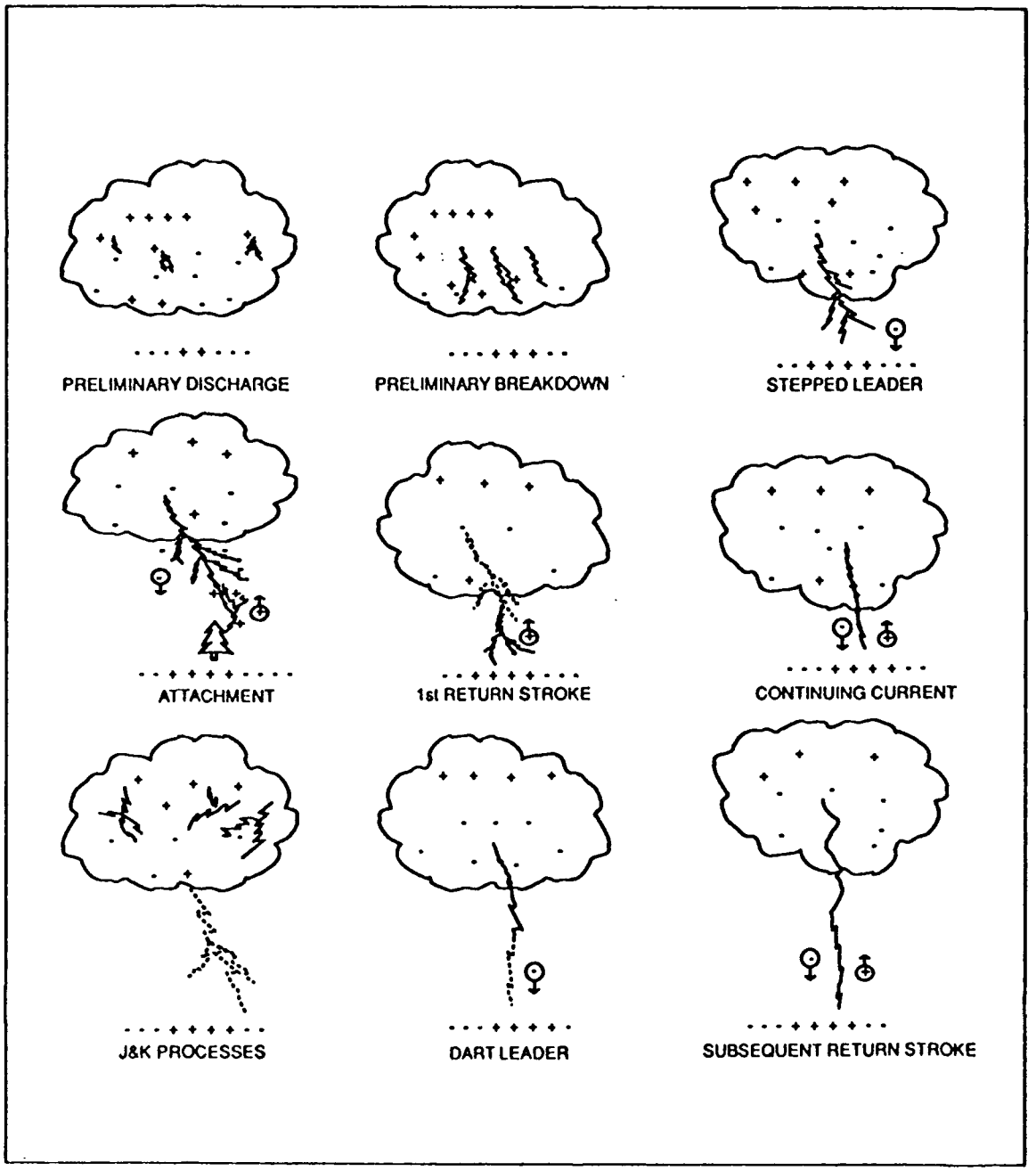

Figure 3.4: Processes of Category 1 Lightning. Adapted from M.A. Uman's *The Lightning Discharge.*

3.2.5 Intracloud Lightning

Even though intracloud discharges occur much more commonly than all types of lightning (including cloud-to-ground), there is not as much data available on its individual phases. One reason for this is that intracloud discharges are not of widespread practical interest. They do not cause as much destruction as do cloud-to-ground discharges (for example, power line outages or setting forest fires)[70]. Also, it is difficult to record and photograph the activity due to visibility limitations. However, the phases of intracloud activity are still important to those in aerospace and aeronautical activity and scientists who are attempting to learn more about thunderstorm charge generation [70].

Intracloud discharges typically occur between the cloud's upper positive Q_P and negative Q_N charged regions (see Figure 3.2), usually have a considerable horizontal component in comparison to cloud-to-ground discharges, and last a total time duration of half a second[7, 51, 67]. A typical intracloud discharge transfers charge over a total spatial extent of 5-10 km[70] and is initiated by either an upward-propagating negative streamer[40, 65] or a downward-propagating positive streamer[51]. The discharge is believed to be a continuously propagating leader that generates weak return strokes (recoil streamers) when it contacts pockets of charge opposite to its own[70]. The recoil streamers originate at the tip of the advancing streamer and travel back along the channel toward the source in a manner similar to that of a return stroke[51].

Recoil streamers involve currents of 1 to 4 kA and travel at velocities of around $2x10^6\ m/s$[51]. Associated with the recoil streamers are rapid electric field changes termed K-Changes, which are similar to but opposite in polarity to the K-Changes observed in cloud-to-ground discharges[70].

3.2.6 Electrostatic Field Observables

Certain attributes of lightning can be determined from its optical luminosity or by measuring the wind shear, acoustics, and radar reflectivity of a thunderstorm. The changes in the earth's E-field are another observable which provide a significant amount of information. For instance, cloud-to-ground flashes are identified by rapid field changes while intracloud discharges are characterized by slow, relatively smooth field changes[4, 65, 70].

The individual stages of cloud-to-ground discharges can be distinguished by the rate of respective E-field changes. "Breakdown processes, leaders, and junction streamers which change the distributions of charge in a gradual way usually cause slow E-field changes during cloud-to-ground flashes. On the other hand, return strokes and recoil streamers produce relatively rapid changes which occur from enhancements in current when a weak discharge encounters a minor charge concentration"[18].

There are three distinct phases of an intracloud discharge, which can be identified by the rate of E-field changes. "*Initiation* is characterized by relatively small amplitude pulsations in the E-field record which last a mean interval of 680 μs while the *Very Active* portion is described by relatively rapid and large pulsed field changes. E-field changes during final intracloud *Junction* phase are similar to cloud-to-ground

J-Changes, slower than the those measured during the Very Active portion, and have occasional K-changes (usually associated with recoil streamers) which occur at intervals from 2 to 20 milliseconds"[7, 20].

3.2.7 Atmospheric Observables

Atmospherics are another important observable that can aid in lightning phase identification. Atmospherics are electromagnetic signals radiated by various phases of the lightning discharge[55]. These radio waves offer some advantages for providing warnings, because they do not suffer visibility limitations imposed by cloud cover that optical systems encounter. Also their velocity of propagation is very high.

It is a misconception that lightning discharges are just one single large spark comparable to the ideal impulse $\delta(t)$ function and that therefore all radio emissions are simultaneously produced as in the case of nuclear EMP[9]. Experimental measurements show that the spectral density for a lightning flash falls off at a rate inversely proportional to frequency $1/f$ as seen in Figure 3.5 [29]. In fact, some researchers believe that at higher frequencies the fall off rate is even greater at $1/f^2$. Also, each phase makes a different and unequal radiation contribution over the wide range of frequencies (from hundred's of Hz to several GHz)[34, 48, 55, 69].

Experimental evidence suggests focusing on LF and VHF radiation levels in order to identify the individual stages of a flash[29]. Return strokes and recoil streamers radiate VLF through LF (3-300 kHz) transients with very high magnitudes. Although the peak transient activity is emitted around 6-10 kHz[36], sizable amounts of LF radiation are measured and result from discharges propagating through relatively long channels (cloud-earth or cloud-cloud)[54, 58, 67]. In addition, these two processes also emit correlated VHF radiation which is caused by the ionization of virgin air and the re-ionization of old channels that have decayed to a nonconducting state within 100 milliseconds after a previous breakdown[32, 57]. However, the primary sources of radiation at frequencies above MF are the aggregate of small-scale and short (in terms of distance) discharges that occur within the cloud particularly during the initial charge separation processes and the acceleration of electrons in the high field region at the tip of the rapidly ($10^7\ m/s$) propagating breakdown or stepped leaders[16, 67, 74].

The differences in the spectral content of each lightning stage provide insight into detecting them. In particular, detection of LF radiation at high magnitudes and correlated VHF activity provides a verification capability for the occurrence of return strokes and recoil streamers. Similarly, levels of increased VHF radiation indicate the occurrence of the initial small scale processes that occur during charge separation. What follows is a more detailed discussion of the various stages of cloud-to-ground and intracloud flashes in terms of experimental observations of their peak RF radiation activity.

Cloud-To-Ground Lightning Atmospherics

Cloud-to-ground flashes emit radiation at all frequencies theoretically, but each phase radiates predominantly in certain bandwidths due to the mechanisms responsible for

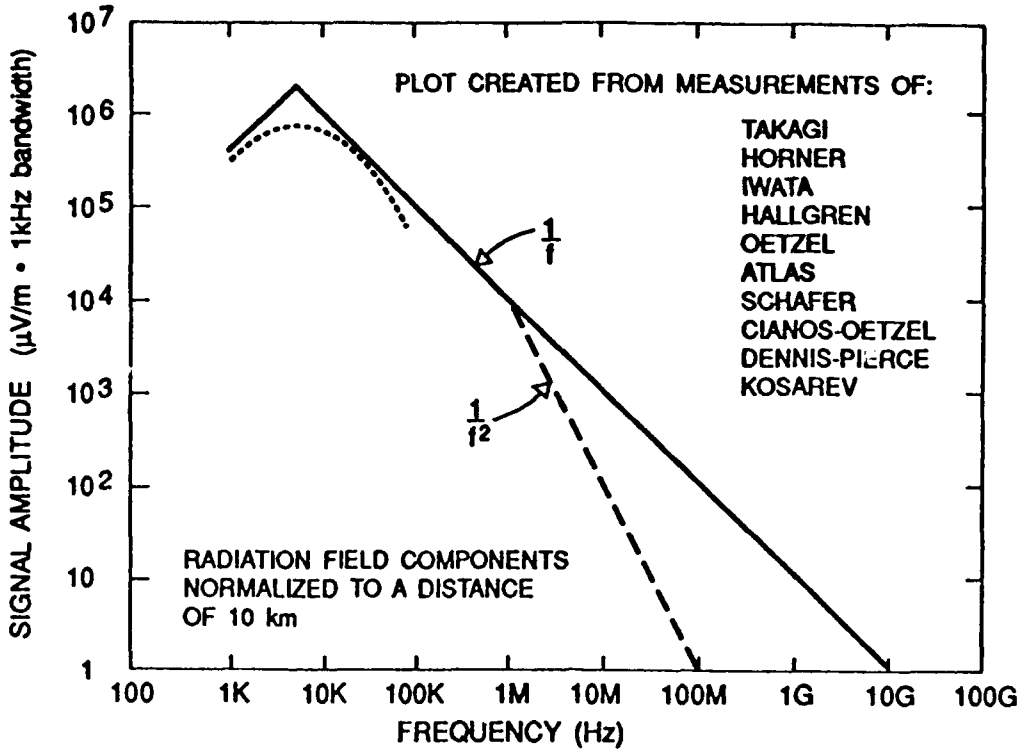

Figure 3.5: Peak Received Amplitude for Signals Radiated by Lightning. Adapted from J.E. Nanevich's, "Observation of Lightning in the Time and Frequency Domains" in *Lightning Electromagnetics.*

that particular phase.

Preliminary Discharges

The best frequency band for detecting this stage is MF-VHF (a few to over 100 MHz). The radiation from this stage typically originates 10 to 15 minutes before the 1st return stroke[76].

Preliminary Breakdown

Generally, researchers agree that the MF (3-30 MHz) and VHF (30-300 MHz) noise during preliminary breakdown is large compared to ambient noise conditions and approximately 20 times as large as the stepped leader[6, 10, 16, 44, 47, 62, 63]. In addition, the actual number of pulses per flash increases as this phase progresses due to probing leaders and small charge transfers within the cloud[9, 47, 48].

Stepped Leader

VHF radiation during this stage is emitted for practically the entire duration and at a level 2-4 times the ambient noise levels[6, 10, 62, 63]. Here too, the number of pulses per flash continues to increase with the stepped leader's multiple steps and branchings[9].

Return Strokes

Return stroke discharges radiate the most intense or largest amplitude VLF-LF signals[37, 44, 49, 54]. Of course, VHF is also radiated by a return stroke due to the extension of the existing leader channel. Even though the peak magnitude of the VHF activity is 25 times larger than that of a stepped leader[62, 63], it does not last as long, nor have a magnitude as large as the activity observed from cloud processes[6, 16, 35].

J-Processes

J-Processes emit very active VHF radiation with a magnitude 5 times greater than the stepped leader's level[62].

Recoil Streamers

Recoil Streamers and associated K-changes emit strong disturbances at VLF (3-30 kHz) [35, 49].

Dart Leaders

High levels of VHF (30-50 MHz) radiation are detected during the dart leader's trip to earth. However, the source of the radiation has been determined to be from within the cloud rather than the dart's leader channel[6, 16, 57, 60, 63, 72].

Intracloud Lightning Atmospherics

From an overall standpoint, intracloud discharges, particularly the ones not usually associated with large scale charge transfers, are the strongest source of VHF and UHF radiation during a thunderstorm[15, 21, 33, 35, 37, 60, 67, 72].

Continuous Propagating Leader

Significant VHF activity (associated with breakdown processes and probing leaders within the cloud) occurs during this stage[9, 46, 54].

Recoil Streamers and K-Changes

A recoil streamer strongly radiates at VLF due to small pulses associated with rapid, but not necessarily the largest, K-changes for frequencies from 3-10 kHz. For LF frequencies and up to 2 MHz, more radiation pulses occur and the largest are associated with K-changes. From 4-12 MHz, the overall radiation becomes continuous and the K-changes can not be distinguished[44, 49].

Atmospherics vs E-field Variations

The choice to focus on atmospherics versus E-field changes stems from the advantages that atmospherics offer in detecting lightning. Experimental results show that RF

radiation is emitted right from the start for both types of lightning. During cloud-to-ground flashes, VHF radiation is always present and lasts an average of 34 ms prior to the initiation of a steady E-field change. E-field changes do not become substantial until the charge transfer between close and oppositely charge pockets becomes significant. This long VHF radiation without a correlated E-field change is the first indication that a cloud-to-ground flash is about to occur. In addition, the preliminary breakdown and stepped leader can be defined by the E-field record and the presence of sharp pulses in VHF radiation[4, 20, 46, 47].

The same holds true for intracloud discharges, where no preliminary breakdown phase is observed and VHF radiation only exists with a correlated steady E-field change[20, 26, 27, 37, 38, 46, 47]. This difference in correlated E-Field and VHF activity allows determination of whether a flash will be cloud-to-ground or intracloud discharge within the first 70 ms[46].

Another advantage is that radio waves can travel a great distance from their generating source (depending on the frequency). The magnitude indicates the source's relative proximity and whether it is moving away or toward a specific location. Also, by detecting radio waves, a sizable local area can be monitored without an investment in multiple sensors or telemetry and the geographic location of VHF sources can be resolved from local storm activity[54].

3.3 Research In Related Areas

Some current investigations concentrate on themes related to this study and continue to search for the mechanisms that explain lightning's behavior or utilize similar observables. For example, several techniques have been developed to map the location and development of lightning by using the atmospheric signals generated. Time-Delay-of-Arrival and Interferometry mapping systems rely on the phase difference of VHF signals at different receiving stations to triangulate the geographic location of lightning sources[2, 61]. VHF radio interferometry has also been used in identifying features of a lightning stroke and pinpointing the three dimensional location of individual processes such as initial breakdown or a dart leader[17, 23, 59, 64]. Other mapping approaches measure transient electric and magnetic fields at the ground surface to estimate location of the lightning and properties of the storm[2, 22].

Another area of research concerns positive cloud-to-ground or Category 3 lightning. Even though Category 3 lightning is rare in its occurrence, it has some unique characteristics. It is usually more prevalent during winter thunderstorms in Japan, spring and summer thunderstorms in the Great Plains, and winter snowstorms in the eastern US. Also, these type of flashes usually have only one return stroke and a 10 kA continuing current amplitude, which is an order of magnitude larger than Category 1 flash levels[3].

The analysis of the electrical breakdown of air at high voltages is also of great importance. Not only does it assist in the understanding of the physical processes of lightning, but it is also useful in analyzing the growing number of extra-high-voltage transmission systems[1]. Most discussions of thundercloud electrification end

with the attainment of significant electric fields, however too far below breakdown to explain the production of a stepped leader[11, 13]. This discrepancy has led to speculation that lightning is initiated by corona discharges from large precipitation particles coupled with some mechanism whereby the local field is enhanced to breakdown values[5, 13]. Also, it is assumed from lightning's behavior, that the initiation processes must be regenerative rather than dissipative[11].

In fact, it was demonstrated in a laboratory environment, that if a parcel of air containing positively charged raindrops was swept in an updraft toward the negative charge center, then the increasing electrical stress on the drops would cause them to yield positive corona streamers. These streamers would then propagate toward the negative center and at the same time expand laterally. The resultant redistribution of charge tended to enhance the electric field at the starting point of the streamer system, so that breakdown would follow if the process was repeated a few more times[41, 42]. The positive streamers could be caused to propagate over large distances if supported by large ambient fields which imparted enough energy to the charge in the streamer tip to replicate itself...which tended to increase the local field even more[13]. In addition, these processes were greatly enhanced by the effects of increased humidity or decreased air density[1, 14].

3.4 Summary of What is Known

- Lightning serves as a battery in the global circuit that transfers negative charge to the earth and positive charge to the atmosphere. In "fair weather" areas across the earth's surface, a relatively small current flows from the ionosphere to earth to complete the circuit.
- Hail, rain, wind shear, and other natural phenomena which usually accompany a thunderstorm have been identified as mechanisms that electrify clouds and cause charge separation.
- The charge structure of a thunderstorm is basically a vertical electric dipole.
- Lightning is subdivided by discharge destination location into cloud and cloud-to-ground flashes.
- Cloud discharges are further subdivided into intracloud, cloud-to-air, and cloud-to-cloud discharges. Of all the types of lightning, intracloud discharges occur the most.
- Cloud-to-ground discharges are categorized depending on the charge polarity and direction of the leader that initiates the flash. Category 1 flashes (initiated by downward-moving negatively charged leaders) account for over 90% of all cloud-to-ground discharges.
- During the preliminary stages of cloud-to-ground lightning, VHF radiation is emitted by small charge-discharge mechanisms and without a correlated change in the E-field initially.

- The cloud-to-ground stepped leader phase radiates a detectable amount of VHF due to the breakdown and ionization of air.
- The cloud-to-ground return stroke is responsible for the largest charge transfer. It also emits high magnitude VLF-LF radiation due to length of the cloud-earth channel involved and correlated VHF due to extension of the leader channel.
- During the continuous propagating leader stage of an intracloud discharge, VHF radiation is emitted in conjunction with correlated E-field changes.
- The intracloud recoil streamer also radiates VLF-LF strongly due to the relatively long channels involved and some correlated VHF due to the extension of the leader channel.
- By correlating E-field changes and VHF activity, the type of flash (cloud or cloud-to-ground) can be determined within the first 70 ms.

3.5 Summary of What is Unknown

- The processes actually responsible for charge separation and cloud electrification are not fully understood.
- The mechanism by which the E-field is locally intensified enough to cause breakdown and propagate a leader is not clear.
- The phenomena responsible for radiating energy at VHF and UHF has not fully been identified.
- During what stage or with how much notice do the preliminary charge-discharge stages start radiating VHF before a return stroke occurs.

Chapter 4

Research Design

4.1 General Method

The general research method utilized to test the precursor hypothesis was a historical type of investigation in order to reconstruct the past accurately without bias. Specifically, time and peak magnitude parameters of VHF and LF transient activity were recorded to compare periods of increased signal activity. These data histories displayed which type (VHF or LF) of atmospherics were emitted first and how much earlier the VHF preceded the LF emissions.

4.2 Research Sample

The observables studied in this research effort were atmospheric signals or transients emitted during electrical discharges in air. Characteristically, these transients were impulsive, had high magnitudes, and were radiated across a wide range of frequencies. This study narrowed the sample to only those signals radiated in narrow VHF and LF bandwidths in order to observe and differentiate lightning's various phases. To detect the atmospherics emitted by transients, receivers tuned to the respective frequency ranges were utilized.

4.3 Instrumentation

4.3.1 Equipment and Set Up

1. 1.22 m Brass Rod VHF Monopole Antenna
2. 160 m of 75 Ω RG-11/U Coaxial Cable
3. 63 MHz Airborne Instruments Laboratory Precision Tuned Receiver (Type 130)
4. HP 54510A Digitizing Oscilloscope
5. HP Vectra Computer

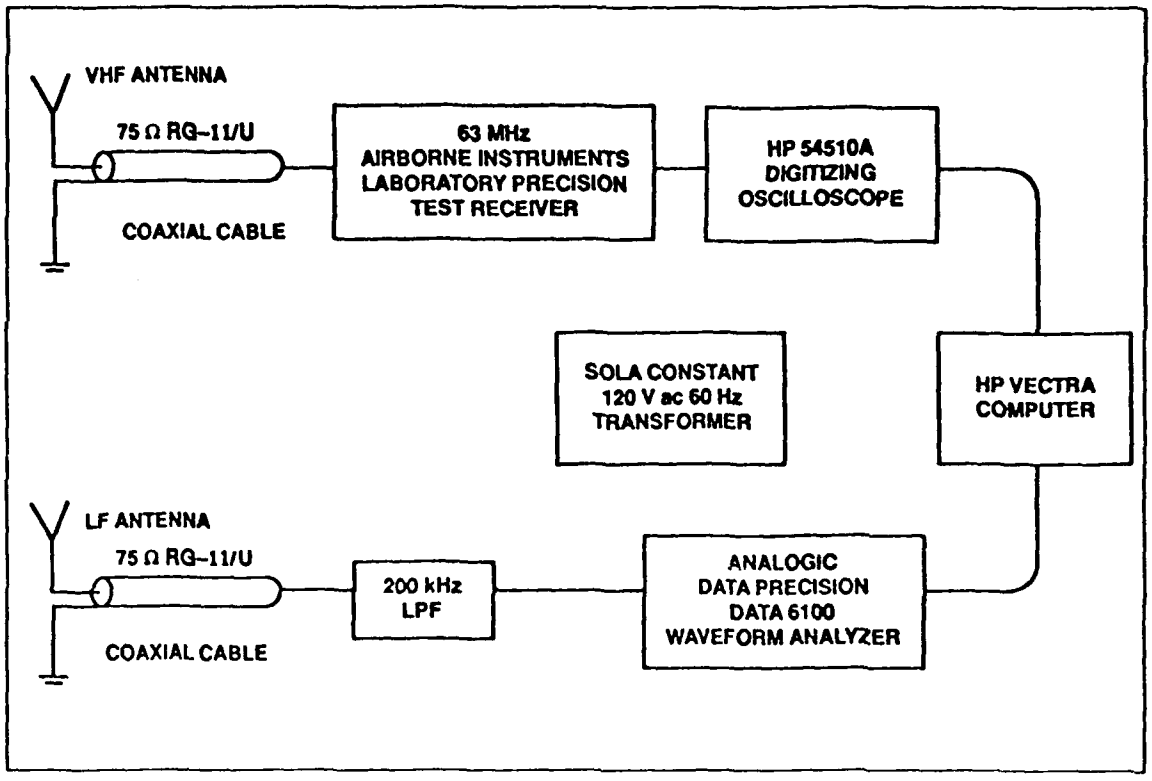

Figure 4.1: *Measurement and Data Collection System*

6. 7 m Aluminum Alloy LF Short-Monopole Antenna (radius 1.65 cm)
7. 200 kHz Anti-Aliasing LPF
8. Analogic Data Precision Data 6100 Waveform Analyzer
9. Sola 120 V 60 Hz Constant Voltage Harmonic Neutralized Transformer
10. Zenith Color TV
11. Model 1246 Digital IC Color Generator "Dynascan"

See Figure 4.1 for Measurement and Data Collection Systems.

4.3.2 VHF Data Collection System Triggering Threshold

The overall voltage gain of the VHF Data Collection System, G_T, was 11.22 (see calculations in Appendix D). This result was utilized to determine the minimum electric field required at the VHF antenna to cause the oscilloscope to trigger as follows:

$$\frac{threshold}{h_e\, G_T} = \frac{.65\, V}{(1.55\, m)\,(11.22)} = .0374\ V/m$$

According to Nanevicz (see Figure 3.5) and based on a receiving bandwidth of 4 MHz in the 60 MHz region, lightning discharges at a distance of 10 km are capable of creating local transient electric fields of anywhere from .04 to 2 V/m.[48] By varying the distance, this also means they are capable of creating local transient electric fields of .08 to 4 V/m at 5 km, .02 to 1 V/m at 20 km, and .01 to .5 V/m at 40 km, etc. The point here is that due to the size of the fields involved and the low VHF triggering threshold of .65 V, transients radiated by lightning as well as small magnitude local discharges were large enough in magnitude to easily trigger the oscilloscope and be recorded. Also important was the fact that the trigger was still set high enough to disregard emissions associated with daily atmospheric noise levels.

4.3.3 LF Data Collection System Triggering Threshold

The LF Data Collection System gain, G_T, was 0.010 as computed in Appendix D. As before, this result was used to calculate the magnitude of the minimum electric field required (at the LF antenna) to cause the waveform analyzer to trigger at .25 V as follows:

$$\frac{threshold}{h_e\, G_T} = \frac{.25\, V}{(6.99\, m)\ (.010)} = 3.58\ V/m$$

Lightning discharges at a distance of 10 km are capable of creating transient local electric fields of 20 V/m based on a receiving bandwidth of 200 kHz in the 100 kHz region as seen in Figure 3.5.[48] This means by varying the distance, they are also capable of creating local transient electric fields of 40 V/m at 5 km, 10 V/m at 20 km, and 5 V/m at 40 km, etc. Therefore, transients from lightning discharges were able to trigger the LF data collection system even if more than 40 km away from the antenna. More importantly, the trigger was still set high enough to disregard the relatively high ambient noise levels in the LF region.

4.4 Pilot Study

The pilot study from 1-24 Jul 1991 accomplished many essential objectives before the main study could begin.

- Selected Operating Frequencies and Bandwidths

  The specific VHF and LF bandwidths were chosen by using a spectrum analyzer. The 4 MHz bandwidth centered at 63 MHz was relatively free from interference and therefore selected as the VHF transient reception channel. The main reason for the lack of interference in the 60-66 MHz range was that this bandwidth was Channel 3 and not used for television broadcast in the Boston area.

In the LF bandwidth, there was much more signal interference activity due to atmospheric noise, Loran, and public service communications. Because of the relatively high field magnitudes associated with lightning in this bandwidth, a 200 kHz bandwidth centered at 100 kHz and a high triggering threshold (previously discussed) were chosen for LF transient reception.

- Acquired and Set-Up Instrumentation

  1. A quarter wavelength vertical antenna designed for 63 MHz was installed.
  2. 85 m of 75 Ω RG-11/U cable was used to connect the VHF antenna to the receiver.
  3. For parts of the pilot study and as a backup VHF receiver, a Zenith color television tuned to channel 3 with an injected carrier signal from the Digital IC Color Generator was employed for VHF reception.
  4. For VHF reception during the main study, an Airborne Instruments Laboratory Precision Test Receiver tuned to 63 MHz was utilized.
  5. The VHF video data from the receiver had a baseband bandwidth of 4-5 MHz and was passed to a HP 54510A Digitizing Oscilloscope set up with a 50 MHz sampling rate and a .65 V single shot trigger.
  6. A short vertical monopole antenna was installed for LF reception.
  7. 73 m of 75 Ω RG-11/U cable was used to connect the antenna to the anti-aliasing low pass filter with a cutoff of 200 kHz.
  8. From the LPF, the signal then passed to an Analogic Data Precision Data 6100 Waveform Analyzer set up with a 1 MHz sampling rate and .25 V single shot trigger.
  9. An HP Vectra Computer was installed with HP-IB software to control the oscilloscope and waveform analyzer and data transfers.
  10. Programs were written in Basic to operate and setup instrumentation and control data transfers (see Appendix E).
  11. A lightning ground protection system was installed to shunt a direct lightning strike to the equipment.
  12. A Sola Harmonic Neutralized Transformer was used to power the receiver, oscilloscope, and waveform analyzer to eliminate equipment triggering from power line voltage transients.

- Tested Data Collection Systems

  1. By using a local oscillator and a dipole antenna, signals transmitted in the LF and VHF regions were correctly detected by each receiver respectively.
  2. By using a static generator, locally radiated transients were detected and caused both data systems to trigger.

3. To ensure the system would provide 24 hour coverage, the data collection systems were operated for days at a time. The resulting data was analyzed to determine normal-day ambient activity in order to set triggering thresholds for the main study.
4. Fixed and variable trigger settings (to adjust for lower noise conditions at night) were tested. The intent was to determine the ambient noise levels in order to ensure that the main study's trigger values were low enough to detect lightning activity, but high enough to avoid ambient noise levels.
5. The system was operated during at least two thunderstorms with confirmed lightning activity to ensure that the equipment could operate and collect meaningful data.

4.5 Main Study

The main study began 18 Aug 91 and ended 24 Nov 91. The VHF and LF data collection systems were set up to run continuously in order to monitor atmospheric conditions.

- Specific Procedures

1. The computer was set up as a controller for the oscilloscope and waveform analyzer operations and to coordinate the data transfers via HP-IB protocols.
2. The HP digitizing oscilloscope was set up with a 50 MHz sampling rate (a 20 ns period), in a single shot triggering mode with a trigger threshold of .65 V (zero to peak), and to acquire the first 8000 data points immediately after triggering. Once adjusted, the oscilloscope sampled input signal magnitudes constantly and when it triggered, 160 μs of data was available for analysis.
3. The Analogic waveform analyzer was configured with a 1 MHz sampling rate (a 1 μs period), in a single shot triggering mode, with a trigger threshold of .25 V (zero to peak), and to acquire the first 1000 points after triggering. Once set up, the waveform analyzer monitored input signal magnitudes constantly and when it triggered, 1 ms of data was available for analysis.
4. When the magnitude of either input signal was greater than the trigger level, the respective device (oscilloscope or waveform analyzer) triggered and sent a "I have triggered !" message to the computer indicating that it had triggered causing the computer to record the time.
5. The triggered device measured the maximum peak value of the transient and then relayed this quantity to the computer.
6. Next, the computer reset the triggered device to start sampling its input signal again and then queried the other device to see if it had also captured a transient.

7. If the other device had also triggered, it measured the maximum peak of its transient and sent this value to the computer, which then would reset the device to start sampling its input signal again.
8. If the other device had not triggered, then the computer merely recorded an amount equal to the respective device's triggering threshold.
9. Lastly, the computer wrote the two data values and time to a hard disk file and example of one such file can be seen in Table 4.1. It then waited for the next device to send a "I have triggered !" message to start the process over again.

- Related Procedures

1. Because it was possible for the equipment to run for hours without ever capturing a transient, the computer reset the oscilloscope and waveform analyzer every three minutes during inactive periods to ensure that they were operating correctly.
2. The equipment was operated many days in order to collect enough data to characterize transient activity during various types of weather conditions.
3. The weather forecasts were monitored to ensure equipment was operating during predicted thunderstorms days.
4. Local surface weather observations that could confirm or deny the existence of lightning activity within the local area were collected.
5. Daily data records of atmospheric activity were downloaded from the computer periodically.

4.6 Data Collection

During the pilot study, the largest zero to peak value and time of occurrence of VHF transients were recorded each 10 s interval to a computer file. This data allowed determination of trigger thresholds and amounted to 8640 (24x60x6) data points per day.

The data collection system during the main study was refined to reduce the size of resulting data files and analysis. As discussed, data samples were only recorded when either the oscilloscope and/or waveform analyzer triggered. Moreover, only one data point (either the transient's peak value or channel trigger threshold) per channel and the respective time were recorded for each trigger. A computer data record for a hypothetical day (with the only activity that day occurring between 0919 and 0925) is shown in Table 4.1.

4.7 Treatment of Data

Data records representing the pilot study's VHF activity were already condensed into maximum transient activity each 10 s interval. This data was then summed into

Table 4.1: Example Day Computer Data Record

Time (hh:mm:ss)	*VHF Peak* (volts)	*LF Peak* (volts)
09:19:24	.65	.37
09:20:17	1.15	.25
09:20:20	.91	.25
09:20:24	.87	.25
09:20:28	1.12	.25
09:20:32	1.12	.25
09:20:35	1.12	.25
09:20:39	.87	.25
09:20:43	1.08	.25
09:20:47	.94	.25
09:20:51	.94	.25
09:20:54	1.26	.25
09:20:58	1.05	.25
09:21:02	1.08	.25
09:21:06	.94	.25
09:21:10	1.22	.25
09:21:13	1.64	.25
09:21:17	.94	.25
09:21:21	.98	.25
09:22:36	.87	.25
09:22:40	.65	.29
09:22:45	.91	.25
09:22:53	.65	.40
09:24:34	.65	.42

values for each 1 minute interval and plotted versus time.

For the main study, daily data records of transient activity like the example in Table 4.1 were condensed into quantities representing the sum of all transient activity that had occurred at each frequency respectively during a 1 minute interval. For example, the data record in Table 4.1 would be consolidated into 1 minute intervals as depicted in Table 4.2. The trigger values of .65 V and .25 V were ignored in the computation of these sums because they indicated that no transient activity had occurred in the respective channel when queried by the computer. This procedure resulted in 2 arrays (1 for each frequency) of 1440 (24x60) points as seen in Table 4.2. Next, both set of data points were plotted on the same graph versus their common metric of time and called "Minute Interval Summaries".

The time period of the study was divided into four categories (clear, overcast, precipitation, and lightning) depending on the most intense weather observations

Table 4.2: Example Day Minute Interval Summary

Time Interval (hh:mm)	*Minute Index*	*VHF Activity* (volts)	*LF Activity* (volts)
00:00 - 00:01	0	0	0
...	...	...	...
09:18 - 09:19	558	0	0
09:19 - 09:20	559	0	.37
09:20 - 09:21	560	12.43	0
09:21 - 09:22	561	6.8	0
09:22 - 09:23	562	1.78	.69
09:23 - 09:24	563	0	0
09:24 - 09:25	564	0	.42
09:25 - 09:26	565	0	0
...	...	...	...
23:59 - 24:00	1439	0	0

reported during that interval. These daily "Minute Interval Summary" plots and the weather reports were used to characterized the VHF, LF, and correlated VHF- LF transient activity for each weather category. Activity during clear periods were used to identify non-lightning days and for the development of an ambient day conditions baseline. This baseline was then used to eliminate daily interference patterns from the plots.

Periods of correlated transient activity during certain intense precipitation and all reported lighting intervals were enlarged and plotted in "Minute-Interval Activity Period" graphs. These graphs were then examined to determine how much earlier the VHF activity began before the LF activity.

4.8 Delimitations and Limitations of the Study

DELIMITATIONS

- Time length of study was limited to Summer-Fall 91.
- Geographic area was limited to local area (within 50 km or 30 miles).
- Only used one LF and one VHF receiver.
- Antennas were nondirectional in azimuth.
- The data values acquired were limited to transient maximums.

LIMITATIONS

- Determining when natural lightning would occur to ensure that the data collection equipment was turned on.
- The choice of frequencies was limited due to man-made interference.
- There was no immediate access to lightning locating or confirmation equipment.

Chapter 5

Findings

5.1 The Procedure

The main study began with a trial run on 18 Aug 91 and was able to record transients emitted during Hurricane Bob the next day. However, the hurricane's high winds eventually removed the antennas and delayed the next start until late August. From 30 Aug 91 through 13 Oct 91, the data collection equipment monitored the atmospheric conditions continuously and triggered on transients when they occurred. For the rest of October and parts of November, the equipment was only operational during periods of possible precipitation or thunderstorms. Due to the seasonal decrease of thunderstorm activity in New England during the fall and winter, 24 Nov 91 was the last day that data was recorded. By the end of the main study period, a total of 56 days of data had been collected.

Using the data treatment methods discussed in the Design chapter, the transient activity was condensed and plotted versus time. The resulting daily graphs were called **Minute Interval Summary** plots and are included in Appendix A. Individual time periods of the "Minute Interval Summaries" were then divided into one of four groups depending on the prevailing weather conditions during that period. The first group was composed of transient data captured when the weather was described as clear or the sky as having scattered or broken cloud cover. Atmospherics measured while the sky was reported as being overcast or hazy made up the second category. The third classification consisted of transient data collected during periods of drizzle, rain, or rain showers. The important distinction with this third group was that no observations of lightning or thunder had been annotated during the respective precipitation. The final category was made up of transient data recorded during time intervals of reported lightning (intracloud, cloud-ground, or cloud-cloud) and thunderstorm activity.

In order to differentiate the four weather periods, surface observations from local weather stations were obtained. These reports were studied to condense the many measurements and observations into entries that represent the most severe weather conditions that existed during each interval. Particular emphasis was placed on utilizing weather observations from Logan International Airport in Boston due to its geographic proximity to the data collection equipment located in Medford, MA.

These condensed weather observations are located in Appendix C.

With the weather periods separated, the overall transient activity during each of the four weather groups was characterized. By analyzing specific time periods (listed in the condensed weather reports) of the "Minute Interval Summaries", the total number of minute intervals in which VHF, LF, and correlated VHF-LF transient activity had occurred was determined. **Average Activity per Hour** amounts were calculated by dividing the transient totals by the number of hours that the particular type of weather was observed. The **Increase Over Ambient** amounts reflected the relative increase in transient activity above levels (see bottom row of Table 5.2) computed for the "clear" or "ambient " weather conditions group.

5.1.1 Clear or Scattered Cloud Cover Periods

During weather periods reported as clear or having scattered cloud cover, the transient activity was minimal. More importantly, the activity that existed was relatively uncorrelated at both frequencies as seen in column 6 of Tables 5.1 and 5.2. There were some examples of significant activity intervals like the VHF data recorded on 20 Oct 91 or LF data on 10 Sep 91, but overall this type of behavior was rare. Because the test equipment was located in an urban area, there were many sources of noise to contend with. Fortunately, the interference from these sources was usually emitted in only one of the bandwidths which implied that lightning discharges were probably not responsible for these atmospherics. Additionally, relatively high triggering thresholds were utilized to also minimize the probability of equipment triggering on interference.

Table 5.1: Clear and Scattered Cloud Cover RF Activity

Date 1991	*Refer To Figure*	*Time Interval*	*Number of Minute Intervals with Transient Activity at*		
			VHF	*LF*	*VHF and LF*
31 Aug	A.3	1030-2400	0	0	0
01 Sep	A.4	0000-2400	8	0	0
02 Sep	A.5	0000-2400	50	0	0
03 Sep	A.6	0000-2400	16	0	0
04 Sep	A.7	0000-0750	1	0	0
06 Sep	A.9	1422-2250	11	1	0
07 Sep	A.10	0450-2400	39	2	0
08 Sep	A.11	0000-2400	15	1	0
09 Sep	A.12	0000-1650	13	2	0
10 Sep	A.13	0000-1650	11	165	4

Table 5.2: Clear and Scattered Cloud Cover RF Activity (cont)

Date 1991	*Refer To Figure*	*Time Interval*	*Number of Minute Intervals with Transient Activity at*		
			VHF	*LF*	*VHF and LF*
11 Sep	A.14	0251-2400	16	1	0
12 Sep	A.15	0000-2400	23	0	0
13 Sep	A.16	0000-2400	30	8	0
17 Sep	A.19	1251-1324	0	0	0
17 Sep	A.19	1400-2210	7	16	0
20 Sep	A.21	1951-2400	7	0	0
21 Sep	A.22	0000-2400	39	0	0
22 Sep	A.23	0000-2400	13	0	0
23 Sep	A.24	0000-0350	0	1	0
26 Sep	A.27	1518-2400	8	4	0
27 Sep	A.28	0000-2400	7	0	0
28 Sep	A.29	0000-2400	1	1	0
29 Sep	A.30	0000-1530	2	1	0
29 Sep	A.30	1556-2400	2	12	1
30 Sep	A.31	0000-2400	18	3	0
01 Oct	A.32	0000-0400	0	2	0
02 Oct	A.33	0000-2400	8	47	0
03 Oct	A.34	1600-2400	6	7	0
04 Oct	A.35	0000-2400	4	24	0
07 Oct	A.37	0200-1200	1	1	0
07 Oct	A.37	1700-2400	4	0	0
08 Oct	A.38	0000-2400	10	1	0
09 Oct	A.39	0000-1100	2	0	0
10 Oct	A.40	0200-0600	0	0	0
10 Oct	A.40	1400-2400	7	0	0
11 Oct	A.41	0000-1300	0	1	0
12 Oct	A.42	1600-2400	2	9	0
13 Oct	A.43	0200-1400	1	9	0
19 Oct	A.46	0000-2400	12	2	0
20 Oct	A.47	0000-2400	119	0	0
21 Oct	A.48	0000-0500	2	0	0
30 Oct	A.49	0000-0400	0	0	0
Totals		633 hours	515	321	5
Average Per Hour			.814	.507	.008

By using the periods of data identified in Tables 5.1 and 5.2, a plot was constructed which represented the daily ambient levels of interference and atmospheric noise in the VHF and LF bandwidths. The resulting plot in Figure 5.1 shows the relative levels of transient activity for the "clear" or "ambient" days. The increased periods of VHF activity around 0700, 1100, and 1500-1830 were probably due to ignition noise from automobiles in rush hour traffic or starting in nearby parking lots when classes ended. The plot also shows that LF transient activity occurred evenly at all hours of the day. However, the data did not show any examples where there was significant daily activity at any one time.

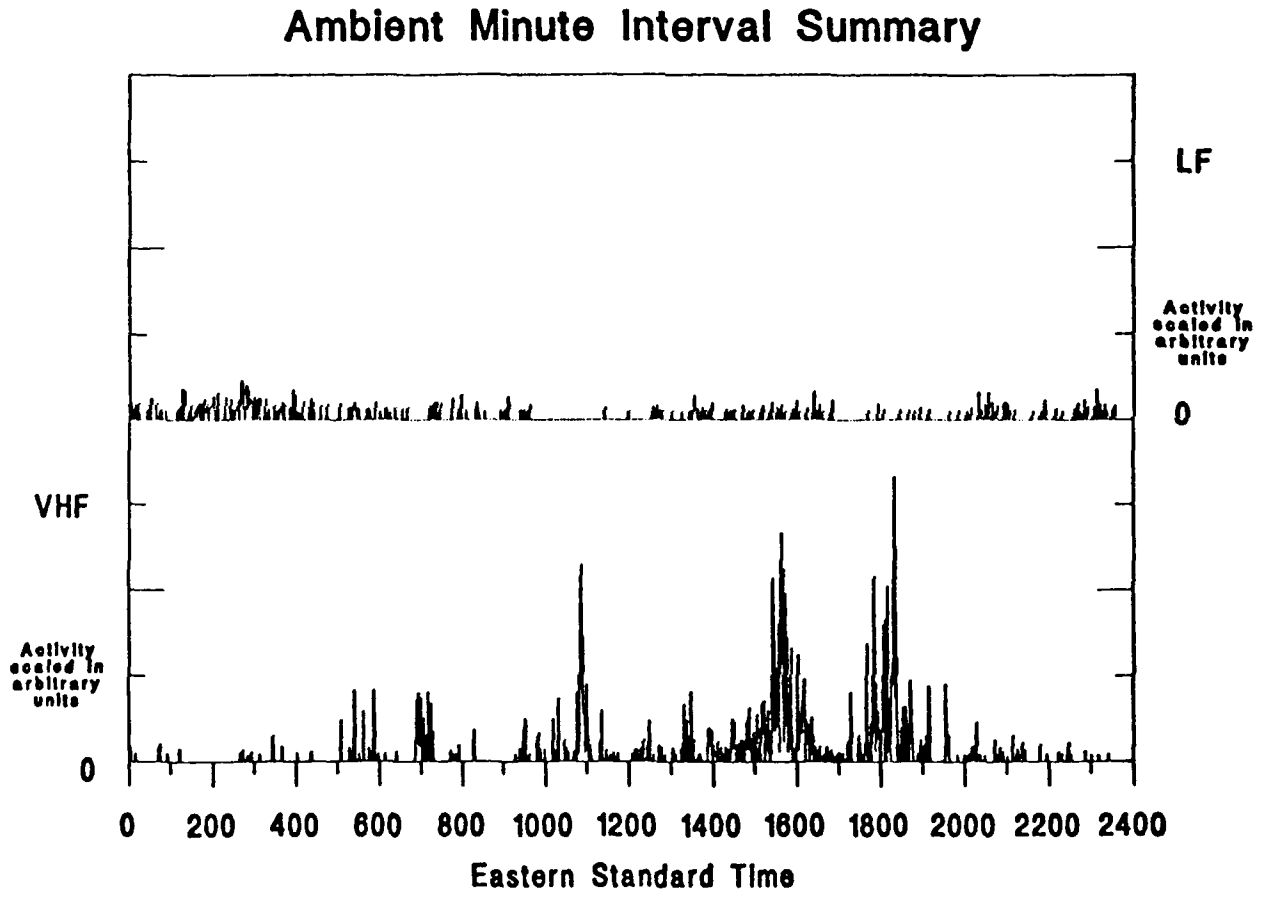

Figure 5.1: Plot of Ambient Activity

5.1.2 Overcast Sky Periods

Data collected during overcast and hazy sky periods showed a two to four times increase in each type of average transient activity per hour over levels measured during "ambient" weather spans. These results are presented in Tables 5.3 and 5.4. The increase in activity during these frontal movements was a surprise and possibly caused by corona point discharges occurring as charged clouds passed over the test location. In addition, small intracloud discharges from developing thunderstorm cells moving through the local area may have also been responsible for the expanded activity.

Table 5.3: Overcast and Hazy Sky RF Activity

Date 1991	*Refer To Figure*	*Time Interval*	*Number of Minute Intervals with Transient Activity at*		
			VHF	*LF*	*VHF and LF*
30 Aug	A.2	0000-2400	53	20	2
31 Aug	A.3	0000-0757	0	0	0
04 Sep	A.7	0750-2400	17	18	0
05 Sep	A.8	1452-2400	8	1	0
06 Sep	A.9	0000-1421	5	4	0
06 Sep	A.9	2251-2400	0	0	0
07 Sep	A.10	0000-0450	0	2	0
09 Sep	A.12	1651-2400	25	92	8
10 Sep	A.13	1651-2400	4	42	0
11 Sep	A.14	0000-0250	0	2	0
14 Sep	A.17	0000-0242	0	0	0
14 Sep	A.17	1221-2400	23	6	1
16 Sep	A.18	0000-0340	0	6	0
16 Sep	A.18	1106-2400	10	8	0
17 Sep	A.19	0000-1219	0	30	0
19 Sep	A.20	0000-1203	0	0	0
20 Sep	A.21	0931-1950	3	19	0
23 Sep	A.24	0600-1219	0	0	0
23 Sep	A.24	1551-2400	9	0	0
24 Sep	A.25	0000-2342	8	1	0
26 Sep	A.27	1349-1517	0	1	0
01 Oct	A.32	0400-1200	0	4	0
01 Oct	A.32	1400-2400	10	30	0
03 Oct	A.34	0000-1400	7	9	0
06 Oct	A.36	0000-0630	0	24	0
06 Oct	A.36	1955-2400	1	44	0
07 Oct	A.37	0000-0200	0	1	0

Table 5.4: Overcast and Hazy Sky RF Activity (cont)

Date 1991	*Refer To Figure*	*Time Interval*	*Number of Minute Intervals with Transient Activity at*		
			VHF	*LF*	*VHF and LF*
07 Oct	A.37	1200-1700	4	0	0
09 Oct	A.39	1100-2400	14	2	0
10 Oct	A.40	0000-0200	0	0	0
10 Oct	A.40	0600-1400	4	3	0
11 Oct	A.41	1300-2000	9	13	0
12 Oct	A.42	0800-1600	7	0	0
13 Oct	A.43	0000-0200	0	2	0
13 Oct	A.43	1400-2400	171	0	0
17 Oct	A.44	0000-1300	16	3	1
18 Oct	A.45	0800-2400	24	3	0
21 Oct	A.48	0500-2400	154	0	0
30 Oct	A.49	0400-1300	2	1	0
01 Nov	A.51	1800-2400	0	9	0
02 Nov	A.52	0700-2400	0	128	0
21 Nov	A.53	0000-0700	3	0	0
23 Nov	A.55	0200-2400	77	2	0
24 Nov	A.56	1800-2400	0	0	0
Totals		415 hours	668	530	12
Average Per Hour			1.61	1.28	.029
Increase Over Ambient			2.0x	2.5x	3.6x

5.1.3 Precipitation Periods

The amount of VHF and LF transient activity per hour also increased two to four times during precipitation periods as seen in Table 5.5. More importantly in terms of this research was the fact that the number of minute intervals with correlated VHF-LF transients per hour increased by over 15 times the level determined for "ambient" weather conditions. Even though the data periods of 5 Sep, 19 Sep, 25 Sep, 6 Oct, 18 Oct, 1 Nov, 21 Nov, and 24 Nov were recorded during moderate rain conditions, significant transient activity was present. The correlated transients were most likely caused by local intracloud lightning discharges that were not observed by any of the weather stations.

Table 5.5: Rain and Rain Shower RF Activity

Date 1991	*Refer To Figure*	*Time Interval*	*Number of Minute Intervals with Transient Activity at*		
			VHF	*LF*	*VHF and LF*
31 Aug	A.3	0758-0814	0	0	0
05 Sep	A.8	0000-0300	23	30	4
05 Sep	A.8	0600-1451	7	9	0
14 Sep	A.17	0242-1220	8	0	0
16 Sep	A.18	0341-1105	0	1	0
17 Sep	A.19	1220-1250	0	0	0
17 Sep	A.19	1325-1400	0	0	0
19 Sep	A.20	1204-1230	0	0	0
19 Sep	A.20	1456-2400	20	32	2
20 Sep	A.21	0000-0930	2	17	0
23 Sep	A.24	0351-0559	0	0	0
23 Sep	A.24	1220-1550	3	0	0
24 Sep	A.25	2343-2400	0	0	0
25 Sep	A.26	0000-0929	28	9	2
25 Sep	A.26	1246-2400	8	117	2
26 Sep	A.27	0000-1348	0	67	0
29 Sep	A.30	1531-1555	0	1	0
01 Oct	A.32	1200-1400	0	0	0
03 Oct	A.34	1400-1600	3	2	0
06 Oct	A.36	0630-1856	10	39	4
11 Oct	A.41	2000-2400	0	14	0
12 Oct	A.42	0000-0800	4	0	0
17 Oct	A.44	1300-2400	51	0	0
18 Oct	A.45	0000-0800	49	5	5
30 Oct	A.49	1300-2400	19	0	0
31 Oct	A.50	0430-2400	4	32	0
01 Nov	A.51	0000-1800	29	26	4
02 Nov	A.52	0000-0700	0	3	0
21 Nov	A.53	0700-2300	6	1	0
22 Nov	A.54	0000-2400	80	13	2
24 Nov	A.56	0000-1800	18	15	6
Totals		251 hours	372	433	31
Average Per Hour			1.48	1.73	.124
Increase Over Ambient			1.8x	3.4x	15.5x

5.1.4 Lightning Periods

The results collected during periods of confirmed lightning discharge and/or thunderstorm weather indicated a significant increase in VHF and LF transient activity as seen in Table 5.6. In fact, the number of minute intervals of transients at both frequencies per hour grew to a value 19-20 times the level calculated for "ambient" weather conditions. More impressive was the fact that the number of minute intervals with correlated transients per hour increased to 500 times the "ambient" level. Due to lightning's wideband transient emission nature, the significant increases in correlated activity were attributed to return strokes and recoil streamer.

Table 5.6: Lightning and Thunderstorm RF Activity

Date 1991	*Refer To Figure*	*Time Interval*	*Number of Minute Intervals with Transient Activity at*		
			VHF	*LF*	*VHF and LF*
19 Aug	A.1	0640-1920	314	39	34
31 Aug	A.3	0815-1030	15	13	11
05 Sep	A.8	0300-0600	34	60	15
17 Sep	A.19	2210-2400	0	81	0
19 Sep	A.20	1230-1455	7	7	2
25 Sep	A.26	0930-1245	57	55	32
06 Oct	A.36	1856-1955	12	24	6
31 Oct	A.50	0000-0430	22	8	6
21 Nov	A.53	2300-2400	28	7	5
23 Nov	A.55	0000-0200	49	29	25
Totals		34 hours	538	323	136
Average Per Hour			15.8	9.50	4.00
Increase Over Ambient			19.4x	18.7x	500x

5.2 Evidence that Supports Hypothesis

Characterization of the four weather groups demonstrated that the increased correlated transient activity recorded during certain periods of precipitation and confirmed intervals of lightning were most likely caused by lightning discharges and not by noise or interference that also existed during "ambient" weather conditions. Based on this assumption, time intervals of correlated VHF-LF activity measured during precipitation, thunderstorm, and lightning periods were enlarged and plotted versus time. These expanded plots clearly showed when the VHF transient activity started in relation to LF transient activity as well as just how many minutes earlier the VHF preceded the LF data. These various expanded graphs were termed **Minute-Interval Activity Period** plots and can be found in Appendix B.

There were two types of predominate results discovered during periods of correlated VHF-LF transient activity. Both groups possessed time spans of significant VHF transient activity before the LF transients began or were detected. Similarly, each group unquestionably displayed the periods of significant correlated activity which were most likely caused by return strokes or recoil streamers. However, the groups differed in their initial VHF behavior. In the majority of instances, which are presented in Table 5.7, initial VHF transients were detected and continued to occur until the LF transient activity began. Then both types of activity occurred in unison at various times for the next one to two minutes. For this "Continuous VHF" group, the VHF transient activity originated on the average at least 3 minutes before the correlated VHF-LF transient activity started.

Table 5.7: Continuous VHF Transient Activity During Precipitation and Lightning Periods

Date 1991	*Refer To Figure*	*Time of Initial Transient Activity at*		*VHF Precursor Lead Time (Minute(s))*
		VHF	*LF*	
19 Aug	B.1	0753	0800	7
19 Aug	B.1	0804	0809	5
19 Aug	B.2	1207	1209	2
19 Aug	B.3	1509	1511	2
19 Aug	B.3	1513	1518	5
31 Aug	B.4	0848	0849	1
05 Sep	B.7	0128	0132	4
05 Sep	B.7	0205	0207	2
05 Sep	B.8	0421	0425	4
05 Sep	B.8	0438	0440	2
05 Sep	B.8	0517	0518	1
19 Sep	B.10	1411	1412	1
19 Sep	B.10	1422	1425	3
19 Sep	B.10	1446	1448	2
19 Sep	B.11	2304	2308	4
19 Sep	B.11	2345	2347	2
25 Sep	B.12	1005	1010	5
25 Sep	B.12	1021	1025	4
25 Sep	B.12	1043	1045	2
25 Sep	B.12	1051	1052	1
25 Sep	B.12	1100	1101	1
25 Sep	B.13	1119	1122	3
25 Sep	B.13	1130	1131	1
06 Oct	B.14	0919	0921	2
06 Oct	B.15	1903	1904	1
06 Oct	B.15	1909	1911	2
31 Oct	B.18	0403	0406	3
01 Nov	B.19	0038	0042	4
21 Nov	B.20	2340	2347	7
22 Nov	B.21	1014	1015	1
22 Nov	B.21	1038	1044	6
22 Nov	B.22	1740	1743	3
23 Nov	B.23	0016	0024	8
23 Nov	B.23	0033	0039	6
23 Nov	B.23	0049	0050	1
23 Nov	B.23	0055	0057	2
24 Nov	B.24	0755	0758	3

For the second group of correlated transient results, which are summarized in Table 5.8, the initial VHF transient activity occurred for a while and then stopped. There was a brief silence in both bandwidths and then the VHF would restart in conjunction with the onset of the initial LF transient activity. Again, both types of activity occurred together in unison for a brief period. The initial VHF activity during this "Two Step VHF" group originated on the average at least 11 minutes before the joint VHF-LF transient activity began.

Table 5.8: Two Step VHF Transient Activity During Precipitation and Lightning Periods

Date 1991	*Refer To Figure*	*Time of Initial Transient Activity at*		*VHF Precursor Lead Time (Minute(s))*
		VHF	*LF*	
19 Aug	B.2	1202	1209	9
19 Aug	B.3	1502	1511	9
05 Sep	B.7	0138	0147	9
05 Sep	B.7	0155	0207	12
05 Sep	B.8	0416	0419	3
19 Sep	B.11	2338	2347	9
06 Oct	B.14	0900	0921	21
18 Oct	B.16	0334	0352	18
31 Oct	B.17	0218	0222	4
31 Oct	B.18	0334	0342	8
01 Nov	B.19	0051	0107	16
21 Nov	B.20	2305	2315	10
22 Nov	B.21	1028	1044	16

5.3 Evidence that Does Not Support Hypothesis

There were also some examples of recorded correlated transient activity in which the VHF transient activity did not start at least 1 minute or more before the joint VHF-LF activity began. These results are illustrated in Table 5.9 and were probably caused by subsequent return strokes. The data results collected after 2200 on 17 Sep 91 were particularly interesting for they may represent the detection of intracloud lightning (as reported by N.A.S. South Weymouth) at a distance quite far away. The absence of any correlated VHF activity indicates that the lightning was probably too far away for the VHF signals to exceed the triggering threshold.

Table 5.9: RF Activity Without VHF Transient Precursors

Date 1991	*Refer To Figure*	*Time of Initial Transient Activity at VHF*	*Time of Initial Transient Activity at LF*	*VHF Precursor Lead Time (Minute(s))*
31 Aug	B.4	0842	0842	0
31 Aug	B.5	1020	1020	.5
17 Sep	B.9	N/A	2210	0
19 Sep	B.10	N/A	1416	0
25 Sep	B.13	1136	1136	0
06 Oct	B.14	N/A	0925	0
18 Oct	B.16	0352	0352	.6
31 Oct	B.18	0348	0348	.7

5.4 Summary Of What Was Found

- "Clear" or "ambient" weather periods were characterized as having relatively very little VHF and LF and hardly any correlated VHF-LF transient activity per hour.
- Intervals with overcast skies exhibited a two to four times increase in VHF, LF, and correlated VHF-LF transient activity per hour.
- Durations of precipitation also exhibited a two to four times increase in VHF and LF transient activity and a 15.5 times increase in correlated VHF-LF transient activity.
- Weather periods reporting lightning discharges and thunderstorm activity demonstrated a 19-20 times increase in VHF and LF transient activity. More significantly, the amount of correlated VHF-LF transient activity per hour drastically increased to 500 times the "ambient" levels.
- Time spans of "Continuous VHF" correlated transient activity illustrated that VHF transients were emitted an average of at least 3 minutes before correlated VHF-LF activity was detected.
- In some cases,which are identified in this study as "Two Step VHF" correlated transient activity, VHF transients initially were radiated an average of at least 11 minutes before the first joint VHF-LF transient activity was measured.

Chapter 6

Conclusions and Implications

6.1 Conclusions

The results of this research showed that "clear" or "ambient" weather periods possessed relatively very little VHF or LF and hardly any correlated VHF-LF transient activity per hour. This finding makes sense due to the lack of any significant mechanisms like lightning which radiate transients in both bandwidths.

Intervals of overcast skies and light precipitation exhibited a two to four times increase above "ambient" levels in VHF and LF transient activity per hour. This small increase was most likely caused by corona point discharges as the earth's electrostatic field conditions changed. Unobserved intracloud discharges were probably responsible for the 15.5 times expansion in correlated VHF-LF transient activity per hour while periods of moderate precipitation existed.

Weather periods reporting observed lightning discharges and thunderstorm activity possessed a 19-20 times increase in VHF and LF transient activity. More importantly, the amount of correlated VHF-LF transient activity per hour multiplied to a value 500 times the "ambient" level. Lightning discharges, which are a known source of atmospherics, were judged to be the cause of this drastic increase in correlated transient activity.

The hypothesis question concerning precursors was tested by more closely examining individual time spans of each of the two observed types of correlated transient activity. The "Continuous VHF" type records illustrated that VHF atmospherics were emitted an average of at least 3 minutes before correlated VHF-LF activity was detected. The more rare "Two Step VHF" type data indicated that initial VHF transients were radiated an average of at least 11 minutes before the first joint VHF-LF transient activity was measured.

Based on these results, this research effort concluded that VHF radiation (precursors) was emitted on the average at least 3 minutes or more before correlated VHF-LF transient activity (return strokes or recoil streamers) was measured during known periods of lightning. This initial VHF activity was attributed to discharges that occur throughout the preliminary charge transfer and breakdown processes of lightning. Of course, there were some examples which do not support this statement, but this activity was most likely due to subsequent return strokes.

6.2 Implications

Because VHF was observed with such a substantial lead time before the return stroke or recoil streamer was launched, warning systems based on detection of these VHF precursors could be developed. These systems would better achieve dynamic protection against lightning by operating continuously, concentrating on the local area, and recognizing the preliminary stages of lightning.

The methods utilized in this study might also be used for other potential applications. The detection technique presented lends itself well to systems that require very fine time resolution for lightning waveform analysis. The data collection system was based on utilizing high-sampling rates and low-quantization errors to digitize the transients. The resulting data could then be Fourier transformed to obtain the magnitude and phase of the frequency domain spectrum[48]. Similarly, the use of high-sampling rates is important to lightning locating systems that determine bearing, range, and azimuth from VHF observables emitted by stepped leaders and return strokes. In particular, time delay of arrival and interferometry require measurements with high-time of arrival accuracy to determine phase variations.

6.3 Recommendations

In terms of future work, the results of this study could be enhanced by adding a few capabilities. Lightning location equipment using time delay of arrival or interferometry techniques would help to pinpoint the location of the various transients. This in turn could be used to isolate the weather conditions at the location, or if there might be a source of man-made interference present.

Likewise, the use of local electric field sensors in conjunction with atmospheric techniques would be useful. In particular, during overcast weather periods, one could determine if the magnitude of the earth's local electrostatic field had increased or changed polarity which might explain the rise in transient activity. Another suggestion would involve utilizing a UHF receiver to detect local transients radiated by preliminary discharges along a distance of approximately 10 cm.

An obstacle that affected this research was overcoming the interference limitations imposed by the noisy urban environment. The major disadvantage was that the local noise conditions pushed the VHF triggering threshold up to levels that hindered detection of the more distant small-scale preliminary discharges. The high signal strength of television broadcasts precluded exploiting fully the wide bandwidth capabilities of the digitizing oscilloscope. Elaborate site-specific trapping filters could have significantly improved the VHF sensitivity to atmospherics. In terms of capturing the atmospherics radiated by return strokes and recoil streamers, the external interference was not a problem because the peak magnitudes of these transients at VHF and LF were substantially above the triggering thresholds.

Bibliography

[1] T.E. Allibone. "The Long Spark". In R.H. Golde, editor, *Lightning Volume I :The Physics of Lightning*, pages 231–280. Academic Press, New York, NY, 1977.

[2] C.E. Baum, J.P. O'Neill, E.L. Breen, D.L. Hall, and C.B. Moore. "Electromagnetic Measurement and Location of Lightning". In R.L. Gardner, editor, *Lightning Electromagnetics*, pages 319–346. Hemisphere Publishing Corporation, New York, NY, 1990.

[3] W.H. Beasley. "Positive Cloud-to-Ground Lightning Observations". *Journal of Geophysical Research*, 90:6131–6138, 1985.

[4] W.H. Beasley, M.A. Uman, and P.L. Rustan. "Electric Fields Preceding Cloud-to-Ground Lightning Flashes". *Journal of Geophysical Research*, 87:4883–4902, 1982.

[5] K. Berger. "The Earth Flash". In R.H. Golde, editor, *Lightning Volume I :The Physics of Lightning*, pages 119–191. Academic Press, New York, NY, 1977.

[6] M. Brook and N. Kitagawa. "Radiation from Lightning Discharges in the Frequency Range 400 to 1,000 Mc/s". *Journal of Geophysical Research*, 69:2431–2434, 1964.

[7] M. Brook and T. Ogawa. "The Cloud Discharge". In R.H. Golde, editor, *Lightning Volume I :The Physics of Lightning*, pages 191–229. Academic Press, New York, NY, 1977.

[8] N.J. Burke and D.B. Watson. "Digital Recorder of Lightning Current Waveforms". *IEEE Transactions on Instrumentation and Measurement*, IM-36(3):750–754, September 1987.

[9] N. Cianos, G.N. Oetzel, and E.T. Pierce. "Structure of Lightning Noise-Especially Above HF". In *Lightning and Static Electricity Conference*, Wright-Patterson AFB, OH, December 1972.

[10] N.D. Clarence and D.J. Malan. "Preliminary Discharge Processes in Lightning Flashes to Ground ". *Quarterly Journal of the Royal Meteorological Society*, 83:161–172, 1957.

[11] G.A. Dawson and D.G. Duff. "Initiation of Cloud-to-Ground Lightning Stokes". *Journal of Geophysical Research*, 75:5858–5867, 1970.

[12] R.J. Doviak, D. Sirmans, and D. Zrnic. "Weather Radar ". In E. Kessler, editor, *Instruments and Techniques for Thunderstorm Observation and Analysis*, pages 137–169. University of Oklahoma Press, Norman, OK, second edition, 1988.

[13] R.F. Griffiths and C.T. Phelps. "A Model of Lightning Initiation Arising from Positive Corona Streamer Development ". *Journal of Geophysical Research*, 31:3671–3676,, 1976.

[14] R.F. Griffiths and C.T. Phelps. "The Effects of Air Pressure and Water Vapour Content on the Propagation of Positive Corona Streamers and Their Implications to Lightning Initiation". *Quarterly Journal of the Royal Meteorological Society*, 102:419–426, April 1976.

[15] R.B. Harvey and E.A. Lewis. "Radio Mapping of 250 and 925 MHz Noise Sources in Clouds". *Journal of Geophysical Research*, 78:1944–1947, 1973.

[16] C.O. Hayenga. "Characteristics of Lightning VHF Radiation Near the Time of Return Strokes". *Journal of Geophysical Research*, 89:1403–1410, 1984.

[17] C.O. Hayenga and J.W. Warwick. "Two-Dimensional Interferometric Positions of VHF Lightning Sources". *Journal of Geophysical Research*, 86:7451–7462, 1981.

[18] F. Horner. "Radio Noise from Thunderstorms ". In J.A. Saxton, editor, *Advances in Radio Research*, volume 2, pages 121–215. Academic Press, New York, NY, 1964.

[19] M.M. Kekez and P. Savic. "Laboratory Simulation of the Stepped Leader in Lightning". *Canadian Journal of Physics*, 54(22):2216–2224, November 1976.

[20] N. Kitagawa and M. Brook. "A Comparison of Intracloud and Cloud-to-Ground Lightning Discharges ". *Journal of Geophysical Research*, 65:1189–1201, 1960.

[21] E.L. Kosarev, V.G. Zattespin, and A.V. Mitrofanov. "Ultrahigh Frequency Radiation from Lightning ". *Journal of Geophysical Research*, 75:7524–7530, 1970.

[22] P.R. Krehbiel, M. Brook, and R.A. McCrory. "An Analysis of the Charge Structure of Lightning Discharges to Ground". *Journal of Geophysical Research*, 84:2432–2456, 1979.

[23] P.R. Krehbiel, X.M. Shao, R.J. Thomas, C.T. Rhodes, and C.O. Hayenga. "VHF Radio Interferometry". In *"Conference of VHF Radio Interferometry"*, Socorro, NM, 1990. National Radio Astronomy Observations.

[24] E.P. Krider and R.C. Noggle. "Broadband Antenna Systems for Lightning Magnetic Fields". *Journal of Geophysical Research*, 14:252–256, 1975.

[25] E.P. Krider and G.J. Radda. "Radiation Waveforms Produced by Lightning Stepped Leaders". *Journal of Geophysical Research*, 80:2653–2657, 1964.

[26] E.P. Krider, G.J. Radda, and R.C. Noggle. "Regular Radiation Field Pulses Produced by Intracloud Discharges". *Journal of Geophysical Research*, 80:3801–3804, 1975.

[27] E.P. Krider, C.D. Weidman, and D.M. LeVine. "The Temporal Structure of the HF and VHF Radiation Produced by Intracloud Lightning Discharges ". *Journal of Geophysical Research*, 84:5760–5762, 1979.

[28] E.P. Krider, C.D. Weidman, and R.C. Noggle. "The Electric Fields Produced by Lightning Stepped Leaders". *Journal of Geophysical Research*, 82:951–960, 1977.

[29] G. Labaune, P. Richard, and A. Bondiou. "Electromagnetic Properties of Lightning Channels Formation and Propagation". In R.L. Gardner, editor, *Lightning Electromagnetics*, pages 285–317. Hemisphere Publishing Corporation, New York, NY, 1990.

[30] J. Latham. "The Electrification of Thunderstorms ". *Quarterly Journal of the Royal Meteorological Society*, 107:277–298, 1981.

[31] J. Latham and I.M. Stromberg. "Point-Discharge". In R.H. Golde, editor, *Lightning Volume I :The Physics of Lightning*, pages 99–117. Academic Press, New York, NY, 1977.

[32] M. LeBoulch, J. Hamelin, and C. Weidman. "UHF-VHF Radiation from Lightning". In R.L. Gardner, editor, *Lightning Electromagnetics*, pages 211–255. Hemisphere Publishing Corporation, New York, NY, 1990.

[33] C. Leteinturier and J. Hamelin. "Experimental Study of the Electromagnetic Characteristics of Lightning Discharge in the 200-20M Hz Band". In R.L. Gardner, editor, *Lightning Electromagnetics*, pages 347–363. Hemisphere Publishing Corporation, New York, NY, 1990.

[34] D.M. LeVine. "RF Radiation from Lightning". In *NASA*, Goddard Space Flight Center, Greenbelt, MD, February 1978.

[35] D.M. LeVine. "Sources of the Strongest RF Radiation from Lightning ". *Journal of Geophysical Research*, 85(C7):4091–4095, July 1980.

[36] D.M. LeVine. "The Spectrum of Radiation from Lightning". In *NASA*, Goddard Space Flight Center, Greenbelt, MD, 1981.

[37] D.M. LeVine and E.P Krider. "The Temporal Structure of HF and VHF Radiation During Florida Lightning Return Strokes ". *Geophysical Research Letters*, 4:13–16, 1977.

[38] D.M. LeVine, E.P Krider, and C.D. Weidman. "RF Radiation Produced by Intracloud Lightning Discharges". In *NASA*, Goddard Space Flight Center, Greenbelt, MD, April 1979.

[39] R.M. Lhermitte and E.R. Williams. "Thunderstorm Electrification: A Case Study". *Journal of Geophysical Research*, 90:6071–6078, 1985.

[40] X. S. Liu and P.R. Krehbiel. "The Initial Streamer of Intracloud Lightning Flashes". *Journal of Geophysical Research*, 90:6211–6218, 1985.

[41] L.B. Loebe. "The Mechanism of Stepped and Dart Leaders in Cloud-to-Ground Lightning Strokes ". *Journal of Geophysical Research*, 71:4711–4721, 1966.

[42] L.B. Loebe. "Mechanism of Charge Drainage from Thunderstorm Clouds". *Journal of Geophysical Research*, 75:5882–5889, 1970.

[43] M. Makino and T. Ogawa. "Quantitative Estimation of the Global Circuit". *Journal of Geophysical Research*, 90:5961–5966, 1985.

[44] D.J. Malan. "Radiation from Lightning Discharges and Its Relation to Discharge Processes". In L.G. Smith, editor, *Recent Advances in Atmospheric Electricity*, pages 557–563. Pergamon, New York, NY, 1959.

[45] C.B. Moore and B. Vonnegut. "The Thundercloud". In R.H. Golde, editor, *Lightning Volume I :The Physics of Lightning*, pages 51–97. Academic Press, New York, NY, 1977.

[46] J.P. Moreau. "Characterization of the Electromagnetic Radiation from Lightning during the Preliminary Phases". *European Space Agency*, January 1986.

[47] J.P. Moreau and P.L. Rustan. "A Study of Lightning Initiation Based on VHF Radiation". In R.L. Gardner, editor, *Lightning Electromagnetics*, pages 257–276. Hemisphere Publishing Corporation, New York, NY, 1990.

[48] J.E. Nanevicz, E.F. Vance, and J.M. Hamm. "Observations of Lightning in the Frequency and Time Domains". In R.L. Gardner, editor, *Lightning Electromagnetics*, pages 191–210. Hemisphere Publishing Corporation, New York, NY, 1990.

[49] G.L. Oetzel and E.T. Pierce. "Radio Emissions from Close Lightning". In S.C. Coroniti and J. Hughes, editors, *Planetary Electrodynamics*, pages 543–569. Gordon and Breach, New York, NY, 1969.

[50] T. Ogawa. "Fair-Weather Electricity". *Journal of Geophysical Research*, 90:5951–5960, 1985.

[51] T. Ogawa and M. Brook. "The Mechanism of the Intracloud Lightning Discharge ". *Journal of Geophysical Research*, 69:5141–5150, 1964.

[52] R.E. Orville. "Spectrum of the Lightning Stepped Leader". *Journal of Geophysical Research*, 73:6999–7008, November 1968.

[53] R.E. Orville. "Spectrum of the Lightning Dart Leader". *Journal of Atmospheric Science*, 32:1829–1837, September 1975.

[54] E.T. Pierce. "Atmospherics and Radio Noise". In R.H. Golde, editor, *Lightning Volume I :The Physics of Lightning*, pages 351–384. Academic Press, New York, NY, 1977.

[55] E.T. Pierce. "Spherics and Other Electrical Techniques for Storm Investigations". In E. Kessler, editor, *Instruments and Techniques for Thunderstorm Observation and Analysis*, pages 83–90. University of Oklahoma Press, Norman, OK, second edition, 1988.

[56] E.T. Pierce. "Storm Electricity and Lightning". In E. Kessler, editor, *Thunderstorm Morphology and Dynamics*, pages 277–285. University of Oklahoma Press, Norman, OK, second edition, 1988.

[57] D.E Proctor. "VHF Radio Pictures of Cloud Flashes ". *Journal of Geophysical Research*, 86:4041–4071, 1981.

[58] L.T. Remizov, A.G. Paskaul, and I.V. Oleynikova. "Characteristics of Impulse VLF Atmospheric Radio Noise Near A Thunderstorm ". *Soviet Journal of Communications Technology & Electronics*, 33(2), February 1988.

[59] P. Richard and G. Auffray. "VHF-UHF Interferometric Measurements, Applications of Lightning Discharge Mapping". *Radio Science*, 20(2):171–192, 1985.

[60] P. Richard, A. Delannoy, G. Labaune, and P. Laroche. "Results of Spatial and Temporal Characterization of the VHF-UHF Radiation of Lightning". *Journal of Geophysical Research*, 91:1248–1260, 1986.

[61] W.D. Rust and D.R. MacGorman. "Techniques for Measuring Electrical Parameters of Thunderstorms". In E. Kessler, editor, *Instruments and Techniques for Thunderstorm Observation and Analysis*, pages 91–118. University of Oklahoma Press, Norman, OK, second edition, 1988.

[62] P.L. Rustan. *"Properties of Lightning Derived from Time Series Analysis of VHF Radiation Data"*. PhD thesis, University of Florida, 1979.

[63] P.L. Rustan, M.A. Uman, D.G. Childers, W.H. Beasley, and C.L. Lennon. "Lightning Source Locations from VHF Radiation Data for a Flash at Kennedy Space Center". *Journal of Geophysical Research*, 85:4893–4903, 1980.

[64] X.M. Shao, P.R. Krehbiel, R. Thomas, and C.T. Rhodes. "Observations of Lightning Using VHF Radio Interferometry". In *Conference on Radio Interferometry*, Socorro, NM, 1990. National Radio Astronomy Observations.

[65] L.G. Smith. "Intracloud Lightning Discharges". *Quarterly Journal of the Royal Meteorological Society*, 83:103–111, 1957.

[66] S. Szpor. "Critical Comparison of Theories of Stepped Leaders ". *Archiwum Elektrotechniki*, 26(2):291–300, 1977.

[67] M. Takagi. "Polarization of VHF Radiation from Lightning Discharges ". *Journal of Geophysical Research*, 80:5011–5014, 1975.

[68] P.C. Thum. "A Review of Lightning Stepped Leader Theories". *Jurnal Fakulti Kejuruteraan Universiti Malaya*, 16:27–34, June 1977.

[69] M.A. Uman. "Lightning Return Stroke Electric and Magnetic Fields". *Journal of Geophysical Research*, 90:6121–6130, 1985.

[70] M.A. Uman. *The Lightning Discharge*. Academic Press, Orlando, FL, 1987.

[71] M.A. Uman and D.K. McLain. "Radiation Field and Current of the Lightning Stepped Leader". *Journal of Geophysical Research*, 75:1058–1066, 1970.

[72] C.D. Weidman, J.H. Hamelin, and M. LeBoulch. "Lightning VHF and UHF Emissions and Fast Time Resolved Measurements of the Associated Electric Field Variations". In *10th International Aerospace and Ground Conference on Lightning and Static Electricity*, Paris, France, December 1985.

[73] C.D. Weidman and E.P. Krider. "The Radiation Field Waveforms Produced by Intracloud Lightning Discharge Processes". *Journal of Geophysical Research*, 84:3157–3164, 1979.

[74] C.D. Weidman and E.P. Krider. "Amplitude Spectra of Lightning Radiation Fields in the Interval from 1 to 20M Hz". *Radio Science*, 21(6):964–970, November 1986.

[75] E.R. Williams, M.E. Weber, and R.E. Orville. "The Relationship Between Lightning Type and Convective State of Thunderclouds". *Journal of Geophysical Research*, 94:13213–13220, 1989.

[76] K.L. Zonge and W.H. Evans. "Prestroke Radiation from Thunderclouds ". *Journal of Geophysical Research*, 71:1519–1523, 1966.

Appendix A

Daily Minute Interval Summary Plots

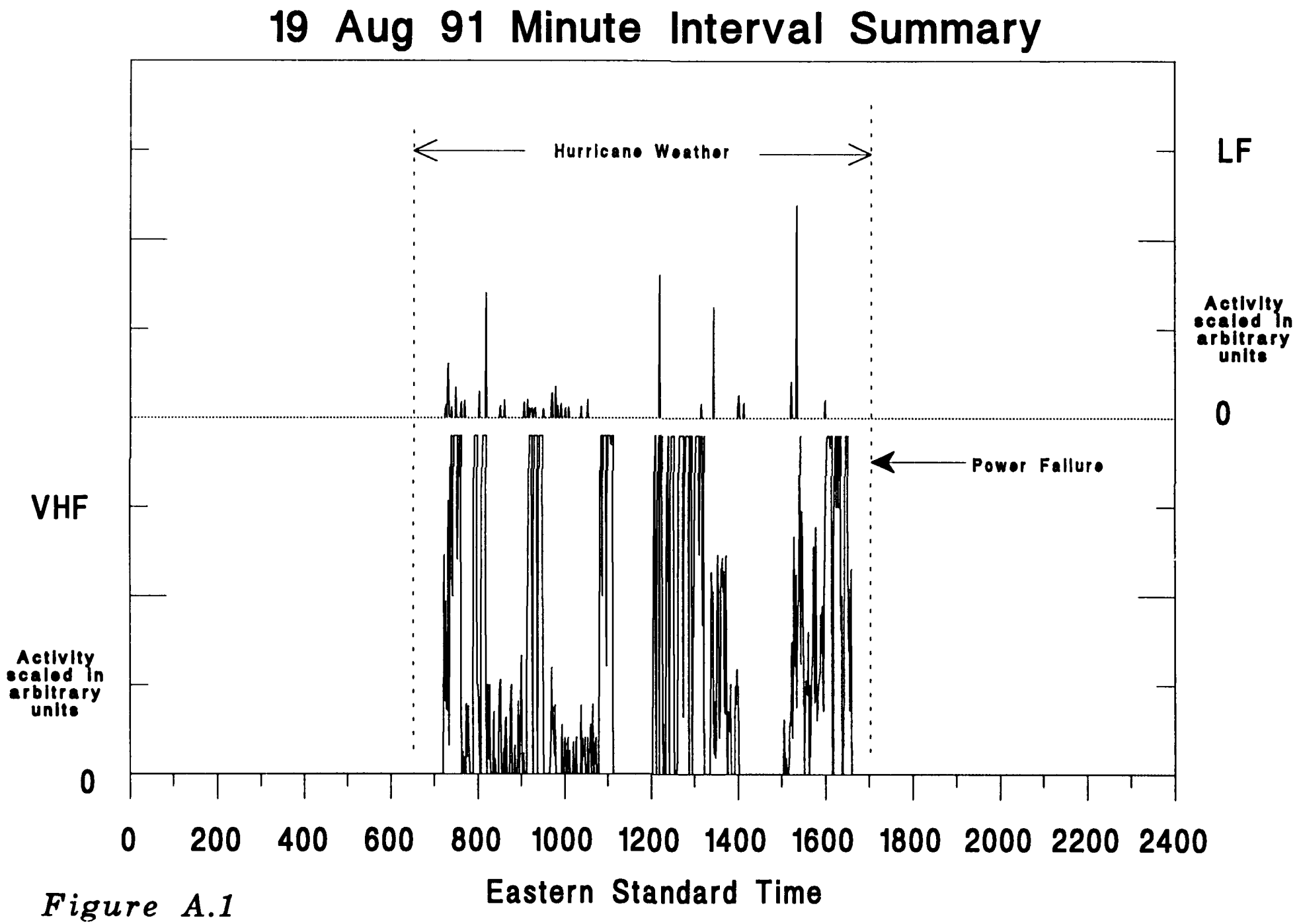
19 Aug 91 Minute Interval Summary
Hurricane Weather
LF
Activity scaled in arbitrary units
0
Power Failure
VHF
Activity scaled in arbitrary units
0
0 200 400 600 800 1000 1200 1400 1600 1800 2000 2200 2400
Eastern Standard Time

Figure A.1

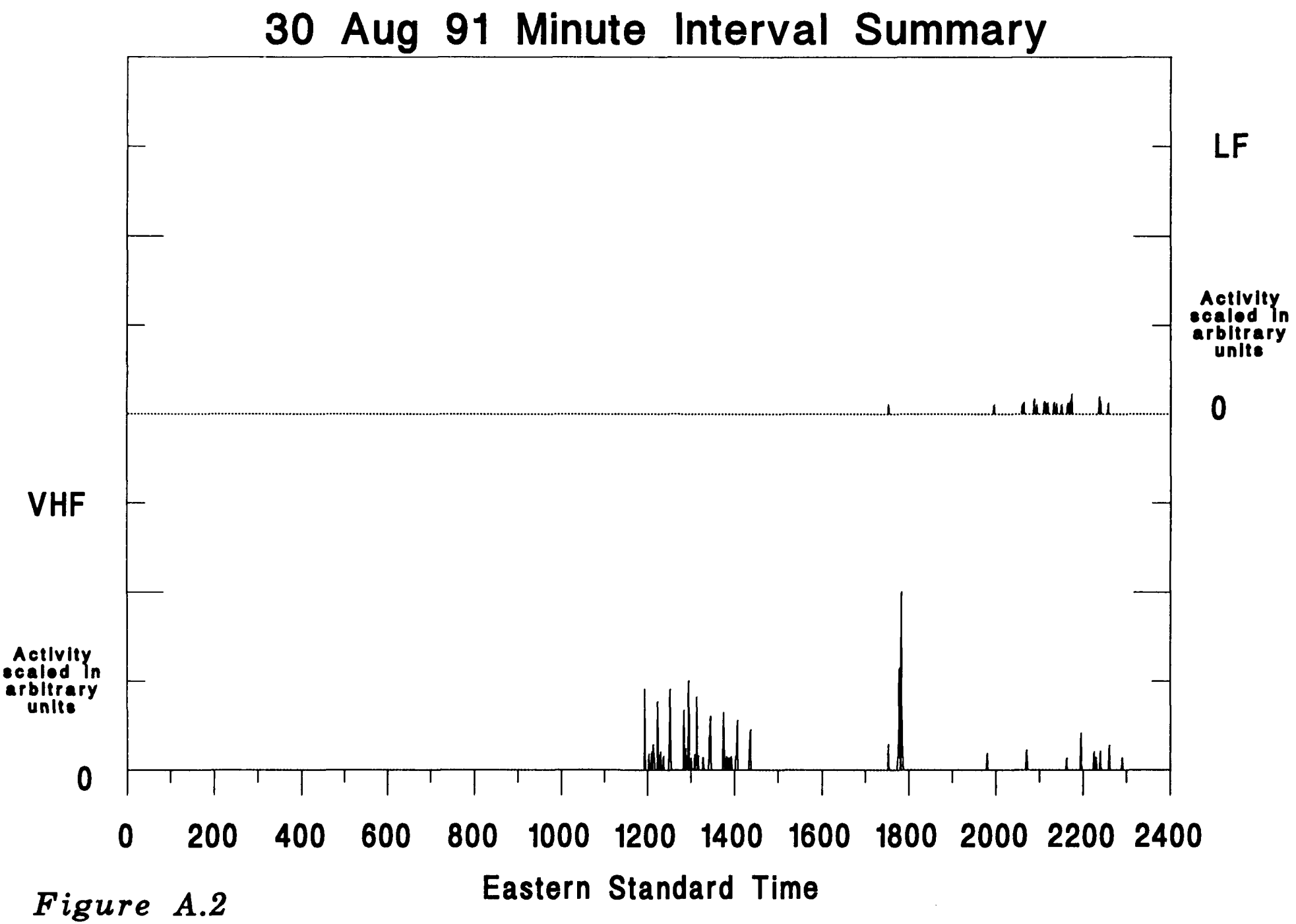
30 Aug 91 Minute Interval Summary
LF
Activity scaled in arbitrary units
0
VHF
Activity scaled in arbitrary units
0
0 200 400 600 800 1000 1200 1400 1600 1800 2000 2200 2400
Eastern Standard Time

Figure A.2

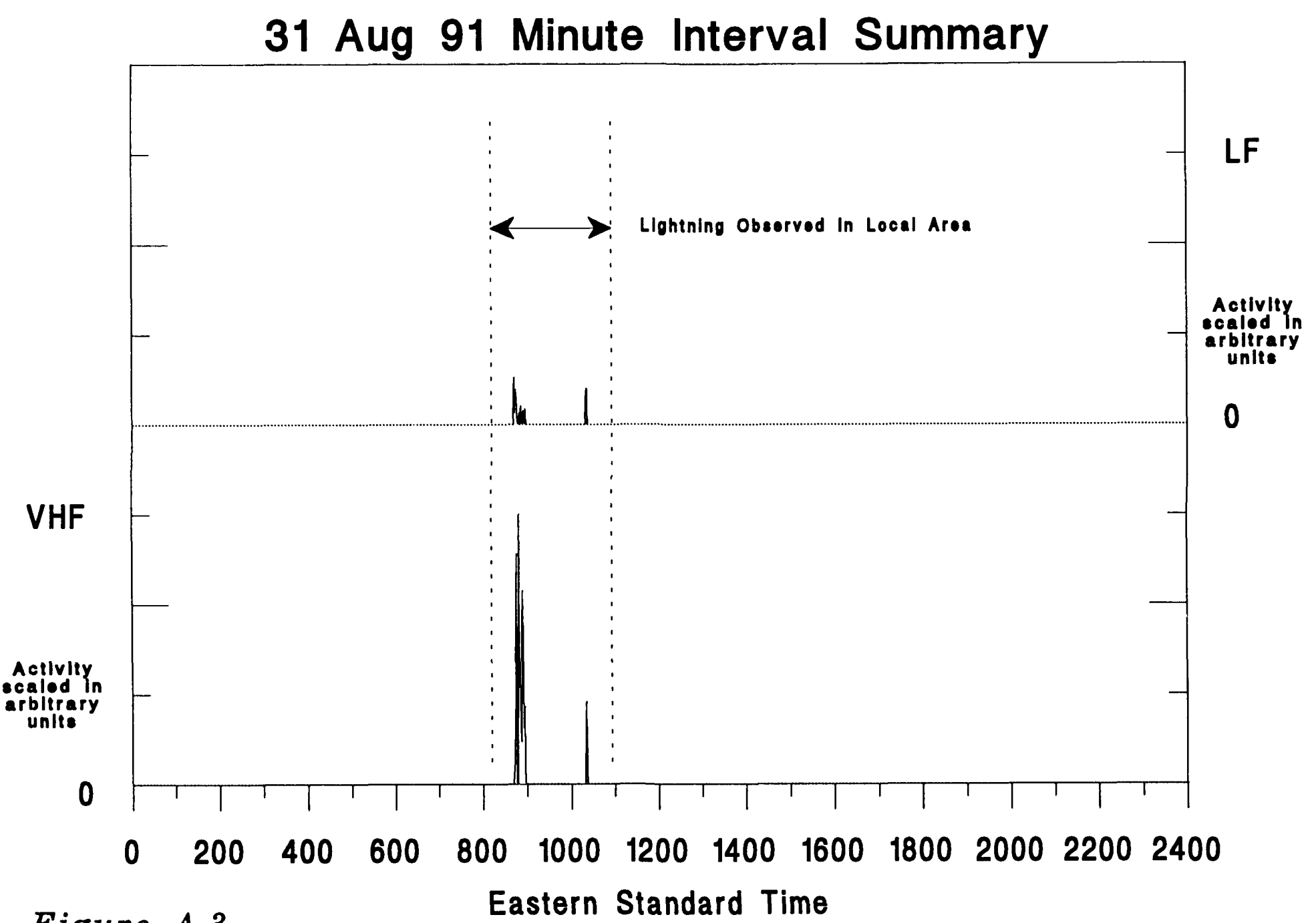
31 Aug 91 Minute Interval Summary
LF
Lightning Observed In Local Area
Activity scaled in arbitrary units
0
VHF
Activity scaled in arbitrary units
0
0 200 400 600 800 1000 1200 1400 1600 1800 2000 2200 2400
Eastern Standard Time

Figure A.3

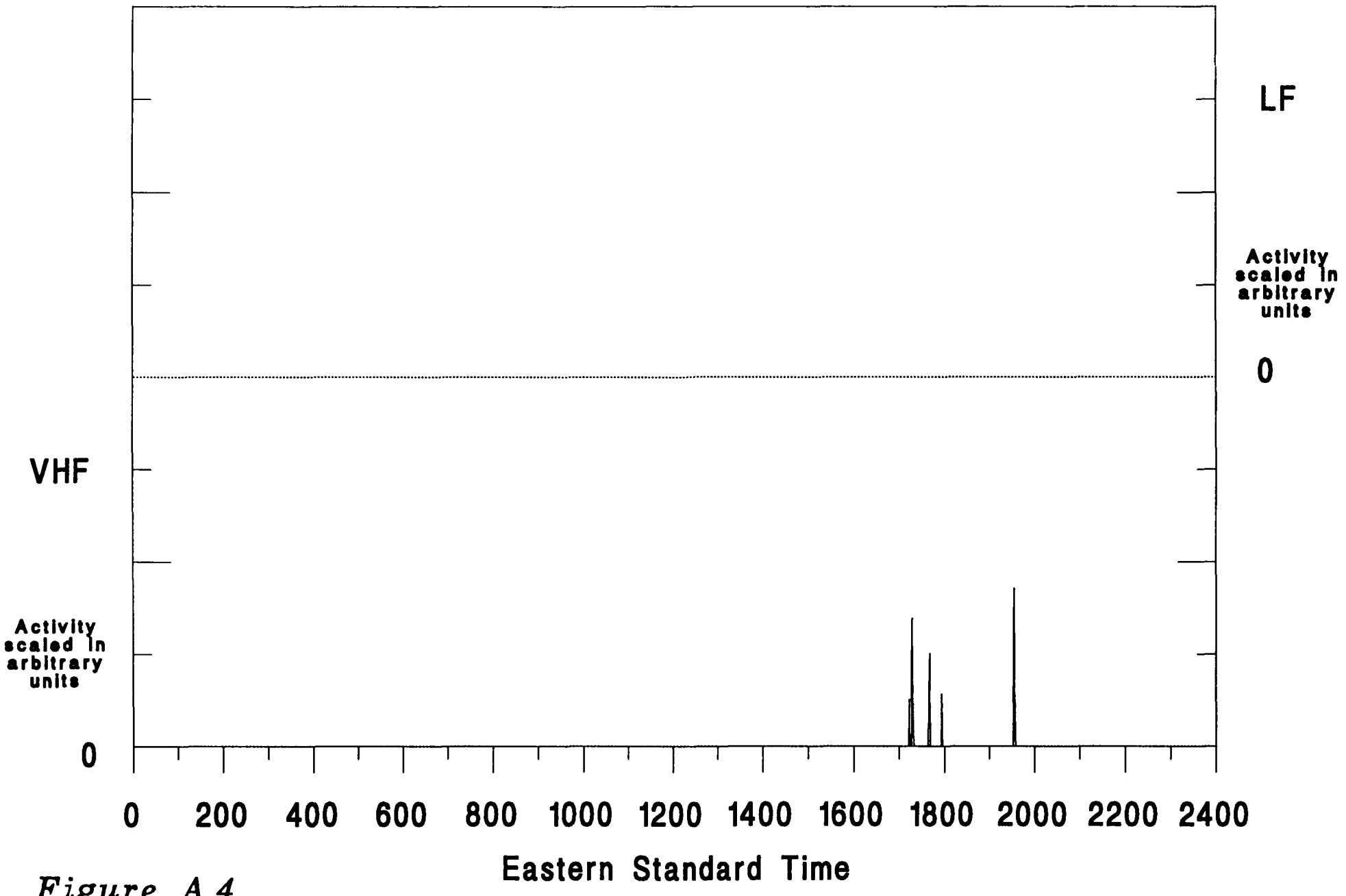
1 Sep 91 Minute Interval Summary
LF
Activity scaled in arbitrary units
0
VHF
Activity scaled in arbitrary units
0
0 200 400 600 800 1000 1200 1400 1600 1800 2000 2200 2400
Eastern Standard Time

Figure A.4

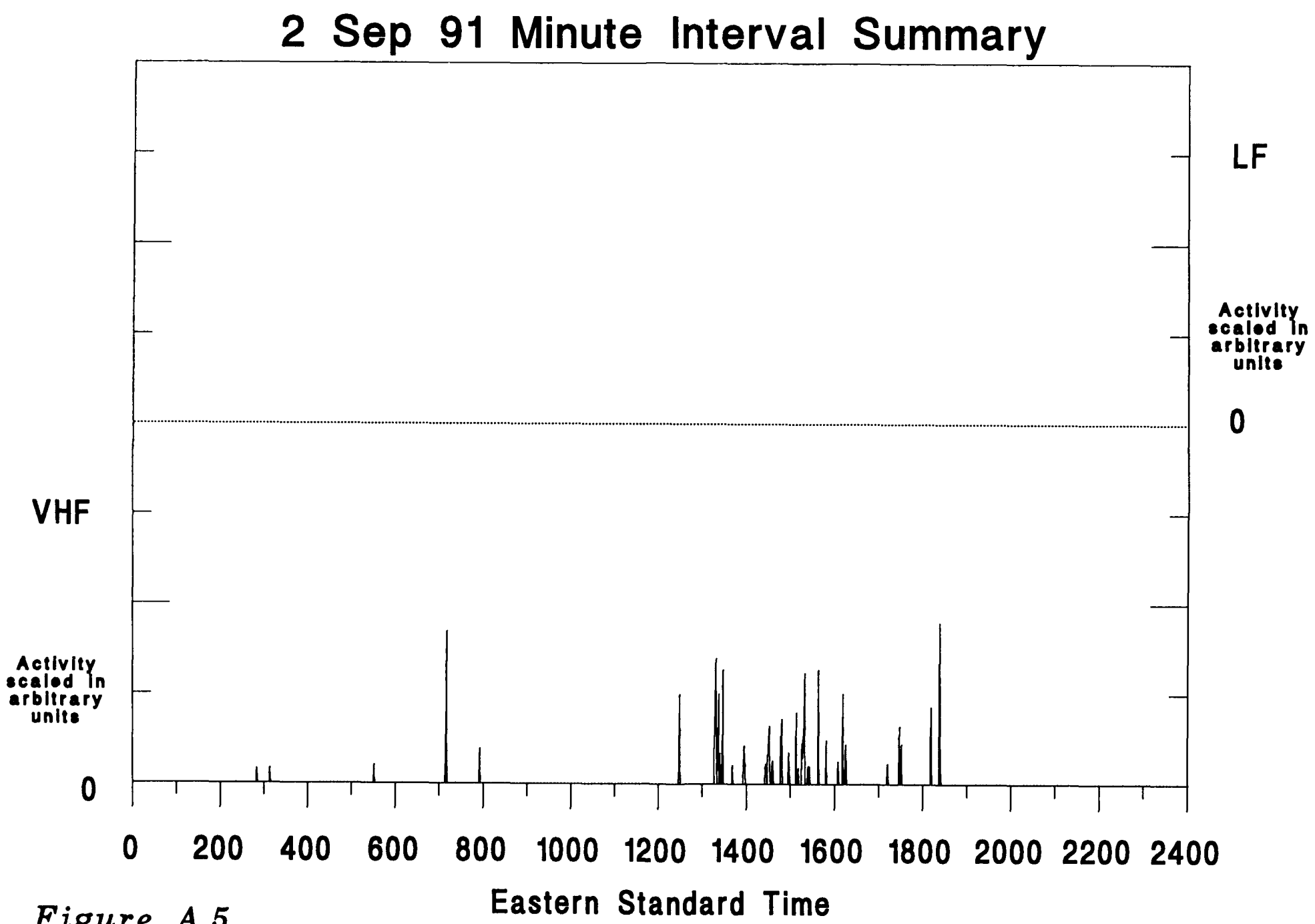
2 Sep 91 Minute Interval Summary
LF
Activity scaled in arbitrary units
0
VHF
Activity scaled in arbitrary units
0
0 200 400 600 800 1000 1200 1400 1600 1800 2000 2200 2400
Eastern Standard Time

Figure A.5

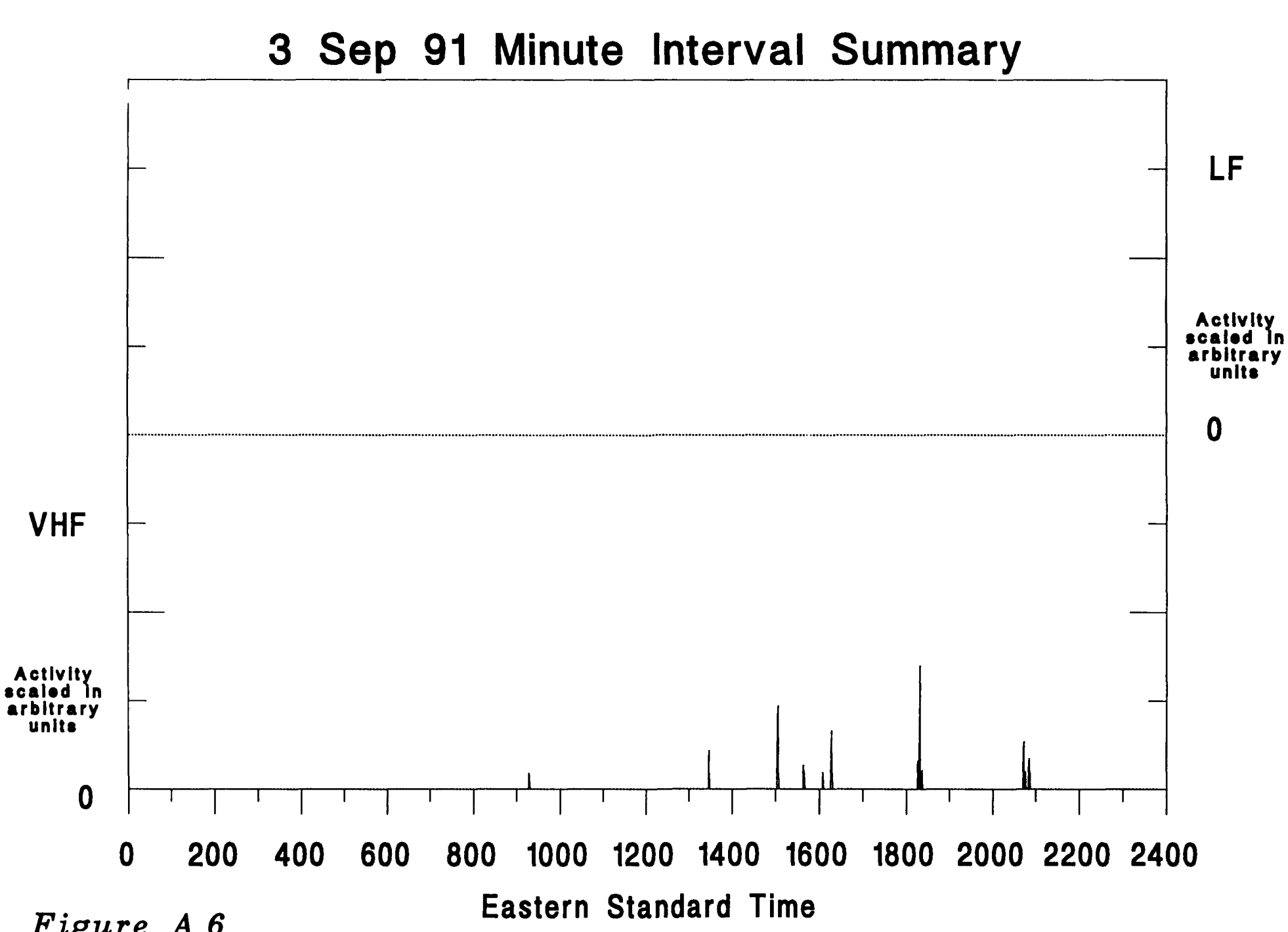
3 Sep 91 Minute Interval Summary
LF
Activity scaled in arbitrary units
0
VHF
Activity scaled in arbitrary units
0
0 200 400 600 800 1000 1200 1400 1600 1800 2000 2200 2400
Eastern Standard Time

Figure A.6

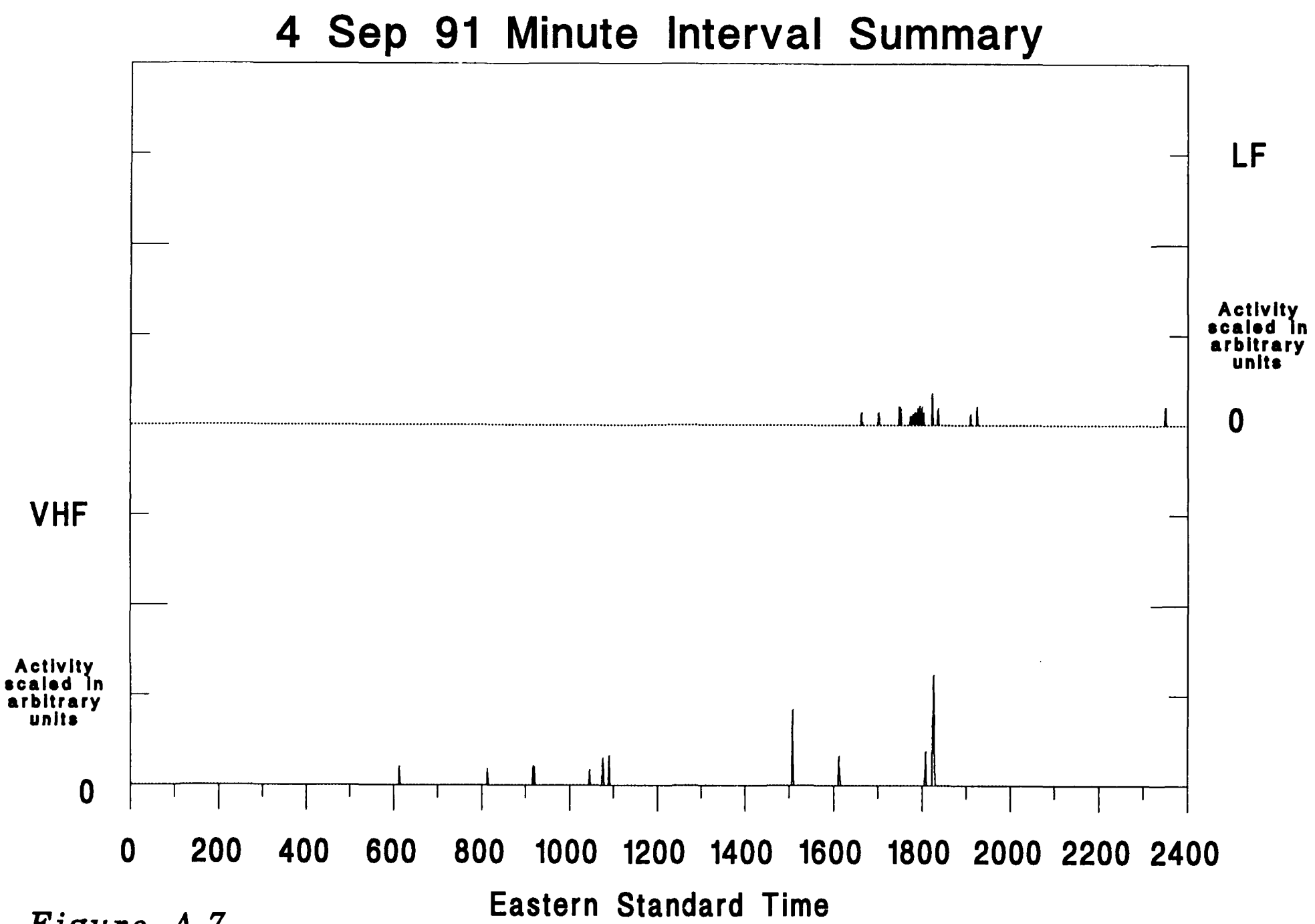
4 Sep 91 Minute Interval Summary
LF
Activity scaled in arbitrary units
0
VHF
Activity scaled in arbitrary units
0
0 200 400 600 800 1000 1200 1400 1600 1800 2000 2200 2400
Eastern Standard Time

Figure A.7

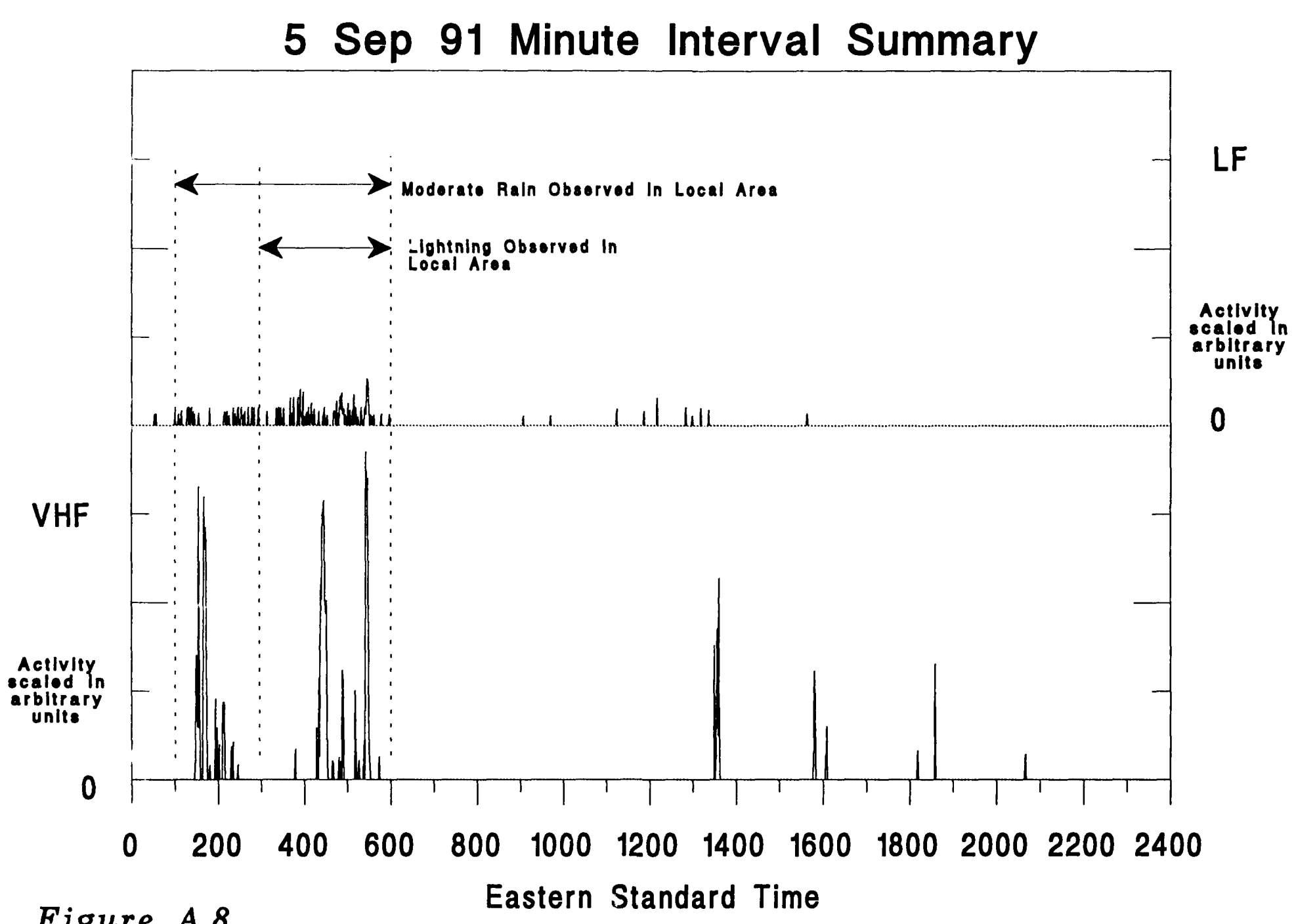
5 Sep 91 Minute Interval Summary
Moderate Rain Observed In Local Area
Lightning Observed In Local Area
LF
Activity scaled in arbitrary units
0
VHF
Activity scaled in arbitrary units
0
0 200 400 600 800 1000 1200 1400 1600 1800 2000 2200 2400
Eastern Standard Time

Figure A.8

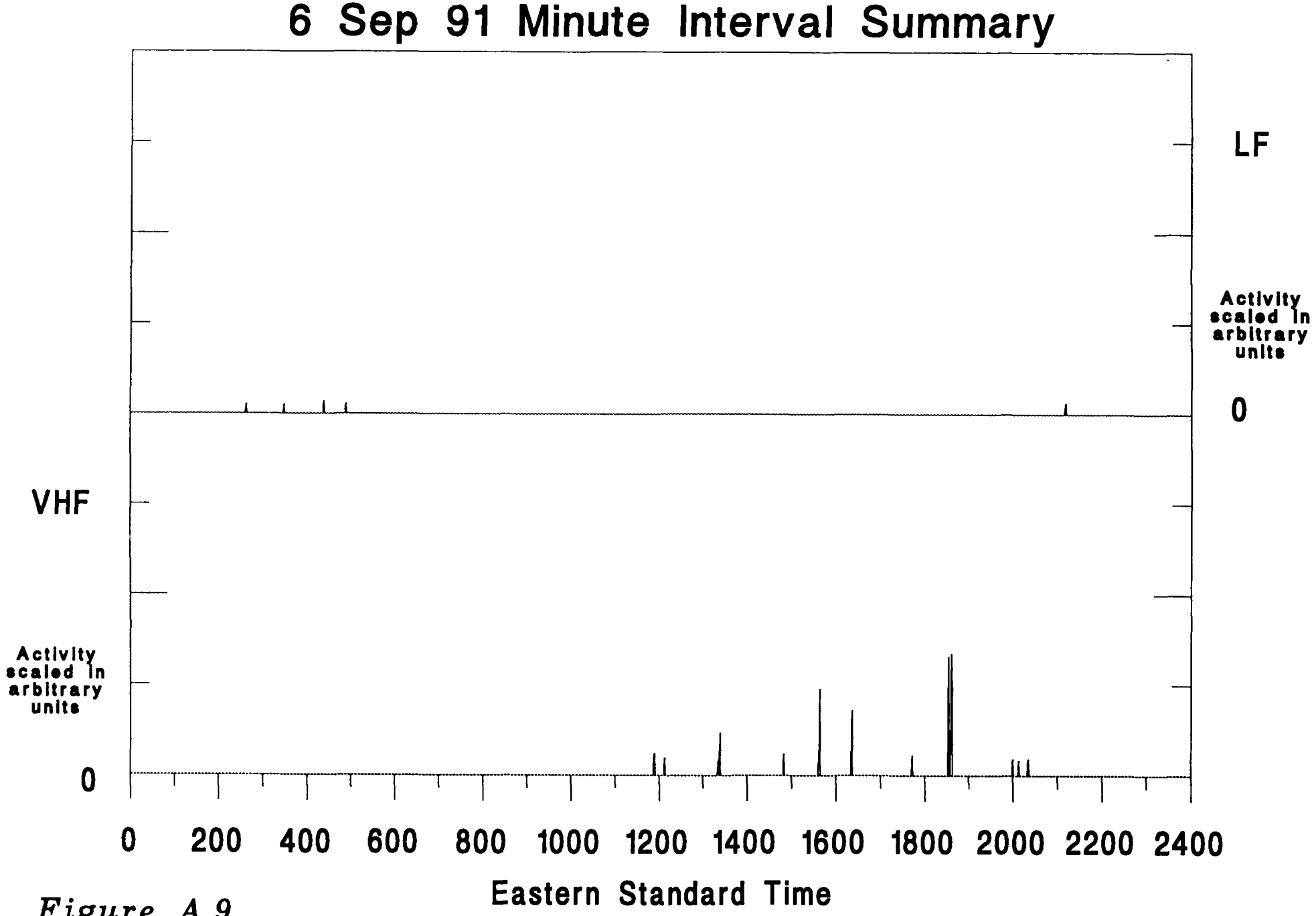
6 Sep 91 Minute Interval Summary
LF
Activity scaled in arbitrary units
0
VHF
Activity scaled in arbitrary units
0
0 200 400 600 800 1000 1200 1400 1600 1800 2000 2200 2400
Eastern Standard Time

Figure A.9

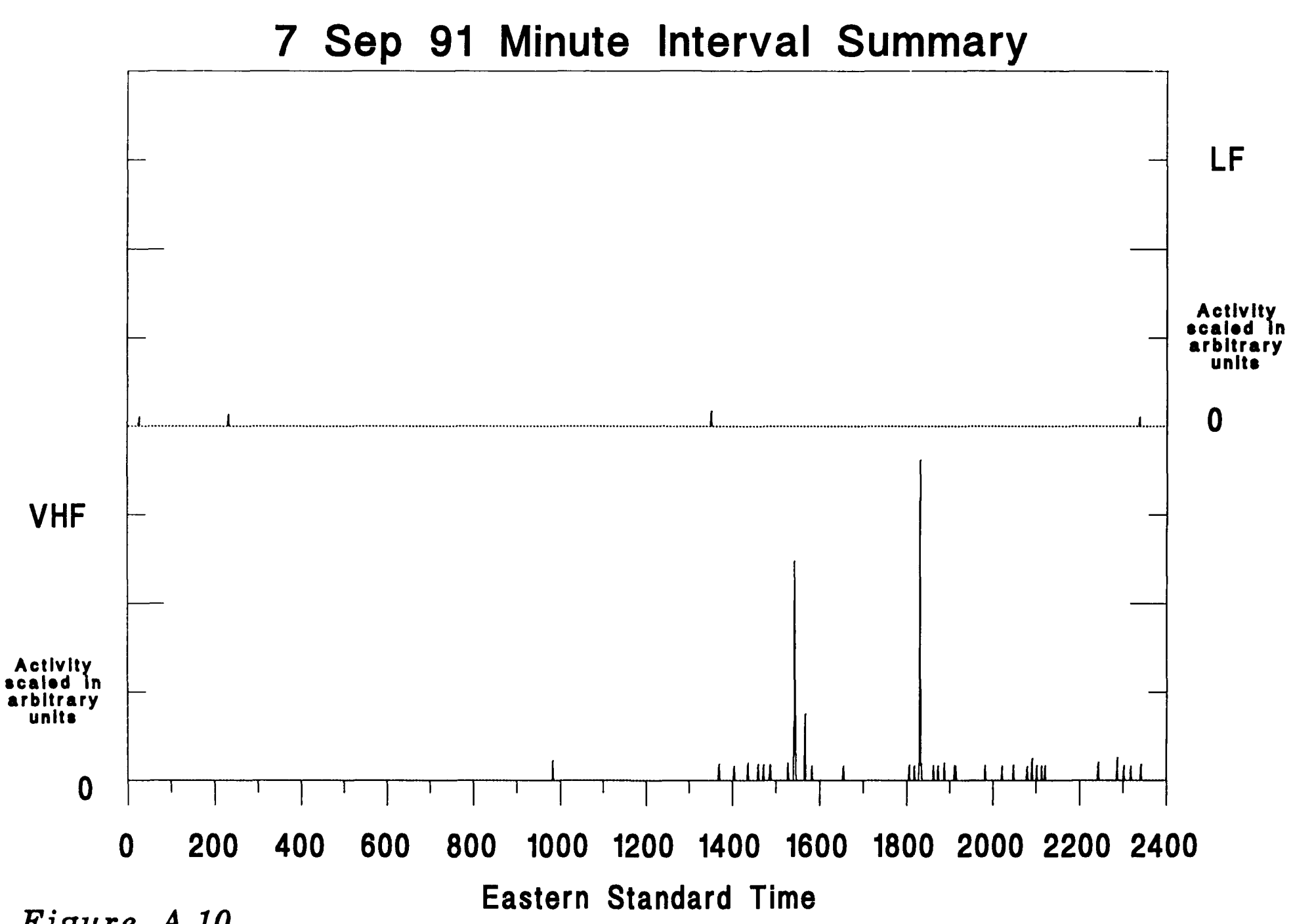
7 Sep 91 Minute Interval Summary
LF
Activity scaled in arbitrary units
0
VHF
Activity scaled in arbitrary units
0
0 200 400 600 800 1000 1200 1400 1600 1800 2000 2200 2400
Eastern Standard Time

Figure A.10

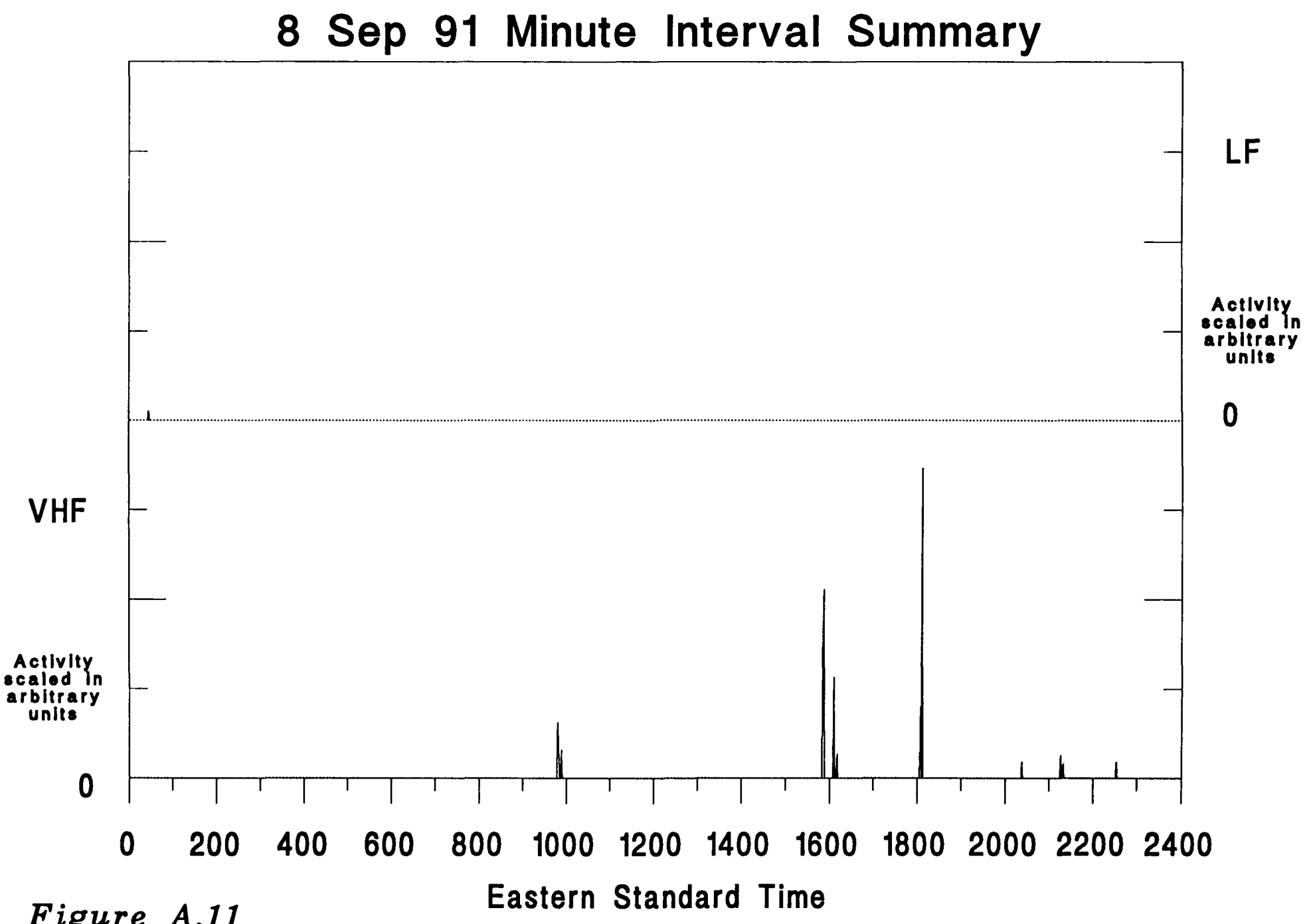
8 Sep 91 Minute Interval Summary
LF
Activity scaled in arbitrary units
0
VHF
Activity scaled in arbitrary units
0
0 200 400 600 800 1000 1200 1400 1600 1800 2000 2200 2400
Eastern Standard Time

Figure A.11

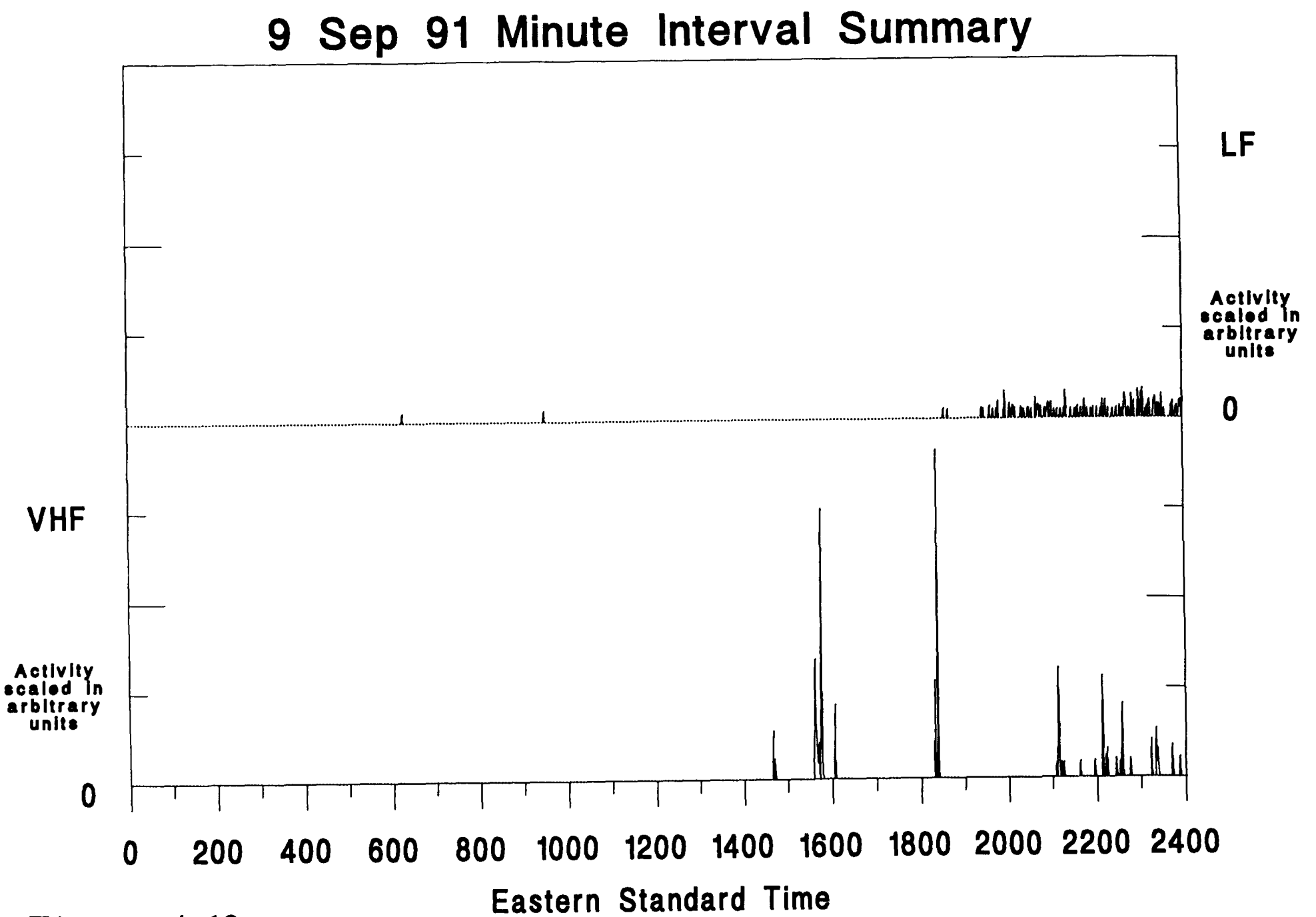
9 Sep 91 Minute Interval Summary
LF
Activity scaled in arbitrary units
0
VHF
Activity scaled in arbitrary units
0
0 200 400 600 800 1000 1200 1400 1600 1800 2000 2200 2400
Eastern Standard Time

Figure A.12

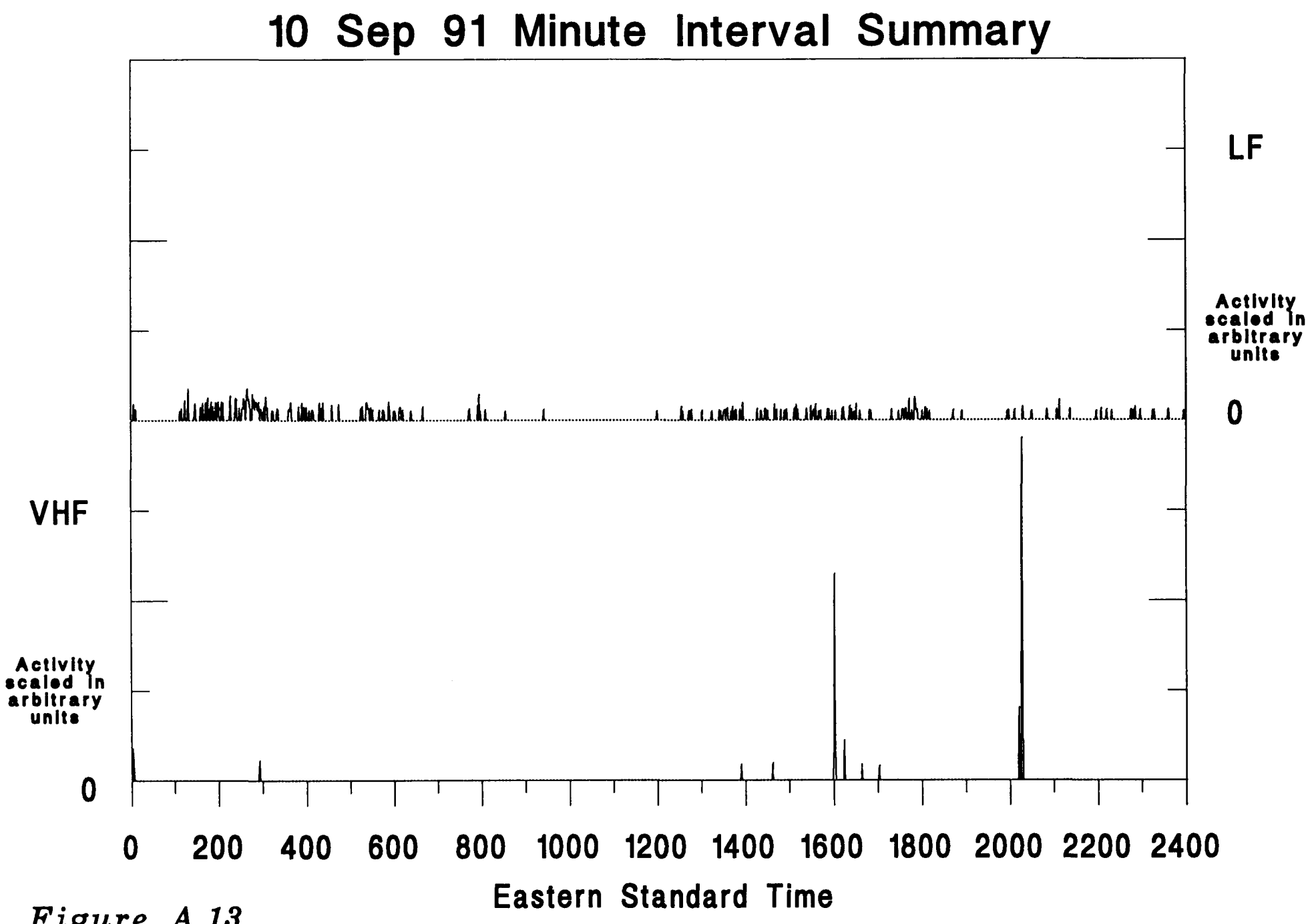
10 Sep 91 Minute Interval Summary
LF
Activity scaled in arbitrary units
0
VHF
Activity scaled in arbitrary units
0
0 200 400 600 800 1000 1200 1400 1600 1800 2000 2200 2400
Eastern Standard Time

Figure A.13

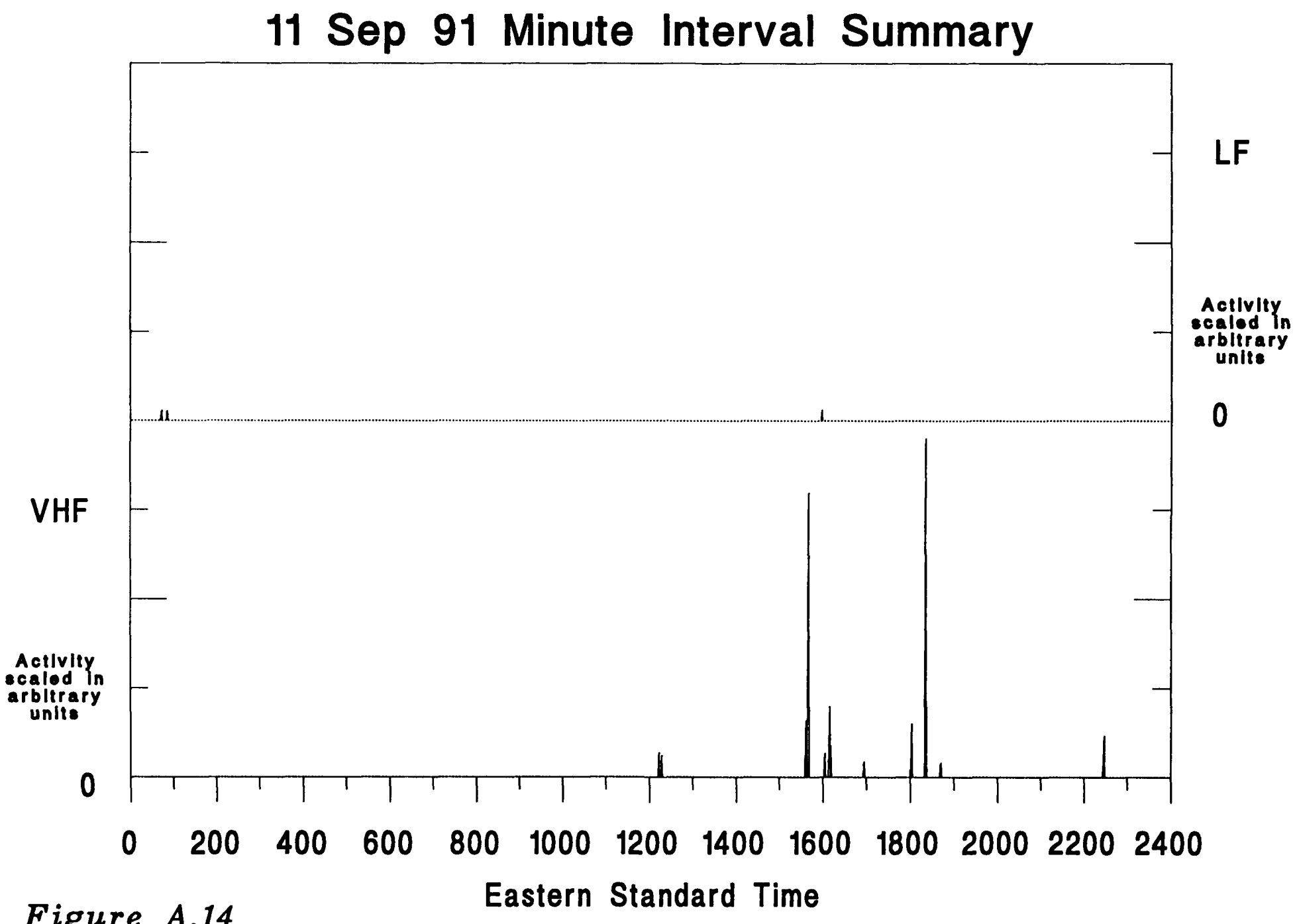
11 Sep 91 Minute Interval Summary
LF
Activity scaled in arbitrary units
0
VHF
Activity scaled in arbitrary units
0
0 200 400 600 800 1000 1200 1400 1600 1800 2000 2200 2400
Eastern Standard Time

Figure A.14

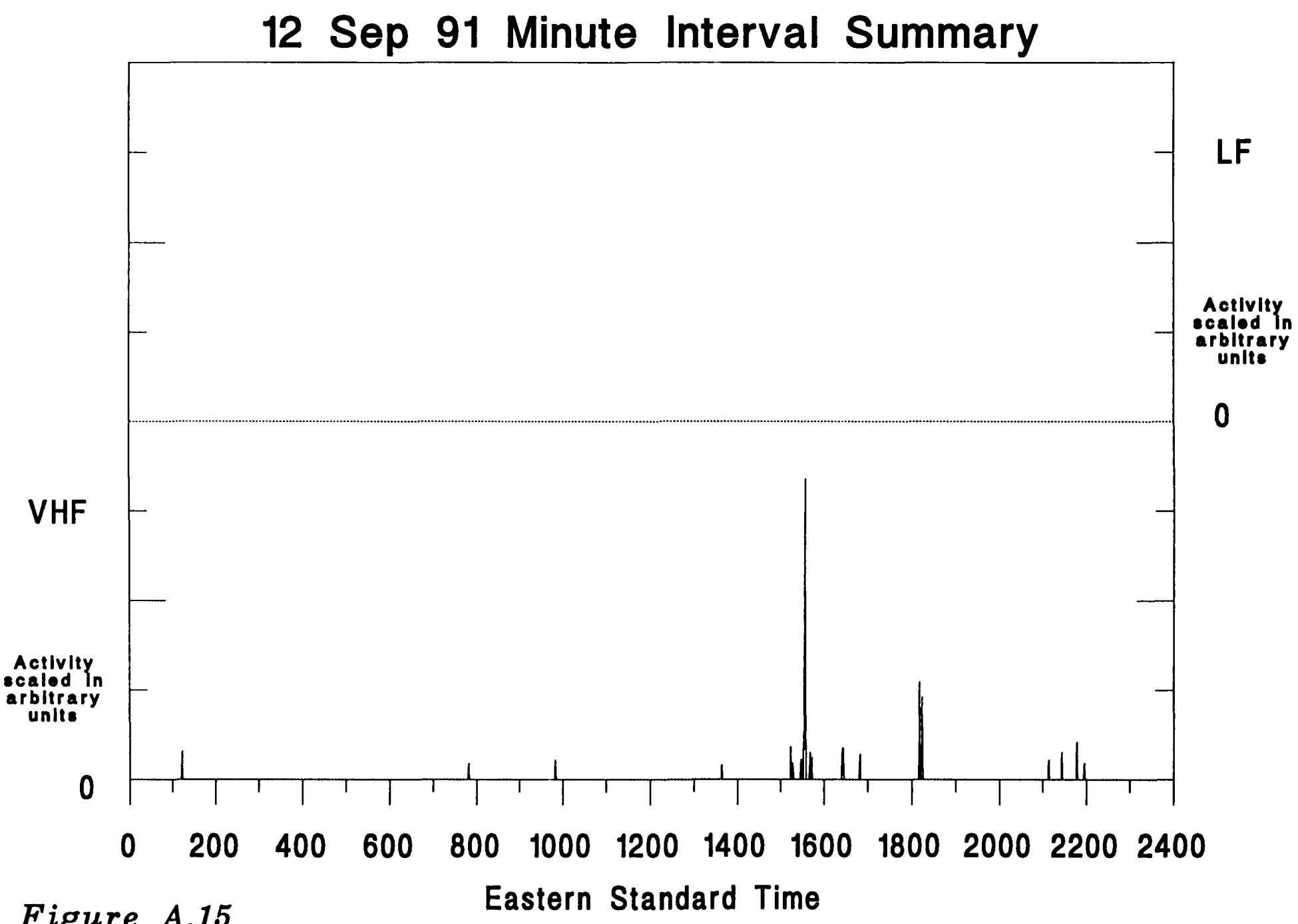
12 Sep 91 Minute Interval Summary
LF
Activity scaled in arbitrary units
0
VHF
Activity scaled in arbitrary units
0
0 200 400 600 800 1000 1200 1400 1600 1800 2000 2200 2400
Eastern Standard Time

Figure A.15

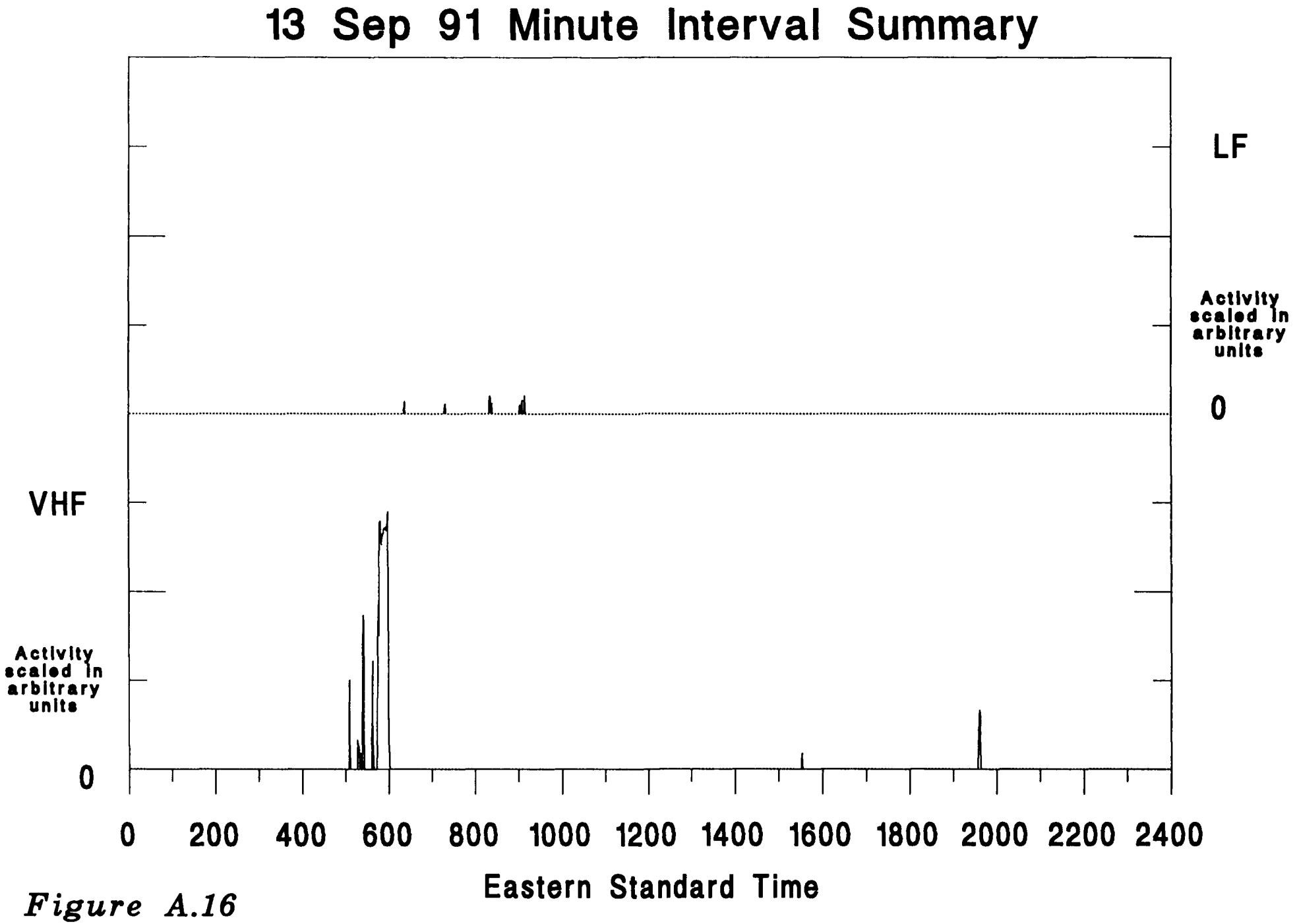
13 Sep 91 Minute Interval Summary
LF
Activity scaled in arbitrary units
0
VHF
Activity scaled in arbitrary units
0
0 200 400 600 800 1000 1200 1400 1600 1800 2000 2200 2400
Eastern Standard Time

Figure A.16

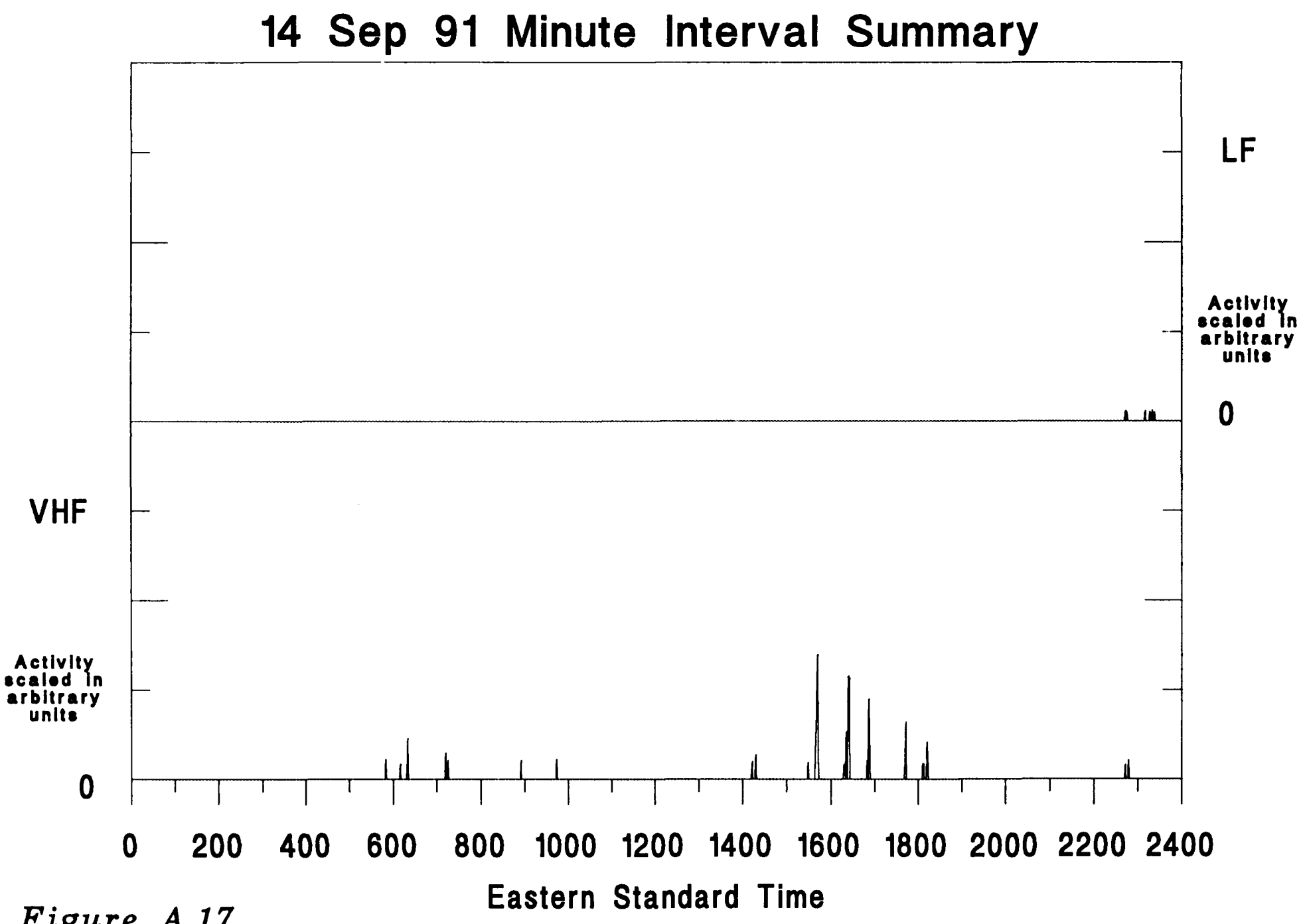
14 Sep 91 Minute Interval Summary
LF
Activity scaled in arbitrary units
0
VHF
Activity scaled in arbitrary units
0
0 200 400 600 800 1000 1200 1400 1600 1800 2000 2200 2400
Eastern Standard Time

Figure A.17

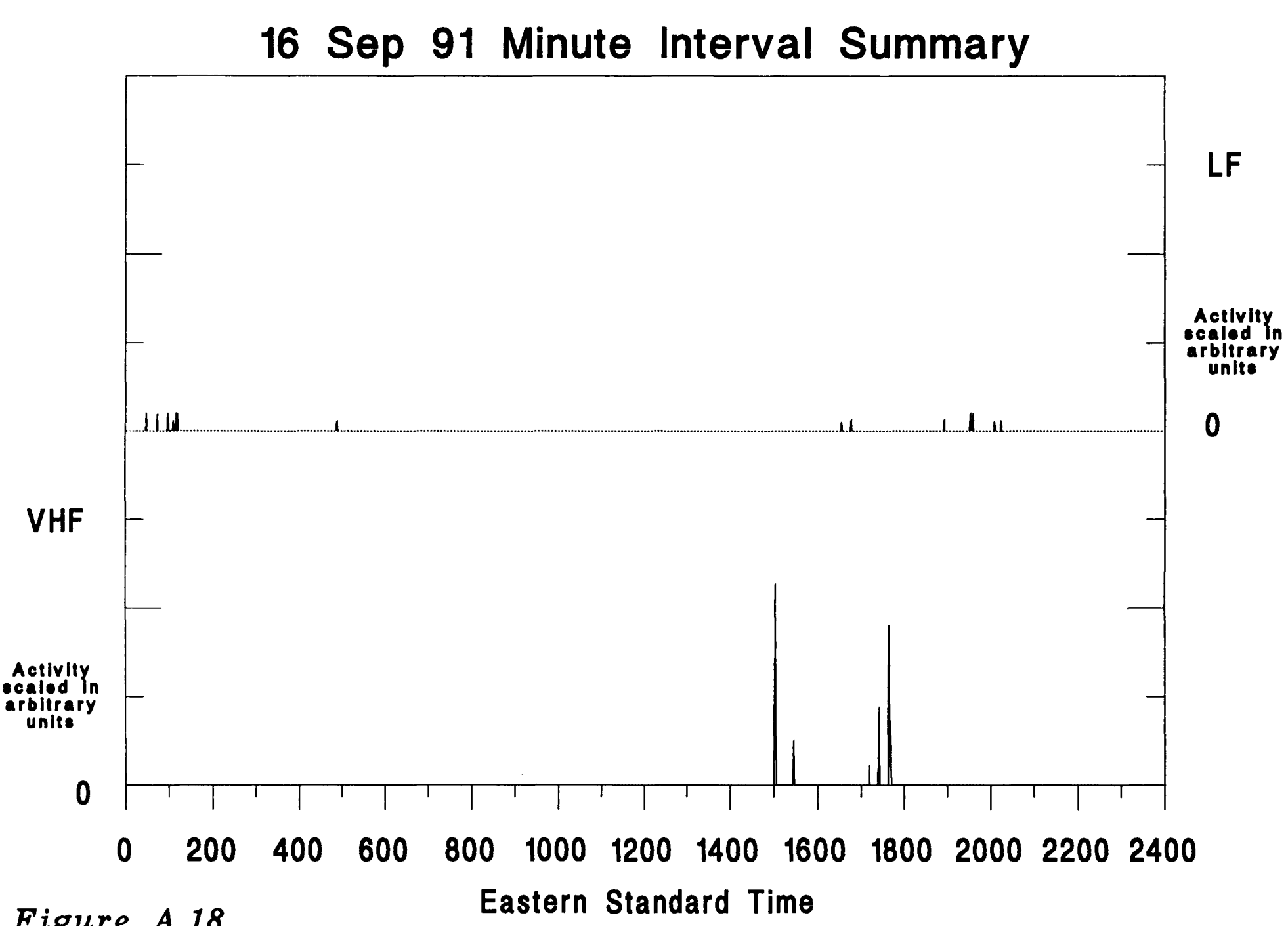
16 Sep 91 Minute Interval Summary
LF
Activity scaled in arbitrary units
0
VHF
Activity scaled in arbitrary units
0
0 200 400 600 800 1000 1200 1400 1600 1800 2000 2200 2400
Eastern Standard Time

Figure A.18

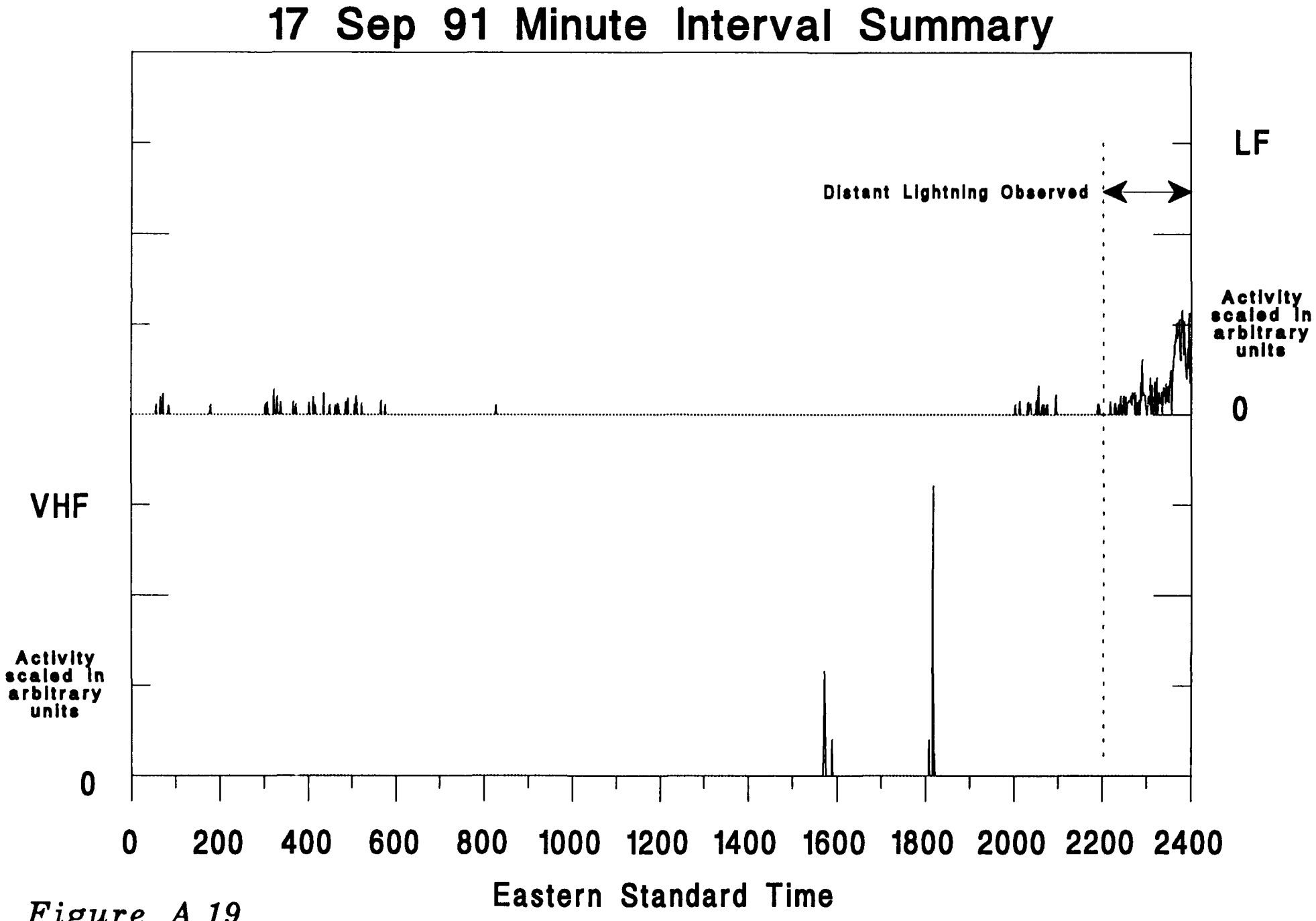
17 Sep 91 Minute Interval Summary
LF
Distant Lightning Observed
Activity scaled in arbitrary units
0
VHF
Activity scaled in arbitrary units
0
0 200 400 600 800 1000 1200 1400 1600 1800 2000 2200 2400
Eastern Standard Time

Figure A.19

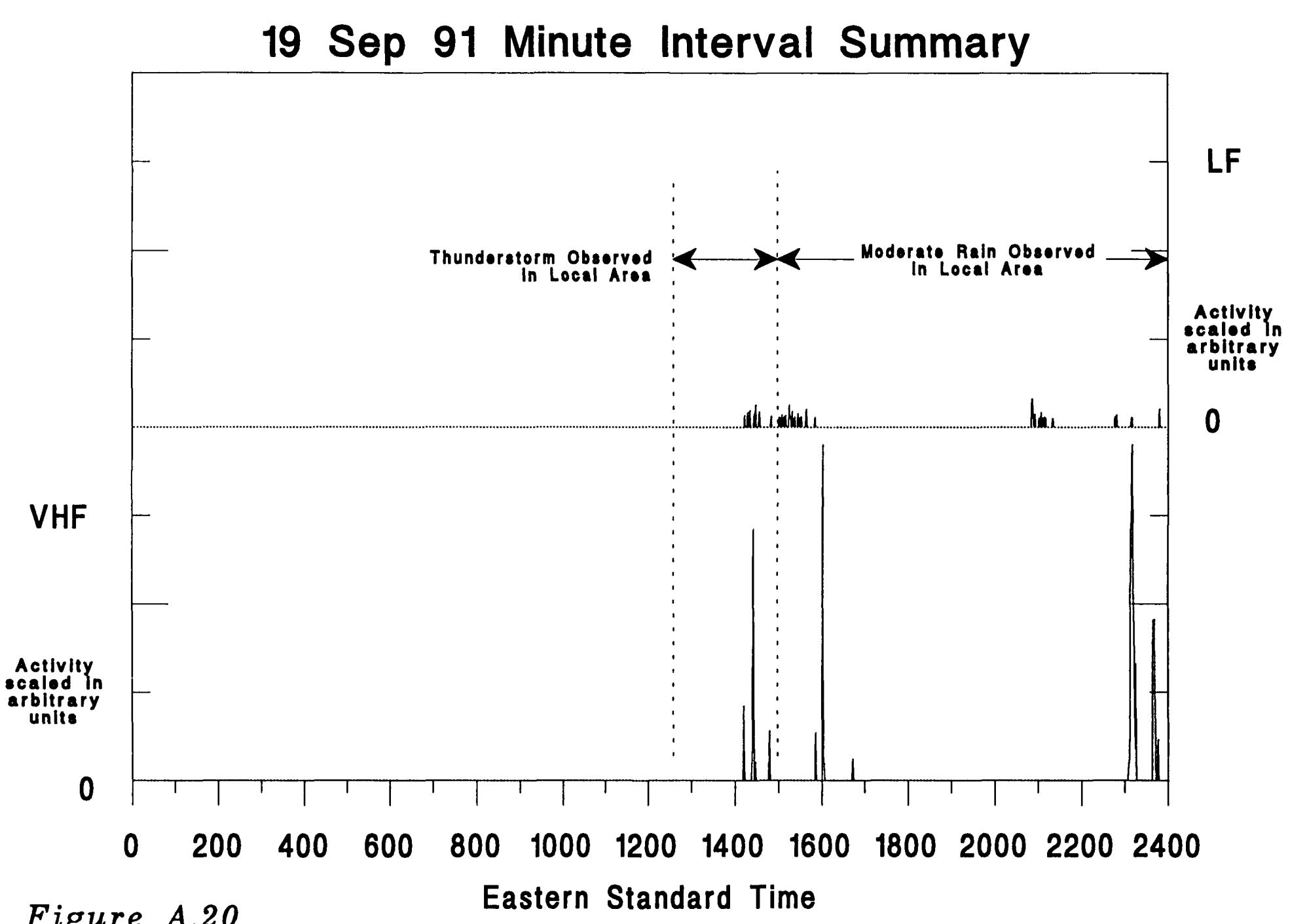
19 Sep 91 Minute Interval Summary
LF
Thunderstorm Observed
In Local Area
Moderate Rain Observed
In Local Area
Activity
scaled in
arbitrary
units
0
VHF
Activity
scaled in
arbitrary
units
0
0 200 400 600 800 1000 1200 1400 1600 1800 2000 2200 2400
Eastern Standard Time

Figure A.20

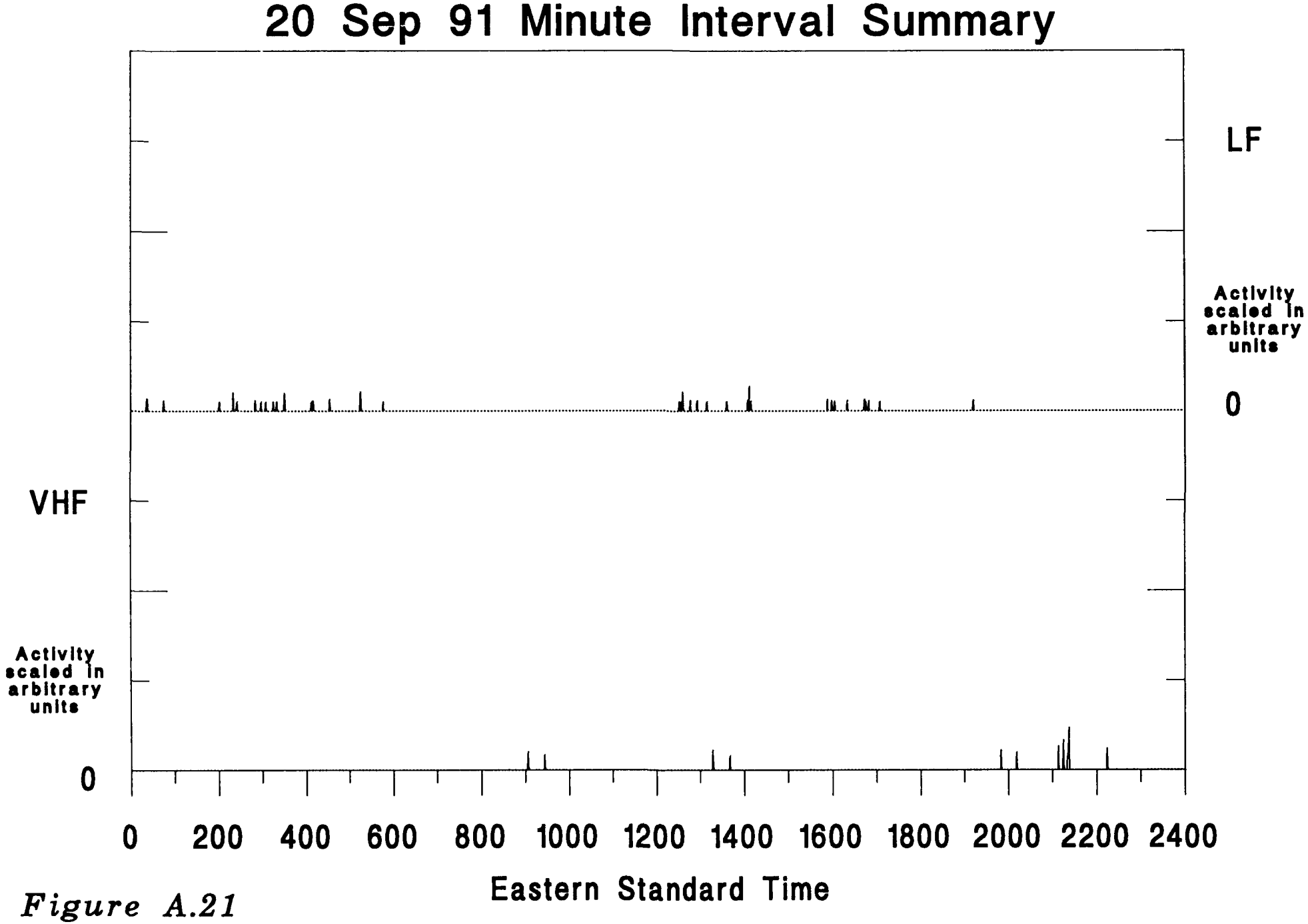
20 Sep 91 Minute Interval Summary
LF
Activity scaled in arbitrary units
0
VHF
Activity scaled in arbitrary units
0
0 200 400 600 800 1000 1200 1400 1600 1800 2000 2200 2400
Eastern Standard Time

Figure A.21

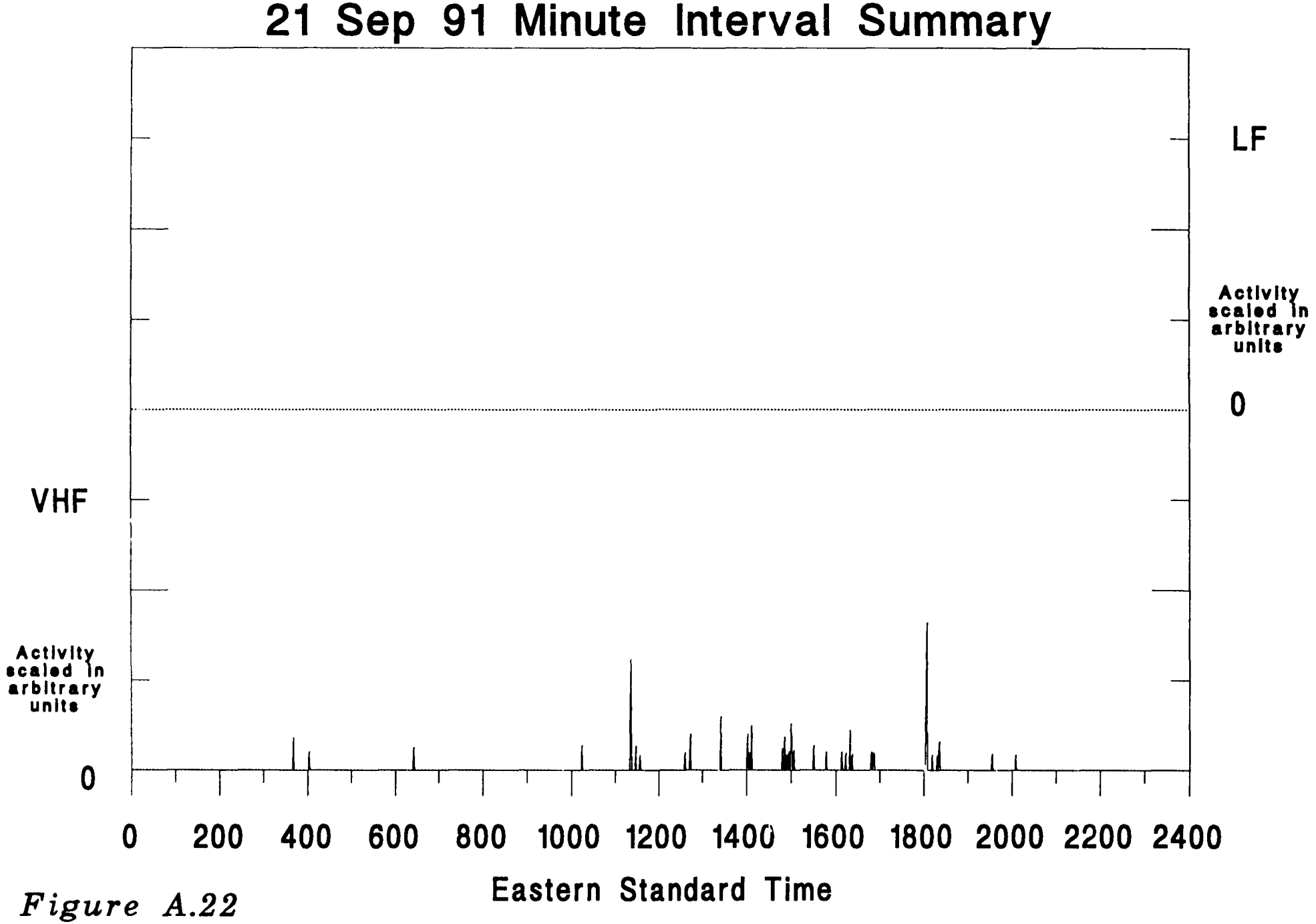
21 Sep 91 Minute Interval Summary
LF
Activity scaled in arbitrary units
0
VHF
Activity scaled in arbitrary units
0
0 200 400 600 800 1000 1200 1400 1600 1800 2000 2200 2400
Eastern Standard Time

Figure A.22

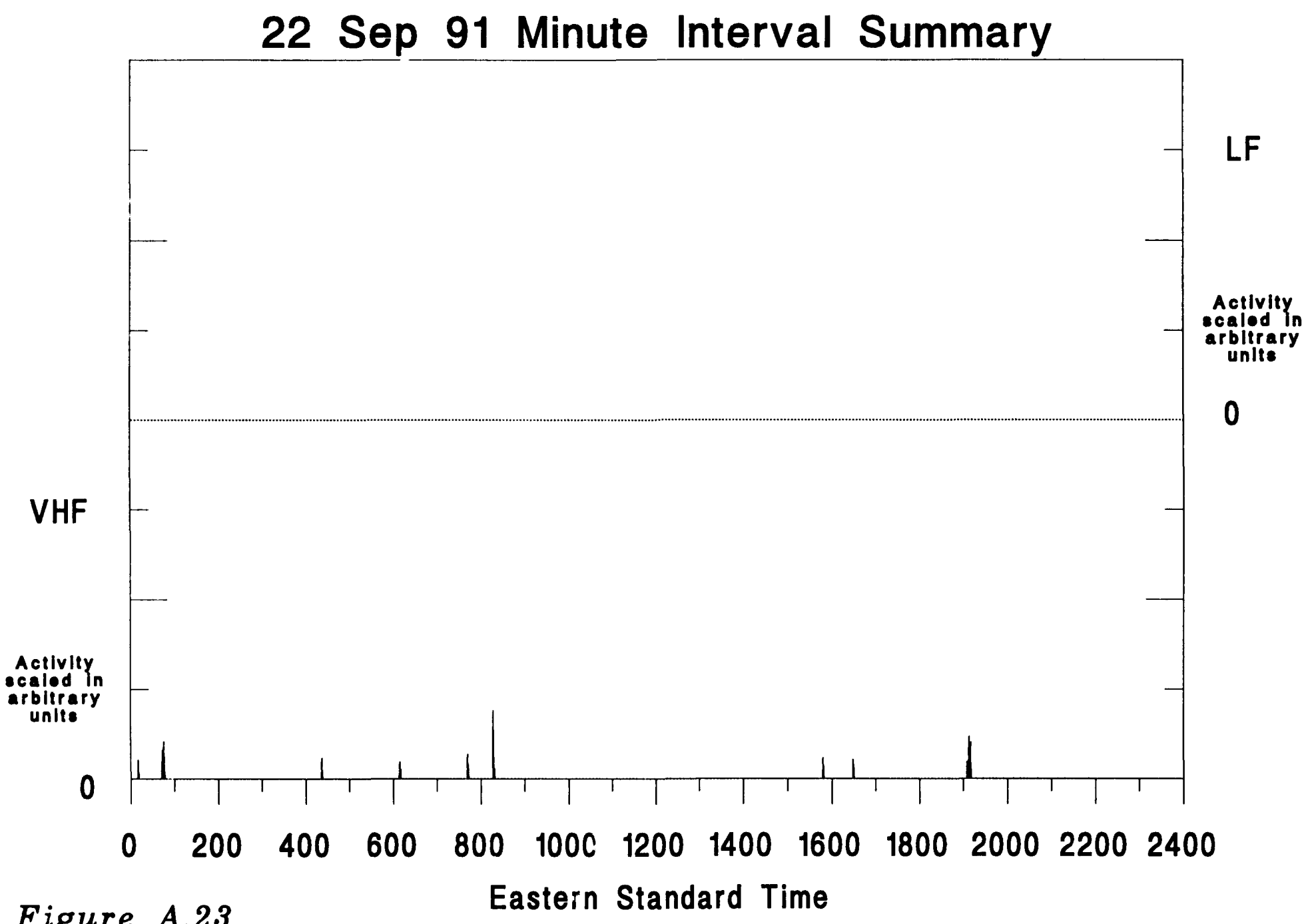
22 Sep 91 Minute Interval Summary
LF
Activity scaled in arbitrary units
0
VHF
Activity scaled in arbitrary units
0
0 200 400 600 800 1000 1200 1400 1600 1800 2000 2200 2400
Eastern Standard Time

Figure A.23

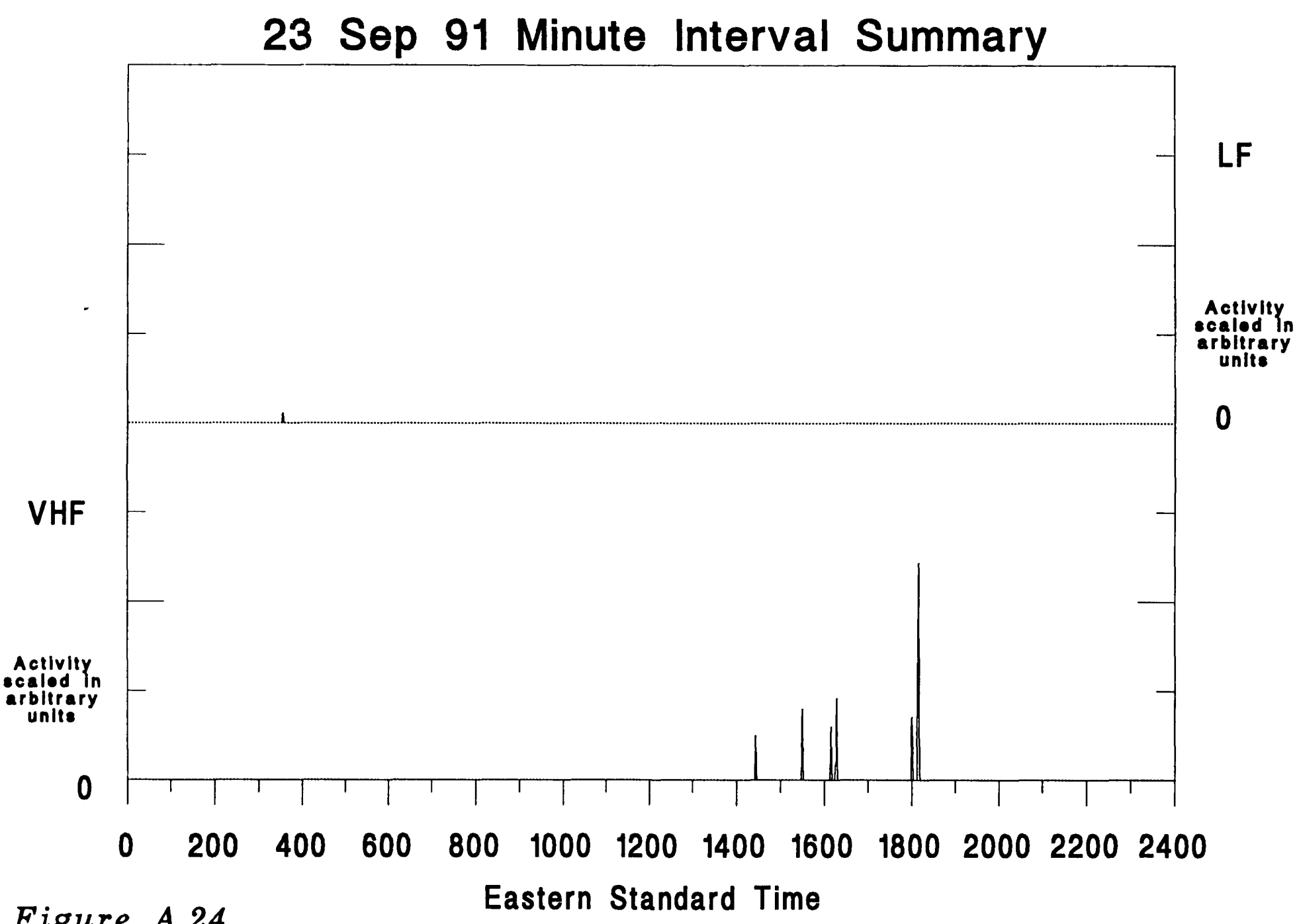
23 Sep 91 Minute Interval Summary
LF
Activity scaled in arbitrary units
0
VHF
Activity scaled in arbitrary units
0
0 200 400 600 800 1000 1200 1400 1600 1800 2000 2200 2400
Eastern Standard Time

Figure A.24

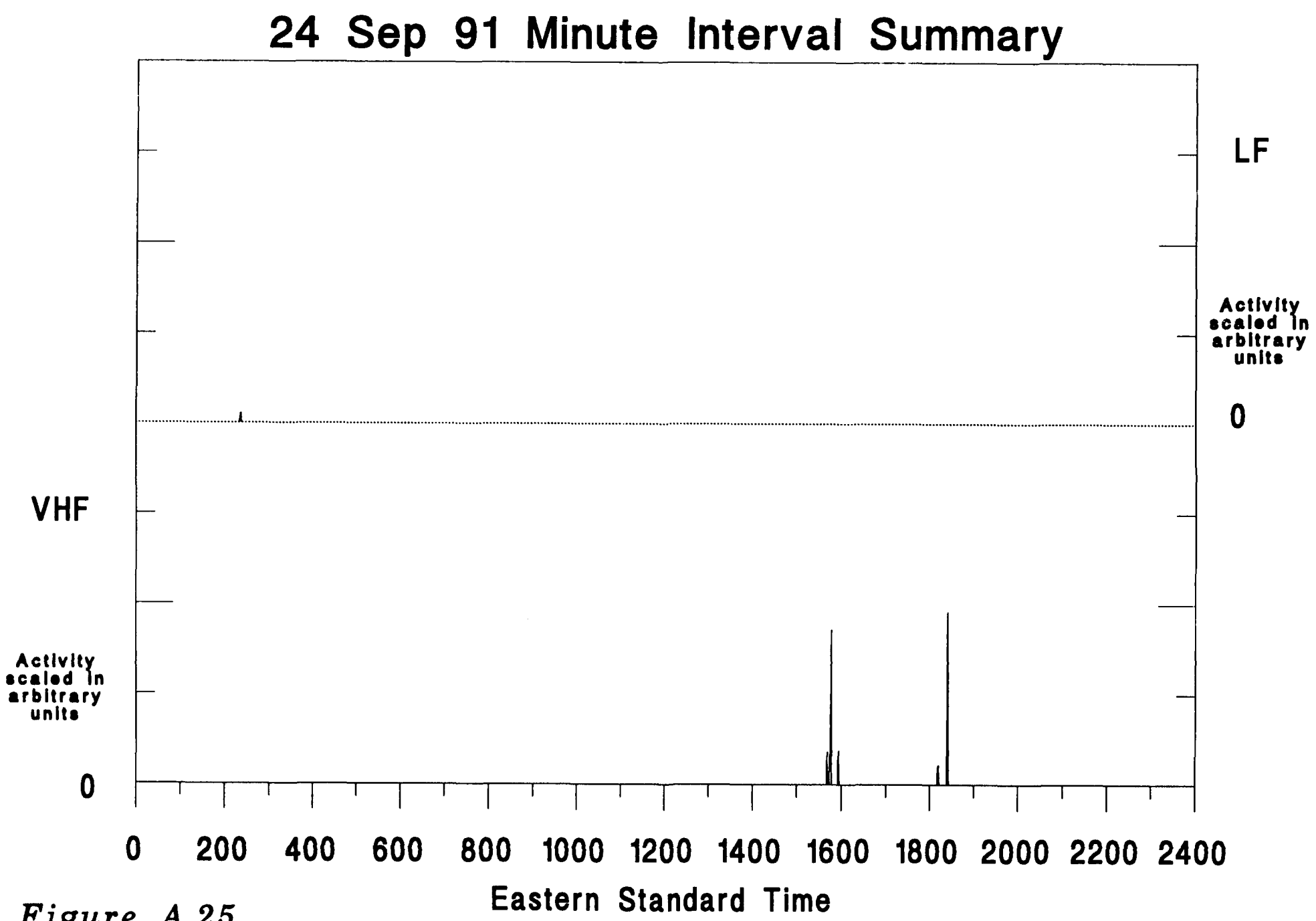
24 Sep 91 Minute Interval Summary
LF
Activity scaled in arbitrary units
0
VHF
Activity scaled in arbitrary units
0
0 200 400 600 800 1000 1200 1400 1600 1800 2000 2200 2400
Eastern Standard Time

Figure A.25

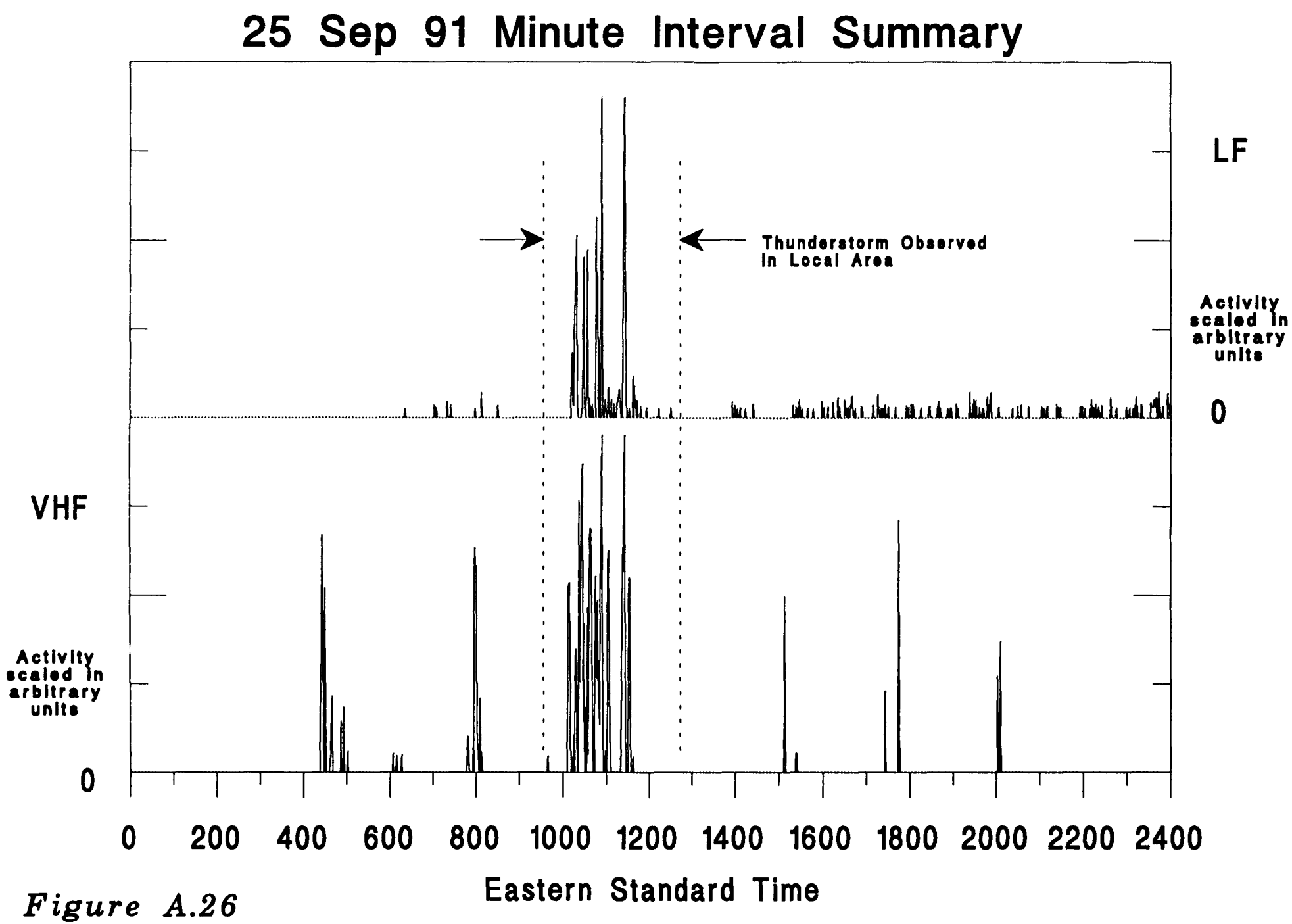
25 Sep 91 Minute Interval Summary
LF
Thunderstorm Observed
In Local Area
Activity
scaled in
arbitrary
units
0
VHF
Activity
scaled in
arbitrary
units
0
0
200
400
600
800
1000
1200
1400
1600
1800
2000
2200
2400
Eastern Standard Time

Figure A.26

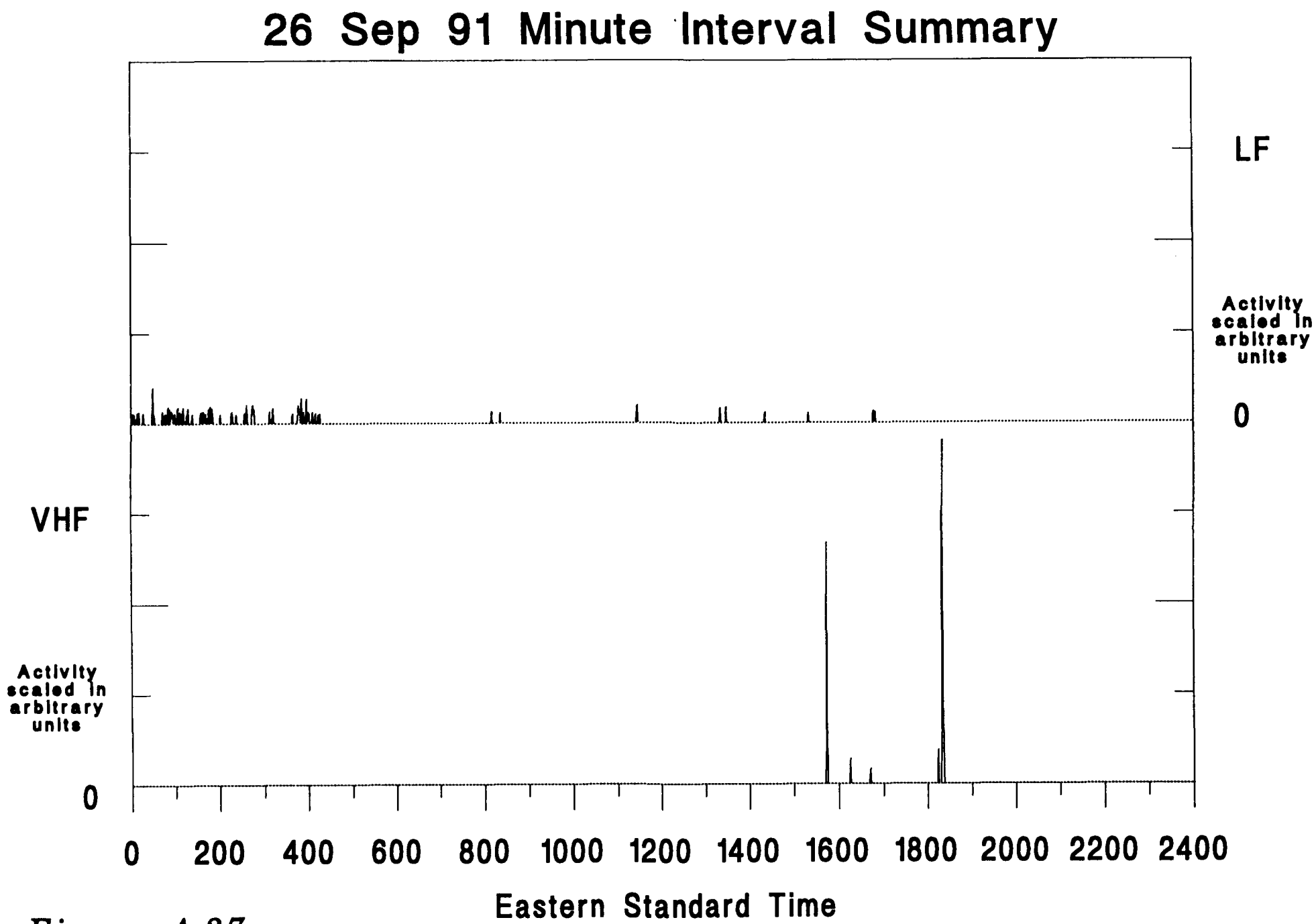
26 Sep 91 Minute Interval Summary
LF
Activity scaled in arbitrary units
0
VHF
Activity scaled in arbitrary units
0
0 200 400 600 800 1000 1200 1400 1600 1800 2000 2200 2400
Eastern Standard Time

Figure A.27

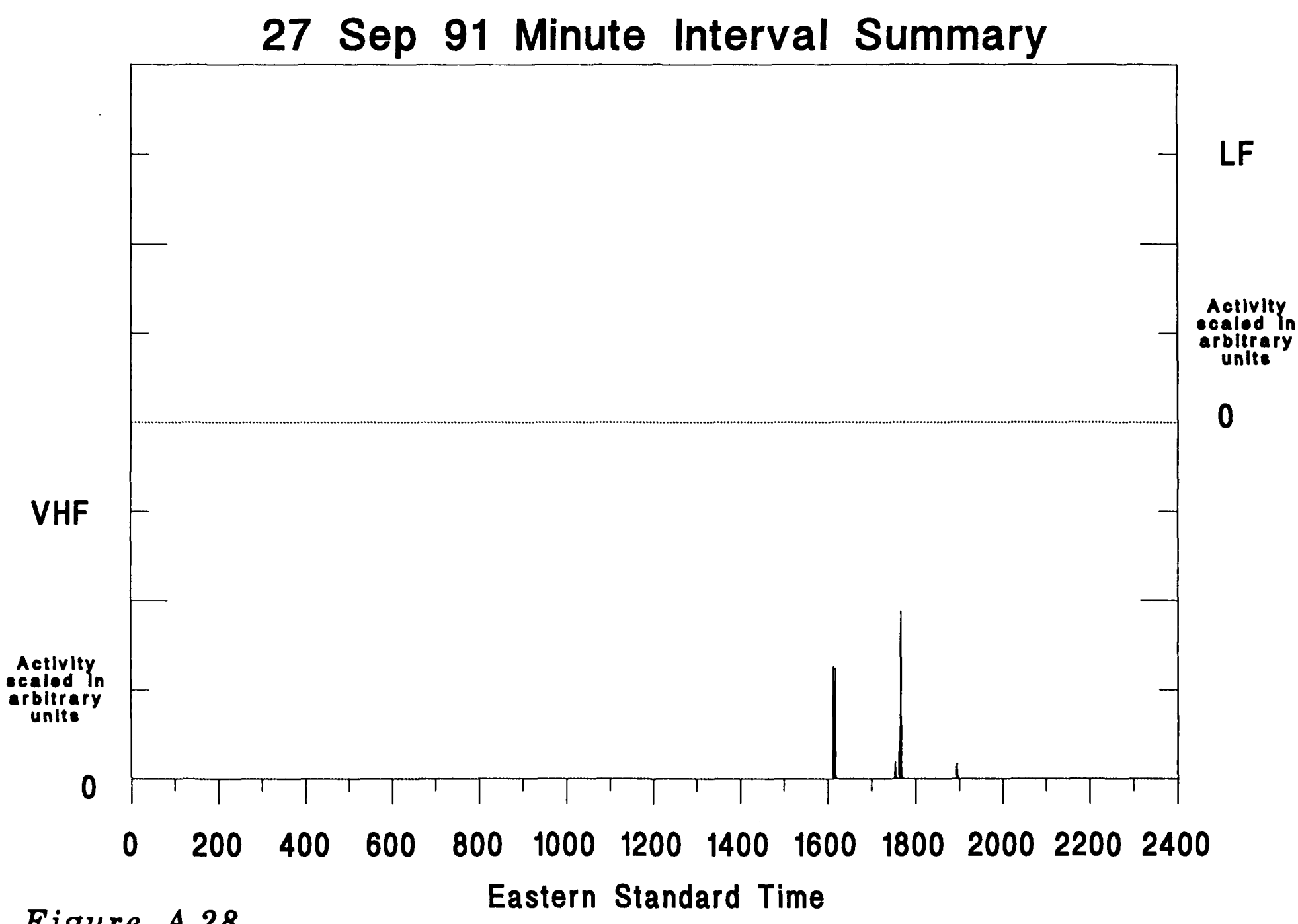
27 Sep 91 Minute Interval Summary
LF
Activity scaled in arbitrary units
0
VHF
Activity scaled in arbitrary units
0
0 200 400 600 800 1000 1200 1400 1600 1800 2000 2200 2400
Eastern Standard Time

Figure A.28

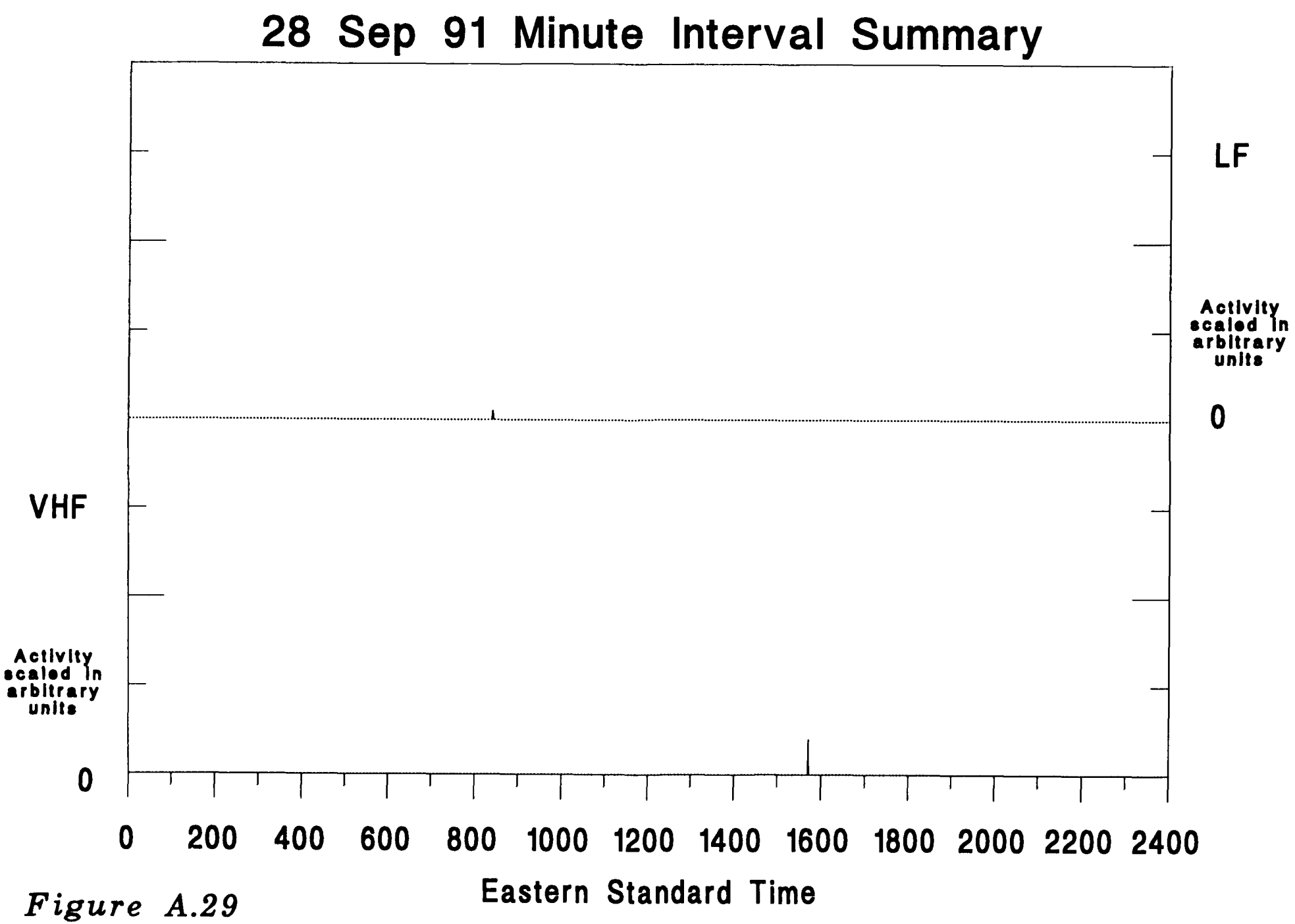
28 Sep 91 Minute Interval Summary
LF
Activity scaled in arbitrary units
0
VHF
Activity scaled in arbitrary units
0
0 200 400 600 800 1000 1200 1400 1600 1800 2000 2200 2400
Eastern Standard Time

Figure A.29

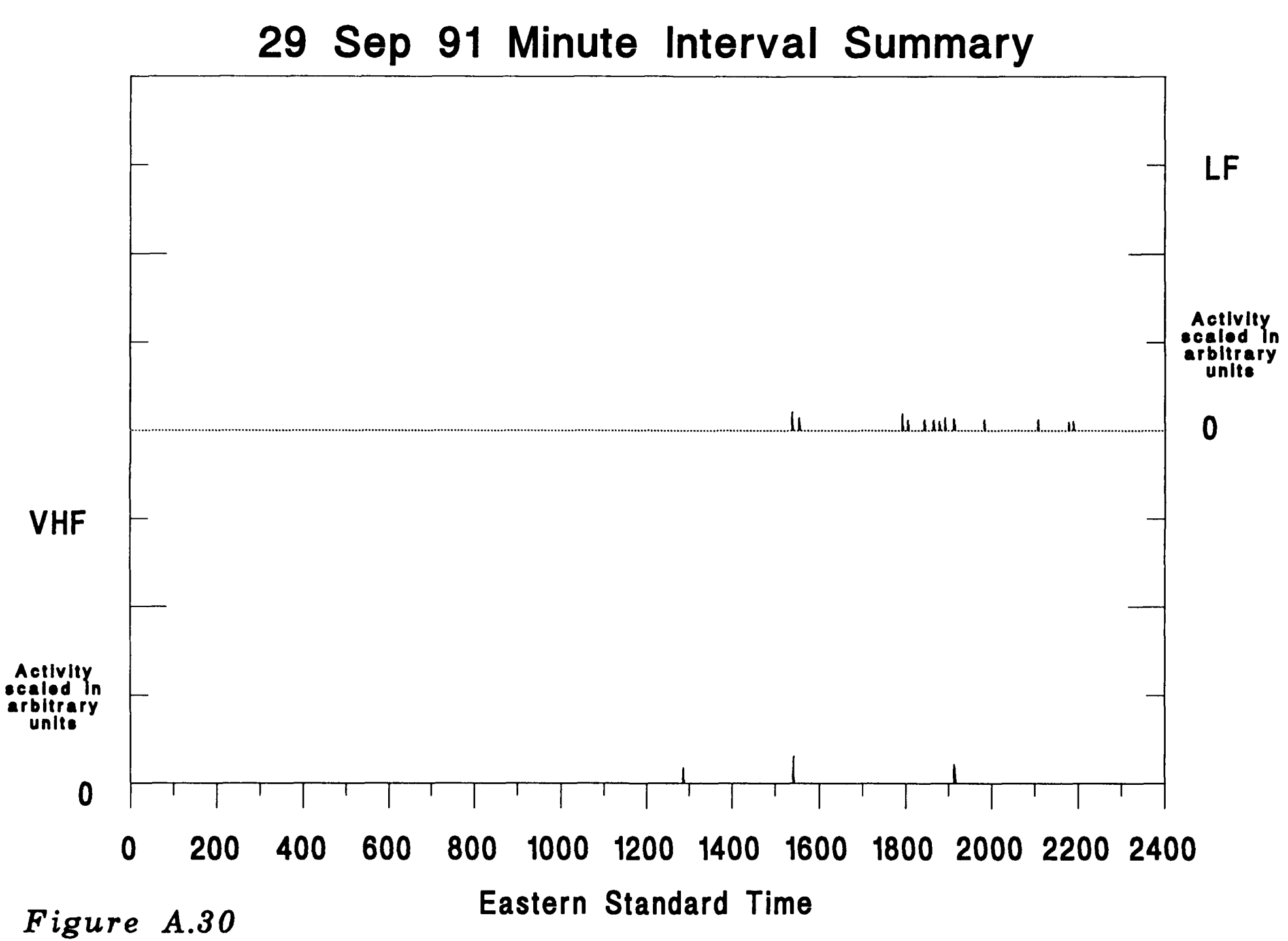
29 Sep 91 Minute Interval Summary
LF
Activity scaled in arbitrary units
0
VHF
Activity scaled in arbitrary units
0
0 200 400 600 800 1000 1200 1400 1600 1800 2000 2200 2400
Eastern Standard Time

Figure A.30

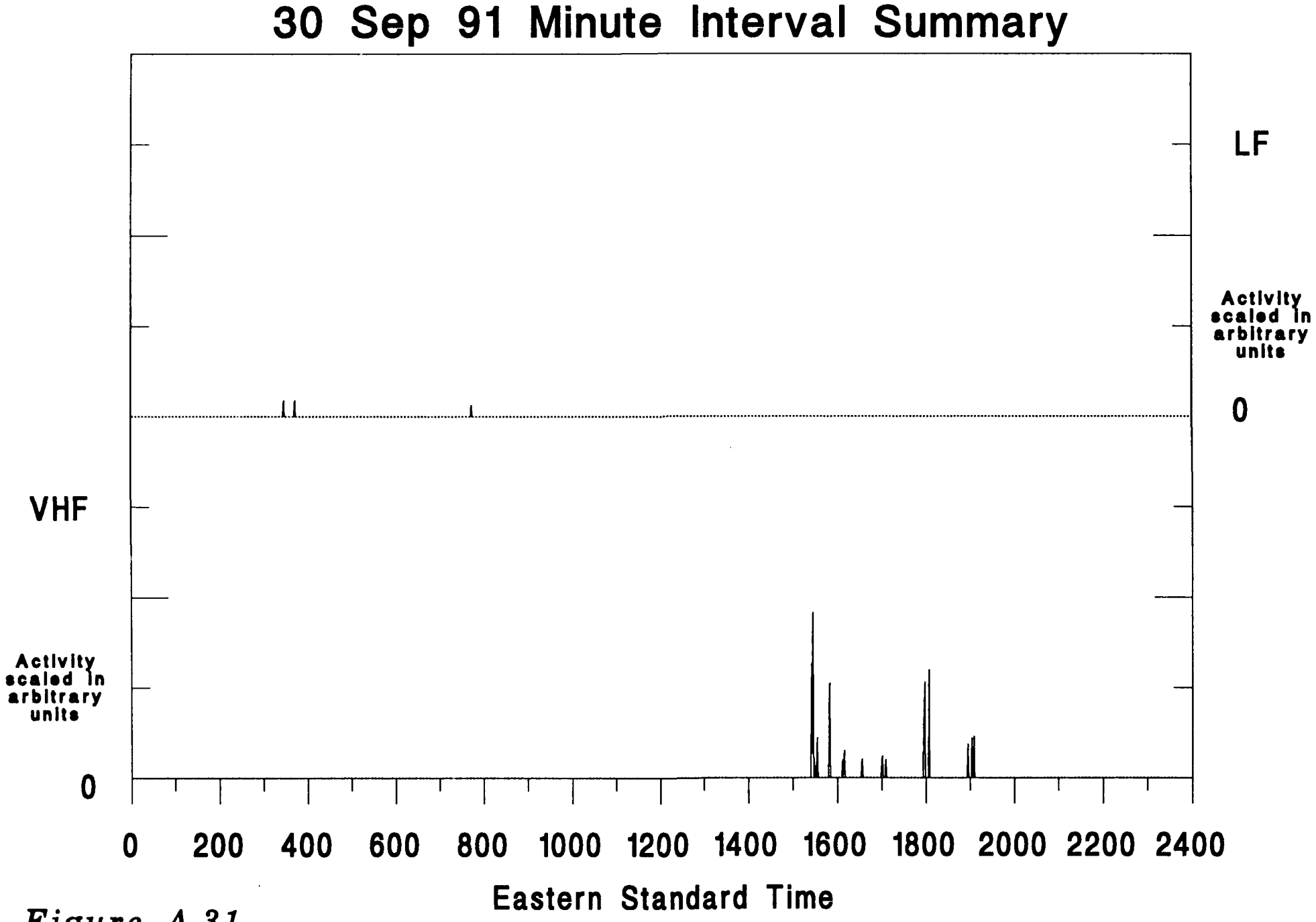
30 Sep 91 Minute Interval Summary
LF
Activity scaled in arbitrary units
0
VHF
Activity scaled in arbitrary units
0
0 200 400 600 800 1000 1200 1400 1600 1800 2000 2200 2400
Eastern Standard Time

Figure A.31

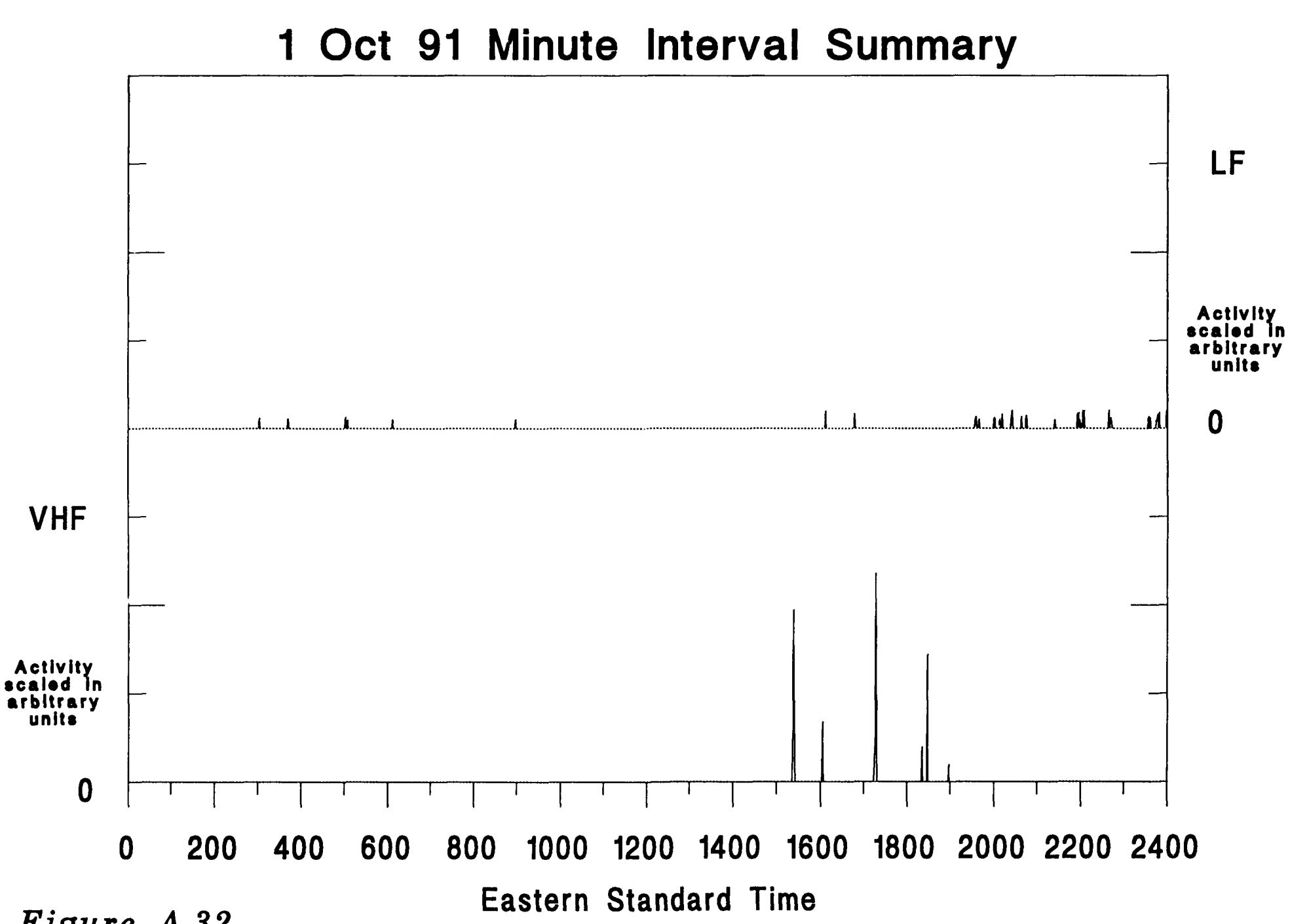
1 Oct 91 Minute Interval Summary
LF
Activity scaled in arbitrary units
0
VHF
Activity scaled in arbitrary units
0
0 200 400 600 800 1000 1200 1400 1600 1800 2000 2200 2400
Eastern Standard Time

Figure A.32

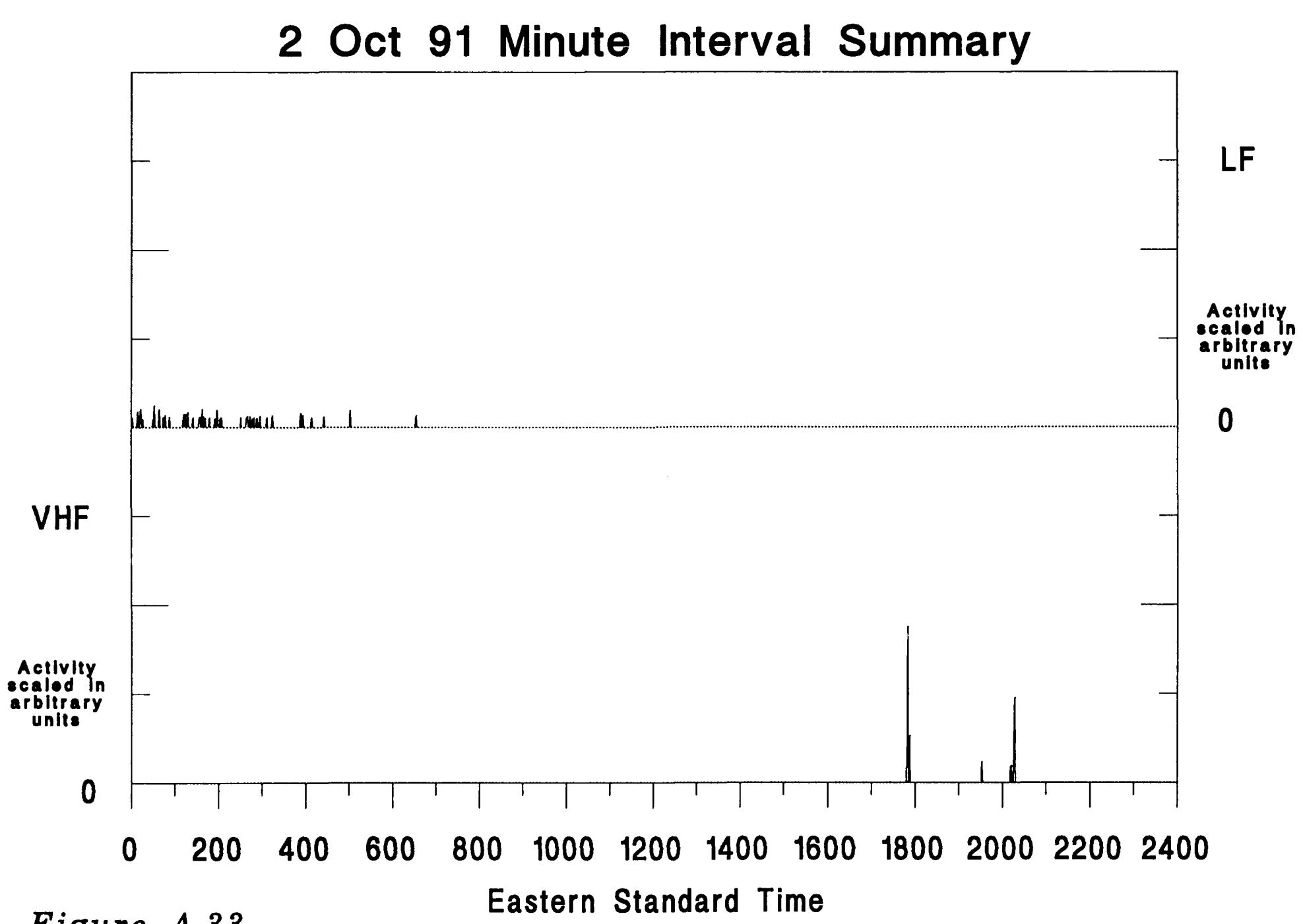
2 Oct 91 Minute Interval Summary
LF
Activity scaled in arbitrary units
0
VHF
Activity scaled in arbitrary units
0
0 200 400 600 800 1000 1200 1400 1600 1800 2000 2200 2400
Eastern Standard Time

Figure A.33

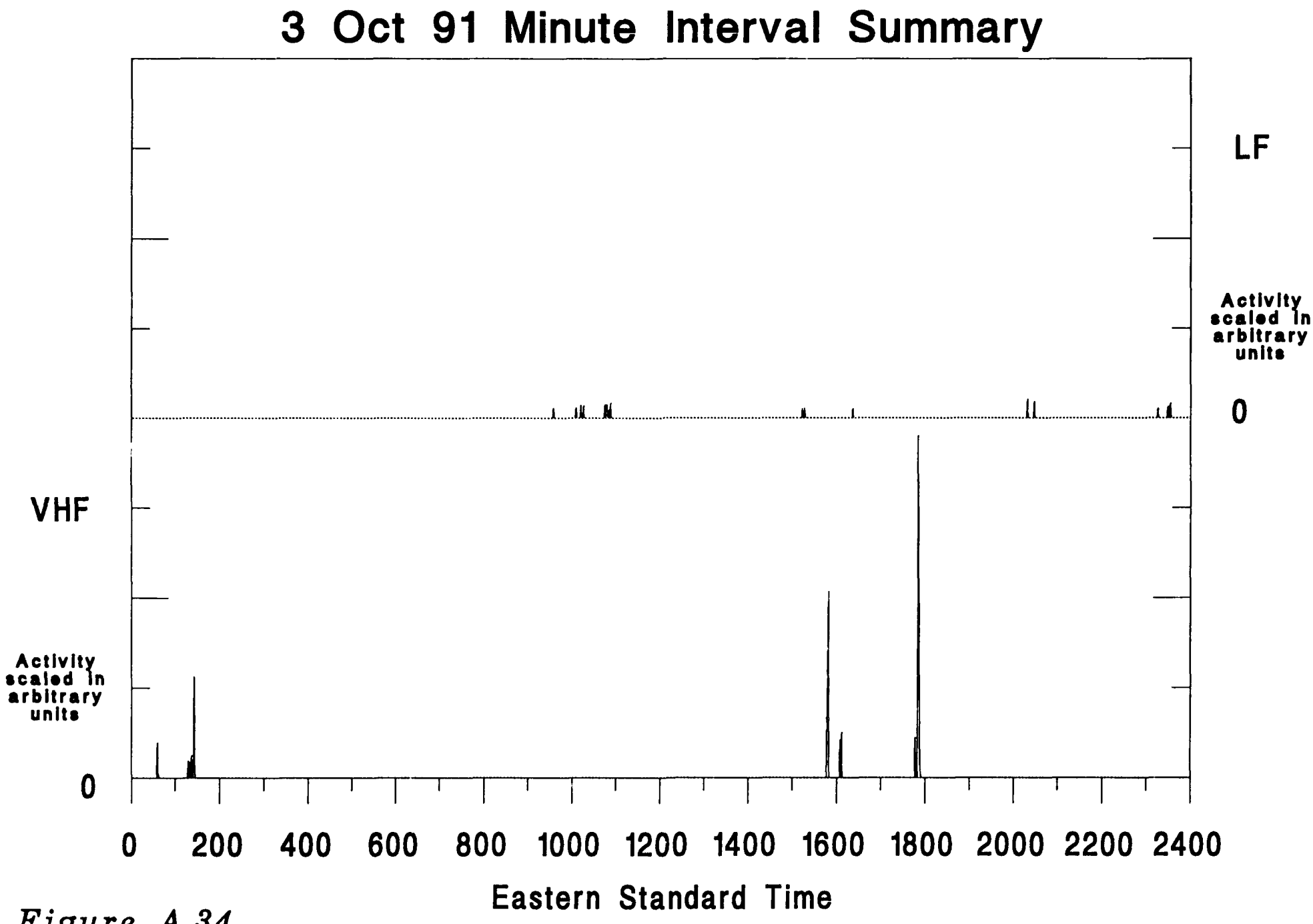
3 Oct 91 Minute Interval Summary
LF
Activity scaled in arbitrary units
0
VHF
Activity scaled in arbitrary units
0
0 200 400 600 800 1000 1200 1400 1600 1800 2000 2200 2400
Eastern Standard Time

Figure A.34

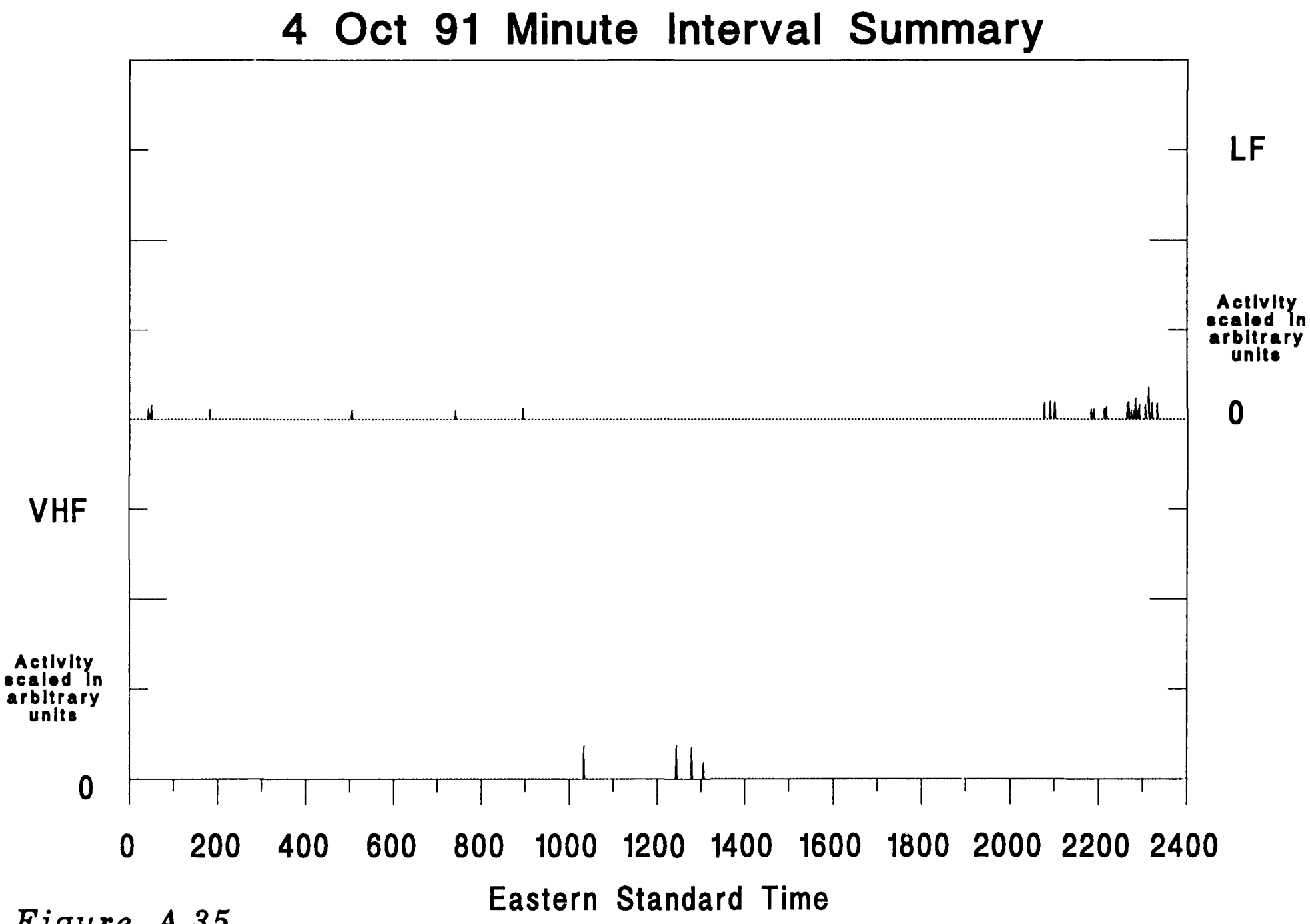
4 Oct 91 Minute Interval Summary
LF
Activity scaled in arbitrary units
0
VHF
Activity scaled in arbitrary units
0
0 200 400 600 800 1000 1200 1400 1600 1800 2000 2200 2400
Eastern Standard Time

Figure A.35

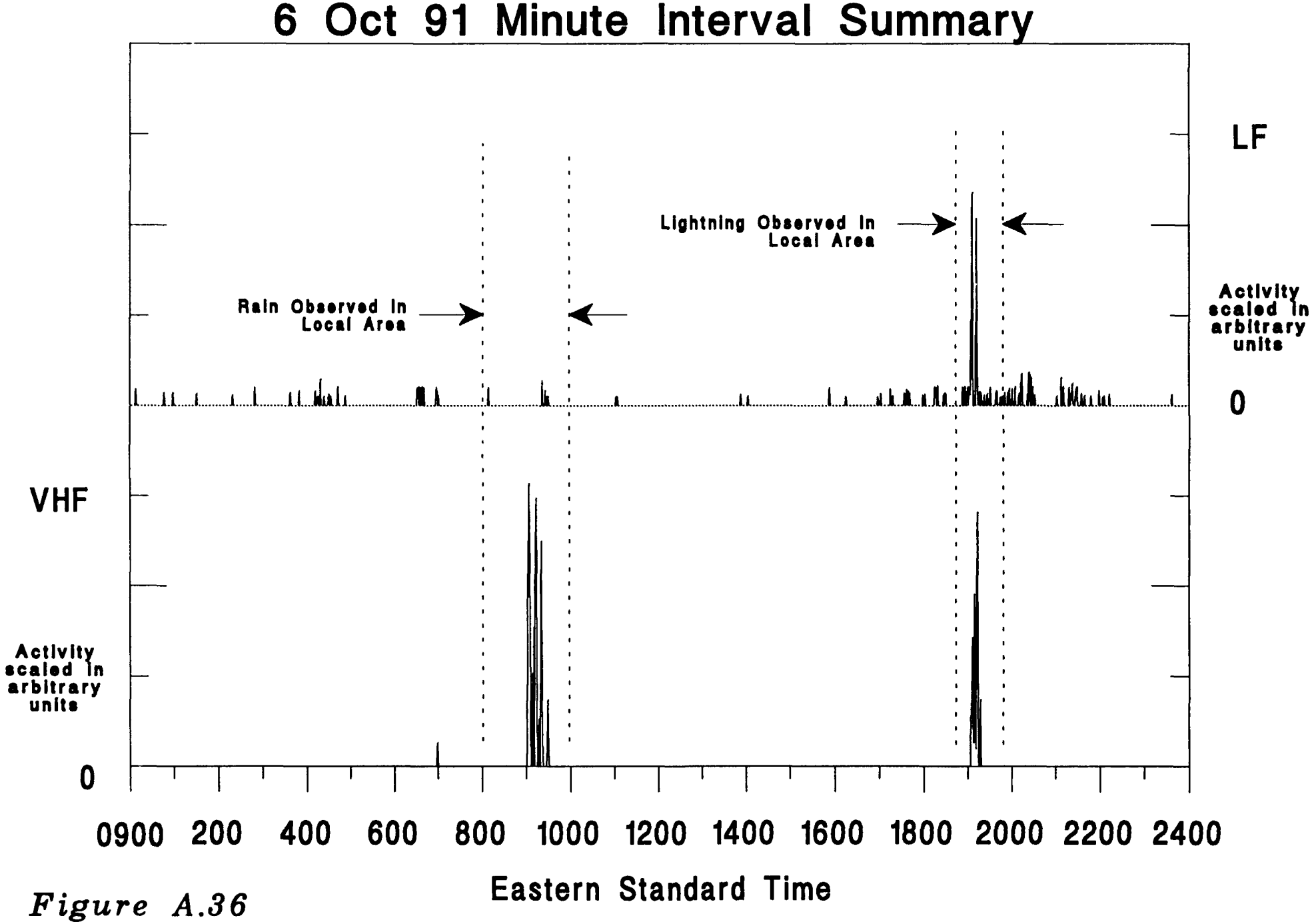
6 Oct 91 Minute Interval Summary
LF
Lightning Observed In Local Area
Rain Observed In Local Area
Activity scaled in arbitrary units
0
VHF
Activity scaled in arbitrary units
0
0900 200 400 600 800 1000 1200 1400 1600 1800 2000 2200 2400
Eastern Standard Time

Figure A.36

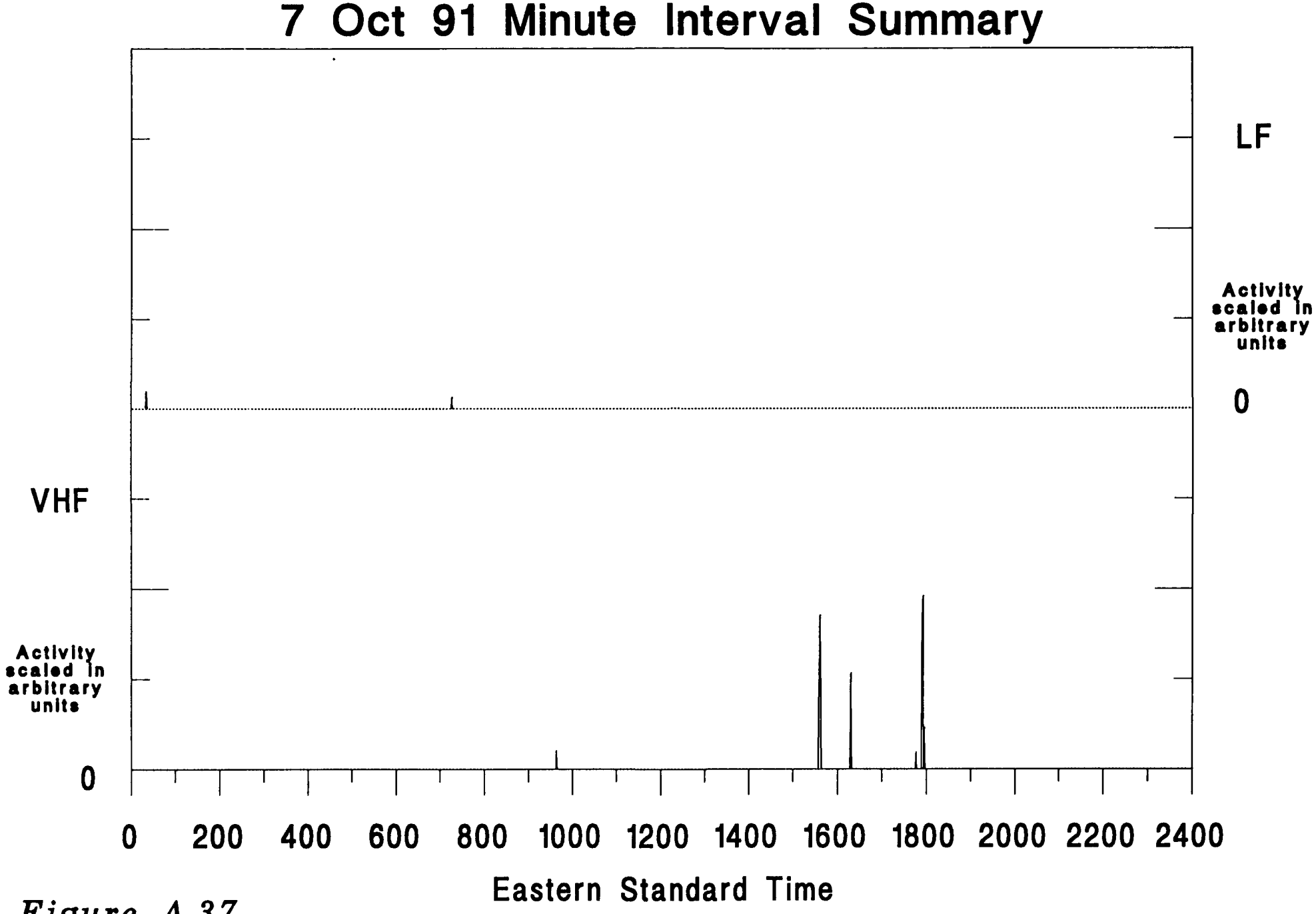
7 Oct 91 Minute Interval Summary
LF
Activity scaled in arbitrary units
0
VHF
Activity scaled in arbitrary units
0
0 200 400 600 800 1000 1200 1400 1600 1800 2000 2200 2400
Eastern Standard Time

Figure A.37

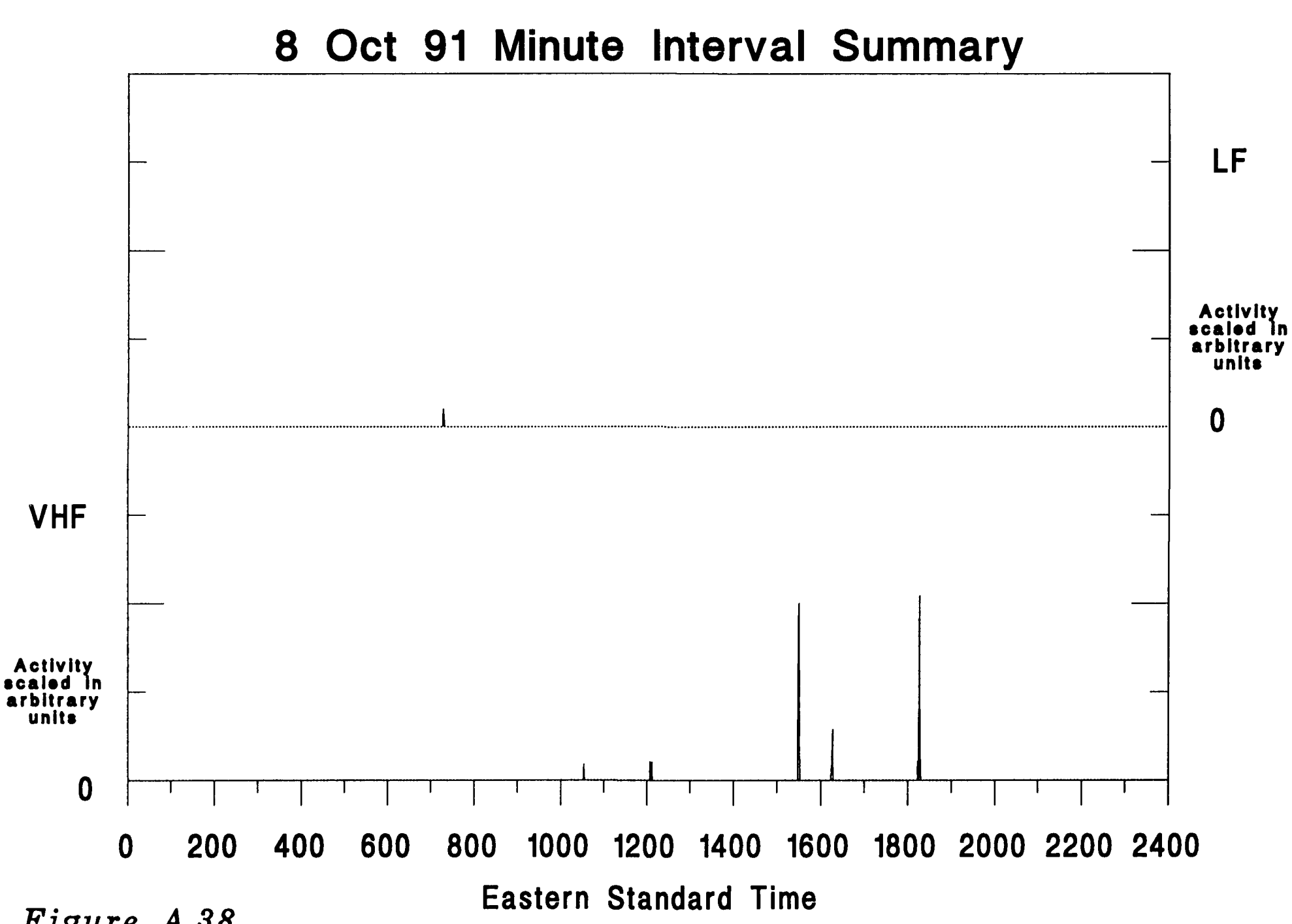
8 Oct 91 Minute Interval Summary
LF
Activity scaled in arbitrary units
0
VHF
Activity scaled in arbitrary units
0
0 200 400 600 800 1000 1200 1400 1600 1800 2000 2200 2400
Eastern Standard Time

Figure A.38

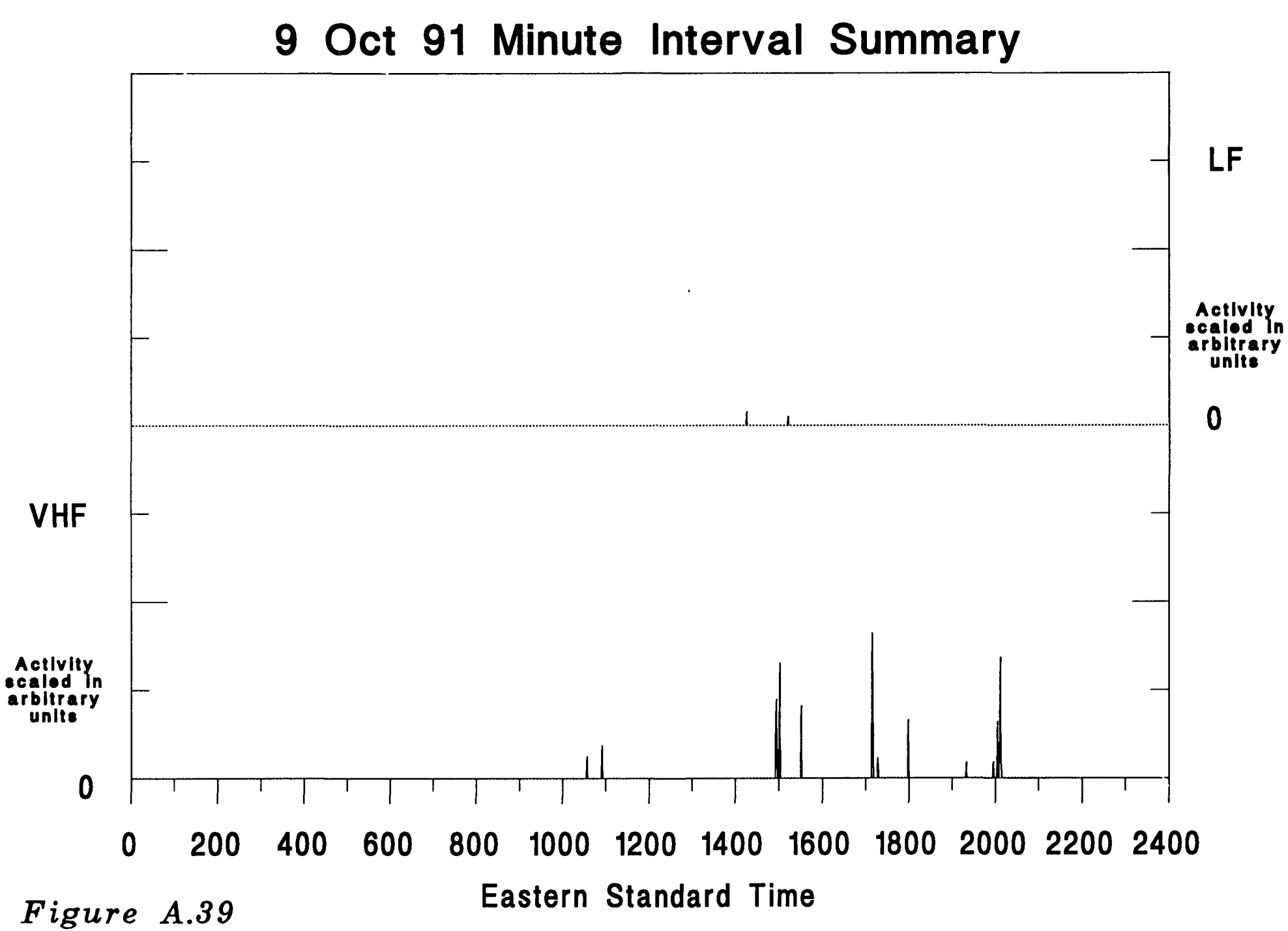
9 Oct 91 Minute Interval Summary
LF
Activity scaled in arbitrary units
0
VHF
Activity scaled in arbitrary units
0
0 200 400 600 800 1000 1200 1400 1600 1800 2000 2200 2400
Eastern Standard Time

Figure A.39

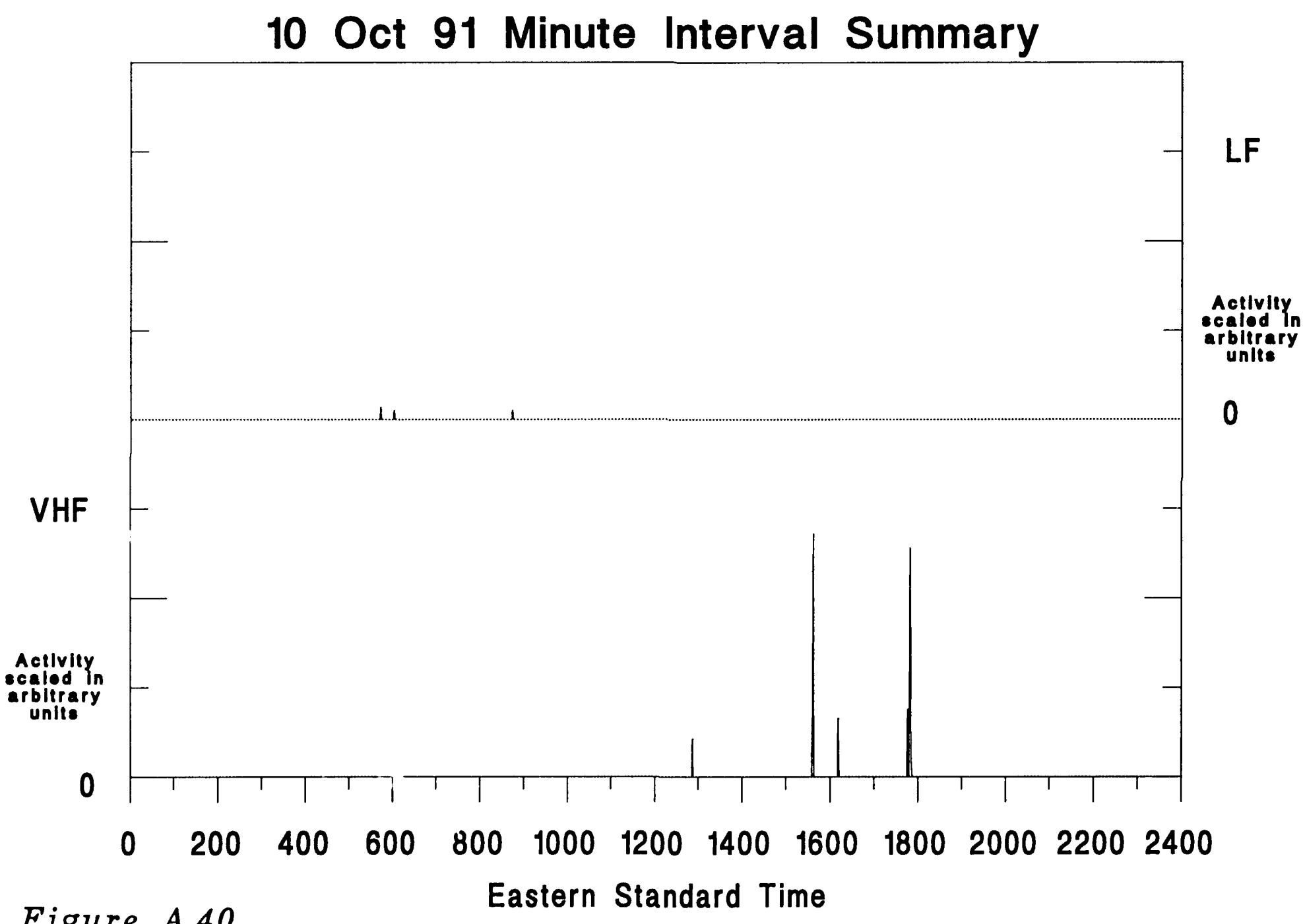
10 Oct 91 Minute Interval Summary
LF
Activity scaled in arbitrary units
0
VHF
Activity scaled in arbitrary units
0
0 200 400 600 800 1000 1200 1400 1600 1800 2000 2200 2400
Eastern Standard Time

Figure A.40

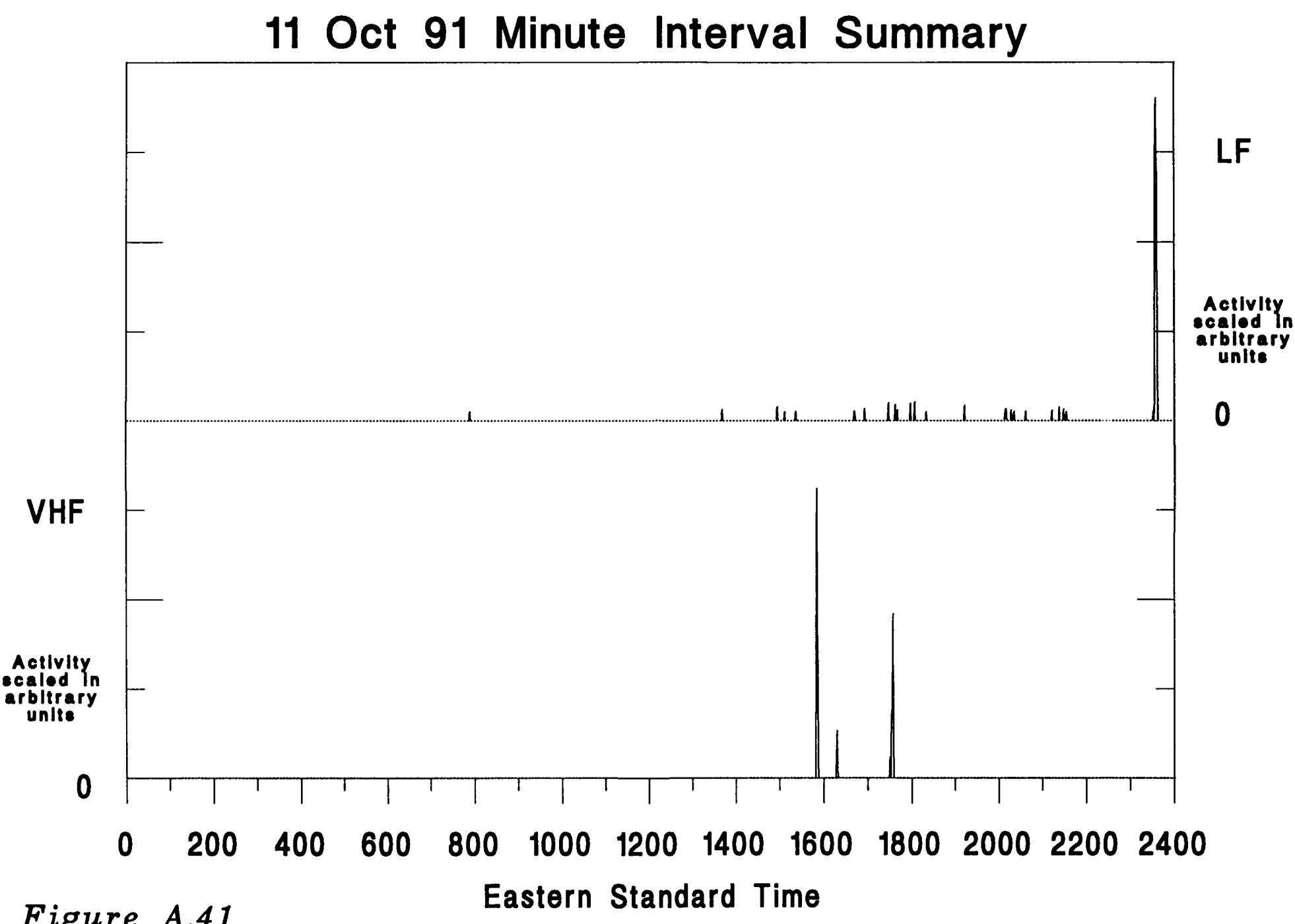
11 Oct 91 Minute Interval Summary
LF
Activity scaled in arbitrary units
0
VHF
Activity scaled in arbitrary units
0
0 200 400 600 800 1000 1200 1400 1600 1800 2000 2200 2400
Eastern Standard Time

Figure A.41

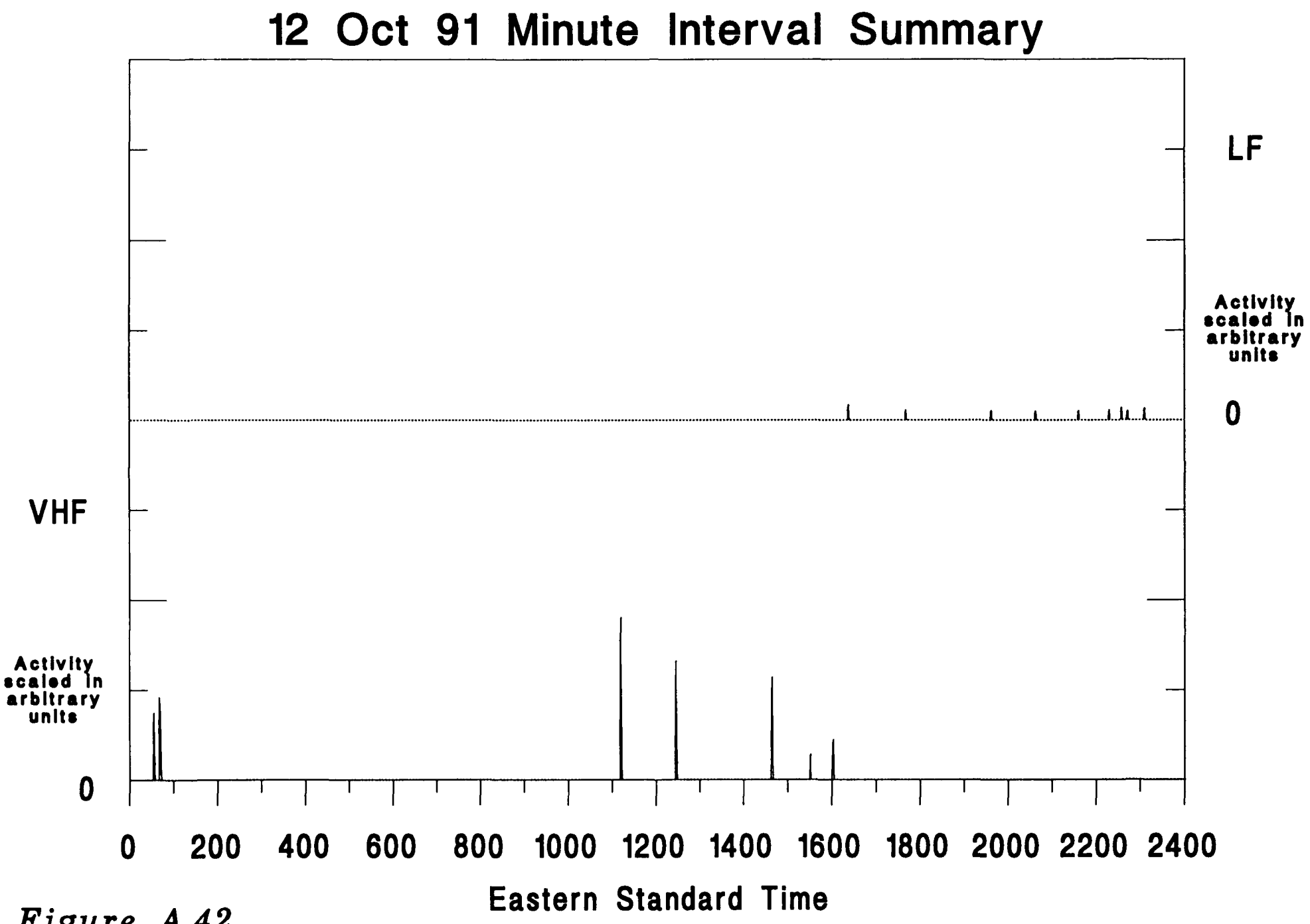
12 Oct 91 Minute Interval Summary
LF
Activity scaled in arbitrary units
0
VHF
Activity scaled in arbitrary units
0
0 200 400 600 800 1000 1200 1400 1600 1800 2000 2200 2400
Eastern Standard Time

Figure A.42

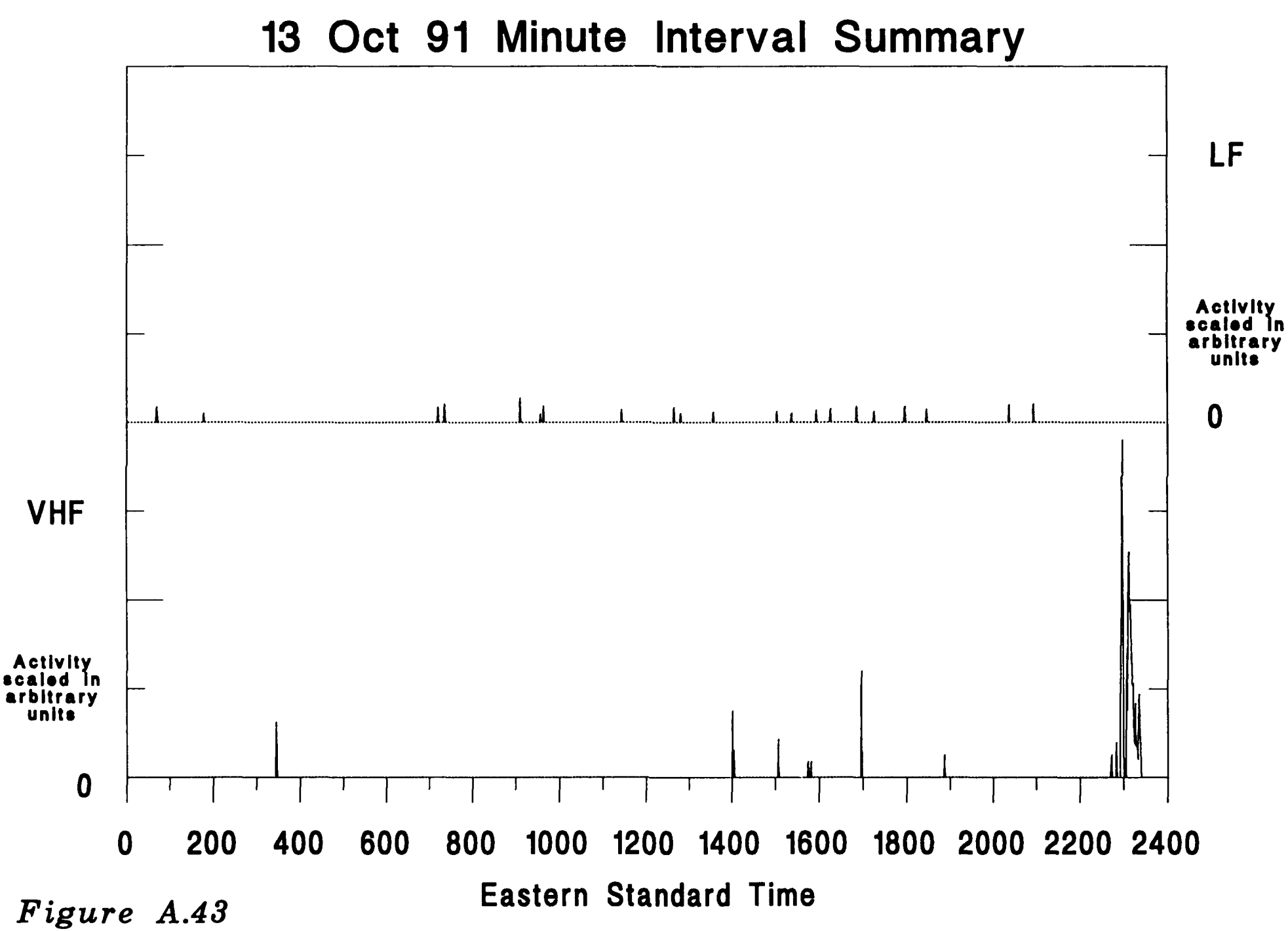
13 Oct 91 Minute Interval Summary
LF
Activity scaled in arbitrary units
0
VHF
Activity scaled in arbitrary units
0
0 200 400 600 800 1000 1200 1400 1600 1800 2000 2200 2400
Eastern Standard Time

Figure A.43

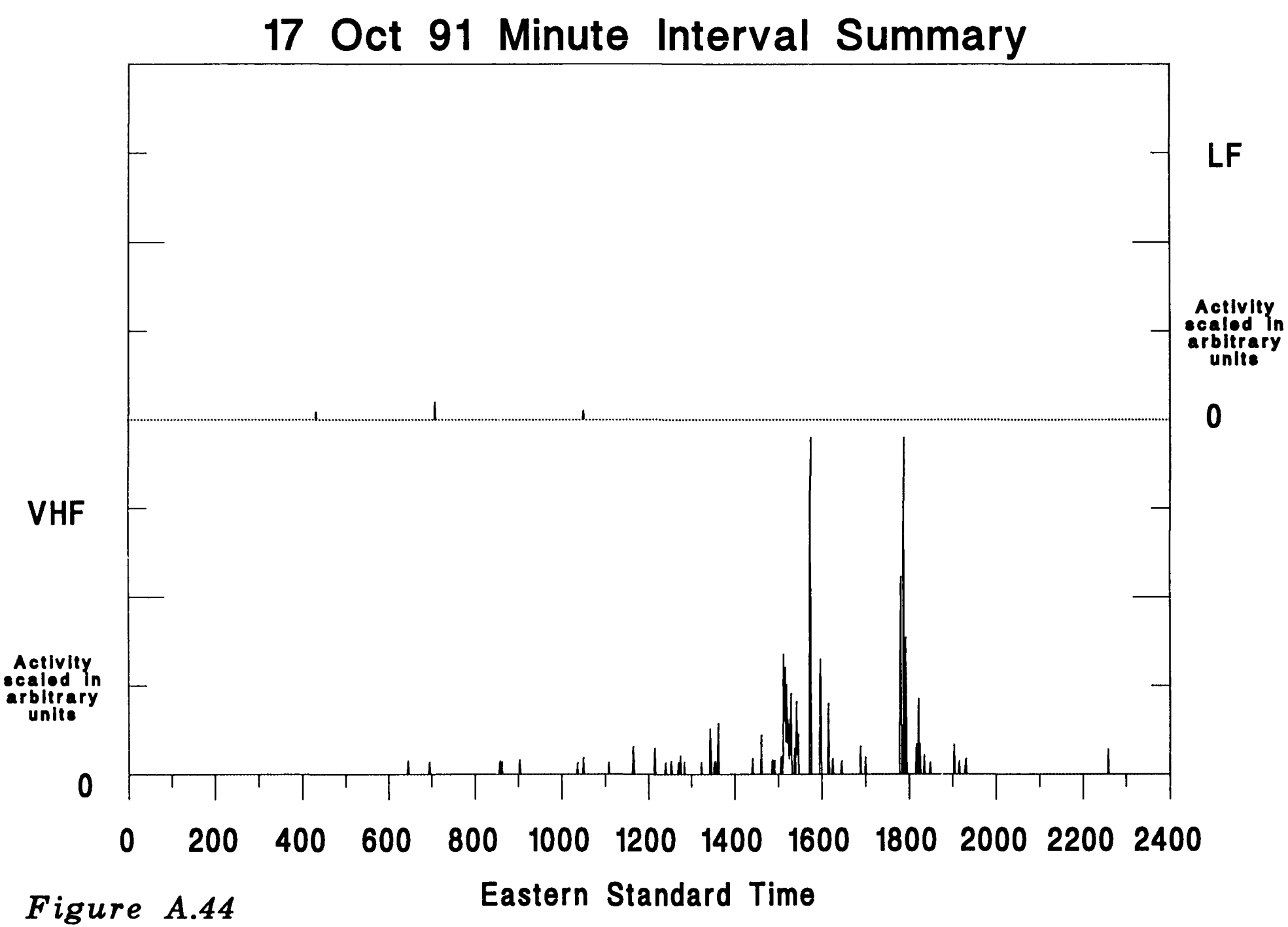
17 Oct 91 Minute Interval Summary
LF
Activity scaled in arbitrary units
0
VHF
Activity scaled in arbitrary units
0
0 200 400 600 800 1000 1200 1400 1600 1800 2000 2200 2400
Eastern Standard Time

Figure A.44

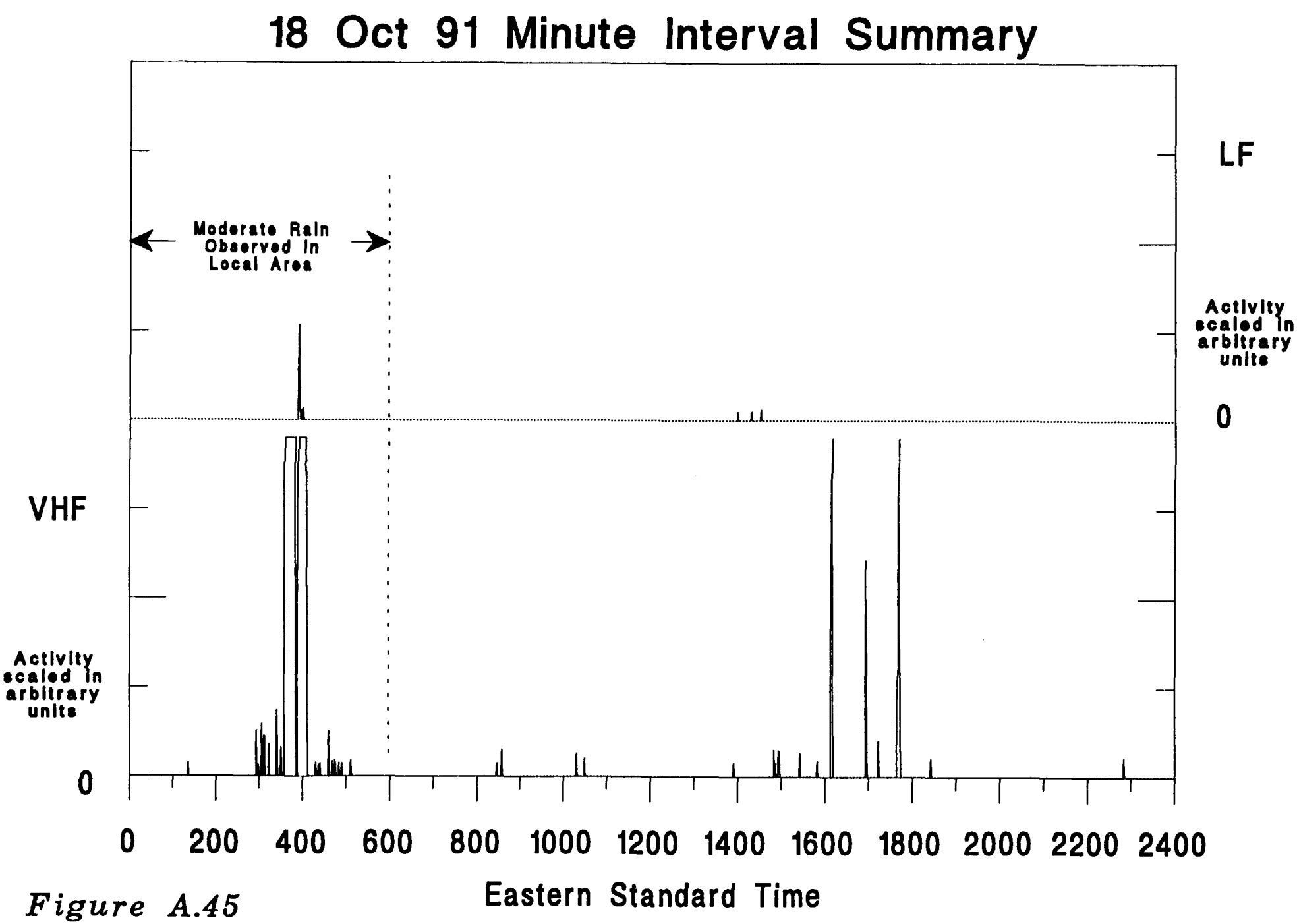
18 Oct 91 Minute Interval Summary
LF
Moderate Rain Observed In Local Area
Activity scaled in arbitrary units
0
VHF
Activity scaled in arbitrary units
0
0 200 400 600 800 1000 1200 1400 1600 1800 2000 2200 2400
Eastern Standard Time

Figure A.45

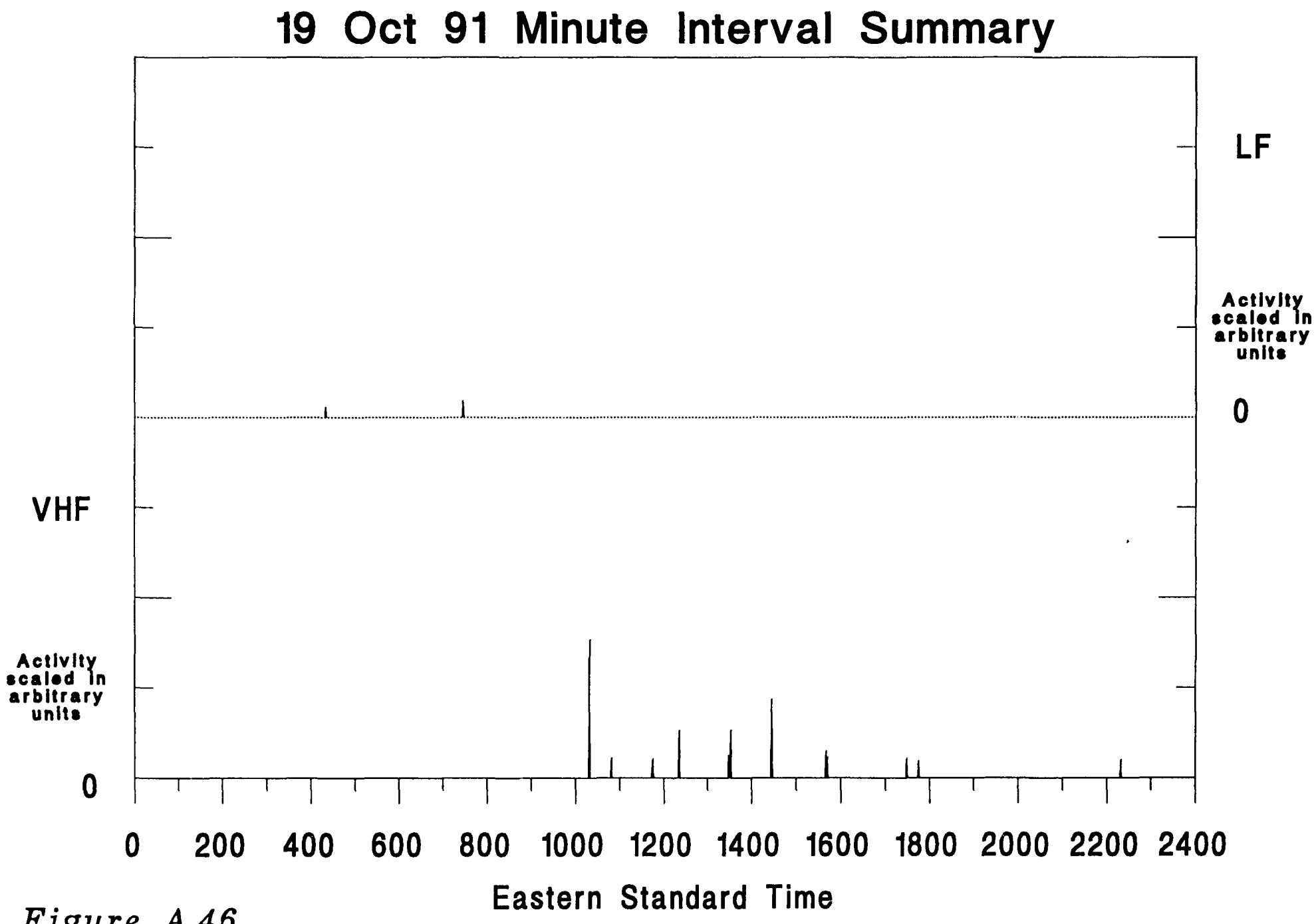
19 Oct 91 Minute Interval Summary
LF
Activity scaled in arbitrary units
0
VHF
Activity scaled in arbitrary units
0
0 200 400 600 800 1000 1200 1400 1600 1800 2000 2200 2400
Eastern Standard Time

Figure A.46

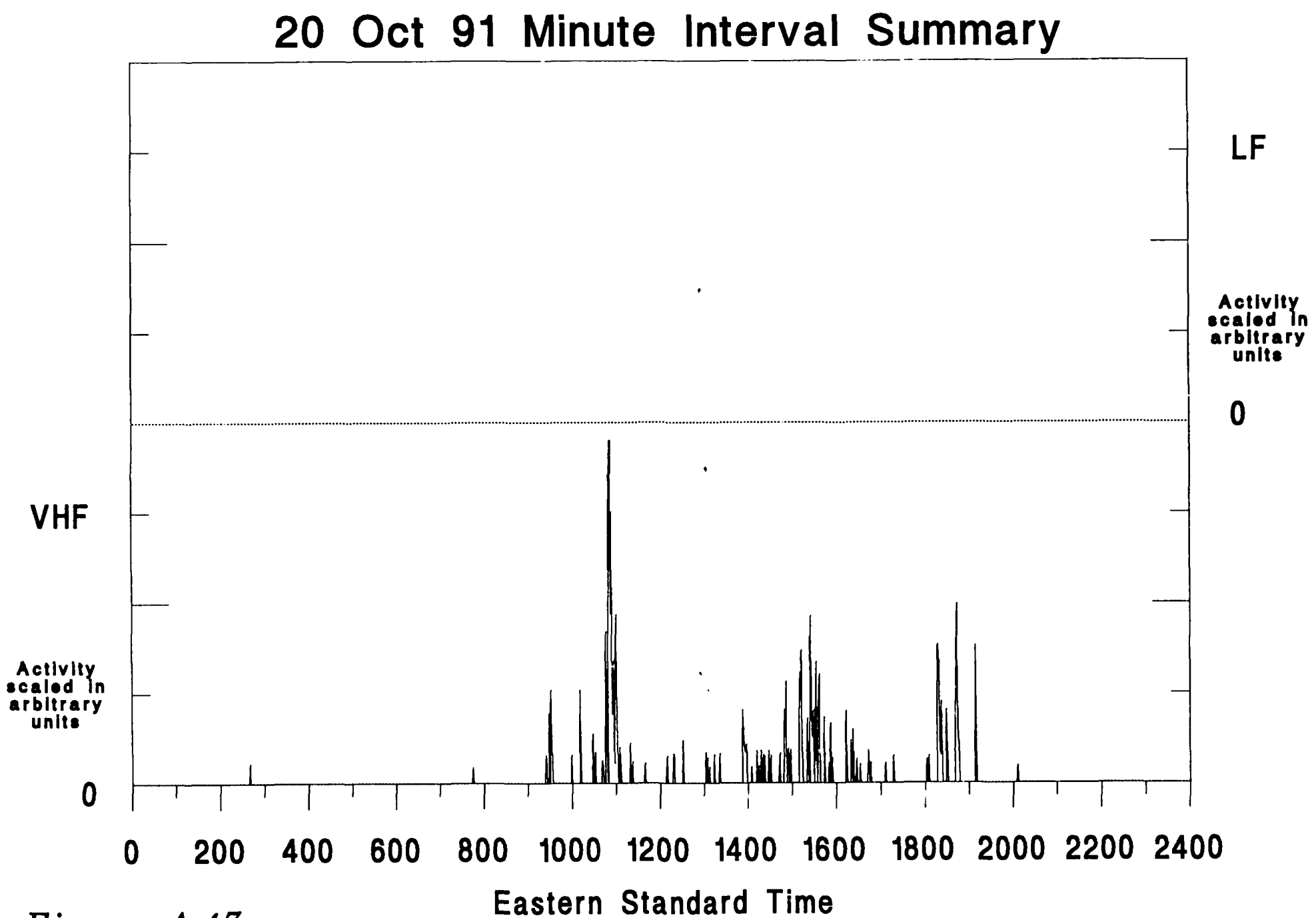
20 Oct 91 Minute Interval Summary
LF
Activity scaled in arbitrary units
0
VHF
Activity scaled in arbitrary units
0
0 200 400 600 800 1000 1200 1400 1600 1800 2000 2200 2400
Eastern Standard Time

Figure A.47

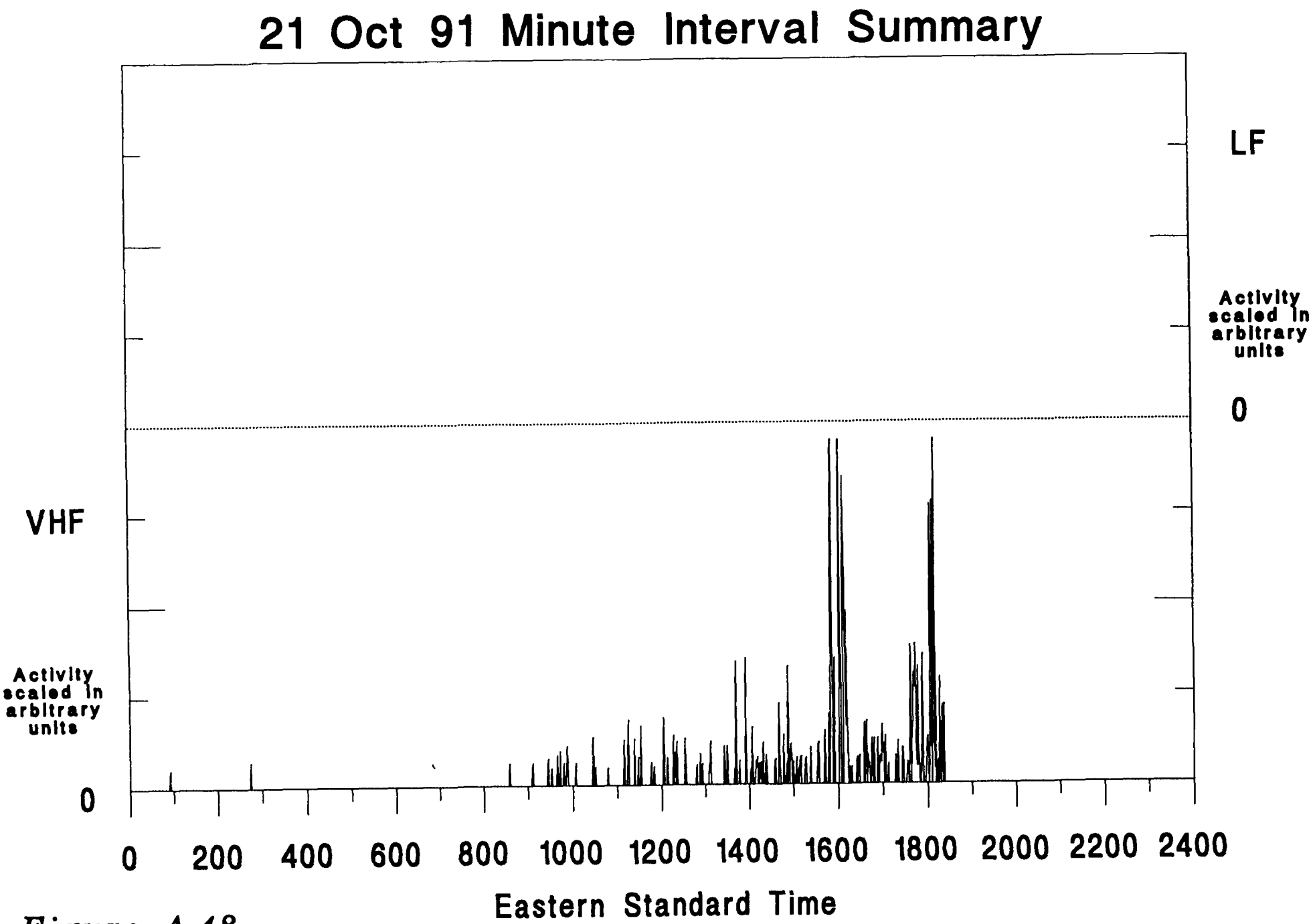
21 Oct 91 Minute Interval Summary
LF
Activity scaled in arbitrary units
0
VHF
Activity scaled in arbitrary units
0
0 200 400 600 800 1000 1200 1400 1600 1800 2000 2200 2400
Eastern Standard Time

Figure A.48

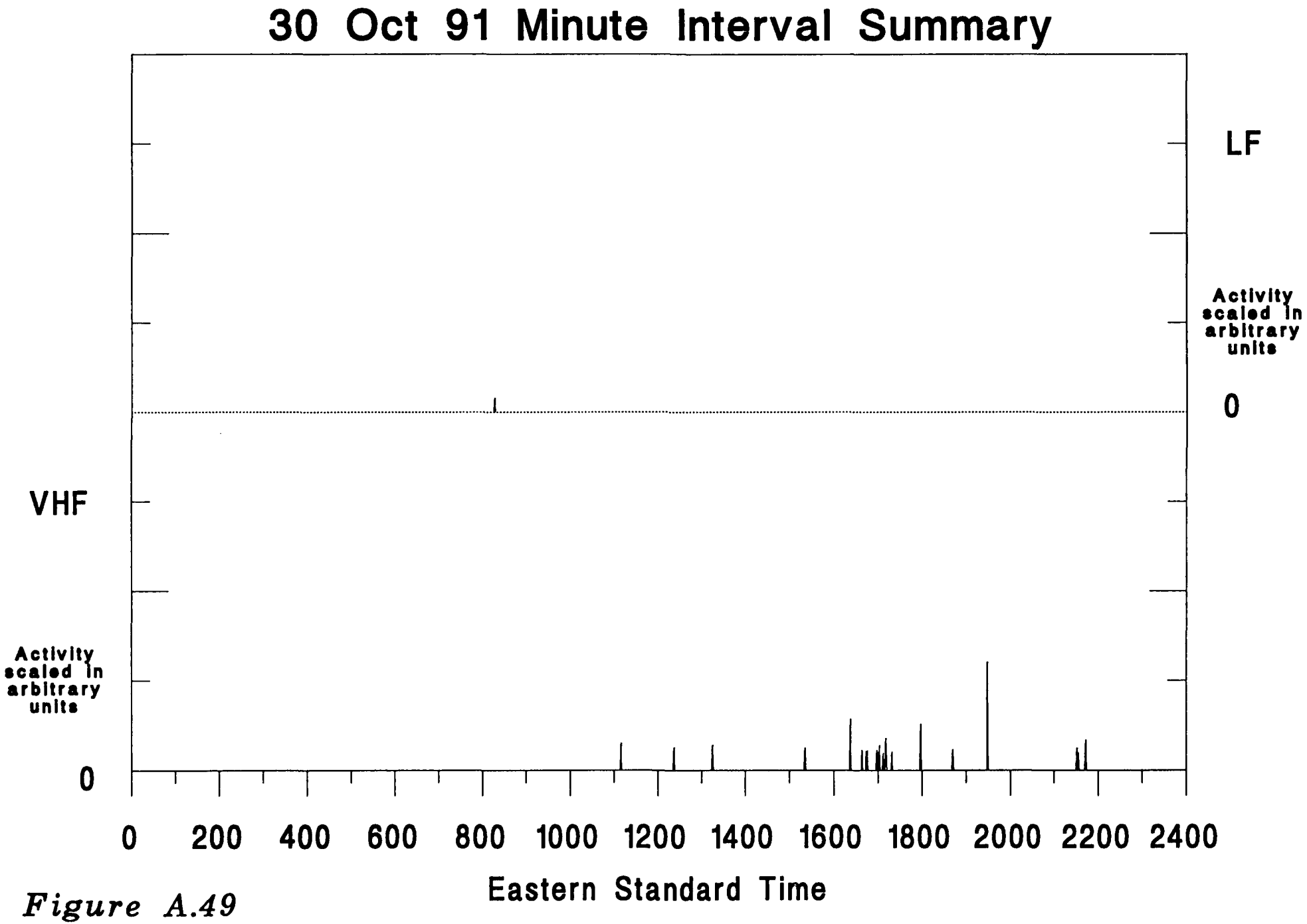
30 Oct 91 Minute Interval Summary
LF
Activity scaled in arbitrary units
0
VHF
Activity scaled in arbitrary units
0
0 200 400 600 800 1000 1200 1400 1600 1800 2000 2200 2400
Eastern Standard Time

Figure A.49

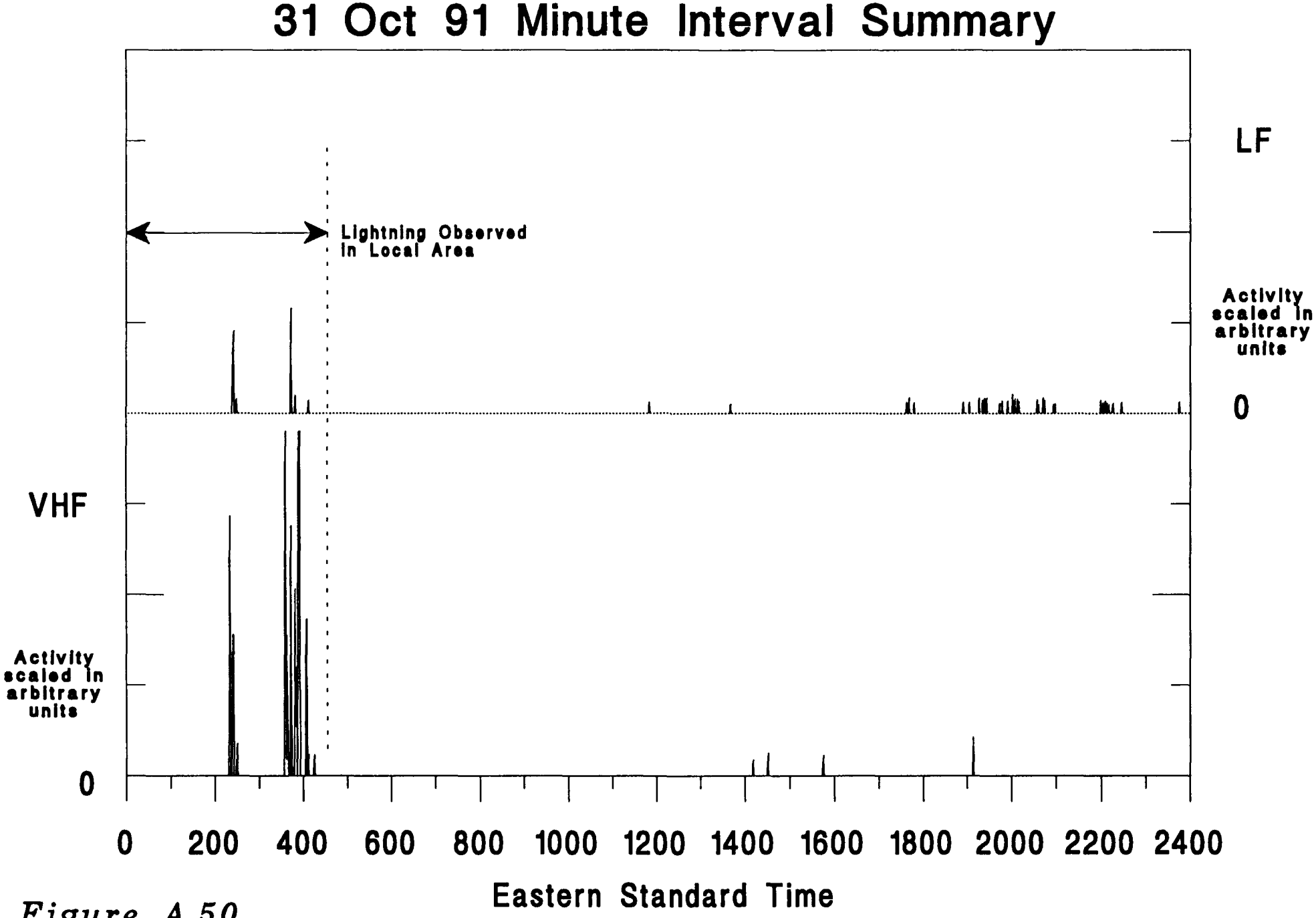
31 Oct 91 Minute Interval Summary
LF
Lightning Observed
in Local Area
Activity
scaled in
arbitrary
units
0
VHF
Activity
scaled in
arbitrary
units
0
0
200
400
600
800
1000
1200
1400
1600
1800
2000
2200
2400
Eastern Standard Time

Figure A.50

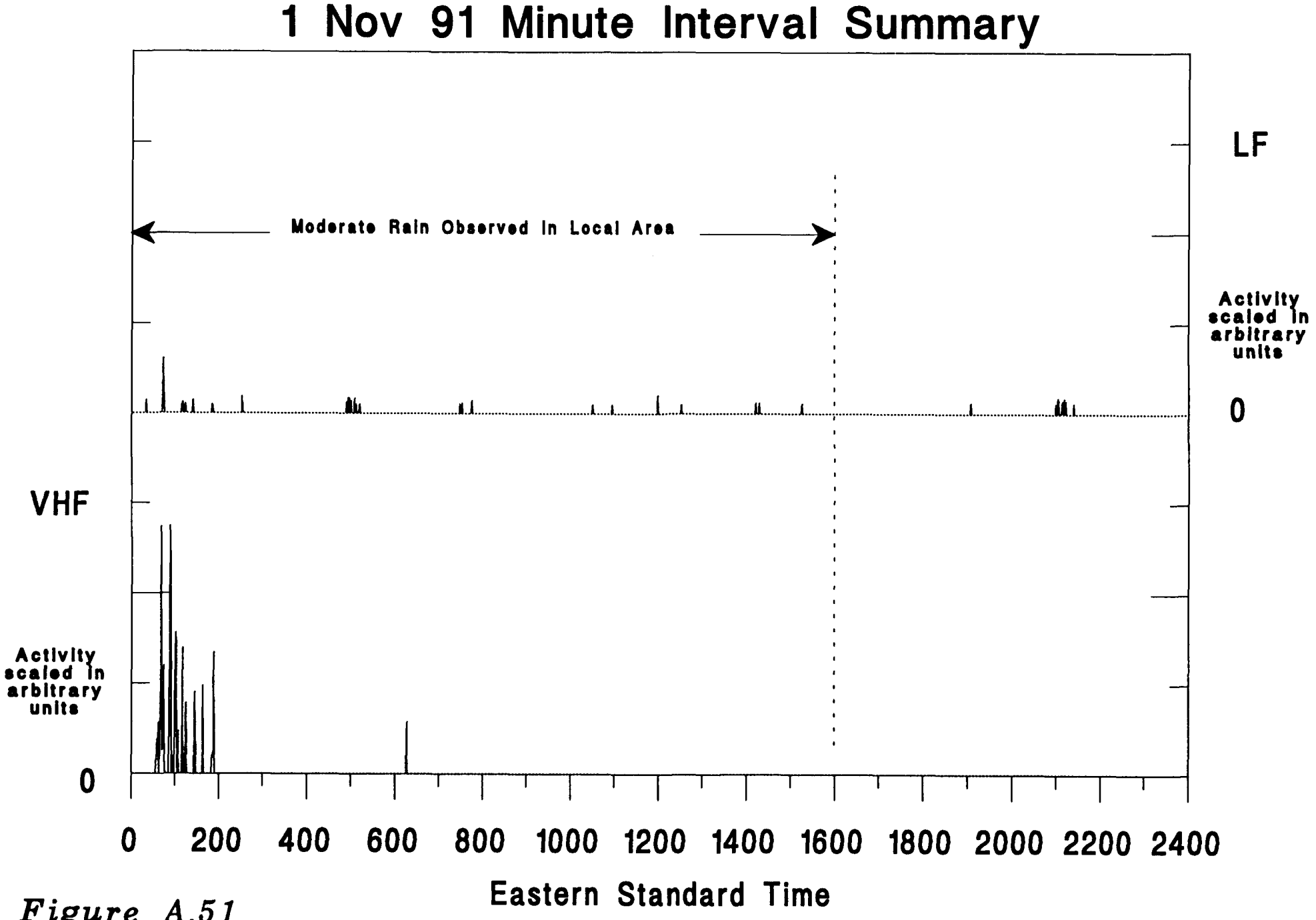
1 Nov 91 Minute Interval Summary
LF
Moderate Rain Observed In Local Area
Activity scaled in arbitrary units
0
VHF
Activity scaled in arbitrary units
0
0 200 400 600 800 1000 1200 1400 1600 1800 2000 2200 2400
Eastern Standard Time

Figure A.51

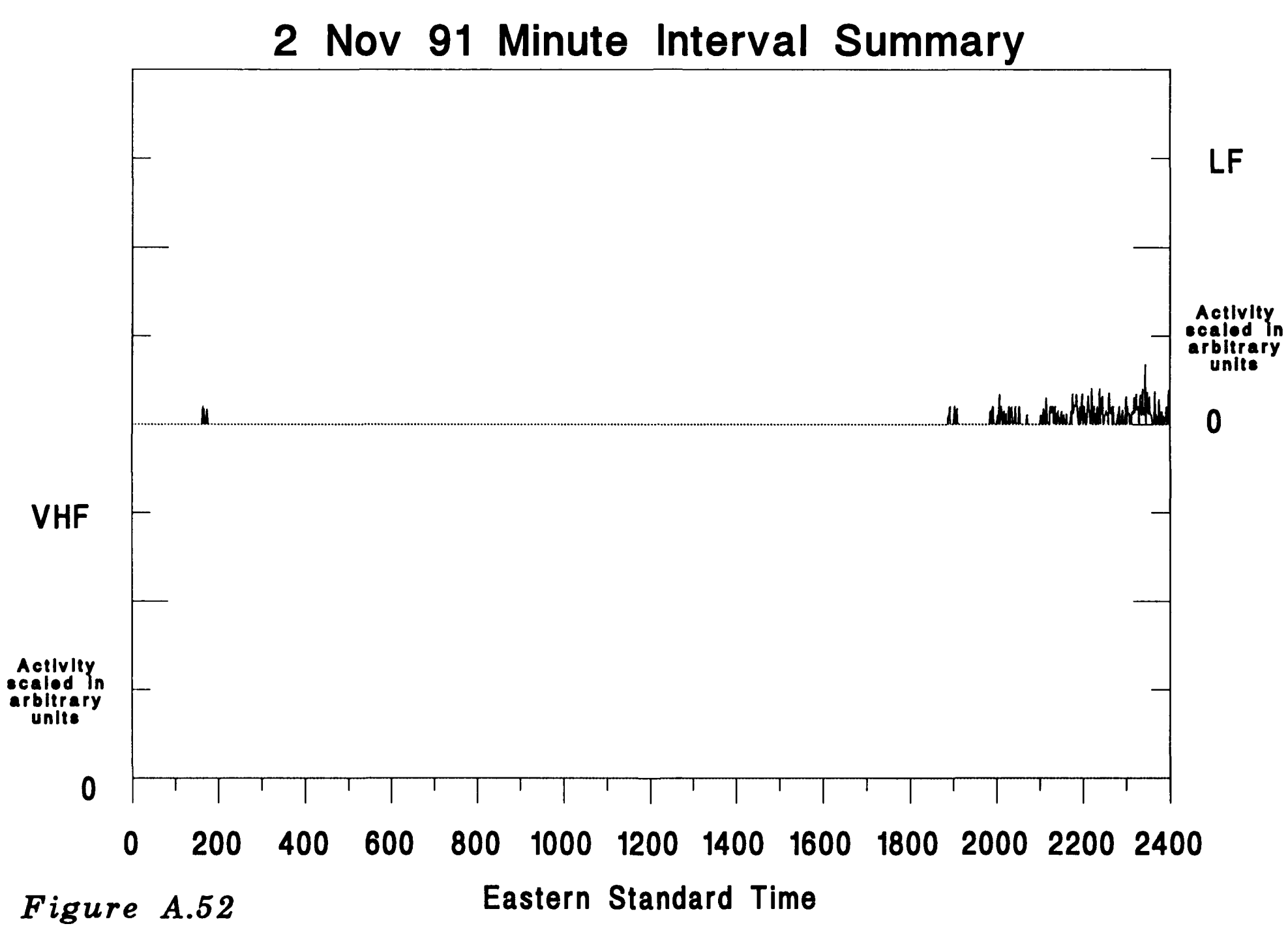
2 Nov 91 Minute Interval Summary
LF
Activity scaled in arbitrary units
0
VHF
Activity scaled in arbitrary units
0
0 200 400 600 800 1000 1200 1400 1600 1800 2000 2200 2400
Eastern Standard Time

Figure A.52

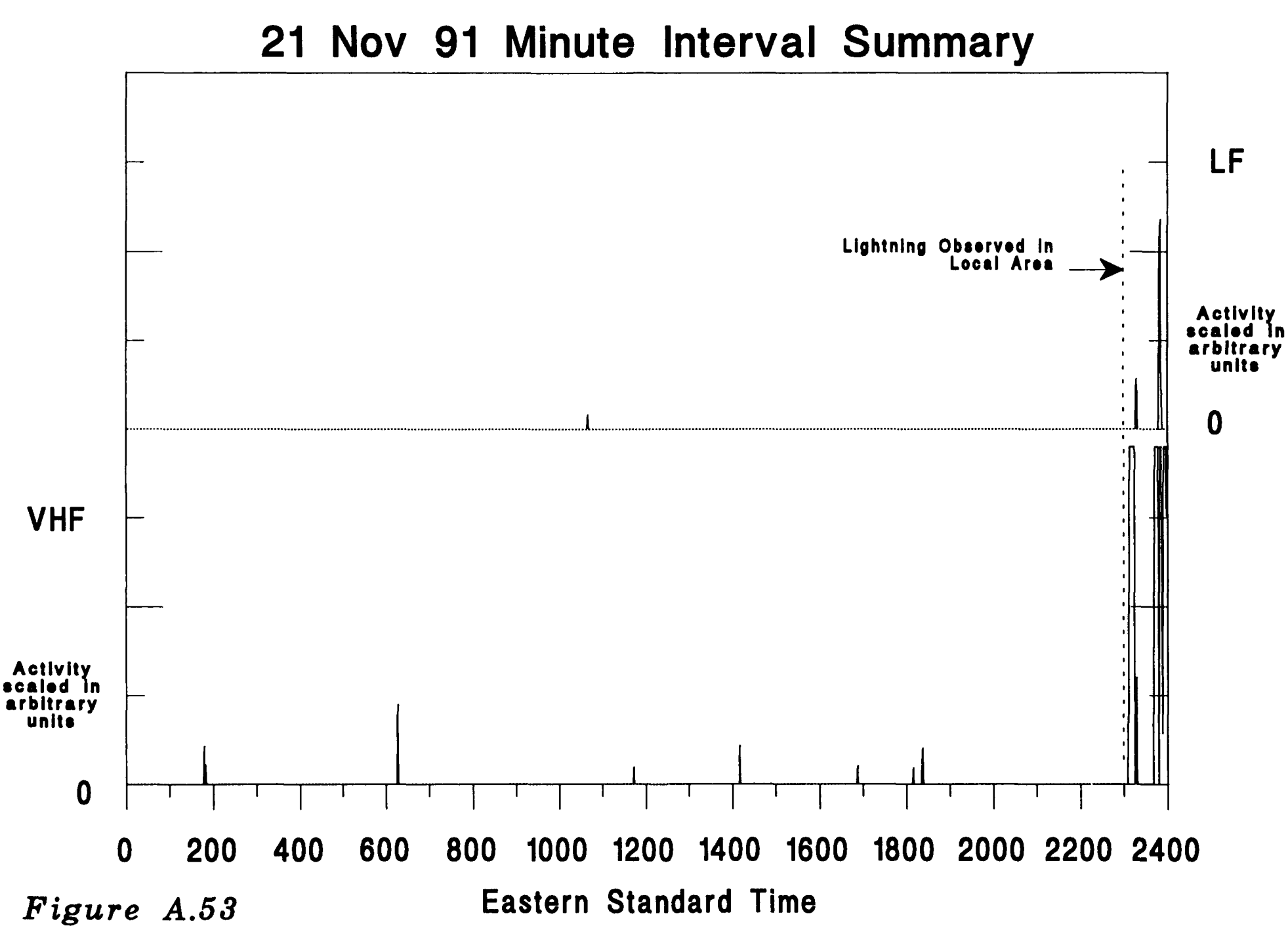
21 Nov 91 Minute Interval Summary
LF
Lightning Observed in Local Area
Activity scaled in arbitrary units
0
VHF
Activity scaled in arbitrary units
0
0 200 400 600 800 1000 1200 1400 1600 1800 2000 2200 2400
Eastern Standard Time

Figure A.53

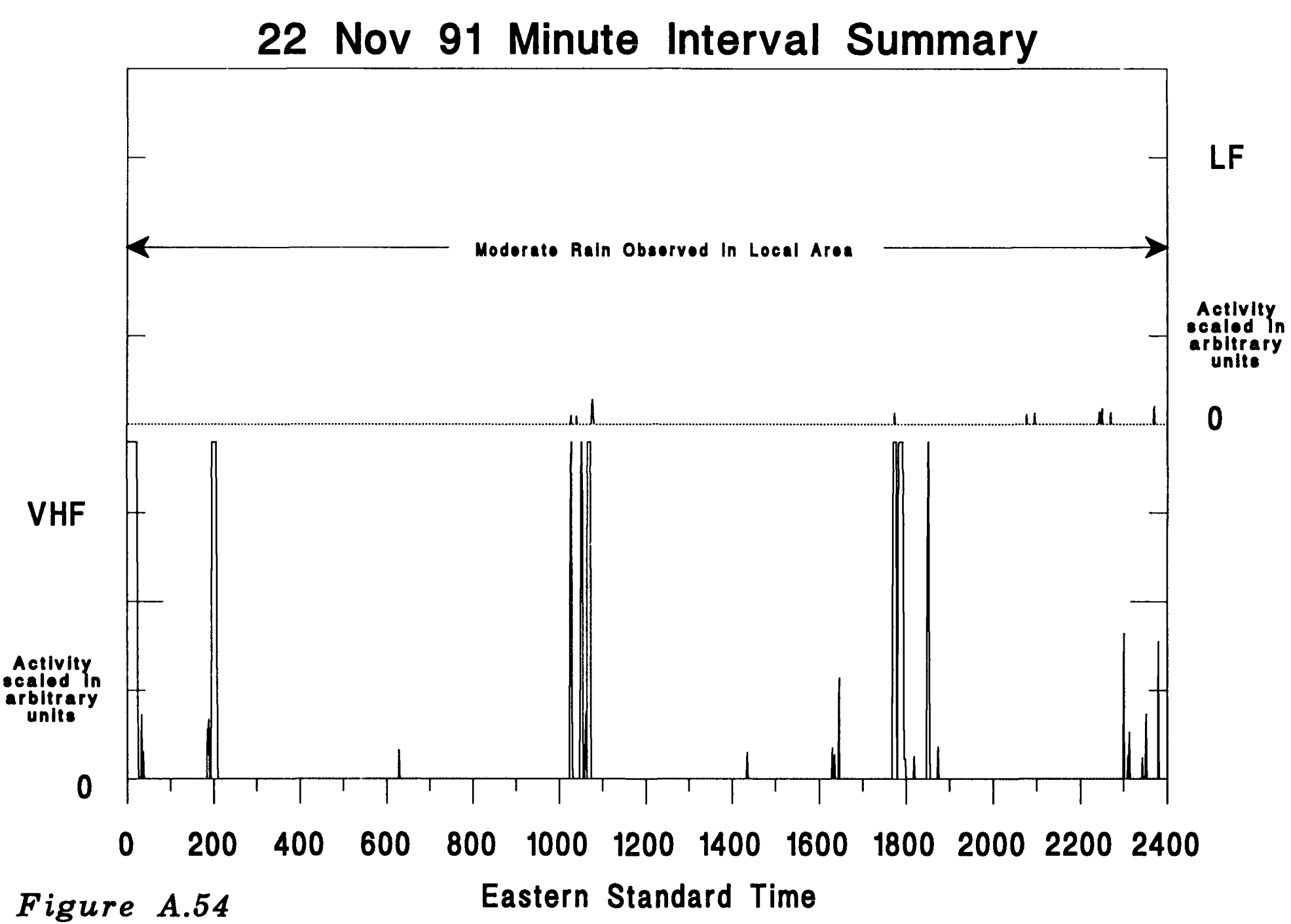
22 Nov 91 Minute Interval Summary
LF
Moderate Rain Observed in Local Area
Activity scaled in arbitrary units
0
VHF
Activity scaled in arbitrary units
0
0 200 400 600 800 1000 1200 1400 1600 1800 2000 2200 2400
Eastern Standard Time

Figure A.54

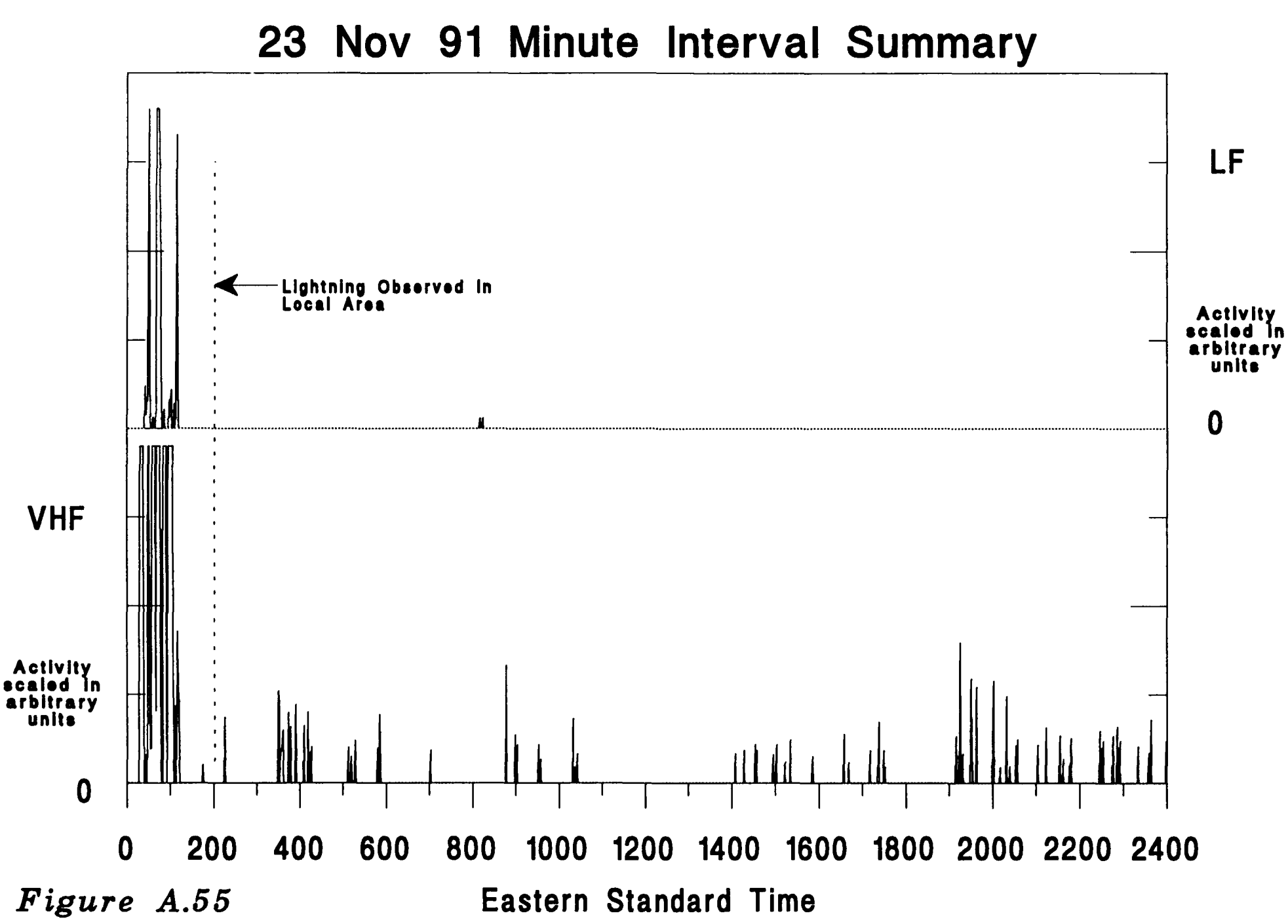
23 Nov 91 Minute Interval Summary
LF
Lightning Observed in Local Area
Activity scaled in arbitrary units
0
VHF
Activity scaled in arbitrary units
0
0 200 400 600 800 1000 1200 1400 1600 1800 2000 2200 2400
Eastern Standard Time

Figure A.55

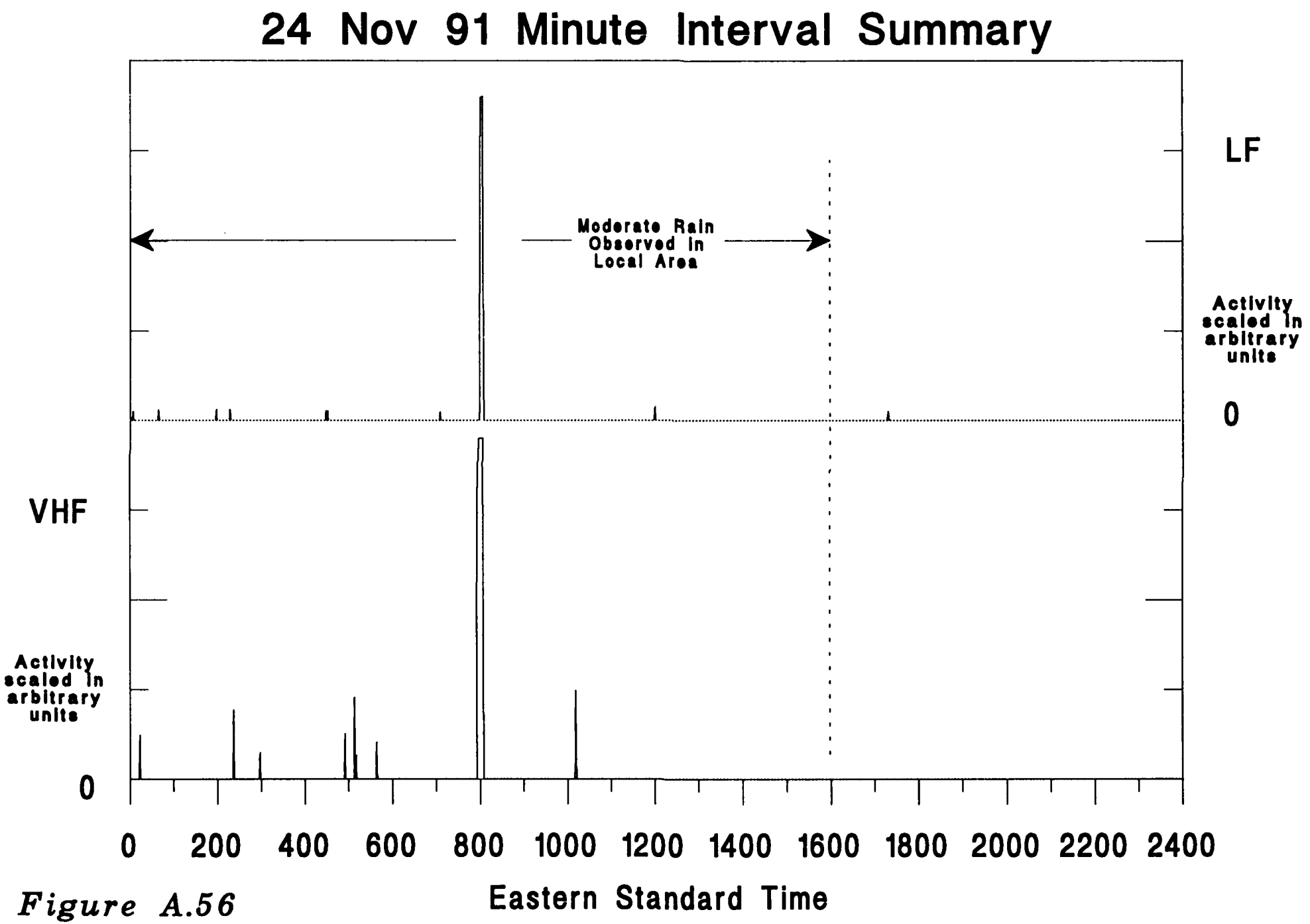
24 Nov 91 Minute Interval Summary
LF
Moderate Rain
Observed In
Local Area
Activity
scaled in
arbitrary
units
0
VHF
Activity
scaled in
arbitrary
units
0
0
200
400
600
800
1000
1200
1400
1600
1800
2000
2200
2400
Eastern Standard Time

Figure A.56

Appendix B

Increased Transient Minute-Interval Activity Period Plots

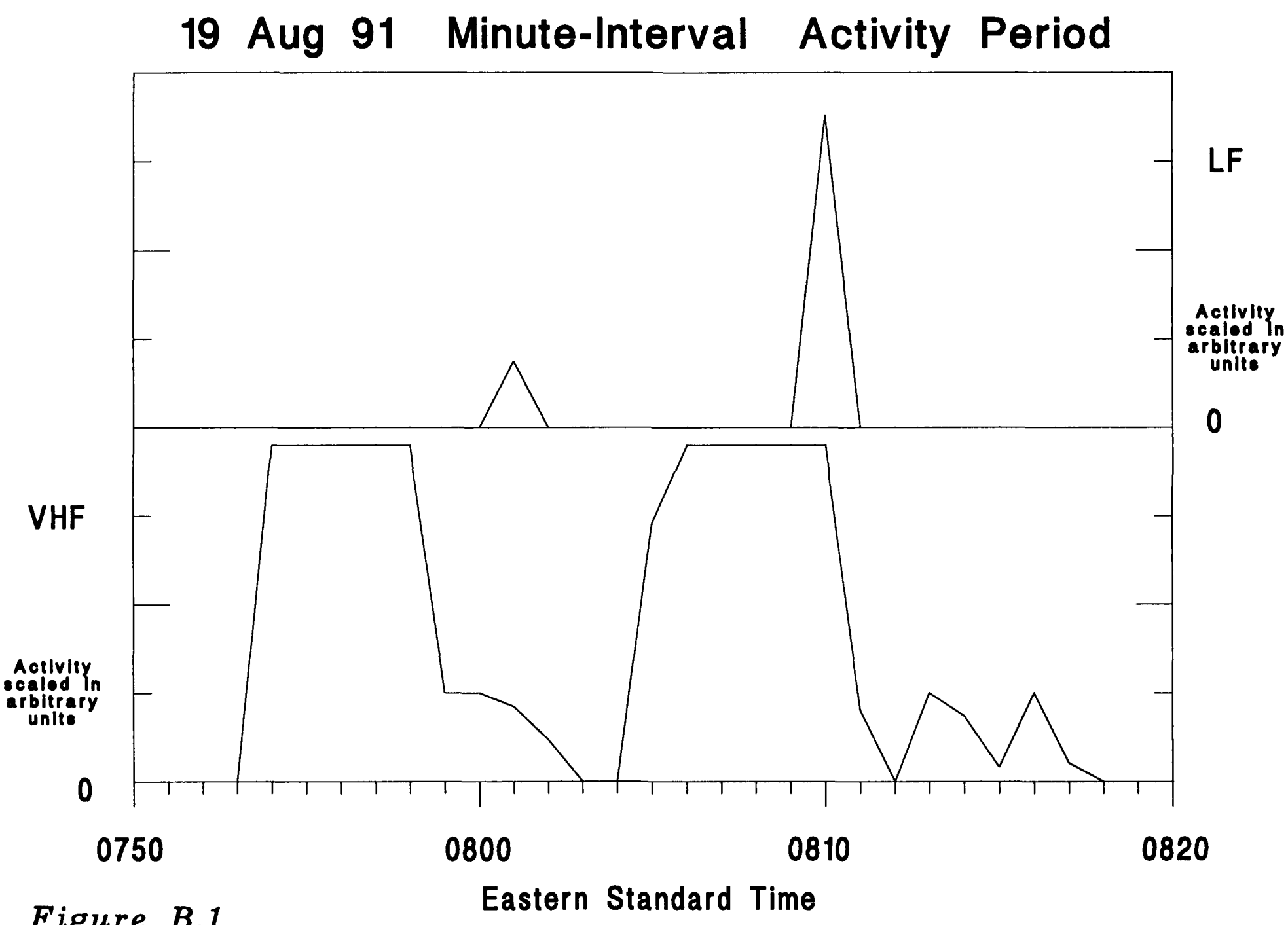
19 Aug 91 Minute-Interval Activity Period
LF
Activity scaled in arbitrary units
0
VHF
Activity scaled in arbitrary units
0
0750
0800
0810
0820
Eastern Standard Time

Figure B.1

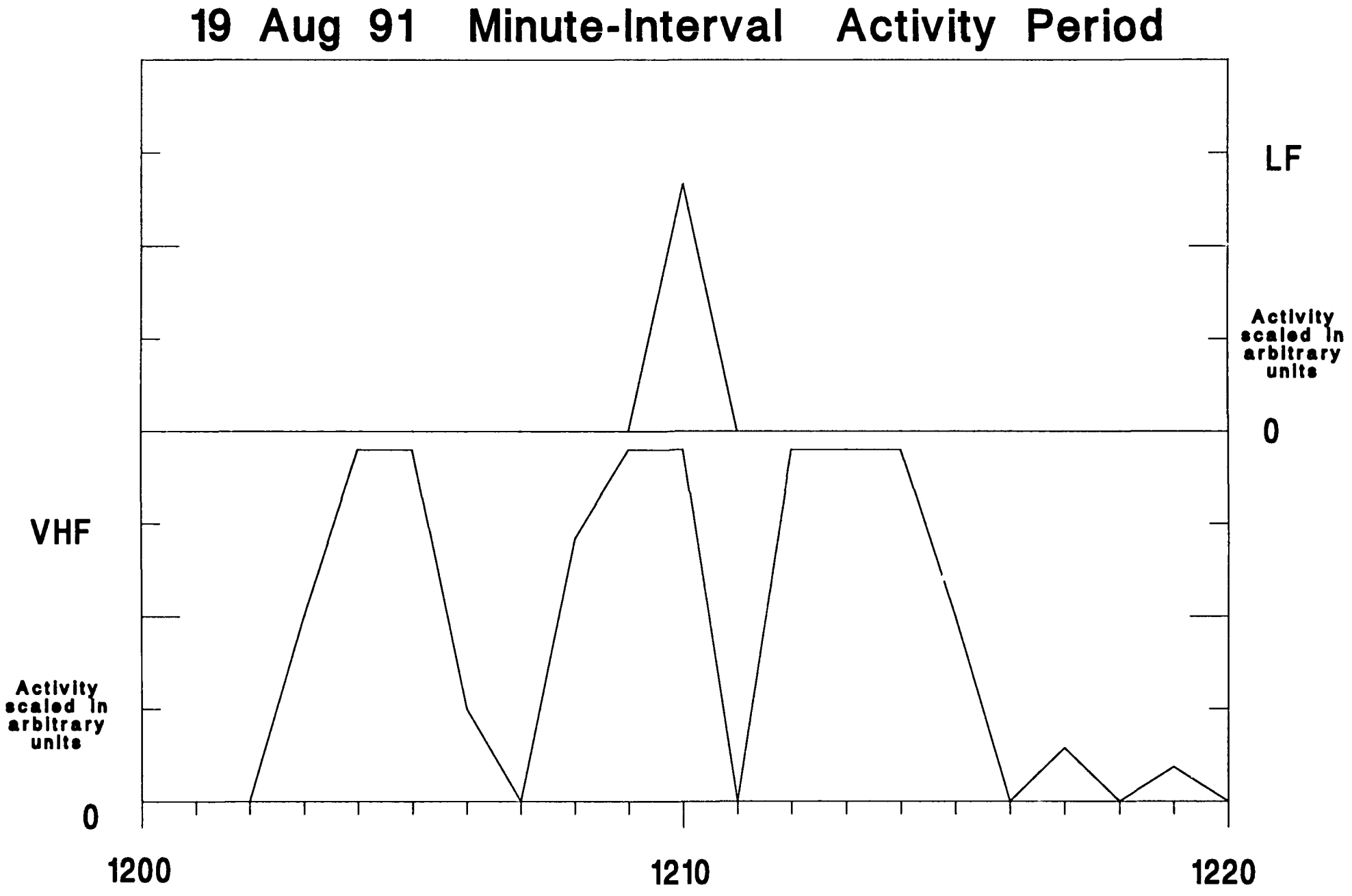
19 Aug 91 Minute-Interval Activity Period
LF
Activity scaled in arbitrary units
0
VHF
Activity scaled in arbitrary units
0
1200
1210
1220
Eastern Standard Time

Figure B.2

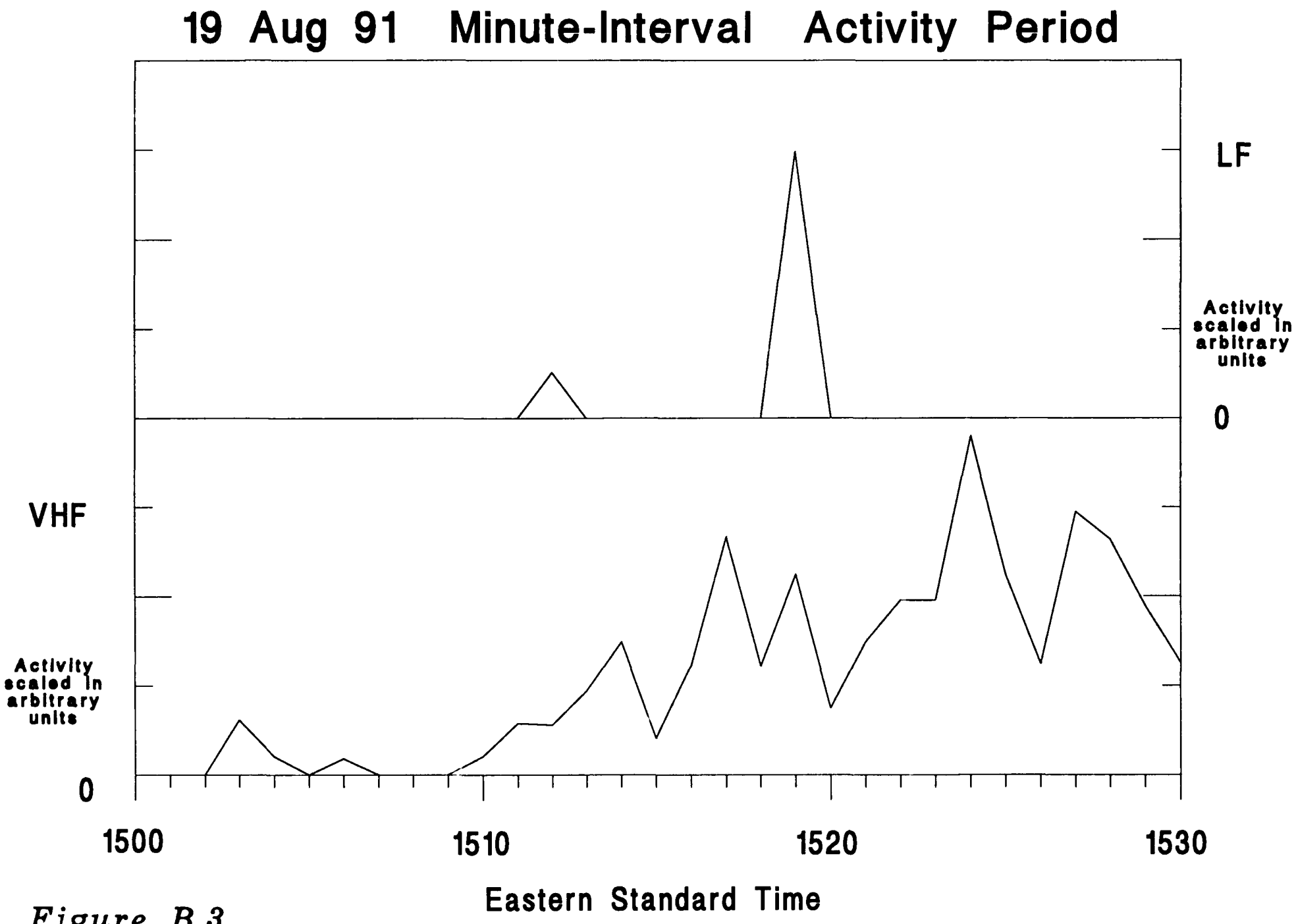
19 Aug 91 Minute-Interval Activity Period
LF
Activity scaled in arbitrary units
0
VHF
Activity scaled in arbitrary units
0
1500
1510
1520
1530
Eastern Standard Time

Figure B.3

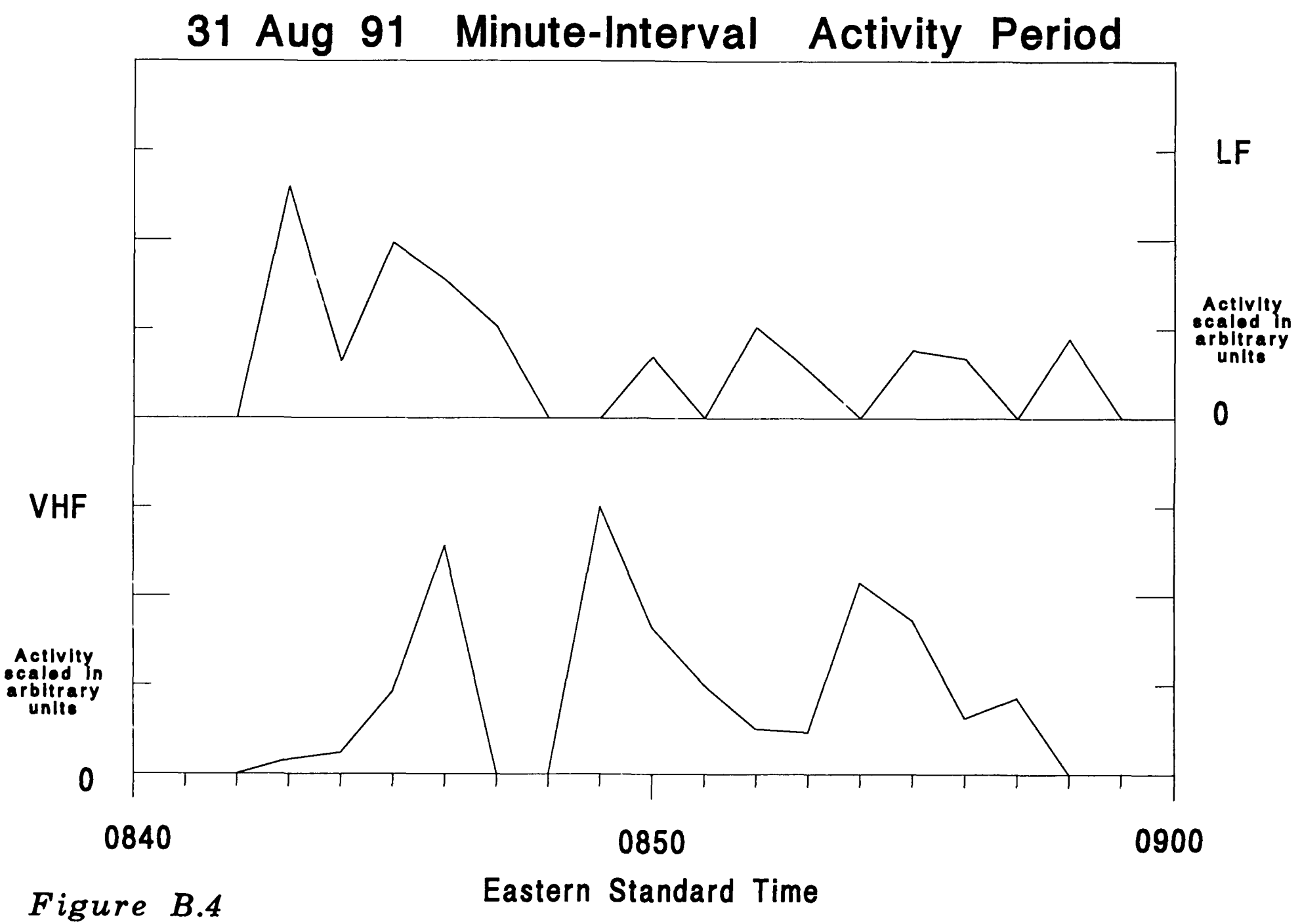
31 Aug 91 Minute-Interval Activity Period
LF
Activity scaled in arbitrary units
0
VHF
Activity scaled in arbitrary units
0
0840
0850
0900
Eastern Standard Time

Figure B.4

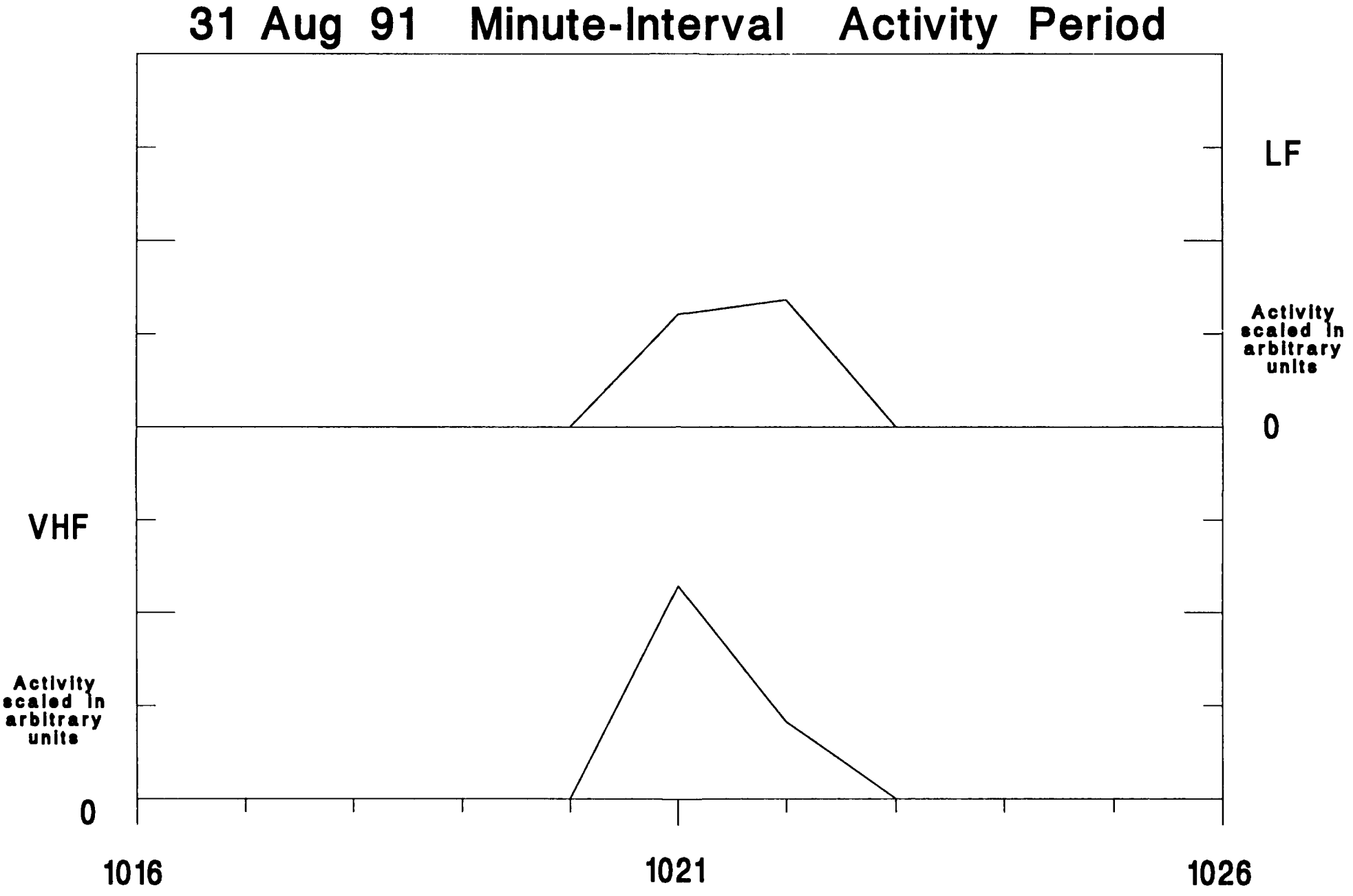
31 Aug 91 Minute-Interval Activity Period
LF
Activity scaled in arbitrary units
0
VHF
Activity scaled in arbitrary units
0
1016
1021
1026
Eastern Standard Time

Figure B.5

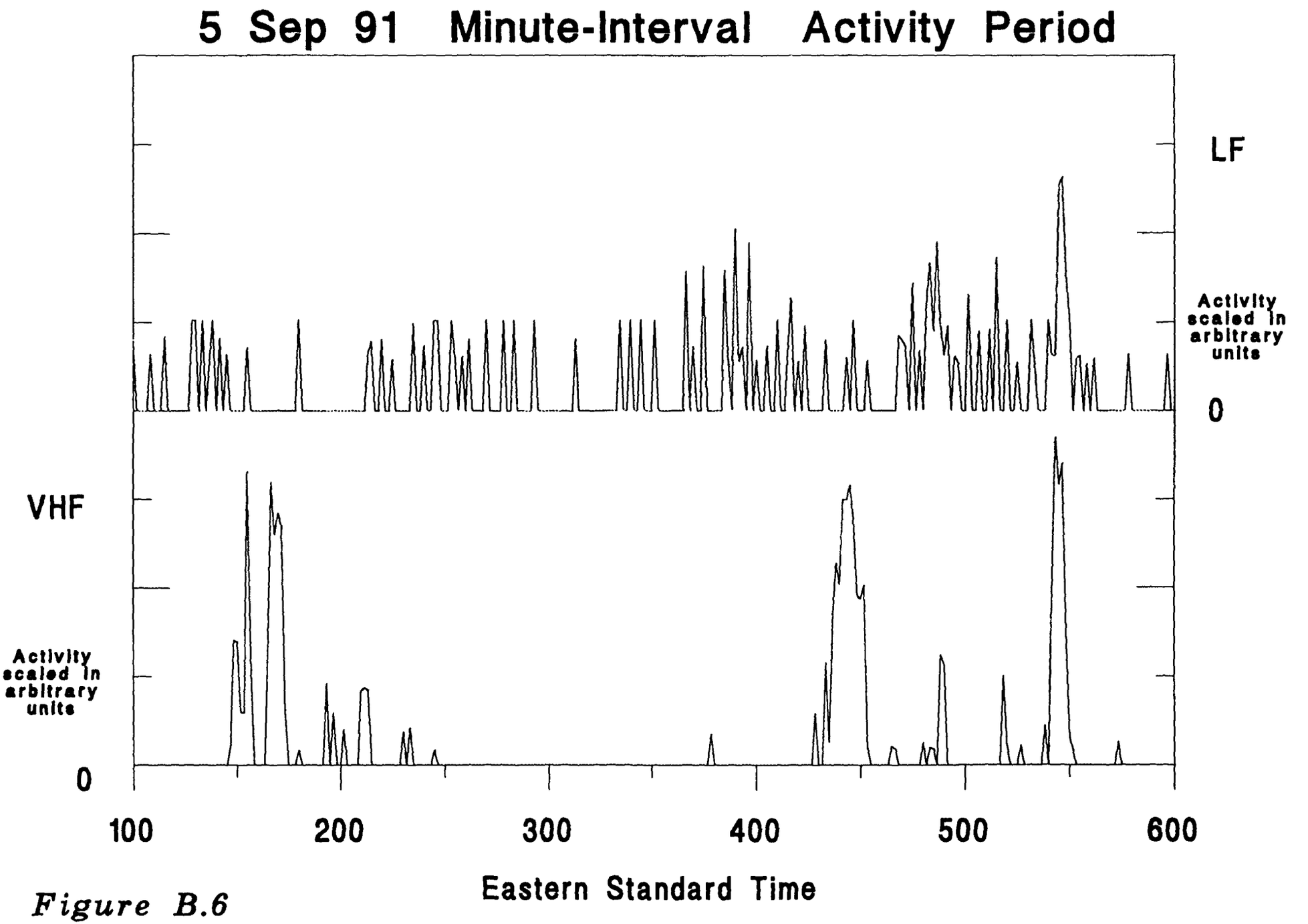
5 Sep 91 Minute-Interval Activity Period
LF
Activity scaled in arbitrary units
0
VHF
Activity scaled in arbitrary units
0
100
200
300
400
500
600
Eastern Standard Time

Figure B.6

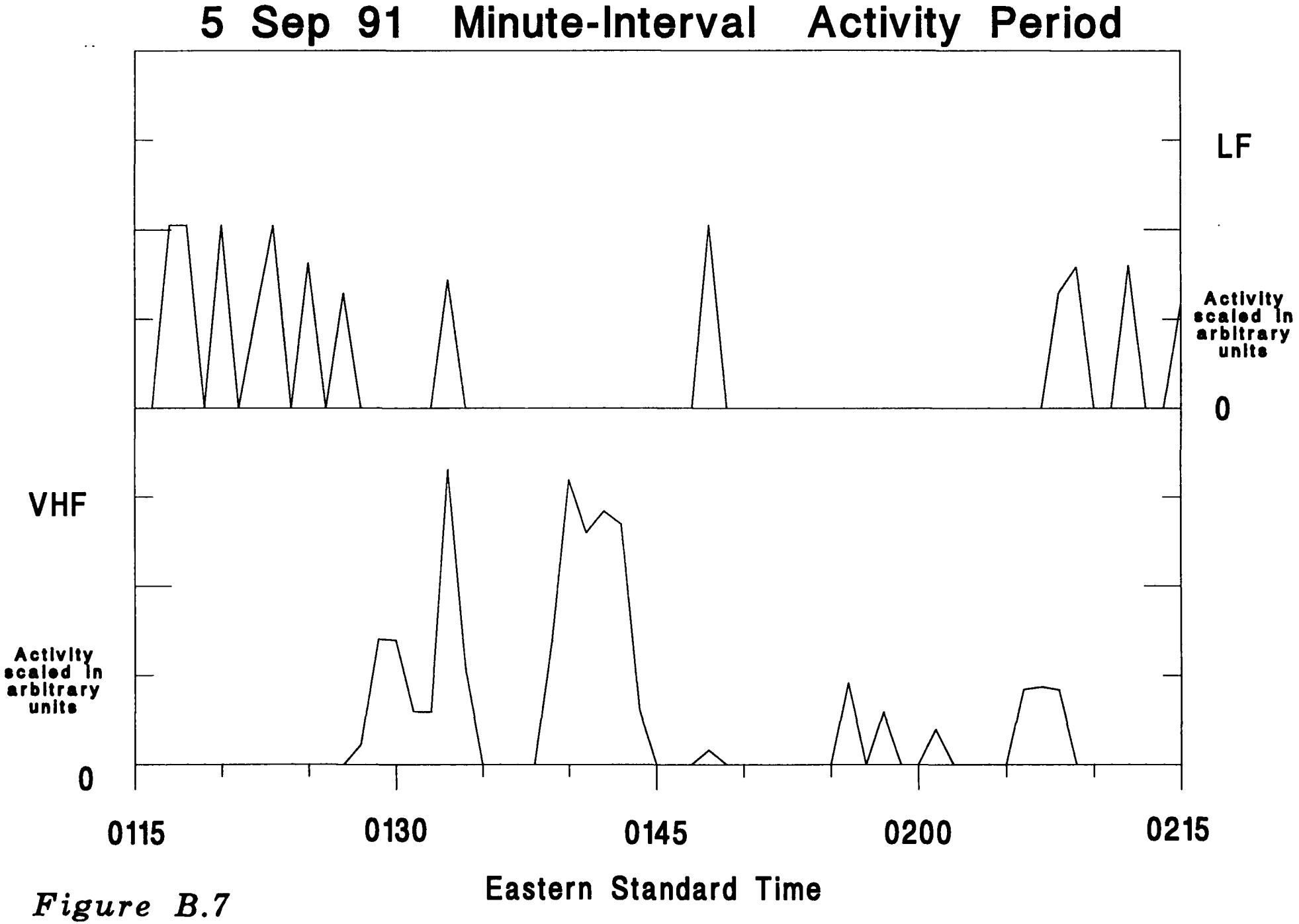
5 Sep 91 Minute-Interval Activity Period
LF
Activity scaled in arbitrary units
0
VHF
Activity scaled in arbitrary units
0
0115
0130
0145
0200
0215
Eastern Standard Time

Figure B.7

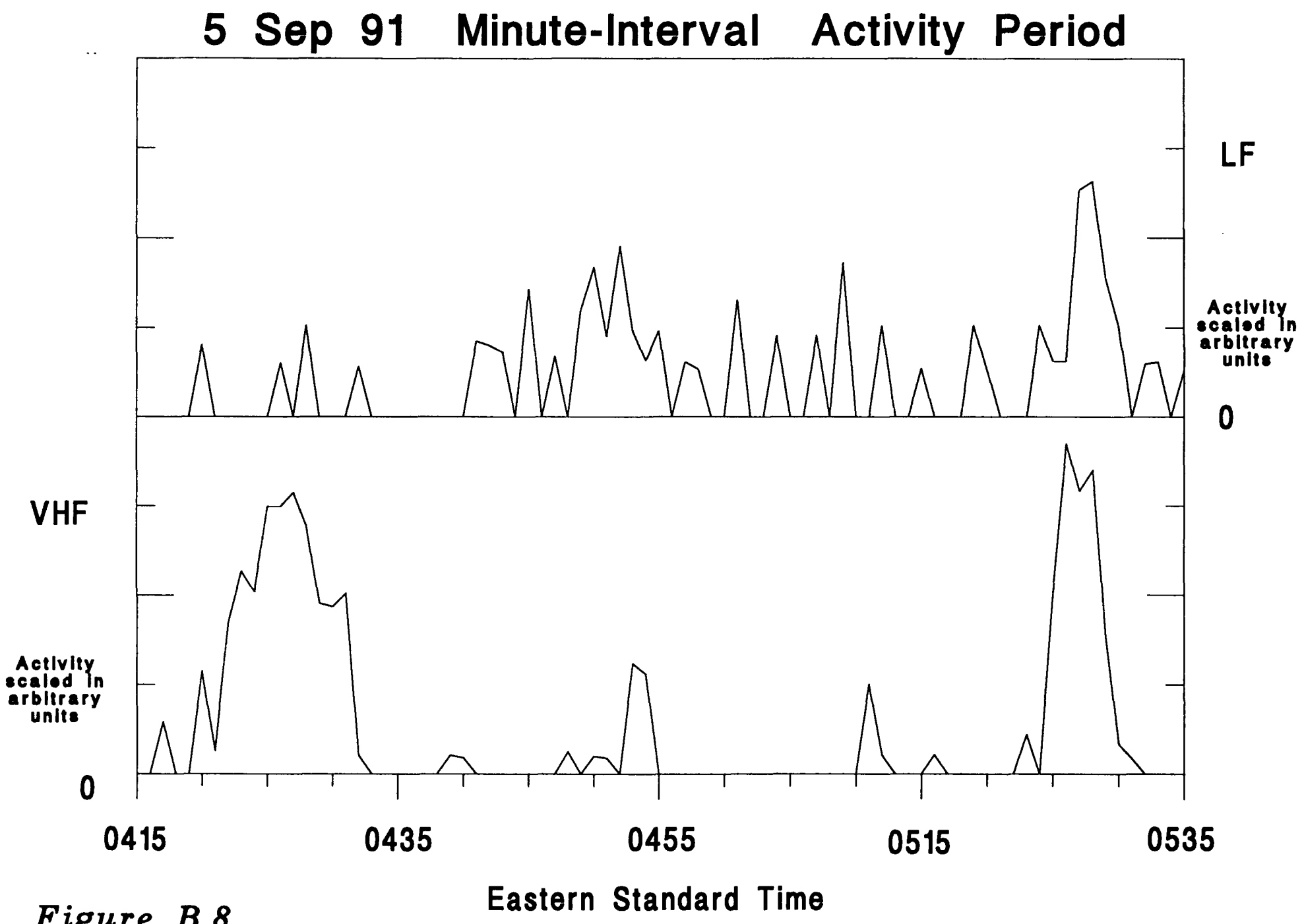
5 Sep 91 Minute-Interval Activity Period
LF
Activity scaled in arbitrary units
0
VHF
Activity scaled in arbitrary units
0
0415
0435
0455
0515
0535
Eastern Standard Time

Figure B.8

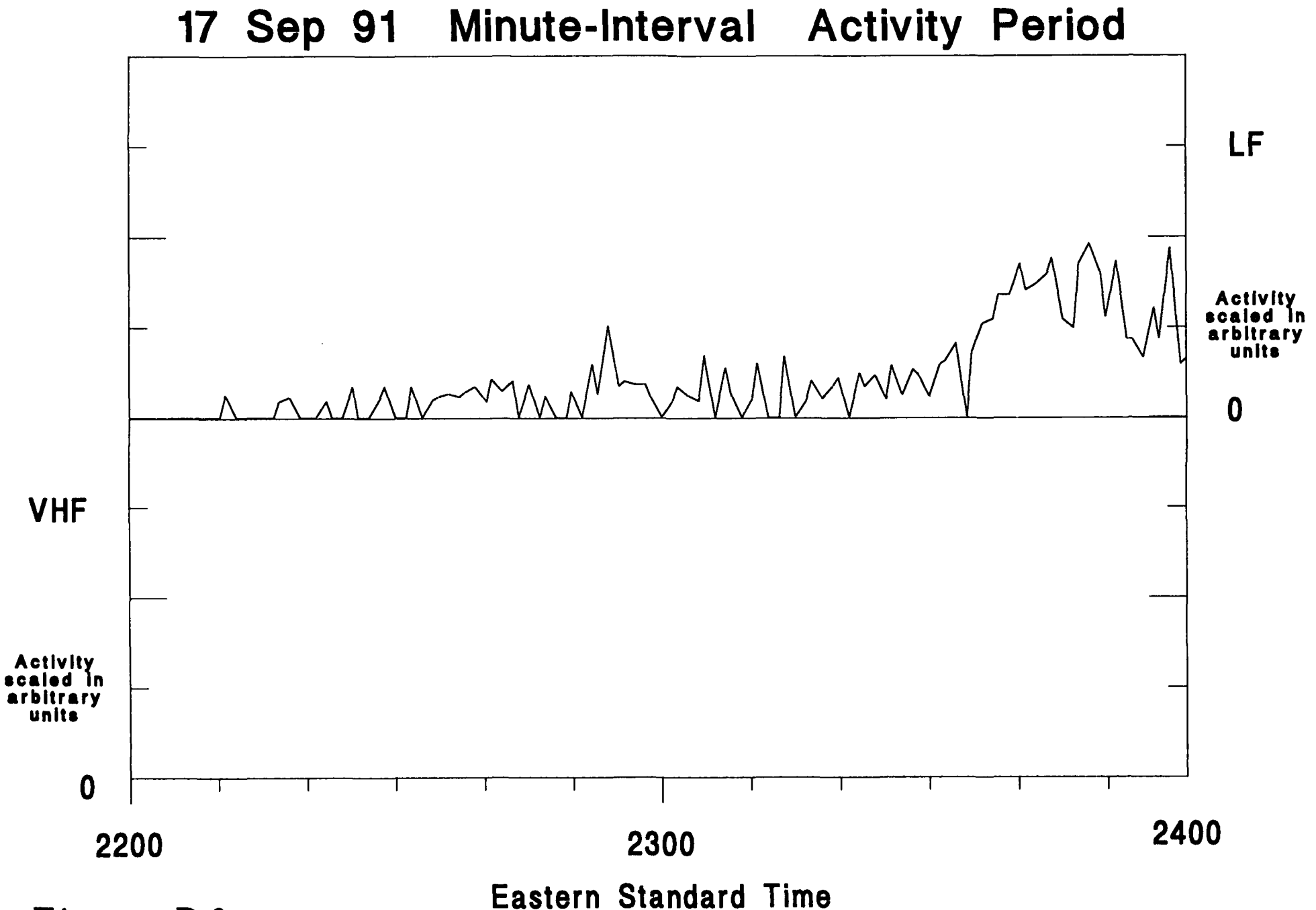
17 Sep 91 Minute-Interval Activity Period
LF
Activity scaled in arbitrary units
0
VHF
Activity scaled in arbitrary units
0
2200
2300
2400
Eastern Standard Time

Figure B.9

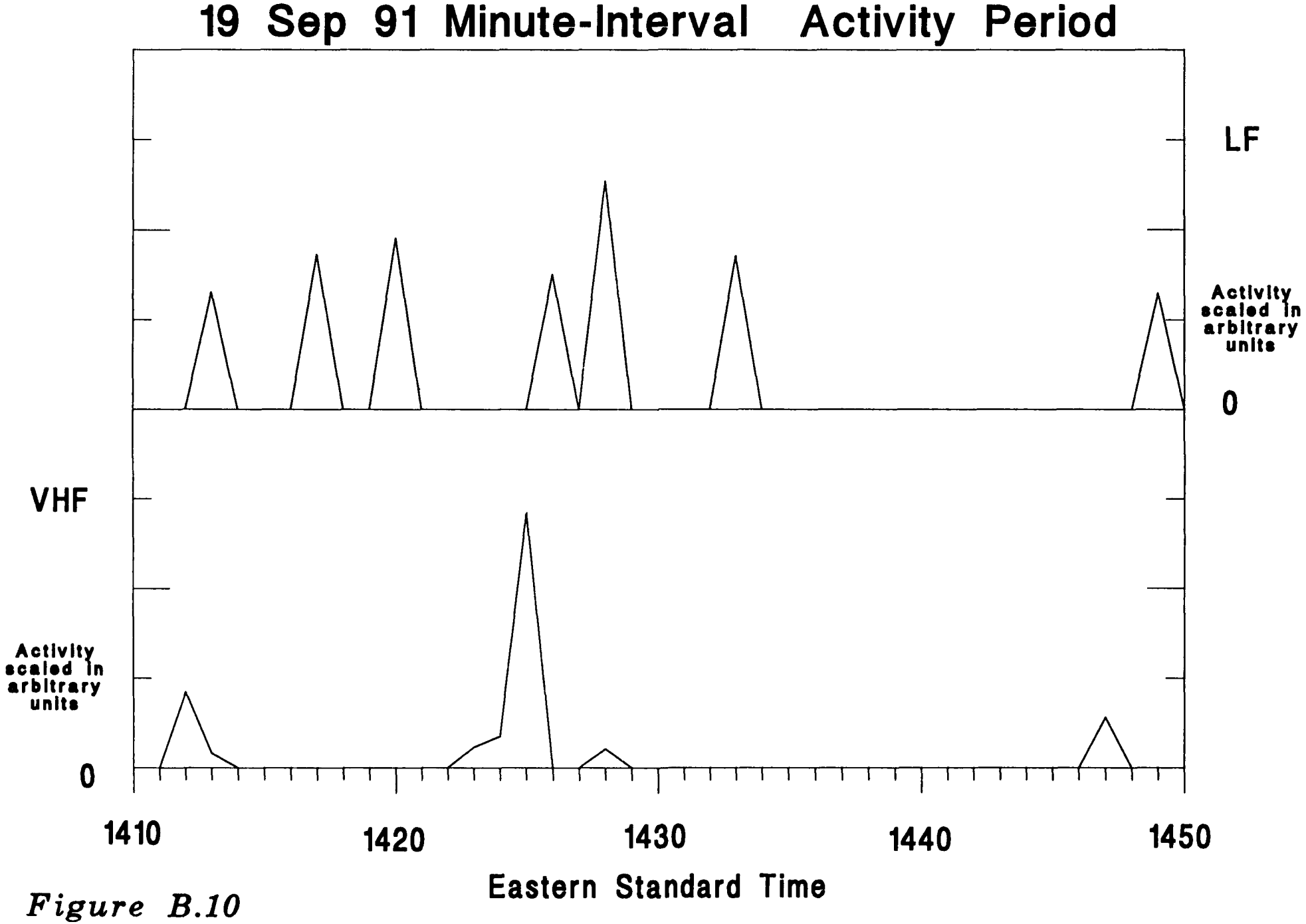
19 Sep 91 Minute-Interval Activity Period
LF
Activity scaled in arbitrary units
0
VHF
Activity scaled in arbitrary units
0
1410
1420
1430
1440
1450
Eastern Standard Time

Figure B.10

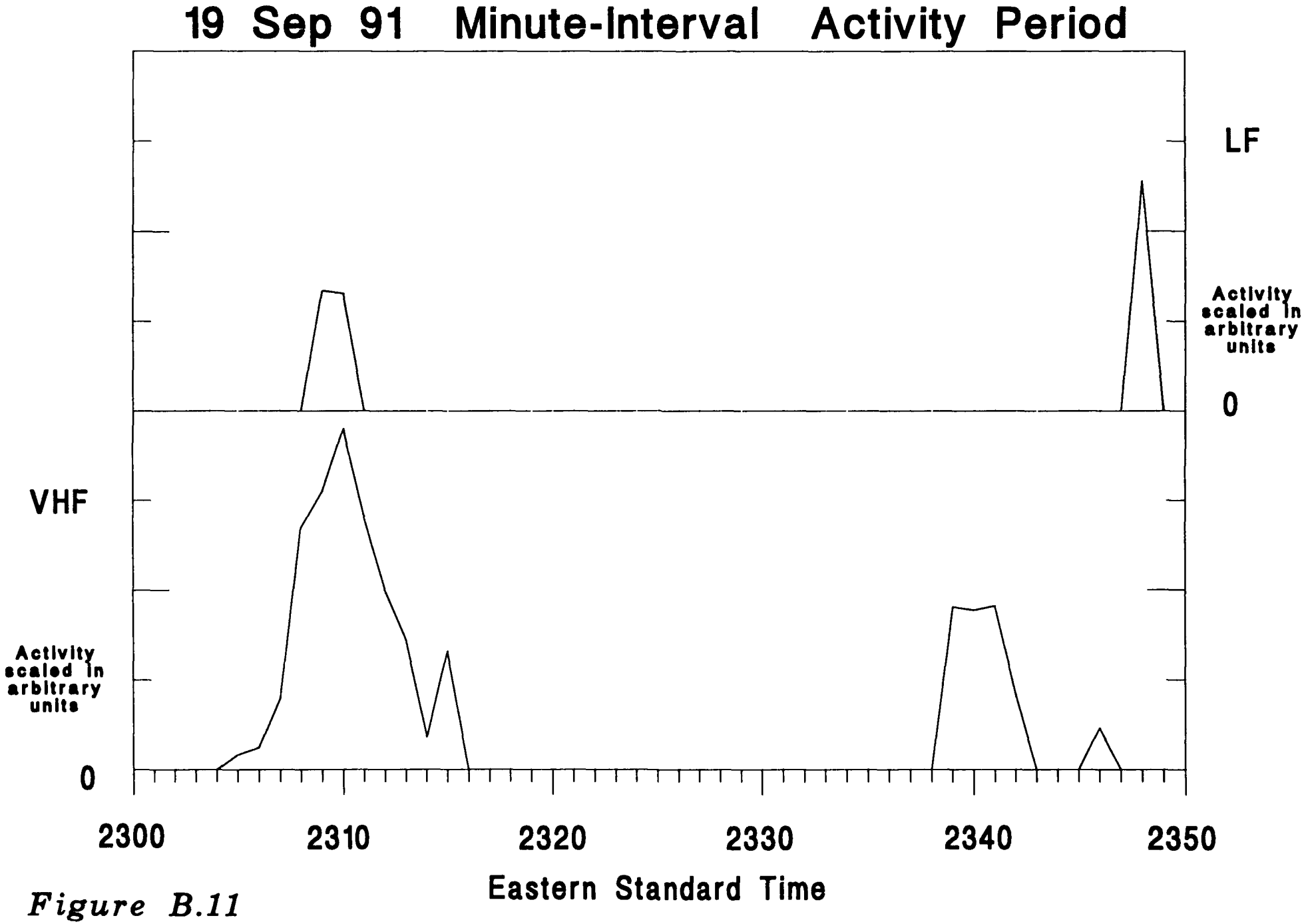
19 Sep 91 Minute-Interval Activity Period
LF
Activity scaled in arbitrary units
0
VHF
Activity scaled in arbitrary units
0
2300
2310
2320
2330
2340
2350
Eastern Standard Time

Figure B.11

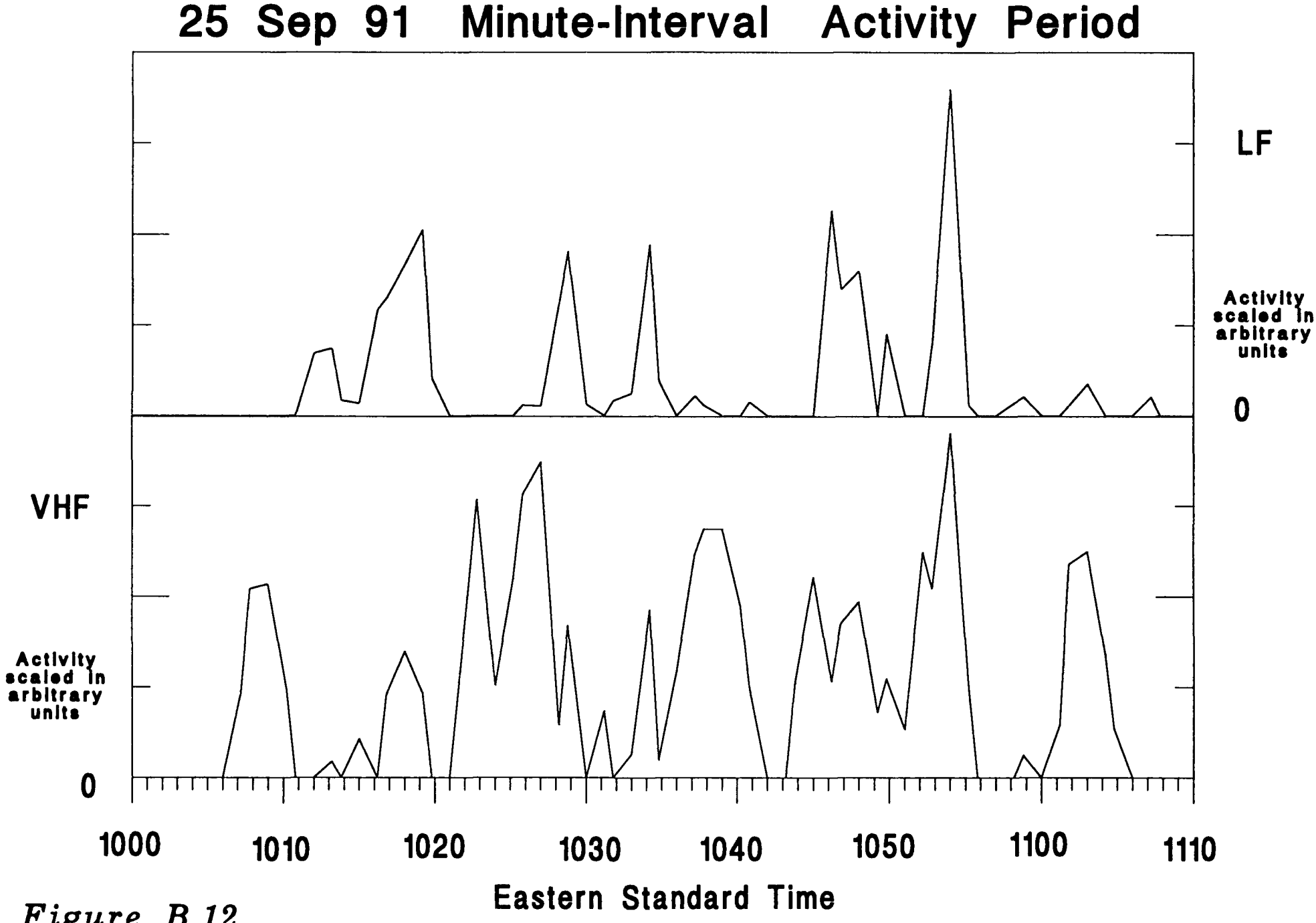
25 Sep 91 Minute-Interval Activity Period
LF
Activity scaled in arbitrary units
0
VHF
Activity scaled in arbitrary units
0
1000
1010
1020
1030
1040
1050
1100
1110
Eastern Standard Time

Figure B.12

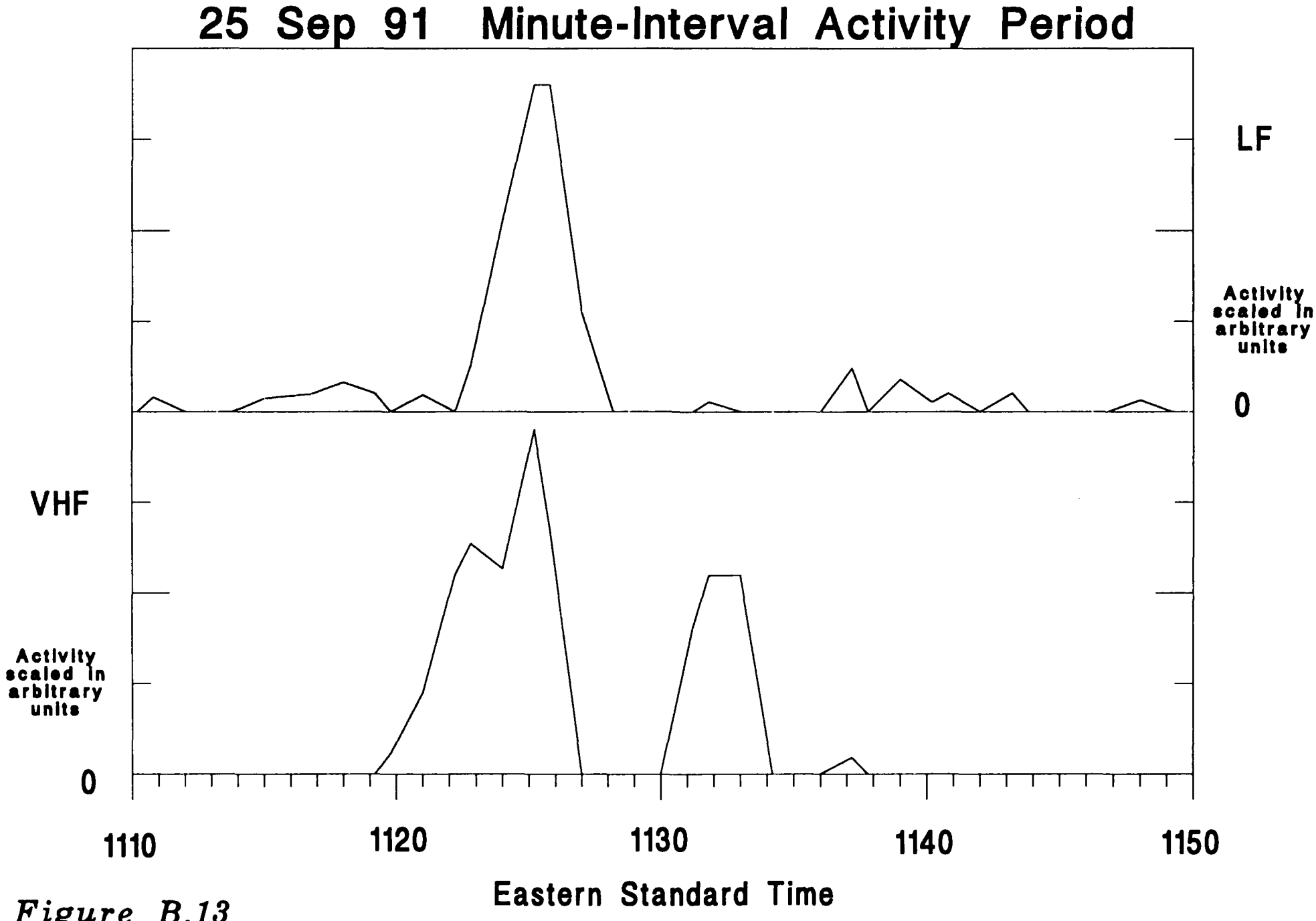
25 Sep 91 Minute-Interval Activity Period
LF
Activity scaled in arbitrary units
0
VHF
Activity scaled in arbitrary units
0
1110
1120
1130
1140
1150
Eastern Standard Time

Figure B.13

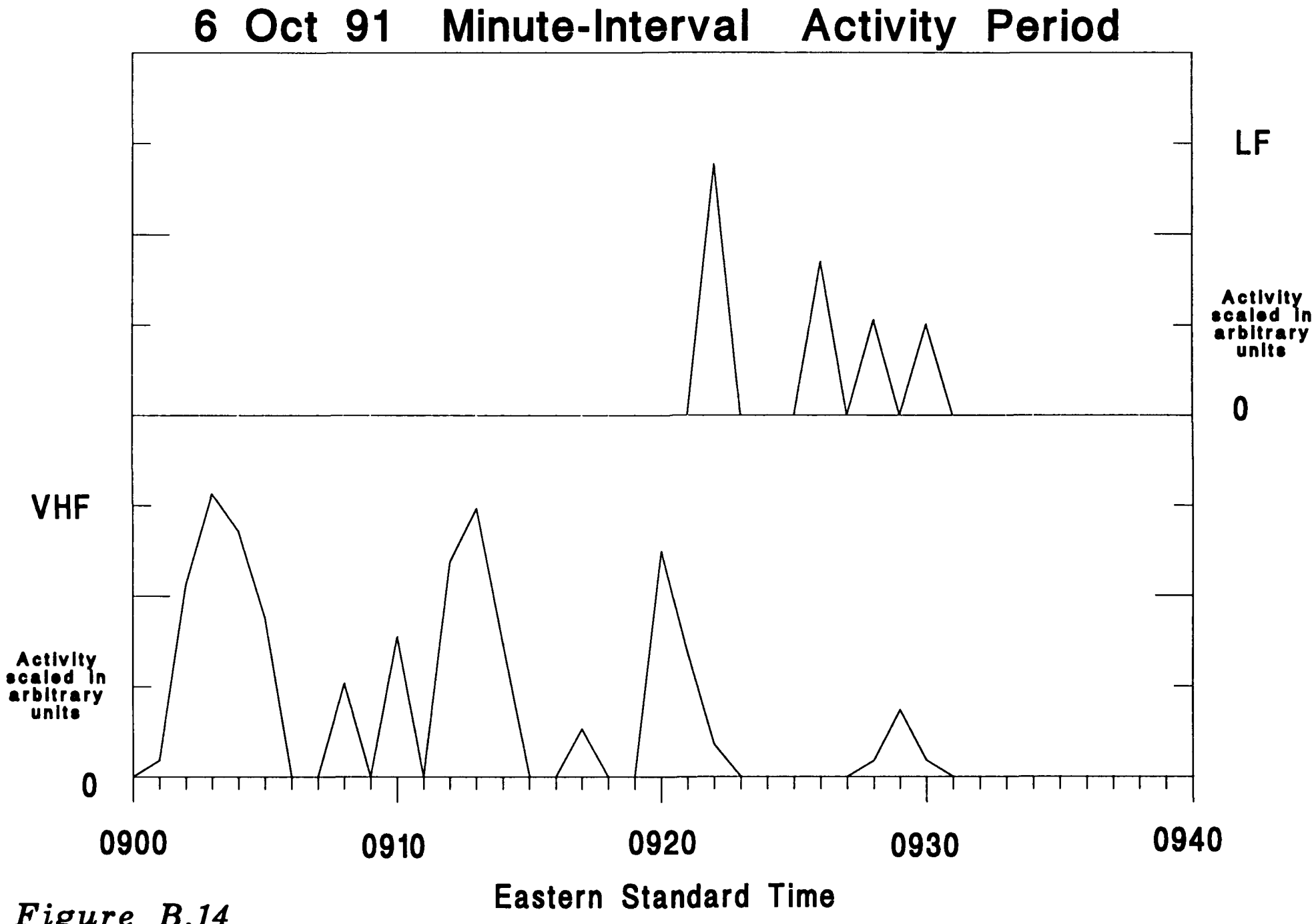
6 Oct 91 Minute-Interval Activity Period
LF
Activity scaled in arbitrary units
0
VHF
Activity scaled in arbitrary units
0
0900
0910
0920
0930
0940
Eastern Standard Time

Figure B.14

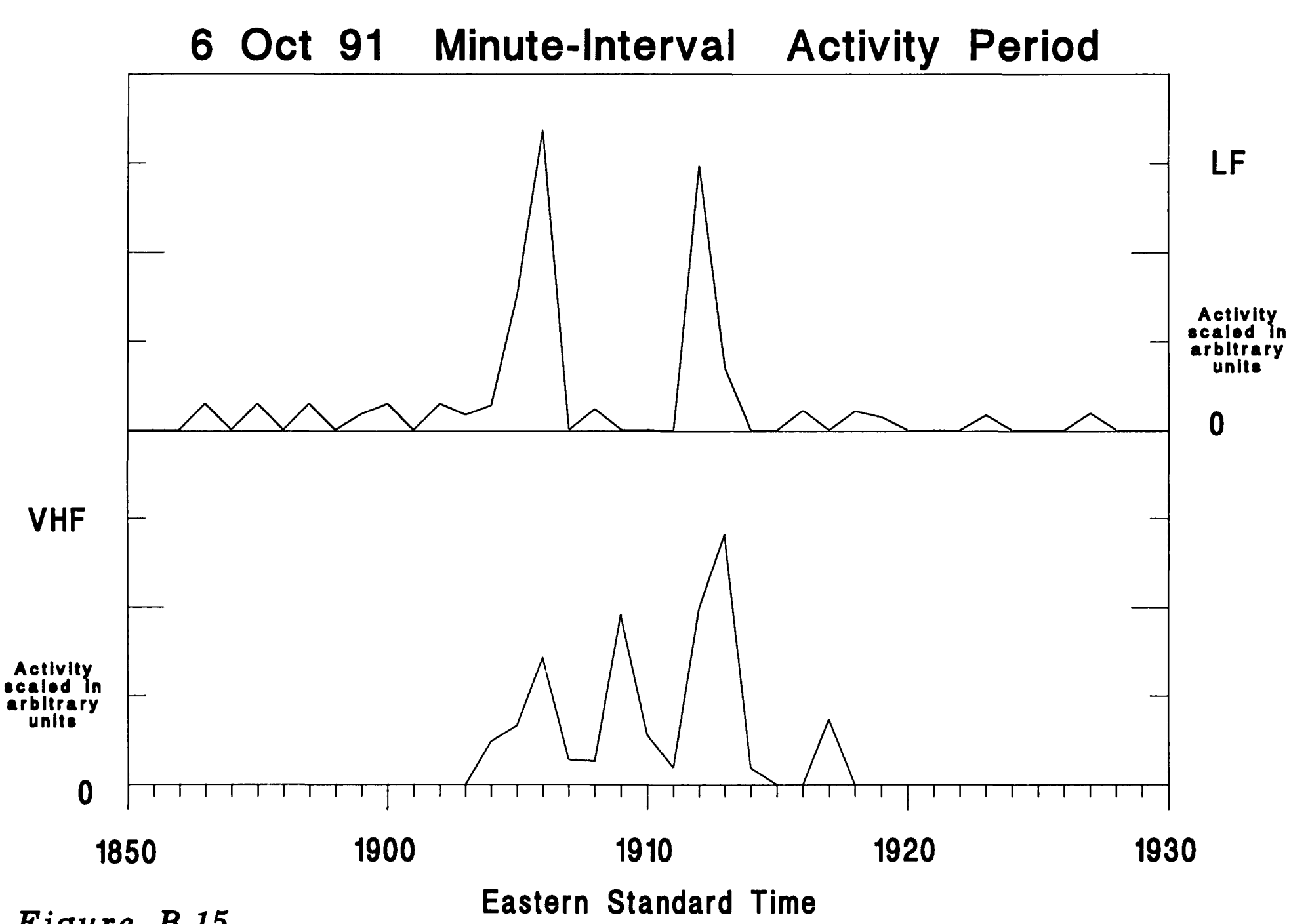
6 Oct 91 Minute-Interval Activity Period
LF
Activity scaled in arbitrary units
0
VHF
Activity scaled in arbitrary units
0
1850
1900
1910
1920
1930
Eastern Standard Time

Figure B.15

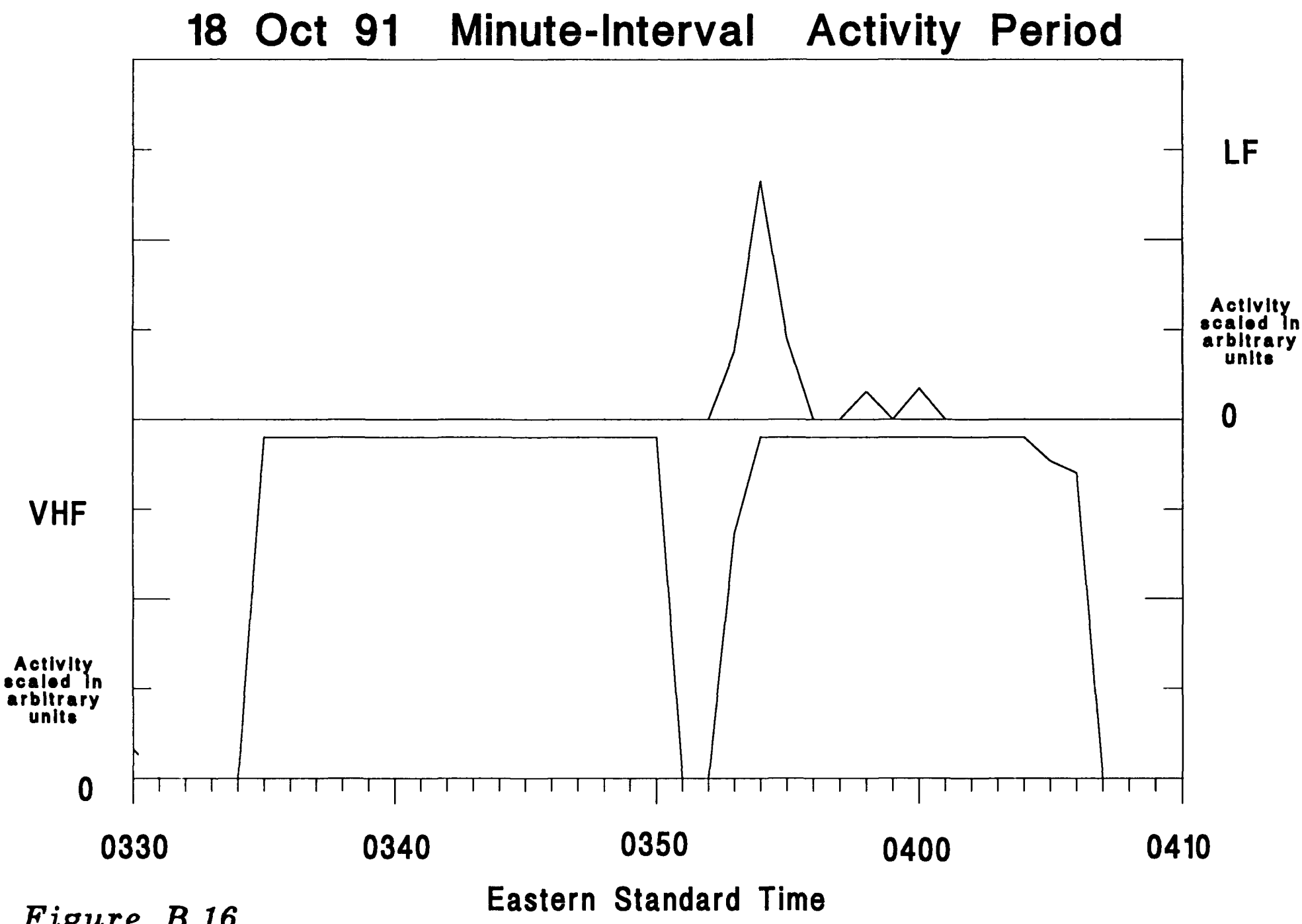
18 Oct 91 Minute-Interval Activity Period
LF
Activity scaled in arbitrary units
0
VHF
Activity scaled in arbitrary units
0
0330
0340
0350
0400
0410
Eastern Standard Time

Figure B.16

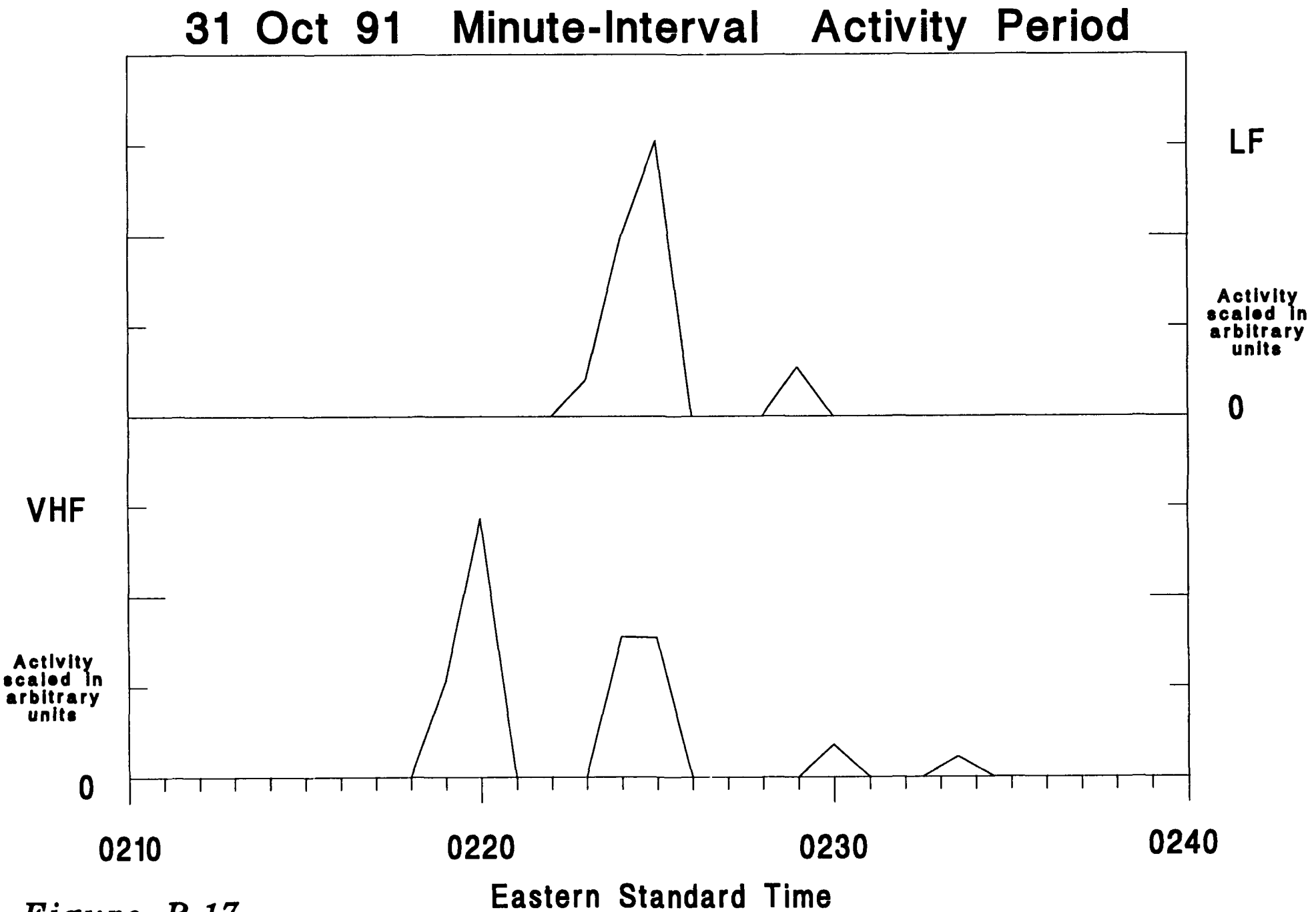
31 Oct 91 Minute-Interval Activity Period
LF
Activity scaled in arbitrary units
0
VHF
Activity scaled in arbitrary units
0
0210
0220
0230
0240
Eastern Standard Time

Figure B.17

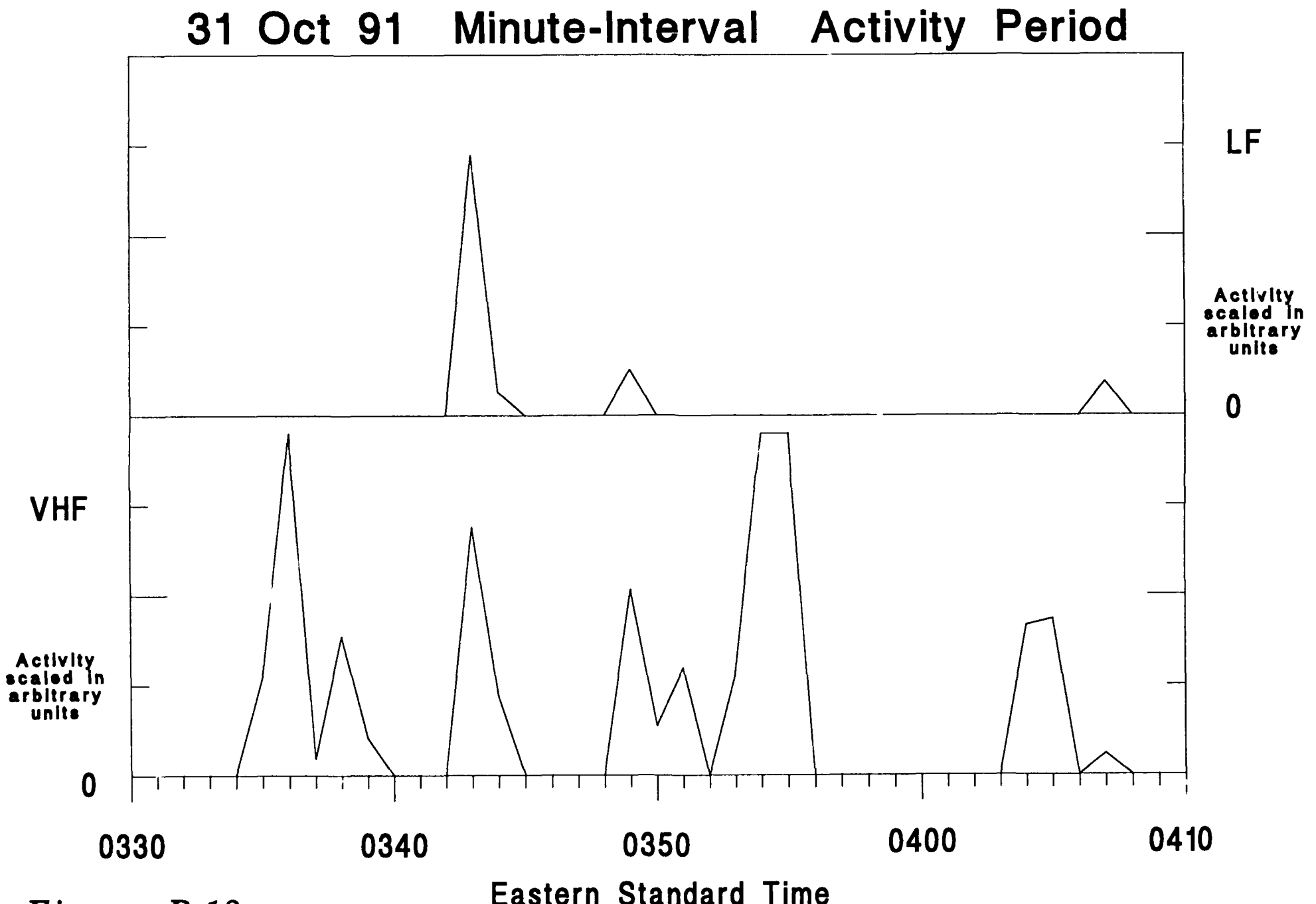
31 Oct 91 Minute-Interval Activity Period
LF
Activity scaled in arbitrary units
0
VHF
Activity scaled in arbitrary units
0
0330
0340
0350
0400
0410
Eastern Standard Time

Figure B.18

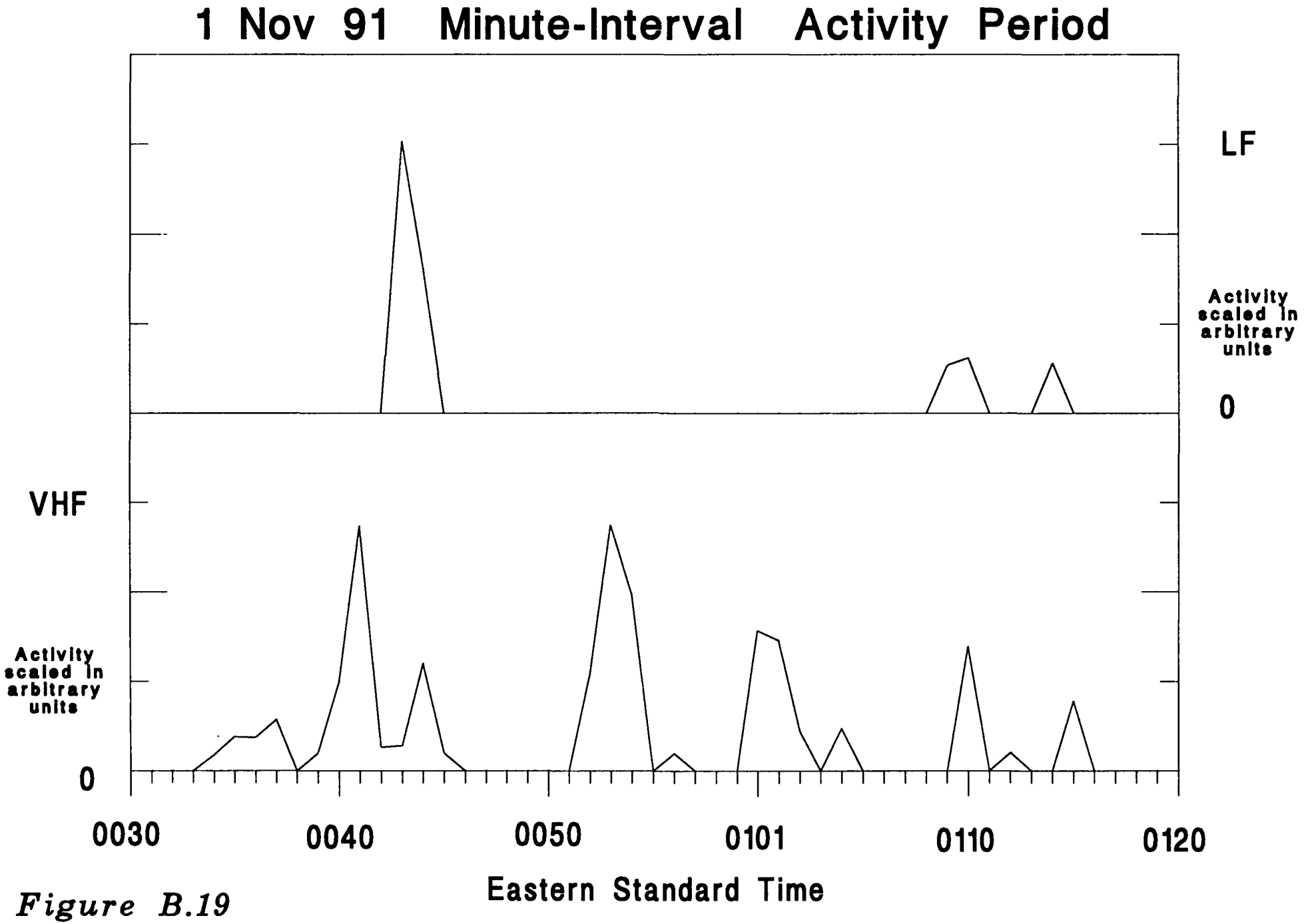
1 Nov 91 Minute-Interval Activity Period
LF
Activity scaled in arbitrary units
0
VHF
Activity scaled in arbitrary units
0
0030
0040
0050
0101
0110
0120
Eastern Standard Time

Figure B.19

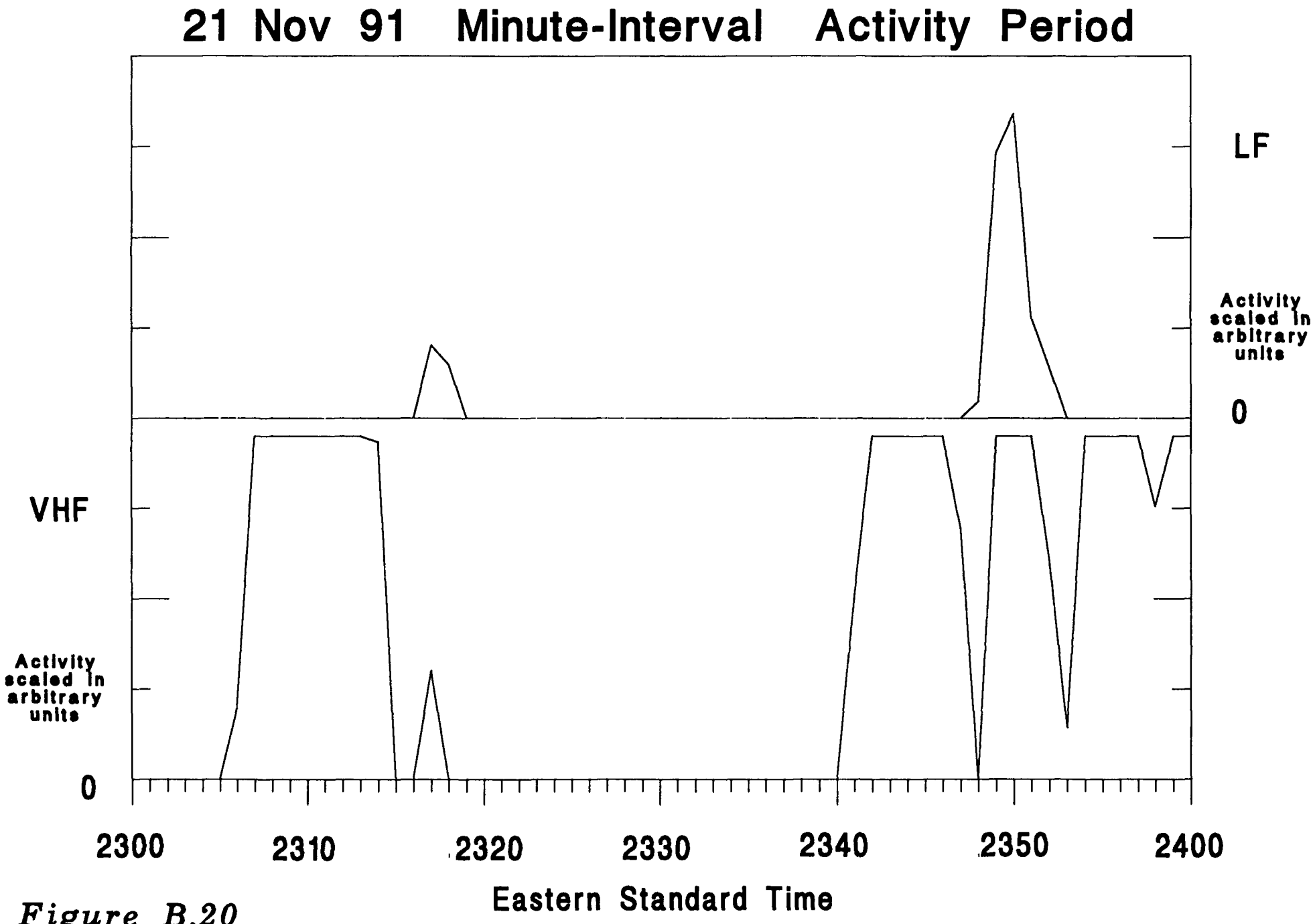
21 Nov 91 Minute-Interval Activity Period
LF
Activity scaled in arbitrary units
0
VHF
Activity scaled in arbitrary units
0
2300
2310
2320
2330
2340
2350
2400
Eastern Standard Time

Figure B.20

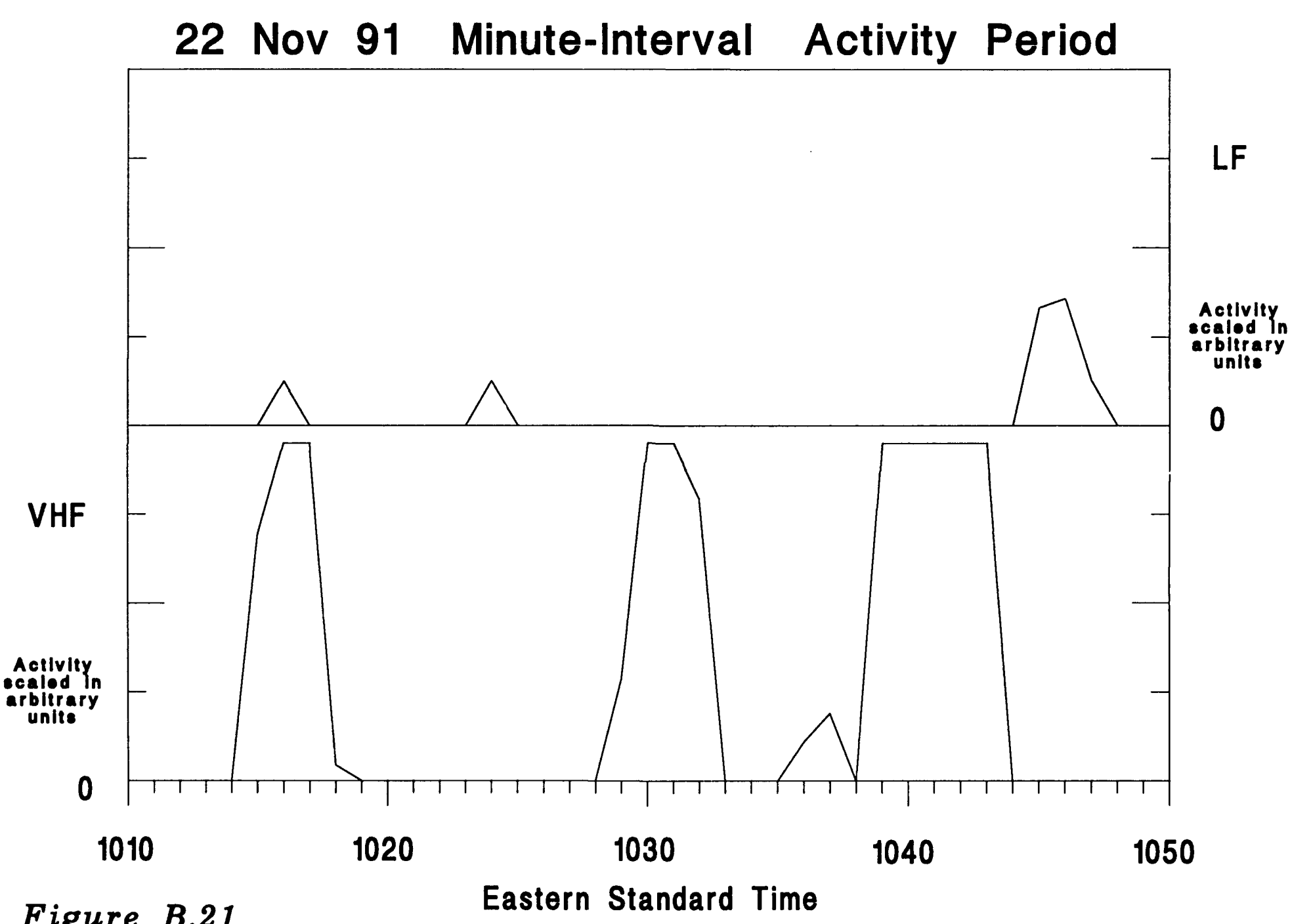
22 Nov 91 Minute-Interval Activity Period
LF
Activity scaled in arbitrary units
0
VHF
Activity scaled in arbitrary units
0
1010
1020
1030
1040
1050
Eastern Standard Time

Figure B.21

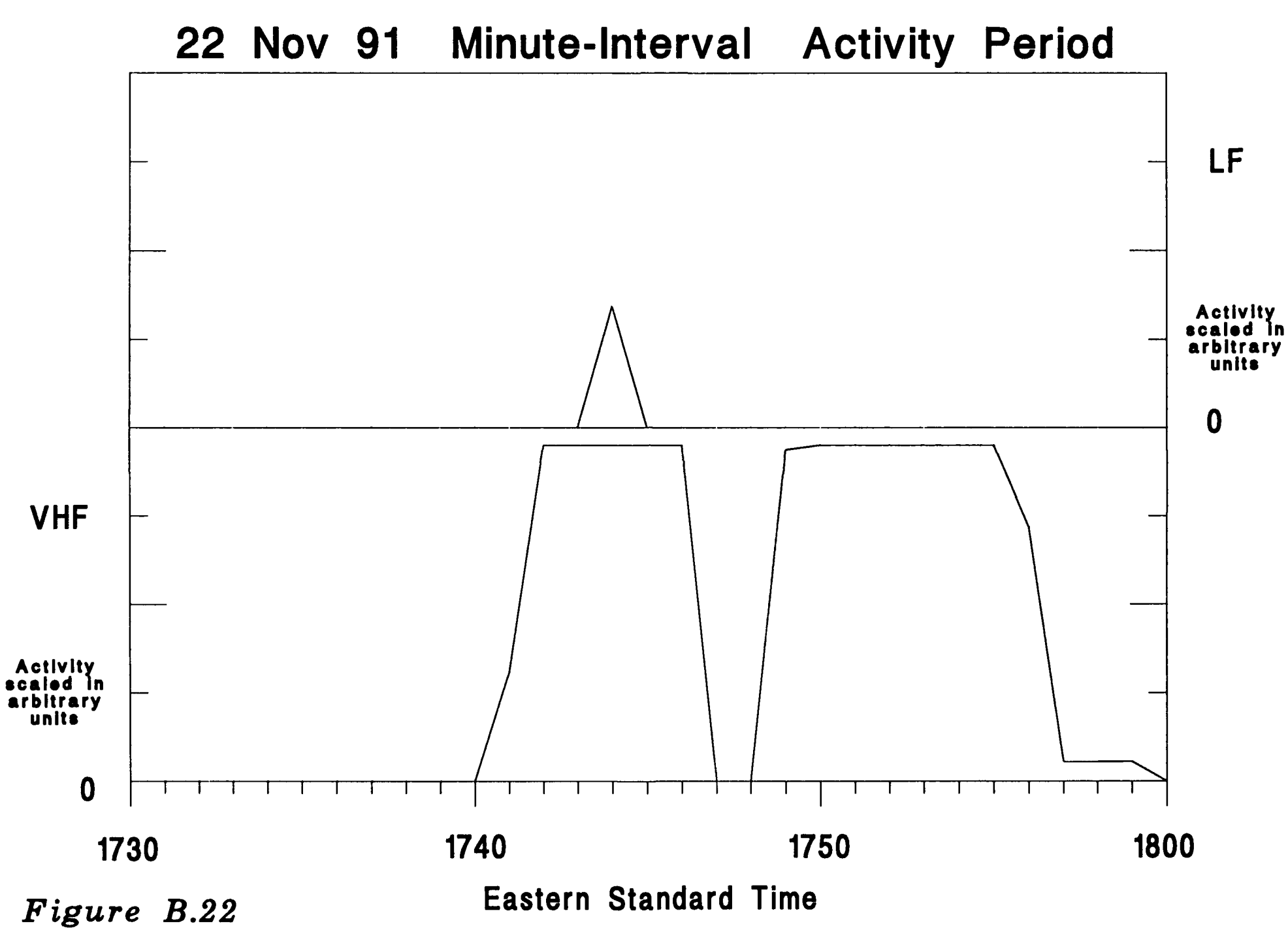
22 Nov 91 Minute-Interval Activity Period
LF
Activity scaled in arbitrary units
0
VHF
Activity scaled in arbitrary units
0
1730
1740
1750
1800
Eastern Standard Time

Figure B.22

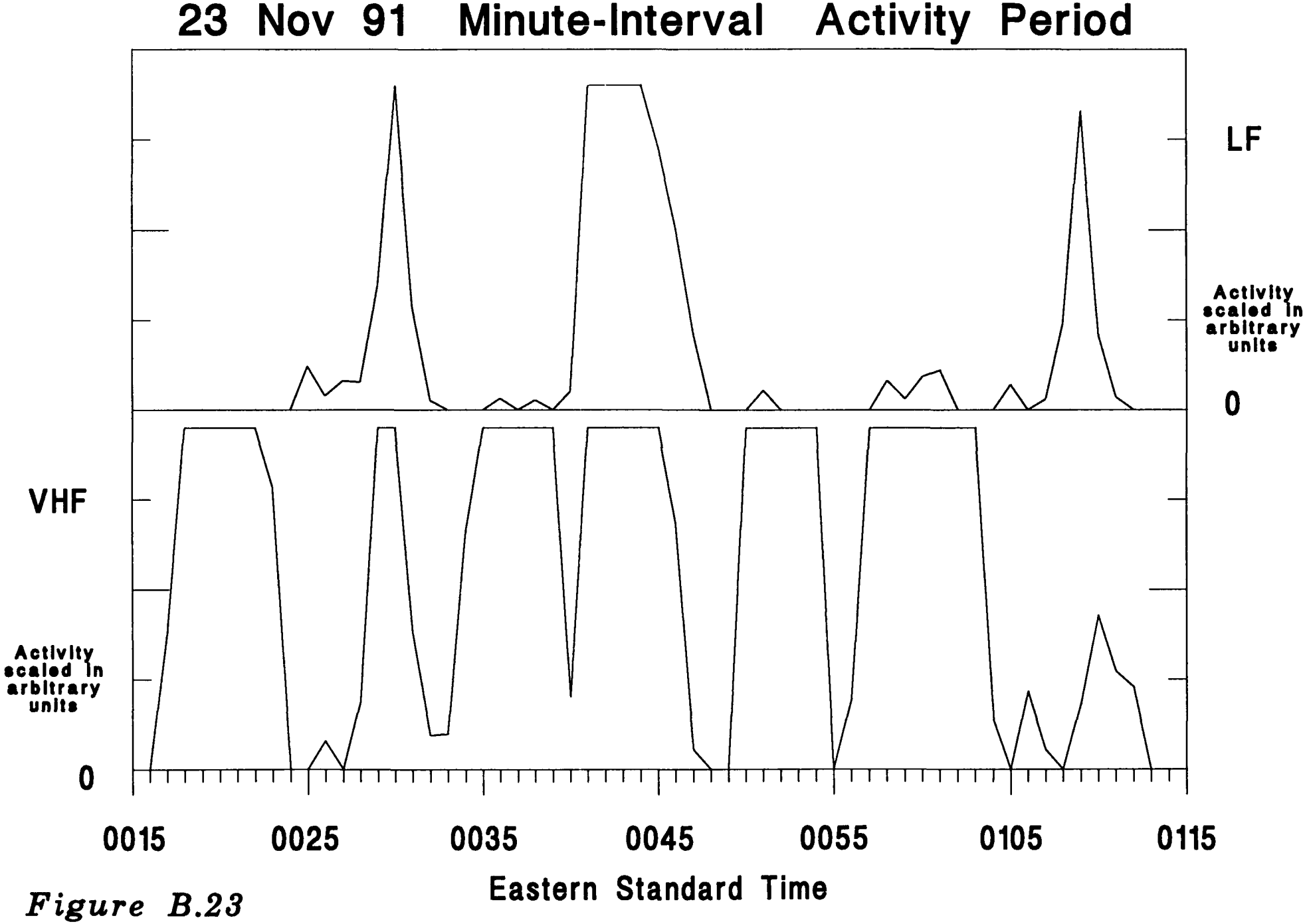
23 Nov 91 Minute-Interval Activity Period
LF
Activity scaled in arbitrary units
0
VHF
Activity scaled in arbitrary units
0
0015
0025
0035
0045
0055
0105
0115
Eastern Standard Time

Figure B.23

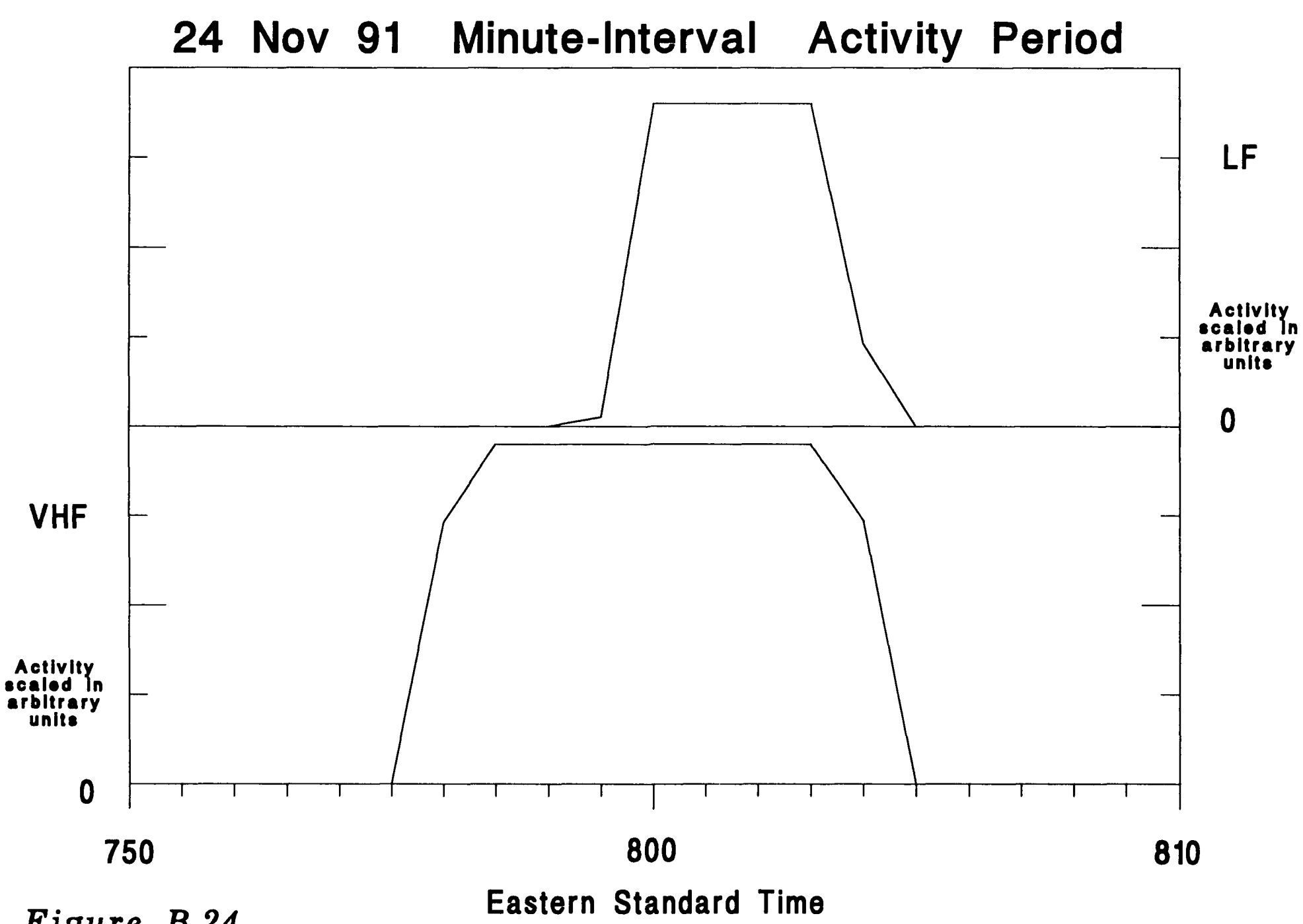
24 Nov 91 Minute-Interval Activity Period
LF
Activity scaled in arbitrary units
0
VHF
Activity scaled in arbitrary units
0
750
800
810
Eastern Standard Time

Figure B.24

Appendix C

Daily Weather Observations

Table C.1 Aug 91 - 14 Sep 91 Weather Observations

1991 Date	*Time* [1] *EST*	*Reporting* [2] *Station*	*Most Intense Weather Conditions Observed* [4]
19 Aug	0646-1920	Logan	Hurricane, Intracloud & Cloud-Cloud
...	...	...	Lightning, Thunderstorms, & Rain
19 Aug	1921-2149	Logan	Overcast Skies
19 Aug	2149-2400	Logan	Clear Skies
30 Aug	0000-2400	Logan	Hazy
31 Aug	0000-0757	Logan	Hazy
31 Aug	0815-0845	Hanscom	Cloud-Ground Lightning, Thunderstorm
31 Aug	0835-1030	Milton	Intracloud Lightning, Thunderstorm
31 Aug	1030-2400	Logan	Clear & Scattered Cloud Cover
01 Sep	0000-2400	Logan	Clear Skies
02 Sep	0000-2400	Logan	Clear Skies
03 Sep	0000-2400	Logan	Clear Skies
04 Sep	0000-0750	Logan	Clear & Scattered Cloud Cover
04 Sep	0750-2400	Logan	Overcast Skies
05 Sep	0000-0300	Logan	Light Rain Showers
05 Sep	0300-0359	Milton	Occasional Intracloud Lightning
05 Sep	0400-0433	Milton	Severe Thunderstorm
05 Sep	0427-0507	Logan	Intracloud Lightning, Thunderstorm
05 Sep	0508-1451	Logan	Moderate & Light Rain
05 Sep	1452-2400	Logan	Overcast Skies
06 Sep	0000-1421	Logan	Overcast Skies
06 Sep	1422-2250	Logan	Broken Cloud Cover & Clear
06 Sep	2251-2400	Logan	Overcast Skies
07 Sep	0000-0450	Logan	Overcast Skies
07 Sep	0450-2400	Logan	Clear or Broken & Scattered Cloud Cover
08 Sep	0000-2400	Logan	Clear Skies
09 Sep	0000-1650	Logan	Clear or Broken & Scattered Cloud Cover
09 Sep	1651-2400	Logan	Overcast Skies
10 Sep	0000-1650	Logan	Scattered Cloud Cover
10 Sep	1651-2400	Logan	Overcast Skies
11 Sep	0000-0250	Logan	Overcast Skies
11 Sep	0251-2400	Logan	Clear or Broken & Scattered Cloud Cover
12 Sep	0000-2400	Logan	Clear Skies
13 Sep	0000-0950	Logan	Clear Skies
13 Sep	0951-2400	Logan	Broken & Scattered Cloud Cover
14 Sep	0000-0242	Logan	Overcast Skies
14 Sep	0242-1220	Logan	Light Rain Showers
14 Sep	1221-2400	Logan	Overcast Skies

Table C.2: 16 Sep 91 - 26 Sep 91 Weather Observations

1991 Date	*Time* [1] *EST*	*Reporting* [2] *Station*	*Most Intense Weather Conditions Observed* [4]
16 Sep	0000-0340	Logan	Overcast Skies
16 Sep	0341-1105	Logan	Light Rain Showers
16 Sep	1106-2400	Logan	Hazy
17 Sep	0000-1219	Logan	Hazy
17 Sep	1220-1250	Worcester [3]	Moderate Rain Showers, Tops 310 at 261/220
17 Sep	1251-1324	Logan	Broken & Scattered Cloud Cover
17 Sep	1325-1400	Worcester [3]	Light Rain Showers, Tops 260 at 263/183
17 Sep	1400-2210	Logan	Broken & Scattered Cloud Cover
17 Sep	2210-2240	Weymouth	IC & Cloud-Ground Lightning, Thunderstorm
17 Sep	2251-2400	Logan	Intracloud Lightning SE Moving East
19 Sep	0000-1203	Logan	Overcast Skies
19 Sep	1204-1230	Logan	Heavy & Light Rain Showers
19 Sep	1230-1300	Worcester [3]	Severe Thunderstorm, Tops 350 at 250/95
19 Sep	1300-1400	Milton	Thunder in vicinity, Heavy Rain Showers
19 Sep	1305-1320	Beverly	Thunderstorm
19 Sep	1430-1455	Weymouth	Thunderstorm
19 Sep	1456-1949	Logan	Heavy & Light Rain Showers
19 Sep	1950-2400	Logan	Moderate & Light Rain
20 Sep	0000-0710	Logan	Moderate & Light Rain
20 Sep	0711-0930	Logan	Light Drizzle
20 Sep	0931-1950	Logan	Overcast Skies
20 Sep	1951-2400	Logan	Clear or Broken & Scattered Cloud Cover
21 Sep	0000-2400	Logan	Clear or Scattered Cloud Cover
22 Sep	0000-2400	Logan	Clear Skies
23 Sep	0000-0350	Logan	Scattered Cloud Cover
23 Sep	0351-0559	Logan	Light Rain Showers
23 Sep	0600-1219	Logan	Overcast Skies
23 Sep	1551-2400	Logan	Overcast Skies
24 Sep	0000-2342	Logan	Overcast Skies
24 Sep	2343-2400	Logan	Light Rain
25 Sep	0000-0929	Logan	Light to Heavy Rain
25 Sep	0930-0955	Norwood	Severe Thunderstorm
25 Sep	0934-0949	Milton	Intracloud Lightning, Thunderstorm
25 Sep	1037-1145	Local	Thunderstorm
25 Sep	1145-1245	Hanscom	Moderate Thunderstorm
25 Sep	1246-2400	Logan	Light to Heavy Rain Shower
26 Sep	0000-1348	Logan	Light to Heavy Rain
26 Sep	1349-1517	Logan	Overcast Skies
26 Sep	1518-2400	Logan	Clear or Broken & Scattered Cloud Cover

Table C.3: 27 Sep 91 - 12 Oct 91 Weather Observations

1991 Date	*Time* [1] *EST*	*Reporting* [2] *Station*	*Most Intense Weather Conditions Observed* [4]
27 Sep	0000-2400	Logan	Clear or Scattered Cloud Cover
28 Sep	0000-2400	Logan	Clear Skies
29 Sep	0000-1530	Logan	Clear or Broken & Scattered Cloud Cover
29 Sep	1531-1555	Logan	Light Rain Showers
29 Sep	1556-2400	Logan	Clear Skies
30 Sep	0000-2400	Logan	Clear or Broken & Scattered Cloud Cover
01 Oct	0000-0400	Logan	Clear Skies
01 Oct	0400-1200	Logan	Overcast Skies
01 Oct	1200-1400	Logan	Light Rain
01 Oct	1400-2400	Logan	Overcast Skies
02 Oct	0000-2400	Logan	Clear Skies
03 Oct	1400-1600	Logan	Light Rain
03 Oct	1600-2400	Logan	Clear Skies
04 Oct	0000-2400	Logan	Clear Skies
06 Oct	0000-0630	Weymouth	Overcast Skies
06 Oct	0630-1745	Weymouth	Light Rain
06 Oct	1745-1856	Hanscom	Heavy Rain
06 Oct	1856-1930	Hanscom	Cloud-Cloud Lightning, Thunderstorm
06 Oct	1937-1955	Weymouth	IC & Cloud-Cloud Lightning, Thunderstorm
06 Oct	1955-2400	Hanscom	Overcast Skies
07 Oct	0000-0200	Logan	Overcast Skies
07 Oct	0200-1200	Logan	Clear Skies
07 Oct	1200-1700	Logan	Overcast Skies
07 Oct	1700-2400	Logan	Clear Skies
08 Oct	0000-2400	Logan	Clear Skies
09 Oct	0000-1100	Logan	Clear Skies
09 Oct	1100-2400	Logan	Overcast Skies
10 Oct	0000-0200	Logan	Overcast Skies
10 Oct	0200-0600	Logan	Clear Skies
10 Oct	0600-1400	Logan	Overcast Skies
10 Oct	1400-2400	Logan	Clear Skies
11 Oct	0000-1300	Logan	Clear Skies
11 Oct	1300-2000	Logan	Overcast Skies
11 Oct	2000-2400	Logan	Drizzle & Light Rain
12 Oct	0000-0800	Logan	Light & Moderate Rain
12 Oct	0800-1600	Logan	Overcast Skies
12 Oct	1600-2400	Logan	Clear Skies

Table C.4: 13 Oct 91 - 24 Nov 91 Weather Observations

1991 Date	*Time* [1] *EST*	*Reporting* [2] *Station*	*Most Intense Weather Conditions Observed* [4]
13 Oct	0000-0200	Logan	Overcast Skies
13 Oct	0200-1400	Logan	Clear Skies
13 Oct	1400-2400	Logan	Overcast Skies
17 Oct	0000-1300	Logan	Overcast Skies
17 Oct	1300-2400	Logan	Moderate Rain
18 Oct	0000-0800	Logan	Moderate Rain
18 Oct	0800-2400	Logan	Overcast Skies
19 Oct	0000-2400	Logan	Clear Skies
20 Oct	0000-2400	Logan	Clear Skies
21 Oct	0000-0500	Logan	Clear Skies
21 Oct	0500-2400	Logan	Overcast Skies
30 Oct	0000-0400	Logan	Clear Skies
30 Oct	0400-1300	Logan	Overcast Skies
30 Oct	1300-2400	Logan	Moderate Rain
31 Oct	0000-0430	Local	Occasional Intracloud Lightning
31 Oct	04302400	Logan	Moderate Rain
01 Nov	0000-1800	Logan	Light & Moderate Rain
01 Nov	1800-2400	Logan	Overcast Skies
02 Nov	0000-0700	Logan	Trace Precipitation
02 Nov	0700-2400	Logan	Overcast Skies
21 Nov	0000-0700	Logan	Overcast Skies
21 Nov	0700-2300	Logan	Moderate Rain
21 Nov	2300-2400	Local	Intracloud Lightning & Thunderstorm
22 Nov	0000-2400	Logan	Moderate Rain
23 Nov	0000-0200	Local	Intracloud Lightning
23 Nov	0200-2400	Logan	Overcast Skies
24 Nov	0000-1800	Logan	Drizzle & Moderate Rain
24 Nov	1800-2400	Logan	Overcast Skies

Notes

All weather observations were provided by Mr. John Walsh of the U.S. Department of Commerce's National Oceanic and Atmospheric Administration: National Environmental Satellite, Data and Information Service located at the National Climatic Data Center, Federal Building, Asheville, NC, 28801.

1. Time

Times from meteorological records have been converted from Universal Time Coordinates, UTC, to Eastern Standard Time, EST, where necessary.

2. Reporting Stations

Beverly - FAA Air Traffic Control Center, Beverly, MA. Located approximately 26 km northeast of data collection equipment.

Hanscom - Air Traffic Control Tower, Hanscom Air Force Base, Bedford, MA. Located approximately 15 km northwest of data collection equipment.

Local - Tufts University, Medford, MA. Location of data collection equipment.

Logan - Air Traffic Control Tower, Logan International Airport, Boston, MA. Located approximately 10 km east of data collection equipment.

Milton - Blue Hill Meteorological Observatory, Milton, MA. Located approximately 21 km south of data collection equipment.

Norwood - Air Traffic Control Tower, Norwood Memorial Airport, Norwood, MA. Located approximately 24 km southwest of data collection equipment.

Weymouth - Air Traffic Control Tower, N.A.S. South Weymouth, South Weymouth, MA. Located approximately 34 km southeast of data collection equipment.

Worcester - Weather Radar Observations, Worcester, MA. Located approximately 62 km west of data collection equipment.

3. Weather Radar

Weather conditions such as the existence of a thunderstorm can be inferred from the intensity of precipitation radar echoes. "Tops 310 at 250/67" is an abbreviation that pinpoints the location of the highest cloud tops. Clouds top observations are important, because as a general rule, they are not usually found at altitudes above 25,000 ft unless a thunderstorm provides the updrafts to lift them there. In this example, the highest cloud tops are located 67 km and at heading 250 from Worcester and at an altitude of 31,000 ft (above mean sea level).

4. Observations

This summary represents an attempt to consolidate the numerous surface weather observations and measurements available from local meteorological stations. Care has been taken to limit the observations to the days of the study and then only includes entries that can possibly confirm or deny the existence of any type of lightning discharge. In terms of this study, the actual sighting of lightning provides the greatest confirmation for the occurrence of lightning discharges. Next, the existence of a thunderstorm in progress or hearing thunder implied that lightning was nearby although it may not have been visible to the observer.

Evidence of rain showers or rain only suggest that lightning might have been occurring elsewhere. Overcast skies hint that lightning might be developing as the front moved through the area. On the other hand, clear or broken and scattered cloud cover conditions were good indications that no lightning activity was occurring.

Appendix D

VHF and LF Data Collection System Gain Analysis

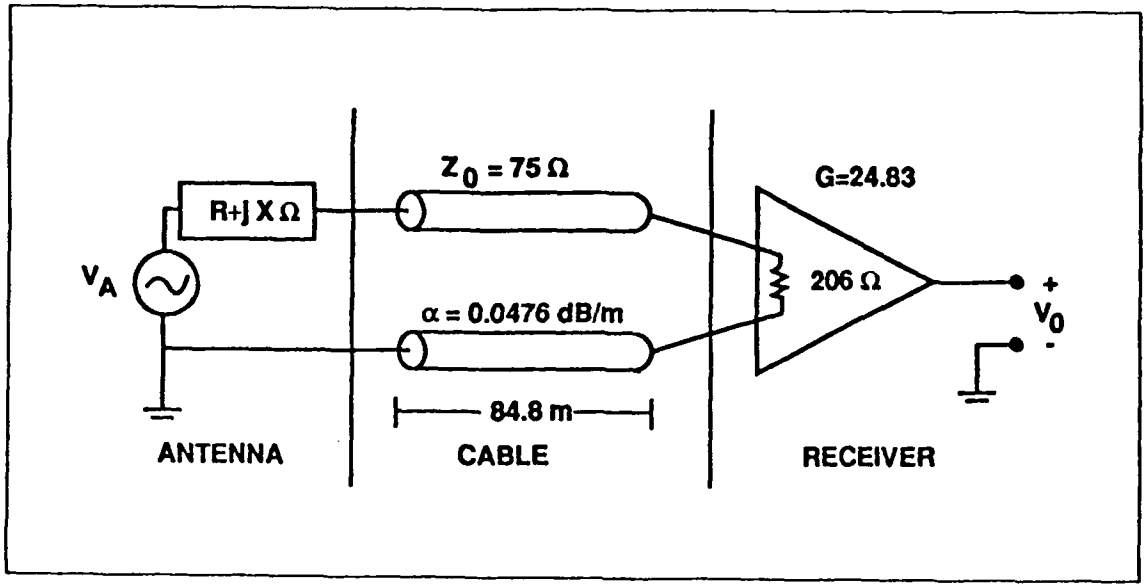

Figure D.1: VHF Data Collection System Circuit Model

D.1 VHF Data Collection System Gain

An equivalent circuit model for the VHF data collection system and following analysis can be seen in Figure D.1.

1. **RG-11/U Coaxial Cable**
   Design Frequency, $f = 63\ MHz$.
   Characteristic Impedance, $Z_o = 75\ \Omega$.
   Characteristic Admittance, $Y_o = 1/75\ \mho$.
   Polyethylene Dielectric[a], $\epsilon_r = 2.26$[b] and $\mu_r = 1$[b].
   Velocity of Propagation,

$$V_p = \frac{c}{\sqrt{\mu_r\,\epsilon_r}} = \frac{3x10^8\ m/s}{\sqrt{2.26}} \simeq 2x10^8\ m/s$$

   Measured One Way Wave Travel Time[c], $t = 425\ ns$.
   Cable Length,

$$l_c = V_p t = (2x10^8\ m/s)(425\ ns) \simeq 84.8\ m$$

[a]From "Transmission Lines" in *Reference Data for Engineers: Radio, Electronics, Computer, and Communications*, p 29-30. Howard W. Sams and Company, Indianapolis, IN, seventh edition, 1989.
[b]From "Properties of Materials" in *Reference Data For Radio Engineers*, p 66. International Telephone and Telegraph Corporation, New York, NY, fourth edition, 1957.
[c]From Time Domain Reflectometry.

Cable Attenuation Constant[d], $\alpha = .0476\ dB/m$.
One Way Cable Attenuation,

$$\alpha l_c = (.0476\ dB/m)(84.8\ m) = 4.036\ dB$$

2. **VHF Antenna**
Design Frequency, $f = 63\ MHz$.
Free Space Quarter Wavelength,

$$\frac{\lambda_o}{4} = \frac{c}{4f} = \frac{3x10^8\ m/s}{(4)\,(63x10^6\ /s)} = 1.19\ m$$

Antenna's Physical Length,

$$l_a = (4\ ft)(.3048\ m/ft) = 1.22\ m$$

Based on it's physical length, the antenna was analyzed as a quarter wavelength monopole, which resulted in an Antenna Effective Height[e] of,

$$h_e = (1.27\ l_a) = (1.27)(1.22\,m) = 1.55\,m$$

Cable-Antenna Combination Measured Admittance[f], $Y_{CA} = .0135 - j.005\ \mho$.

Normalized Admittance of the Cable-Antenna Combination,

$$\overline{Y_{CA}} = \frac{Y_{CA}}{Y_o} = (.0135 - j.005)(75) = 1.01 - j.375$$

Cable-Antenna Combination Reflection Coefficient,

$$\Gamma_{CA} = \frac{\overline{Y_{CA}} - 1}{\overline{Y_{CA}} + 1} = \frac{.01 - j.375}{2.01 - j.375} = .1835\angle - 77.9°$$

Voltage Standing-Wave Ratio of Cable-Antenna Combination,

$$VSWR_{CA} = \frac{1 + |\Gamma_{CA}|}{1 - |\Gamma_{CA}|} = \frac{1 + .183}{1 - .183} = 1.45$$

[d] From "Coaxial Cables" in Cooper Industries' *Belden Wire and Cable Catalog*, p 125. Richmond, IN, 1989.

[e] From "Gain, Capture Area, And Transmission Loss For Grounded Monopoles And Elevated Dipoles", in *RF Design*, p 45. November-December, 1978.

[f] From an admittance bridge tuned to 63 MHz.

Return Loss of the Cable-Antenna Combination,

$$Ret\ Loss_{CA} = 10\ \log \frac{1}{|\Gamma_{CA}|^2} = 10\ \log \frac{1}{|.183|^2} = 14.73\ dB$$

Return Loss of Antenna,

$$Ret\ Loss_A = Ret\ Loss_{CA} - 2(\alpha l_c) = 14.73\,dB - 2(4.036\,dB) = 6.66\ dB$$

Magnitude of Antenna Reflection Coefficient,

$$|\Gamma_A| = \sqrt{10^{-\frac{Ret\ Loss_A}{10}}} = \sqrt{10^{-\frac{6.66}{10}}} = .465$$

Reflection Loss of Antenna,

$$Ref\ Loss_A = 10\ \log \frac{1}{1 - |\Gamma_A|^2} = 10\ \log \frac{1}{1 - .465^2} = 1.06\,dB$$

3. **Airborne Instruments Laboratory Precision Tuned Receiver**
Input Impedance, $Z_L = 206\ \Omega$.
Receiver Voltage Gain at 63 MHZ, $G_r = 24.83$ or $27.9\,dB$.
Receiver Reflection Coefficient,

$$\Gamma_L = \frac{Z_L - Z_o}{Z_L + Z_o} = \frac{206 - 75}{206 + 75} = .466\angle 0°$$

Voltage Standing-Wave Ratio of Receiver,

$$VSWR_L = \frac{1 + |\Gamma_L|}{1 - |\Gamma_L|} = \frac{1 + .466}{1 - .466} = 2.75$$

Maximum Voltage Standing-Wave Ratio Due to Multiple Reflections,

$$VSWR_{max} = (VSWR_{CA})(VSWR_L) = (1.45)(2.75) = 3.98$$

Maximum Reflection Loss Due To Multiple Reflections,

$$Ref\ Loss_{max} = 10 \log \frac{(VSWR_{max} + 1)^2}{4\,VSWR_{max}} = 10 \log \frac{(3.98 + 1)^2}{(4)\,(3.98)} = 1.93\,dB$$

Minimum VHF System Gain,

$$G_{min} = G_r - Ref\ Loss_A - \alpha l_c - Ref\ Loss_{max} = 27.90 - 1.06 - 4.04 - 1.93 = 20.87\,dB$$

or a minimum voltage gain of 11.05.

Minimum Voltage Standing-Wave Ratio Due to Multiple Reflections,

$$VSWR_{min} = \frac{VSWR_L}{VSWR_{CA}} = \frac{2.75}{1.45} = 1.90$$

Minimum Reflection Loss Due To Multiple Reflections,

$$Ref\ Loss_{min} = 10\log\frac{(VSWR_{min}+1)^2}{4\,VSWR_{min}} = 10\log\frac{(1.90+1)^2}{(4)\,(1.90)} = .46\,dB$$

Maximum VHF System Gain,

$$G_{max} = G_r - Ref\ Loss_A - \alpha l_c - Ref\ Loss_{min} = 27.90 - 1.06 - 4.04 - .46 = 22.34\,dB$$

or a maximum voltage gain of 13.09.

Although a more rigorous flow graph calculation to determine the system's minimum-maximum range of gain could have been used, it would not have appreciably altered these results. Therefore, a conservative gain of 21 dB was chosen. This quantity corresponded to an **Overall VHF Voltage Gain**, G_T, of 11.22.

D.2 LF Data Collection System Gain

An equivalent circuit model for the LF data collection system and following discussion is illustrated in Figure D.2.

1. **LF Aluminum Alloy Antenna**
   Design Frequency, $f = 100kHz$.
   Free Space Wavelength,

$$\lambda_o = \frac{c}{f} = \frac{3x10^8\ m/s}{100x10^3\ /s} = 3\ km$$

   Physical Length,

$$l_a = (275\ in)(1\ ft/12\ in)(.3048\ m/ft) = 6.99\ m$$

   Based on it's physical length, the antenna was analyzed as a short monopole

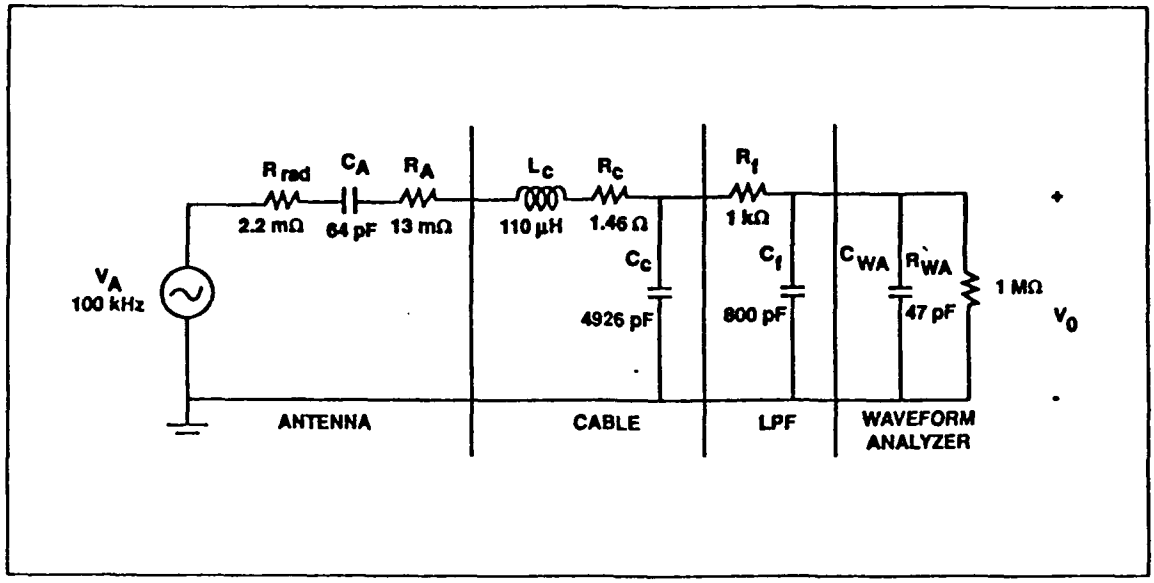

Figure D.2: LF Data Collection System Equivalent Circuit

which resulted in an Antenna Effective Height[e], h_e, of just l_a or $6.99\,m$.

Antenna Radius, $r = (.65\,in)(2.54\,cm/in) = 1.65\,cm$.
Phase Constant,

$$\beta\, l_a = \frac{2\pi f\, l_a}{c} = \frac{2\pi\, 100x10^3\,/s\; 6.99\,m}{3x10^8\; m/s} = .01463\; rad$$

Short Monopole Antenna Impedance[g],

$$Z_A = .5\left(20\,(\beta\, l_a)^2 - j\frac{120}{\beta\, l_a}\,\ln\left(\frac{l_a}{r} - 1\right)\right) =$$

$$.5\left(20\,(.01463)^2 - j\frac{120}{.01463}\,\ln\left(\frac{699\,cm}{1.65\,cm} - 1\right)\right) = .0022 - j\,24,713\;\Omega$$

Antenna Radiation Resistance, $R_{rad} = 2.2\,m\Omega$.
Antenna Capacitance,

$$C_A = \frac{1}{2\pi\, f\, X_A} = \frac{1}{(2\pi)\,(100x10^3\,/s)\,(24,713\,\Omega)}\left(\frac{\Omega\, F}{s}\right) = 64\,pF$$

Aluminum Alloy Conductivity Constant, $\sigma \simeq 1x10^7\; \mho/m$.

[g] From "Dipoles and Monopoles" in R.C. Johnson and H. Jasik's *Antenna Engineering Handbook*, p 4-5 and 4-26. McGraw-Hill Book Company, New York, NY, second edition, 1984.

Aluminum Alloy Relative Permeability, $\mu_r = 1$.
Permeability of Free Space, $\mu_o = 4\,\pi\,x10^{-7}\ H/m$.
Antenna Skin Depth,

$$\delta \equiv \frac{1}{\sqrt{\pi\, f\, \mu_r\, \mu_o\, \sigma}} = \frac{1}{\sqrt{(\pi)(100x10^3)(1)(4\,\pi\,x10^{-7})(1x10^7)}} = 503\ \mu m$$

Antenna Resistance,

$$R_A = \frac{l_a}{\sigma\, \delta\, w} = \frac{6.99\,m}{(1x10^7\,\mho/m)(503\,\mu m)(2\,\pi\,1.65\,cm)} = 13\ m\Omega$$

2. **RG-11/U Coaxial Cable**
For the LF system, the coaxial cable length was short enough in comparison to the design frequency's wavelength of 3 km to be modeled as lumped circuit elements.

Polyethylene Dielectric[a], $\epsilon_r = 2.26$[b] and $\mu_r = 1$[b].
Velocity of Propagation,

$$V_p = \frac{c}{\sqrt{\mu_r\, \epsilon_r}} = \frac{3x10^8\ m/s}{\sqrt{2.26}} \simeq 2x10^8\ m/s$$

One Way Wave Travel Time[c], $t = 366\,ns$.
Cable Length,

$$l_c = V_p t = (2x10^8\ m/s)(366\ ns) \simeq 73.2\ m$$

Cable Capacitance Constant[d], $C = 67.3\,pF/m$.
Total Cable Capacitance,

$$C_c = C\, l_c = (67.3\,pF/m)(73.2\,m) = 4926\ pF$$

Cable DC Resistance Constant[d], $R_{dc} = .0199\,\Omega/m$.
Total Cable DC Resistance,

$$R_c = R_{dc}\, l_c = (.0199\,\Omega/m)(73.2\,m) = 1.46\ \Omega$$

Cable Inductance Constant[h], $L = 1.5\ \mu H/m$.
Total Cable Inductance,

$$L_c = L\, l_c = (1.5\,\mu H/m)(73.2\,m) = 110\ \mu H$$

[h] From "Ground Conductor Properties" in H. W. Denny's *Grounding for the Control of EMI*, p 2.7. Interference Control Technologies, Inc., Gainesville, VA, 1983.

3. **Low Pass Filter**
   $R_f = 1\,k\Omega$ and $C_f = 800\,pF$.

4. **Waveform Analyzer Input Impedance**
   $R_r = 1\,M\Omega$ and $C_r = 47\,pF$.

   Spice (computer circuit analysis) was used to analyze the resulting circuit in Figure D.2. Based on a 1 V input signal, V_A, at 100 kHz, an output voltage, V_O, of $10.0\,mV$ was produced. This resulting output voltage corresponded to an **Overall LF Voltage gain**, G_T, of .010.

Appendix E

Computer Program

The program, *Trigonly.Bas*, was utilized for the entire main study period. It set-up the instrumentation, controlled the equipment, opened data files, coordinated data transfers, and reset timers at midnight.

In order to use this program, one must also ensure that the HP Digitizing Oscilloscope (HPDO) and Analogic Waveform Analyzer (WA) are addressed appropriately using the proper HP-IB menus. In this program, an ISC of 7 was used to identity the Vectra computer input/output board. Similarly, 07 and 15 were used to address the Oscilloscope and Waveform Analyzer respectively. The actual code of interest begins after line 1170.

Trigonly.Bas

```
10 ' Copyright Hewlett-Packard 1984, 1985
20 ' Set up program for MS-DOS HP-IB I/O Library
30 ' For use independent of the PC instrument bus system
40 DEF SEG
50 CLEAR , &HFE00
60 I = &HFE00
70 ' PCIB.DIR$ represents the directory where the library
80 ' files are located
90 ' PCIB is an environment variable which should be set
100 ' from MS-DOS i.e. A:> SET PCIB = A:\LIB
110 '
120 ' If there is insufficient environment space a direct
130 ' assignment can be made here, i.e
140 ' PCIB.DIR$ = "A:\LIB"
150 ' Using the environment variable is the preferred method
160 '
170 PCIB.DIR$ = ENVIRON$("PCIB")
180 I$ = PCIB.DIR$ + "\PCIBILC.BLD"
190 BLOAD I$, &HFE00
200 CALL I(PCIB.DIR$, I%, J%)
210 PCIB.SEG = I%
220 IF J% = 0 THEN GOTO 290
230 PRINT "Unable to load.";
240 PRINT " (Error #";J%;")"
250 STOP
260 '
270 ' Define entry points for setup routines
280 '
290 DEF SEG = PCIB.SEG
300 O.S = 5
310 C.S = 10
320 I.V = 15
330 I.C = 20
340 L.P = 25
```

```
350 LD.FILE = 30
360 GET.MEM = 35
370 L.S = 40
380 PANELS = 45
390 '
400 ' Establish error variables and ON ERROR branching
410 '
420 DEF.ERR = 50
430 PCIB.ERR$ = STRING$(64, 32)
440 PCIB.NAME$ = STRING$(16, 32)
450 CALL DEF.ERR(PCIB.ERR, PCIB.ERR$, PCIB.NAME$, PCIB.GLBERR)
460 PCIB.BASERR = 255
470 ON ERROR GOTO 790
480 '
490 J = -1
500 I$ = PCIB.DIR$+"\HPIB.SYN"
510 CALL O.S(I$)
520 IF PCIB.ERR<>0 THEN ERROR PCIB.BASERR
530 '
540 ' Determine entry points for HP-IB Library routines
550 '
560 I = 0
570 CALL I.V(I, IOABORT, IOCLEAR, IOCONTROL, IOENTER)
580 IF PCIB.ERR<>0 THEN ERROR PCIB.BASERR
590 CALL I.V(I, IOENTERA, IOENTERS, IOEOI, IOEOL)
600 IF PCIB.ERR<>0 THEN ERROR PCIB.BASERR
610 CALL I.V(I, IOGETTERM, IOLLOCKOUT, IOLOCAL, IOMATCH)
620 IF PCIB.ERR<>0 THEN ERROR PCIB.BASERR
630 CALL I.V(I, IOOUTPUT, IOOUTPUTA, IOOUTPUTS, IOPPOLL)
640 IF PCIB.ERR<>0 THEN ERROR PCIB.BASERR
650 CALL I.V(I, IOPPOLLC, IOPPOLLU, IOREMOTE, IORESET)
660 IF PCIB.ERR<>0 THEN ERROR PCIB.BASERR
670 CALL I.V(I, IOSEND, IOSPOLL, IOSTATUS, IOTIMEOUT)
680 IF PCIB.ERR<>0 THEN ERROR PCIB.BASERR
690 CALL I.V(I, IOTRIGGER, J, J, J)
700 IF PCIB.ERR<>0 THEN ERROR PCIB.BASERR
710 CALL C.S
720 I$ = PCIB.DIR$+"\HPIB.PLD"
730 CALL L.P(I$)
740 IF PCIB.ERR<>0 THEN ERROR PCIB.BASERR
750 GOTO 930
760 '
770 ' Error handling routine
780 '
790 IF ERR = PCIB.BASERR THEN GOTO 820
```

```
800 PRINT "BASIC error #";ERR;" occurred in line ";ERL
810 STOP
820 TMPERR = PCIB.ERR
830 IF TMPERR = 0 THEN TMPERR = PCIB.GLBERR
840 PRINT "PC error #";TMPERR;" detected at line ";ERL
850 PRINT "Error: ";PCIB.ERR$
860 STOP
870 '
880 ' COMMON declarations are needed if your program is
890 ' going to chain to other programs. When chaining,
900 ' be sure to call DEF.ERR as well upon entering the
910 ' chained-to program
920 '
930 COMMON PCIB.DIR$, PCIB.SEG
940 COMMON LD.FILE, GET.MEM, PANELS, DEF.ERR
950 COMMON PCIB.BASERR, PCIB.ERR, PCIB.ERR$, PCIB.NAME$
960 COMMON PCIB.GLBERR, IOABORT, IOCLEAR, IOCONTROL, IOENTER
970 COMMON IOENTERA, IOENTERS, IOEOI, IOEOL, IOGETTERM
980 COMMON IOLLOCKOUT, IOLOCAL, IOMATCH, IOOUTPUT
990 COMMON IOOUTPUTA, IOOUTPUTS, IOPPOLL, IOPPOLLC
1000 COMMON IOPPOLLU, IOREMOTE, IORESET, IOSEND, IOSPOLL
1010 COMMON IOSTATUS, IOTIMEOUT, IOTRIGGER
1020 '
1030 FALSE = 0
1040 TRUE = NOT FALSE
1050 NOERR = 0
1060 EUNKNOWN = 100001!
1070 ESEL = 100002!
1080 ERANGE = 100003!
1090 ETIME = 100004!
1100 ECTRL = 100005!
1110 EPASS = 100006!
1120 ENUM = 100007!
1130 EADDR = 100008!
1140 COMMON FALSE, TRUE, NOERR, EUNKNOWN, ESEL, ERANGE
1112 COMMON ETIME, ECTRL, EPASS, ENUM, EADDR
1150 '
1160 ' End Program Set-up
1170 ' User program begins at this point
1180 ISC = 7
1190 HPDO = 707 'HP Oscilloscope Address
1200 WA = 715 'Analogic Waveform Analyzer Address
1210 CALL IORESET (ISC)
1220 IF PCIB.ERR <> NOERR THEN ERROR PCIB.BASERR
1230 TIMEOUT = 5
```

```
1240 CALL IOTIMEOUT (ISC, TIMEOUT)
1250 IF PCIB.ERR <> NOERR THEN ERROR PCIB.BASERR
1260 CALL IOCLEAR (ISC)
1270 IF PCIB.ERR <> NOERR THEN ERROR PCIB.BASERR
1280 D$ = DATE$
1290 MID$(D$, 7) = "91 "
1300 V! = TIMER
1310 Y! = V/100
1320 A = INT(Y)
1330 OPEN "C:\"+D$+"."+MID$(STR$(A), 2) FOR OUTPUT AS #2
1340 ' Oscilloscope Setup
1350 MAX.LEN = 50
1360 ACT.LEN = 0
1370 REP$ = SPACE$(MAX.LEN)
1380 FOR D = 1 TO 32
1390 READ C$
1400 L = LEN(C$)
1410 CALL IOOUTPUTS (HPDO, C$, L)
1420 IF PCIB.ERR <> NOERR THEN ERROR PCIB.BASERR
1430 NEXT D
1440 DATA ":AUTOSCALE"
1450 DATA ":TIM:MODE SING"
1460 DATA ":TIM:SAMP REAL"
1470 DATA ":TIM:REF CENT"
1480 DATA ":TIM:RANG 10 us"
1490 DATA ":TIM:DEL 3 us"
1500 DATA ":CHAN1:PROB 1"
1510 DATA ":CHAN1:RANGE 9"
1520 DATA ":CHAN1:OFFS 2.0"
1530 DATA ":CHAN1:COUP AC"
1540 DATA ":CHAN1:LFR ON"
1550 DATA ":TRIG:MODE EDGE"
1560 DATA ":TRIG:SOUR CHAN1"
1570 DATA ":TRIG:LEV .650"
1580 DATA ":TRIG:SLOP POS"
1590 DATA ":TRIG:HOLD TIME, 320ms"
1600 DATA ":ACQ:TYPE NORM"
1610 DATA ":ACQ:COMP 100"
1620 DATA ":ACQ:POIN 8000"
1630 DATA ":ACQ:COUN 1"
1640 DATA ":WAV:FORM ASCII"
1650 DATA ":WAV:SOUR CHAN1"
1660 DATA ":SYSTEM:HEADER OFF"
1670 DATA ":SYSTEM:LONGFORM OFF"
1680 DATA ":DISP:GRAT FRAM"
```

```
1690 DATA ":DISP:CONN ON"
1700 DATA ":DISP:FORM 1"
1710 DATA ":MEAS:SOUR CHAN1"
1720 DATA ":MEAS:MODE STAN"
1730 DATA ":RUN"
1740 DATA "*SRE 1"
1750 DATA ":TER?"
1760 CALL IOENTERS (HPDO, REP$, MAX.LEN, ACT.LEN)
1770 IF PCIB.ERR <> NOERR THEN ERROR PCIB.BASERR
1780 'Waveform Analyzer Setup
1790 FOR D = 1 TO 31
1800 READ C$
1810 L = LEN(C$)
1820 CALL IOOUTPUTS (WA, C$, L)
1830 IF PCIB.ERR <> NOERR THEN ERROR PCIB.BASERR
1840 NEXT D
1850 DATA "PORT = 3", "FLDDLM = 6", "INTEN = 10"
1860 DATA "INP", "PROBE = 1", "RANGE(1) = 1", "COUPLE = AC"
1870 DATA "TMB", "NPTS(1) = 1000", "PERIOD = 1E-6", "DELAY = -50E-6"
1880 DATA "TRIG", "TRGLEV = .250", "TMOD = 3", "HLDOFF = 9"
1890 DATA "MARK", "CROSS = 4"
1900 DATA "X", "XSCL = 3", "XOFF = 200E-6"
1910 DATA "Y", "YSCL = 4", "YOFF = 75E-3"
1920 DATA "DISP", "DSPM = 1"
1930 DATA "CLRERR", "CLRSRQ", "CLRKEY", "CLRAQU"
1940 DATA "DARM", "ARM"
1950 ' Intitialize
1960 ' Start
1970 T! = TIMER
1980 VMAX! = .65
1990 VMAXY! = .65
2000 UMAX! = .25
2010 UMAXY! = .25
2020 REPL = 0
2030 MEANY = 0
2040 TST = 0
2050 'Has O'Scope Triggered ?
2060 C$ = ":TER?"
2070 L = LEN(C$)
2080 CALL IOOUTPUTS (HPDO, C$, L)
2090 IF PCIB.ERR <> NOERR THEN ERROR PCIB.BASERR
2100 CALL IOENTER (HPDO, REPL)
2110 IF PCIB.ERR <> NOERR THEN ERROR PCIB.BASERR
2120 IF REPL<>1 THEN 2270
2130 'If O'Scope Has Triggered, Then Find Peak Value Of VHF Transient.
```

```
2140 C$ = ":STOP"
2150 L = LEN(C$)
2160 CALL IOOUTPUTS (HPDO, C$, L)
2170 IF PCIB.ERR <> NOERR THEN ERROR PCIB.BASERR
2180 TST = 1
2190 C$ = ":MEAS:VMAX?"
2200 L = LEN(C$)
2210 CALL IOOUTPUTS (HPDO, C$, L)
2220 IF PCIB.ERR <> NOERR THEN ERROR PCIB.BASERR
2230 CALL IOENTER (HPDO, VMAXY)
2240 IF PCIB.ERR <> NOERR THEN ERROR PCIB.BASERR
2250 GOSUB 2630
2260 IF VMAXY>VMAX THEN VMAX = VMAXY
2270 'Has Waveform Analyzer Triggered ?
2280 C$ = "SRQ"
2290 L = LEN(C$)
2300 CALL IOOUTPUTS (WA, C$, L)
2310 IF PCIB.ERR <> NOERR THEN ERROR PCIB.BASERR
2320 CALL IOENTER (WA, MEANY)
2330 IF PCIB.ERR <> NOERR THEN ERROR PCIB.BASERR
2340 IF MEANY<> 19 THEN 2450
2350 'If Waveform Analyzer Has Triggered, Then Find Peak Value Of LF Transient.
2360 TST = 1
2370 C$ = "MAX"
2380 L = LEN(C$)
2390 CALL IOOUTPUTS (WA, C$, L)
2400 IF PCIB.ERR <> NOERR THEN ERROR PCIB.BASERR
2410 CALL IOENTER (WA, UMAXY)
2420 IF PCIB.ERR <> NOERR THEN ERROR PCIB.BASERR
2430 GOSUB 2730
2440 IF UMAXY>UMAX THEN UMAX = UMAXY
2450 'Has Either Device Triggered ?
2460 IF TST = 1 THEN 2590 'If Either Triggered, Then Write Results To A File.
2470 'Is The Time Near Midnite ?
2480 S! = TIMER
2490 IF S>86392! THEN GOSUB 2930
2500 'If Neither Device Has Triggered, Then Wait 2 s.
2510 W! = TIMER
2520 S! = TIMER
2530 IF S<(W+2!) THEN 2520
2540 IF S<(T+180) THEN GOTO 2580 'If Neither Device Has Triggered After
2545                              '180 seconds, Then Reset Them.
2550 GOSUB 2630
2560 GOSUB 2730
2570 T! = TIMER
```

```
2580 GOTO 2050
2590 ' Write Results to a File
2600 WRITE #2, TIME$, VMAX, UMAX
2610 PRINT TIME$, VMAX, UMAX
2620 GOTO 1960
2630 'O'Scope Clear Sub-routine
2640 C$ = "*CLS"
2650 L = LEN(C$)
2660 CALL IOOUTPUTS (HPDO, C$, L)
2670 IF PCIB.ERR <> NOERR THEN ERROR PCIB.BASERR
2680 C$ = ":RUN"
2690 L = LEN(C$)
2700 CALL IOOUTPUTS (HPDO, C$, L)
2710 IF PCIB.ERR <> NOERR THEN ERROR PCIB.BASERR
2720 RETURN
2730 'Waveform Analyzer Clear Sub-routine
2740 C$ = "CLRERR"
2750 L = LEN(C$)
2760 CALL IOOUTPUTS (WA, C$, L)
2770 C$ = "CLRSRQ"
2780 L = LEN(C$)
2790 CALL IOOUTPUTS (WA, C$, L)
2800 C$ = "CLRKEY"
2810 L = LEN(C$)
2820 CALL IOOUTPUTS (WA, C$, L)
2830 C$ = "CLRAQU"
2840 L = LEN(C$)
2850 CALL IOOUTPUTS (WA, C$, L)
2860 C$ = "DARM"
2870 L = LEN(C$)
2880 CALL IOOUTPUTS (WA, C$, L)
2890 C$ = "ARM"
2900 L = LEN(C$)
2910 CALL IOOUTPUTS (WA, C$, L)
2920 RETURN
2930 'Midnite Sub-routine
2940 S! = TIMER
2950 IF S<1 THEN 2970
2960 GOTO 2940
2970 T = TIMER
2980 RETURN
2990 END
```

Bibliography

[1] T.E. Allibone. "The Long Spark". In R.H. Golde, editor, *Lightning Volume I :The Physics of Lightning*, pages 231–280. Academic Press, New York, NY, 1977.

[2] C.E. Baum, J.P. O'Neill, E.L. Breen, D.L. Hall, and C.B. Moore. "Electromagnetic Measurement and Location of Lightning". In R.L. Gardner, editor, *Lightning Electromagnetics*, pages 319–346. Hemisphere Publishing Corporation, New York, NY, 1990.

[3] W.H. Beasley. "Positive Cloud-to-Ground Lightning Observations". *Journal of Geophysical Research*, 90:6131–6138, 1985.

[4] W.H. Beasley, M.A. Uman, and P.L. Rustan. "Electric Fields Preceding Cloud-to-Ground Lightning Flashes". *Journal of Geophysical Research*, 87:4883–4902, 1982.

[5] K. Berger. "The Earth Flash". In R.H. Golde, editor, *Lightning Volume I :The Physics of Lightning*, pages 119–191. Academic Press, New York, NY, 1977.

[6] M. Brook and N. Kitagawa. "Radiation from Lightning Discharges in the Frequency Range 400 to 1,000 Mc/s". *Journal of Geophysical Research*, 69:2431–2434, 1964.

[7] M. Brook and T. Ogawa. "The Cloud Discharge". In R.H. Golde, editor, *Lightning Volume I :The Physics of Lightning*, pages 191–229. Academic Press, New York, NY, 1977.

[8] N.J. Burke and D.B. Watson. "Digital Recorder of Lightning Current Waveforms". *IEEE Transactions on Instrumentation and Measurement*, IM-36(3):750–754, September 1987.

[9] N. Cianos, G.N. Oetzel, and E.T. Pierce. "Structure of Lightning Noise-Especially Above HF". In *Lightning and Static Electricity Conference*, Wright-Patterson AFB, OH, December 1972.

[10] N.D. Clarence and D.J. Malan. "Preliminary Discharge Processes in Lightning Flashes to Ground ". *Quarterly Journal of the Royal Meteorological Society*, 83:161–172, 1957.

[11] G.A. Dawson and D.G. Duff. "Initiation of Cloud-to-Ground Lightning Stokes". *Journal of Geophysical Research*, 75:5858–5867, 1970.

[12] R.J. Doviak, D. Sirmans, and D. Zrnic. "Weather Radar ". In E. Kessler, editor, *Instruments and Techniques for Thunderstorm Observation and Analysis*, pages 137–169. University of Oklahoma Press, Norman, OK, second edition, 1988.

[13] R.F. Griffiths and C.T. Phelps. "A Model of Lightning Initiation Arising from Positive Corona Streamer Development ". *Journal of Geophysical Research*, 31:3671–3676,, 1976.

[14] R.F. Griffiths and C.T. Phelps. "The Effects of Air Pressure and Water Vapour Content on the Propagation of Positive Corona Streamers and Their Implications to Lightning Initiation". *Quarterly Journal of the Royal Meteorological Society*, 102:419–426, April 1976.

[15] R.B. Harvey and E.A. Lewis. "Radio Mapping of 250 and 925 MHz Noise Sources in Clouds". *Journal of Geophysical Research*, 78:1944–1947, 1973.

[16] C.O. Hayenga. "Characteristics of Lightning VHF Radiation Near the Time of Return Strokes". *Journal of Geophysical Research*, 89:1403–1410, 1984.

[17] C.O. Hayenga and J.W. Warwick. "Two-Dimensional Interferometric Positions of VHF Lightning Sources". *Journal of Geophysical Research*, 86:7451–7462, 1981.

[18] F. Horner. "Radio Noise from Thunderstorms ". In J.A. Saxton, editor, *Advances in Radio Research*, volume 2, pages 121–215. Academic Press, New York, NY, 1964.

[19] M.M. Kekez and P. Savic. "Laboratory Simulation of the Stepped Leader in Lightning". *Canadian Journal of Physics*, 54(22):2216–2224, November 1976.

[20] N. Kitagawa and M. Brook. "A Comparison of Intracloud and Cloud-to-Ground Lightning Discharges ". *Journal of Geophysical Research*, 65:1189–1201, 1960.

[21] E.L. Kosarev, V.G. Zattespin, and A.V. Mitrofanov. "Ultrahigh Frequency Radiation from Lightning ". *Journal of Geophysical Research*, 75:7524–7530, 1970.

[22] P.R. Krehbiel, M. Brook, and R.A. McCrory. "An Analysis of the Charge Structure of Lightning Discharges to Ground". *Journal of Geophysical Research*, 84:2432–2456, 1979.

[23] P.R. Krehbiel, X.M. Shao, R.J. Thomas, C.T. Rhodes, and C.O. Hayenga. "VHF Radio Interferometry". In *"Conference of VHF Radio Interferometry"*, Socorro, NM, 1990. National Radio Astronomy Observations.

[24] E.P. Krider and R.C. Noggle. "Broadband Antenna Systems for Lightning Magnetic Fields". *Journal of Geophysical Research*, 14:252–256, 1975.

[25] E.P. Krider and G.J. Radda. "Radiation Waveforms Produced by Lightning Stepped Leaders". *Journal of Geophysical Research*, 80:2653–2657, 1964.

[26] E.P. Krider, G.J. Radda, and R.C. Noggle. "Regular Radiation Field Pulses Produced by Intracloud Discharges". *Journal of Geophysical Research*, 80:3801–3804, 1975.

[27] E.P. Krider, C.D. Weidman, and D.M. LeVine. "The Temporal Structure of the HF and VHF Radiation Produced by Intracloud Lightning Discharges ". *Journal of Geophysical Research*, 84:5760–5762, 1979.

[28] E.P. Krider, C.D. Weidman, and R.C. Noggle. "The Electric Fields Produced by Lightning Stepped Leaders". *Journal of Geophysical Research*, 82:951–960, 1977.

[29] G. Labaune, P. Richard, and A. Bondiou. "Electromagnetic Properties of Lightning Channels Formation and Propagation". In R.L. Gardner, editor, *Lightning Electromagnetics*, pages 285–317. Hemisphere Publishing Corporation, New York, NY, 1990.

[30] J. Latham. "The Electrification of Thunderstorms ". *Quarterly Journal of the Royal Meteorological Society*, 107:277–298, 1981.

[31] J. Latham and I.M. Stromberg. "Point-Discharge". In R.H. Golde, editor, *Lightning Volume I :The Physics of Lightning*, pages 99–117. Academic Press, New York, NY, 1977.

[32] M. LeBoulch, J. Hamelin, and C. Weidman. "UHF-VHF Radiation from Lightning". In R.L. Gardner, editor, *Lightning Electromagnetics*, pages 211–255. Hemisphere Publishing Corporation, New York, NY, 1990.

[33] C. Leteinturier and J. Hamelin. "Experimental Study of the Electromagnetic Characteristics of Lightning Discharge in the 200-20M Hz Band". In R.L. Gardner, editor, *Lightning Electromagnetics*, pages 347–363. Hemisphere Publishing Corporation, New York, NY, 1990.

[34] D.M. LeVine. "RF Radiation from Lightning". In *NASA*, Goddard Space Flight Center, Greenbelt, MD, February 1978.

[35] D.M. LeVine. "Sources of the Strongest RF Radiation from Lightning ". *Journal of Geophysical Research*, 85(C7):4091–4095, July 1980.

[36] D.M. LeVine. "The Spectrum of Radiation from Lightning". In *NASA*, Goddard Space Flight Center, Greenbelt, MD, 1981.

[37] D.M. LeVine and E.P Krider. "The Temporal Structure of HF and VHF Radiation During Florida Lightning Return Strokes ". *Geophysical Research Letters*, 4:13–16, 1977.

[38] D.M. LeVine, E.P Krider, and C.D. Weidman. "RF Radiation Produced by Intracloud Lightning Discharges". In *NASA*, Goddard Space Flight Center, Greenbelt, MD, April 1979.

[39] R.M. Lhermitte and E.R. Williams. "Thunderstorm Electrification: A Case Study". *Journal of Geophysical Research*, 90:6071–6078, 1985.

[40] X. S. Liu and P.R. Krehbiel. "The Initial Streamer of Intracloud Lightning Flashes". *Journal of Geophysical Research*, 90:6211–6218, 1985.

[41] L.B. Loebe. "The Mechanism of Stepped and Dart Leaders in Cloud-to-Ground Lightning Strokes ". *Journal of Geophysical Research*, 71:4711–4721, 1966.

[42] L.B. Loebe. "Mechanism of Charge Drainage from Thunderstorm Clouds". *Journal of Geophysical Research*, 75:5882–5889, 1970.

[43] M. Makino and T. Ogawa. "Quantitative Estimation of the Global Circuit". *Journal of Geophysical Research*, 90:5961–5966, 1985.

[44] D.J. Malan. "Radiation from Lightning Discharges and Its Relation to Discharge Processes". In L.G. Smith, editor, *Recent Advances in Atmospheric Electricity*, pages 557–563. Pergamon, New York, NY, 1959.

[45] C.B. Moore and B. Vonnegut. "The Thundercloud". In R.H. Golde, editor, *Lightning Volume I :The Physics of Lightning*, pages 51–97. Academic Press, New York, NY, 1977.

[46] J.P. Moreau. "Characterization of the Electromagnetic Radiation from Lightning during the Preliminary Phases". *European Space Agency*, January 1986.

[47] J.P. Moreau and P.L. Rustan. "A Study of Lightning Initiation Based on VHF Radiation". In R.L. Gardner, editor, *Lightning Electromagnetics*, pages 257–276. Hemisphere Publishing Corporation, New York, NY, 1990.

[48] J.E. Nanevicz, E.F. Vance, and J.M. Hamm. "Observations of Lightning in the Frequency and Time Domains". In R.L. Gardner, editor, *Lightning Electromagnetics*, pages 191–210. Hemisphere Publishing Corporation, New York, NY, 1990.

[49] G.L. Oetzel and E.T. Pierce. "Radio Emissions from Close Lightning". In S.C. Coroniti and J. Hughes, editors, *Planetary Electrodynamics*, pages 543–569. Gordon and Breach, New York, NY, 1969.

[50] T. Ogawa. "Fair-Weather Electricity". *Journal of Geophysical Research*, 90:5951–5960, 1985.

[51] T. Ogawa and M. Brook. "The Mechanism of the Intracloud Lightning Discharge ". *Journal of Geophysical Research*, 69:5141–5150, 1964.

[52] R.E. Orville. "Spectrum of the Lightning Stepped Leader". *Journal of Geophysical Research*, 73:6999–7008, November 1968.

[53] R.E. Orville. "Spectrum of the Lightning Dart Leader". *Journal of Atmospheric Science*, 32:1829–1837, September 1975.

[54] E.T. Pierce. "Atmospherics and Radio Noise". In R.H. Golde, editor, *Lightning Volume I :The Physics of Lightning*, pages 351–384. Academic Press, New York, NY, 1977.

[55] E.T. Pierce. "Spherics and Other Electrical Techniques for Storm Investigations". In E. Kessler, editor, *Instruments and Techniques for Thunderstorm Observation and Analysis*, pages 83–90. University of Oklahoma Press, Norman, OK, second edition, 1988.

[56] E.T. Pierce. "Storm Electricity and Lightning". In E. Kessler, editor, *Thunderstorm Morphology and Dynamics*, pages 277–285. University of Oklahoma Press, Norman, OK, second edition, 1988.

[57] D.E Proctor. "VHF Radio Pictures of Cloud Flashes ". *Journal of Geophysical Research*, 86:4041–4071, 1981.

[58] L.T. Remizov, A.G. Paskaul, and I.V. Oleynikova. "Characteristics of Impulse VLF Atmospheric Radio Noise Near A Thunderstorm ". *Soviet Journal of Communications Technology & Electronics*, 33(2), February 1988.

[59] P. Richard and G. Auffray. "VHF-UHF Interferometric Measurements, Applications of Lightning Discharge Mapping". *Radio Science*, 20(2):171–192, 1985.

[60] P. Richard, A. Delannoy, G. Labaune, and P. Laroche. "Results of Spatial and Temporal Characterization of the VHF-UHF Radiation of Lightning". *Journal of Geophysical Research*, 91:1248–1260, 1986.

[61] W.D. Rust and D.R. MacGorman. "Techniques for Measuring Electrical Parameters of Thunderstorms". In E. Kessler, editor, *Instruments and Techniques for Thunderstorm Observation and Analysis*, pages 91–118. University of Oklahoma Press, Norman, OK, second edition, 1988.

[62] P.L. Rustan. *"Properties of Lightning Derived from Time Series Analysis of VHF Radiation Data"*. PhD thesis, University of Florida, 1979.

[63] P.L. Rustan, M.A. Uman, D.G. Childers, W.H. Beasley, and C.L. Lennon. "Lightning Source Locations from VHF Radiation Data for a Flash at Kennedy Space Center". *Journal of Geophysical Research*, 85:4893–4903, 1980.

[64] X.M. Shao, P.R. Krehbiel, R. Thomas, and C.T. Rhodes. "Observations of Lightning Using VHF Radio Interferometry". In *Conference on Radio Interferometry*, Socorro, NM, 1990. National Radio Astronomy Observations.

[65] L.G. Smith. "Intracloud Lightning Discharges". *Quarterly Journal of the Royal Meteorological Society*, 83:103–111, 1957.

[66] S. Szpor. "Critical Comparison of Theories of Stepped Leaders ". *Archiwum Elektrotechniki*, 26(2):291–300, 1977.

[67] M. Takagi. "Polarization of VHF Radiation from Lightning Discharges ". *Journal of Geophysical Research*, 80:5011–5014, 1975.

[68] P.C. Thum. "A Review of Lightning Stepped Leader Theories". *Jurnal Fakulti Kejuruteraan Universiti Malaya*, 16:27–34, June 1977.

[69] M.A. Uman. "Lightning Return Stroke Electric and Magnetic Fields". *Journal of Geophysical Research*, 90:6121–6130, 1985.

[70] M.A. Uman. *The Lightning Discharge.* Academic Press, Orlando, FL, 1987.

[71] M.A. Uman and D.K. McLain. "Radiation Field and Current of the Lightning Stepped Leader". *Journal of Geophysical Research*, 75:1058–1066, 1970.

[72] C.D. Weidman, J.H. Hamelin, and M. LeBoulch. "Lightning VHF and UHF Emissions and Fast Time Resolved Measurements of the Associated Electric Field Variations". In *10th International Aerospace and Ground Conference on Lightning and Static Electricity*, Paris, France, December 1985.

[73] C.D. Weidman and E.P. Krider. "The Radiation Field Waveforms Produced by Intracloud Lightning Discharge Processes". *Journal of Geophysical Research*, 84:3157–3164, 1979.

[74] C.D. Weidman and E.P. Krider. "Amplitude Spectra of Lightning Radiation Fields in the Interval from 1 to 20M Hz". *Radio Science*, 21(6):964–970, November 1986.

[75] E.R. Williams, M.E. Weber, and R.E. Orville. "The Relationship Between Lightning Type and Convective State of Thunderclouds". *Journal of Geophysical Research*, 94:13213–13220, 1989.

[76] K.L. Zonge and W.H. Evans. "Prestroke Radiation from Thunderclouds ". *Journal of Geophysical Research*, 71:1519–1523, 1966.